

Characterization of the ACC-1 Family of Cys-Loop Ligand Gated Ion Channels from the Parasitic Nematode *Haemonchus contortus*.

by

Sarah A. Habibi

A thesis submitted to the  
School of Graduate and Postdoctoral Studies in partial  
fulfillment of the requirements for the degree of

**Doctor of Philosophy in Applied Bioscience**

University of Ontario Institute of Technology (Ontario Tech University), Faculty of Science

Oshawa, Ontario, Canada

December 2020

© Sarah A. Habibi

## THESIS EXAMINATION INFORMATION

Submitted by: **Sarah Habibi**

**Doctor of Philosophy in Applied Biosciences**

Thesis title: Characterization of the ACC-1 Family of Cys-Loop Ligand Gated Ion Channels from the Parasitic Nematode *Haemonchus contortus*.

An oral defense of this thesis took place on November 17, 2020 in front of the following examining committee:

**Examining Committee:**

Chair of Examining Committee	Dr. Holly Jones Taggart
Research Supervisor	Dr. Sean Forrester
Examining Committee Member	Dr. Julia Green-Johnson
Examining Committee Member	Dr. Janice Strap
University Examiner	Dr. Bernadette Murphy
External Examiner	Dr. Robert Greenberg

The above committee determined that the thesis is acceptable in form and content and that a satisfactory knowledge of the field covered by the thesis was demonstrated by the candidate during an oral examination. A signed copy of the Certificate of Approval is available from the School of Graduate and Postdoctoral Studies.

## Abstract

Nematode cys-loop ligand-gated ion channels (LGICs) have been extensively studied for decades because of their role in current anthelmintic action and potential as targets for future drugs. Many families of cys-loop receptors have not yet been pharmacologically characterized in parasitic nematodes, and thus provides an opportunity for further exploration into their role in the nervous system of these pathogens, and relevance for anthelmintic action. The ACC-1 family of receptors is a group of inhibitory acetylcholine-gated chloride channels that are unique to invertebrate species. Specifically, the ACCs have been identified in both free-living (*Caenorhabditis elegans*) and parasitic (*Haemonchus contortus*) nematodes. However, their pharmacological properties in *H. contortus* have yet to be explored. My PhD thesis focused on identifying and characterizing the role of the ACC-1 family of receptors in *H. contortus*, using molecular cloning, pharmacological characterization and an investigation of the ligand-binding pockets using site-directed mutagenesis and computational protein modelling. I conducted an extensive pharmacological characterization of the following receptors, ACC-2, ACC-1/ACC-2, ACC-1/LGC-46, LGC-46, LGC-39/ACC-1, and LGC-40/ACC-1, and generated homology models for each with various ligands bound. The ACC receptors from *H. contortus* are sensitive to various cholinergic ligands, nicotinic acetylcholine receptor anthelmintics, classical antagonists, and minimally sensitive to nicotine. Although one particular subunit, ACC-1, does not form a functional channel alone, it does associate with other members of the ACC family, ACC-2 and LGC-46, as well the previously uncharacterized cholinergic receptors, LGC-39 and 40, to form unique heteromeric channels. In addition, it was found that a single point mutation of a phenylalanine residue to a tyrosine in Loop C of the ACC binding pocket results in a hypersensitive receptor. Finally, sequence analysis of the ACCs revealed that the characteristic tryptophan residue, which contributes to  $\pi$ -cationic stabilizing interactions with ligands in the binding pocket, is located in Loop C of these receptors, whereas this residue is commonly found in Loop B of mammalian nAChRs. Together, this dissertation provides the first characterization of these inhibitory ACh receptors in parasitic nematodes and further sheds light into cholinergic neurotransmission in *H. contortus*.

Key words:

Acetylcholine; ACC; *Haemonchus contortus*; Cys-loop receptors; Anthelmintic resistance;

## Author's Declaration

I hereby declare that this thesis consists of original work of which I have authored. This is a true copy of the thesis, including any required final revisions, as accepted by my examiners.

I authorize the University of Ontario Institute of Technology (Ontario Tech University) to lend this thesis to other institutions or individuals for the purpose of scholarly research. I further authorize University of Ontario Institute of Technology (Ontario Tech University) to reproduce this thesis by photocopying or by other means, in total or in part, at the request of other institutions or individuals for the purpose of scholarly research. I understand that my thesis will be made electronically available to the public.

The research work in this thesis that was performed in compliance with the regulations of Animal Care Committee under **the Animal care certificate file number 0002.**

Sarah A Habibi

A handwritten signature in black ink that reads "SARAH.H". The letters are stylized and connected, with a prominent "S" and "H".

## Statement of Contributions

**Published Manuscript I (Chapter II): Habibi, S.A.,** Callanan, M. and Forrester, S.G. (2018) Molecular and pharmacological characterization of an acetylcholine-gated chloride channel (ACC-2) from the parasitic nematode *Haemonchus contortus*. *International Journal for Parasitology: Drugs and Drug Resistance*. 8(3): 518-525

Sarah Habibi conducted all of the electrophysiological experiments for the various receptors studied, generated the protein models and ligand docks, created all of the figures, and wrote the manuscript. Micah Callanan cloned the acc-2 receptor and generated two of the five ACC-2 mutants.

**Published Manuscript II (Chapter III): Callanan, M., Habibi, S.A.\*,** Law, W.J., Nazareth, K., Komuniecki, R., and Forrester, S.G. (2018) Investigating the function and possible biological role of an acetylcholine-gated chloride channel subunit (ACC-1) from the parasitic nematode *Haemonchus contortus*. *International Journal for Parasitology: Drugs and Drug Resistance*. 8(3): 526-533 **\*Joint first author**

Sarah Habibi conducted all of the electrophysiology experiments listed in the manuscript, generated the protein models and ligand docks, created figures 1 and 2, and co-wrote the manuscript. Micah Callanan cloned the *acc-1* receptor, conducted PCR expression tests, completed the immunolocalization studies, and co-wrote the manuscript. Kristen Nazareth generated the phylogenetic tree.

**Published Manuscript III (Chapter IV): Habibi, S.A.,** Blazie, S., Jin, Y. and Forrester, S.G. (2019) Isolation and characterization of a novel member of the ACC ligand-gated chloride channel family, Hco-LCG-46, from the parasitic nematode *Haemonchus contortus*. *Molecular & Biochemical Parasitology*. 237(111276)

Sarah Habibi cloned the LGC-46 receptor, conducted all of the electrophysiology experiments, generated the protein models and ligand docks, generated all figures (except figure 6), and wrote the manuscript (except results related to figure 6). Steven Blazie conducted the *in vivo lgc-46* experiment, generated figure 6, and wrote the result section related to figure 6 (section 3.4). Yishi Jin provided funding for work completed by Steven Blazie. Micah Callanan cloned the *hco-acc-4* gene and published it on GenBank. Sarah Habibi confirmed the ACC-4 sequence through sub-cloning into the pGEMHE vector.

**Preparation Manuscript IV (Chapter V):** Investigation of subunit co-assembly of members of the ACC family with other cys-loop receptors.

Sarah Habibi conducted all electrophysiology experiments related to characterization of the LGC-39, LGC-39/ACC-1, LGC-40/ACC-1, ACC-2, and ACC-1/ACC-2 receptors, generated the protein models and ligand docks, created all figures, and wrote the chapter. Kristen Nazareth cloned LGC-39 and LGC-40 and conducted initial pharmacological characterization of homomeric receptors.

**Published Technical Manuscript V (Appendix 1): Abdelmassih, S.A., Cochrane, E. and Forrester, S.G.** (2018) Evaluating the longevity of surgically extracted *Xenopus laevis* oocytes for the study of nematode ligand-gated ion channels. *Invertebrate Neuroscience*. 18(1): 1-6

Sarah Habibi conducted all of the experiments week-to-week, created all of the figures, and wrote the entirety of the manuscript. Everett Cochrane completed 1 week of data collection. This manuscript is included here because all of the oocyte studies carried out in this thesis followed the protocol outlined in this paper.

## Acknowledgements

First, I would like to thank the Faculty of Science at Ontario Tech University for the opportunity to complete my graduate studies here. Thank you to both of my committee members, Dr. Janice Strap and Dr. Julia Green-Johnson. I would especially like to thank my PhD supervisor Dr. Sean Forrester for taking the chance with me back during my honours thesis project and supporting me through my desire to continue into a PhD. Your support, guidance, encouragement, and overall good vibes, made for a wonderful graduate study experience. I appreciate all of our long chats over frog surgeries, as they made for positive starts to the workweek and allowed us to be comfortable being ourselves while working in the lab.

I would also like to thank my lab colleagues over the years. First, thank you Micah for showing me the ropes during my undergrad, and teaching me everything I needed to know about molecular cloning and mutagenesis. Thank you Everett for being my desk buddy for the first year of my master's degree and always being down to grab whoppers on Wednesdays to eat outside of the labs. Your calm soul helped me power through my first year (and most difficult year) of graduate studies. Thank you Kristen for being the absolute positivity our lab needed. Your huge smile, constant laughter, and huge heart made for an amazing lab environment. I appreciate your positive guidance regarding my research and social media passion projects. Thank you Sierra for always being down to help in any way you could in the lab. I appreciate you taking the time to discuss process and techniques with me to help solve research problems. Finally, thank you to my two closest girlfriends on the 4<sup>th</sup> floor, Lidya and Samira. The frequent coffee breaks, sushi lunches, and girls nights out, really helped us to unwind and remember the good things in life. I can honestly say these are friendships that will last a lifetime. I can't wait to all celebrate as doctors really soon!

Finally, I would like to thank my family and my beautiful husband for your constant support and encouragement every step of the way. Mom and Dad, I appreciate you always showing interest in my project and praying for me when roads got rough. Saman, I can't express enough how grateful I am for having you by my side throughout this process. The countless mornings and nights you listened to me bore you with my research, let out my frustration, repeat myself, and over think (literally everything). You are the real MVP. As much as your logical and calm approach made me crazy at times, it also taught me a lot about how I handle situations, reflect from them, and grow both personally and professionally. I can't wait to start growing our family together and see where life takes us. I have a strong feeling our future is bright. Love you.

## Table of Contents

---

Thesis Examination Information .....	I
Abstract .....	II
Authors Declaration .....	III
Statement of Contributions .....	IV
Acknowledgements .....	VI
Table of contents .....	VII
List of Tables .....	XI
Fist of Figures .....	XII
List of Abbreviations and Symbols .....	XIV

### Chapter I: Literature Review

---

1.1: Phylum <i>Nematoda</i> .....	1
1.1.1: The nervous system of nematodes .....	2
1.1.2: Parasitic nematodes: <i>Haemonchus contortus</i> .....	2
1.2: Current Control Mechanisms .....	4
1.3: Mechanisms of resistance .....	4
1.3.1: Benzimidazole .....	5
1.3.2: Macrocyclic lactones .....	5
1.3.3: nAChR agonists .....	6
1.3.4: Amino-acetonitrile derivatives .....	7
1.4: Cys-loop Ligand Gated Ion Channels .....	7
1.4.1: The binding site .....	8
1.4.2: The channel pore .....	9
1.5: Diversity of Cys-Loop Receptors in Nematodes .....	9
1.6: Cholinergic neurotransmission .....	12
1.7: The ACC family .....	12
1.7: Goals and objectives .....	15

### Chapter II – Manuscript I: Molecular and pharmacological characterization of an acetylcholine-gated chloride channel (ACC-2) from the parasitic nematode *Haemonchus contortus*.

---

2.0: Abstract .....	17
2.1: Introduction .....	17
2.2: Methods .....	19
2.2.1: Isolation of <i>hco-acc-2</i> .....	19
2.2.2: Site-directed mutagenesis .....	20
2.2.3: Expression in <i>Xenopus laevis</i> oocytes .....	20
2.2.4: Electrophysiological recordings .....	21
2.2.5: Homology modeling .....	22
2.3: Results .....	22



2.3.1: Isolation of <i>hco-acc-2</i> .....	22
2.3.2: Expression of <i>hco-acc-2</i> in <i>Xenopus</i> oocytes .....	23
2.3.3: Pharmacological analysis .....	25
2.3.4: Homology modelling .....	26
2.3.5: Mutational analysis .....	29
2.3.6: Nicotine activates Hco-ACC-2 F200Y .....	32
2.4: Discussion .....	33
2.5: Acknowledgements .....	35
2.6: References .....	35
Connecting Statement I.....	39

Chapter III – Manuscript II: Investigating the function and possible biological role of an acetylcholine-gated chloride channel subunit (ACC-1) from the parasitic nematode *Haemonchus contortus*. 40

3.0: Abstract .....	41
3.1: Introduction .....	43
3.2: Materials and Methods .....	43
3.2.1: RNA/cDNA .....	43
3.2.2: Isolation of <i>hco-acc-1</i> and sequence analysis .....	43
3.2.3: Expression in <i>Xenopus</i> oocytes .....	44
3.2.4: Electrophysiology recordings .....	45
3.2.5: <i>In silico</i> modelling .....	46
3.2.6: Immunolocalization in <i>H. contortus</i> .....	46
3.2.7: Expression of <i>acc-1</i> in <i>C. elegans</i> .....	47
3.3: Results .....	48
3.3.1: Hco-ACC-1 isolation and polypeptide analysis .....	48
3.3.2: Functional Characterization of Hco-ACC-1 .....	49
3.3.3: Ligand docking analysis .....	51
3.3.4: Immunolocalization .....	51
3.3.5: Expression of <i>hco-acc-1</i> in <i>C. elegans</i> .....	52
3.4: Discussion .....	54
3.5: Acknowledgements .....	56
3.7: References .....	56
Connecting Statement II.....	60

Chapter IV – Manuscript III: Isolation and characterization of a novel member of the ACC ligand-gated chloride channel family, Hco-LCG-46, from the parasitic nematode *Haemonchus contortus*. 61

4.0: Abstract .....	62
4.1: Introduction .....	62
4.2: Methods .....	64
4.2.1: Isolation of <i>hco-lgc-46</i> and <i>hco-acc-4</i> .....	64
4.2.2: Expression in <i>Xenopus laevis</i> oocytes .....	64

4.2.3: Electrophysiological recordings .....	65
4.2.4: <i>In silico</i> modelling .....	66
4.2.5: Expression of <i>hco-lgc-46</i> in <i>C. elegans</i> .....	66
4.3: Results .....	67
4.3.1: Isolation of <i>hco-lgc-46</i> and <i>hco-acc-4</i> .....	67
4.3.2: Expression of <i>hco-lgc-46</i> and <i>hco-acc-1</i> in <i>Xenopus</i> oocytes .....	69
4.3.3: Homology modelling .....	72
4.3.4: Expression of <i>hco-lgc-46</i> in <i>C. elegans</i> .....	74
4.3.5: Expression of Hco-ACC-4 in oocytes .....	75
4.4: Discussion .....	77
4.5: Acknowledgements .....	79
4.7: References .....	79
Connecting Statement III.....	83
 Chapter V – Manuscript IV: Investigation of subunit co-assembly of members of the ACC family with other cys-loop receptors.	 84
<hr/>	
5.1: Introduction .....	85
5.2: Methods .....	86
5.2.1: Expression in <i>Xenopus laevis</i> oocytes .....	86
5.2.2: Electrophysiological recordings .....	87
5.2.3: <i>In silico</i> modelling .....	88
5.3: Results .....	88
5.3.1: Expression in <i>Xenopus</i> oocytes .....	88
5.3.2: Pharmacological analysis of homomeric and heteromeric channels .....	90
5.3.3: Action of antagonist on members of the ACC-1 and GGR-1 family .....	93
5.3.4: Homology modelling .....	95
5.4: Discussion .....	100
5.4: Acknowledgements .....	103
 Chapter VI – General Discussion	 104
<hr/>	
Chapter VII – References	108
<hr/>	
Appendix 1 – Technical Manuscript V: Evaluating the longevity of surgically extracted <i>Xenopus laevis</i> oocytes for the study of nematode ligand-gated ion channels.	119
<hr/>	
A1.0: Abstract .....	120
A1.1: Introduction .....	120
A1.2: Methods .....	122
A1.2.1: Oocyte extraction and preparation .....	122
A1.2.2: cRNA injection .....	122
A1.2.3: Electrophysiological recordings .....	123

A1.3: Results .....	124
A1.4: Discussion .....	127
A1.5: Acknowledgements .....	129
A1.5: Compliance with ethical standards .....	129
A1.6: List of Figures .....	130
A1.7: List of Tables .....	130
A1.8: References .....	130
A1.9. Manuscript V .....	132
<b>Appendix 2: Chapter II</b> .....	<b>139</b>
<hr/>	
A2.1: Manuscript I .....	140
<b>Appendix 3: Chapter III</b> .....	<b>148</b>
<hr/>	
A3.1: Manuscript II .....	149
A3.2: Supplementary Information .....	157
A3.2.1: Figures .....	157
<b>Appendix 4: Chapter IV</b> .....	<b>158</b>
<hr/>	
A4.1: Manuscript III .....	159
A4.2: Supplementary Information .....	170
A4.2.1: Tables .....	170
<b>Appendix 5: Copyright Permission from Co-Authors</b> .....	<b>171</b>
<hr/>	

## List of Tables

### Chapter II

**Table 2.1:** Summary of EC<sub>50</sub> values ± standard error for each channel with all of the compounds listed. N.R<sup>a</sup> indicates the channel did not respond to concentrations of indicated compound at concentrations ≥1 mM which is a concentration that elicited a maximal response on the WT channel. N.R<sup>b</sup> indicated that the channel did not respond to concentration up to 20 mM. n ≥ 5 oocytes. NR = no response; ND = not determined. \*indicates significant difference compared to WT (P < 0.01). \*\*indicates significant difference compared to WT (P < 0.001). NOTE: For each molecule (row), statistical analysis compared EC<sub>50</sub> values between WT and each mutant.

### Chapter IV

**Table 4.1:** Pharmacological summary of ACC-1 family of receptors from *H. contortus* in response to various cholinergic ligands and nAChR anthelmintics. Pharmacological responses are represented by EC<sub>50</sub> ± SE. N.R refers to no observed response of receptor to 20 mM concentration of ligand.

### Chapter V

**Table 5.1:** Pharmacological summary of the various ACC receptors from *H. contortus* in response to various cholinergic ligands, nAChR anthelmintics, and classic antagonists.

## List of Figures

### Chapter I

**Figure 1.1:** Life cycle of *Haemonchus contortus*.

**Figure 1.2:** Visual representation of a pentameric cys-loop ligand-gated ion channel.

### Chapter II

**Figure 2.1:** Protein sequence alignment of the *H. contortus* Hco-ACC-2 receptor with *C. elegans* Cel-ACC-2 and *D. rerio* Dre-GLY- $\alpha$ 1 receptors.

**Figure 2.2:** Pharmacological representation of the Hco-ACC-2 homomeric receptor.

**Figure 2.3:** Pharmacological characterization of the Hco-ACC-2 homomeric receptor in the presence of cholinergic ligands and anthelmintics.

**Figure 2.4:** Homology model of Hco-ACC-2 homodimer.

**Figure 2.5:** Homology models of Hco-ACC-2 with docked agonists.

**Figure 2.6:** Pharmacological characterization of the mutant Hco-ACC-2 receptors.

**Figure 2.7:** Impact of mutations at key aromatic residues in the Hco-ACC-2 binding pocket.

**Figure 2.8:** Pharmacology characterization and homology model of the Hco-ACC-2 homomeric receptor in the presence of Nicotine.

### Chapter III

**Figure 3.1:** Isolation of *hco-acc-1* and protein sequence analysis.

**Figure 3.2:** Pharmacological characterization and homology models of the Hco-ACC-1/Hco-ACC-2 heterodimer.

**Figure 3.3:** Immunolocalization of Hco-ACC-1 in adult female *H. contortus* worms.

**Figure 3.4:** Mean time to reverse of *C. elegans* in the presence of 30% octanol.

**Figure 3.5:** Confocal image of N2 *Caenorhabditis elegans* worms expressing *hco-acc-1* under control of the *cel-acc-1* wild type promoter.

### Chapter IV

**Figure 4.1:** Protein sequence alignment of the *H. contortus* Hco-LGC-46 and Hco-ACC-4 receptors with *C. elegans* Cel-LGC-46 and Cel-ACC-4 and *D. rerio* Dre-GLY- $\alpha$ 1 receptors.

**Figure 4.2:** Pharmacological characterization of the Hco-LGC-46 and Hco-ACC-/Hco-LGC-46 receptors.

**Figure 4.3:** Current-voltage analysis of the Hco-LGC-46 and Hco-ACC-/Hco-LGC-46 receptors.

**Figure 4.4:** Homology model of the LGC-46 homodimer with ligands docked.

**Figure 4.5:** Homology model of Hco-ACC-1/ Hco-LGC-46 heterodimer with ligands docked.

**Figure 4.6:** *in vivo* expression of Hco-LGC-46.

**Figure 4.7:** Average maximal currents shown for the Hco-LGC-46 and Hco-ACC-2 receptors in comparison to the heteromeric channels with Hco-ACC-4 present.

## **Chapter V**

**Figure 5.1:** Protein sequence alignment of the *H. contortus* Hco-ACC-1, Hco-ACC-2, Hco-LGC-39, and Hco-LGC-40 receptors with *C. elegans* Cel-LGC-39 and Cel-LGC-40 receptors.

**Figure 5.2:** Pharmacological characterization of the Hco-LGC-39 and Hco-LGC-39/ACC-1 receptors.

**Figure 5.3:** Pharmacological characterization of the Hco-LGC-40 and Hco-LGC-40/ACC-1 receptors.

**Figure 5.4:** Pharmacological characterization of the Hco-LGC-39, Hco-LGC-39/Hco-ACC-1, Hco-ACC-2, Hco-ACC-1/Hco-ACC-2, and Hco-ACC-2 F200Y in the presence of antagonists.

**Figure 5.5:** Homology model of the LGC-39 homodimer and LGC-39/ACC-1 heterodimer with ligands docked.

**Figure 5.6:** Homology model of the LGC-40 homodimer and LGC-40/ACC-1 heterodimer with ligands docked.

**Figure 5.7:** Strychnine docked in the ACC-2 and ACC-1/ACC-2 binding pockets.

**Figure 5.8:** (A) View of the Hco-ACC-2 homodimer binding pocket with strychnine docked. (B) View of the crystal structure of the *Aplysia* AChBP binding pocket with strychnine bound. PDB model retrieved from Brams et al. 2011.

## List of Abbreviations and Symbols

$\pi$ : Pie

Å: Angstrom (Unit of measurement)

$\alpha$ : Greek symbol alpha

$\beta$ : Greek symbol beta

$\gamma$ : Greek symbol gamma

5-HT: 5-Hydroxytryptamine (Serotonin)

ACC: Acetylcholine-gated chloride channel

AChR: Acetylcholine receptor

ADDs: Amino-acetonitrile derivatives

ACh: Acetylcholine

Ala (A): Alanine

Asn (N): Asparagine

Atro: Atropine

*A. suum*: *Ascaris suum*

Carbachol (Carb): Carbamylcholine

ChAT: Choline acetyltransferase

Chol: Choline chloride

*C. elegans (Cel)*: *Caenorhabditis elegans*

Cys(C): Cysteine

Cys-loop: Cysteine-Loop (Super family of ligand-gated ion channels)

*D. rerio (Dre)*: *Danio rerio*

DOPE: Discrete optimized protein energy

EC<sub>50</sub>: Half-maximal response concentration

ECD: Extracellular domain

GABA:  $\gamma$ -aminobutyric acid

GFP/YFP: Green/Yellow fluorescent protein

GGR: Subunit notation for some genes of the GABA/Glycine Receptor family.

Glu (E): Glutamate

GluCl: Glutamate-gated Chloride (Channel)

GlyR: Glycine Receptor

*H. contortus* (*Hco*): *Haemonchus contortus*

IC<sub>50</sub>: Half-maximal inhibitory concentration

IVM: Ivermectin

Lev: Levamisole chloride

LGIC: Ligand-gated ion channel

LGC: Ligand-gated channel

LGCC: Ligand-gated chloride channel

L1: Larval stage 1

L2: Larval stage 2

L3: Larval stage 3

L4: Larval stage 4

Meth: Methacholine (Acetyl- $\beta$ -methylcholine chloride)

nAChR: Nicotinic Acetylcholine Receptor

NGM: Nematode growth medium

NMJ: Neuromuscular junction



PAR: proline-alanine-arginine motif

PCR: Polymerase-chain reaction

Phe (F): Phenylalanine

RDL: Resistance to dieldrin

Strya: Strychnine hydrochloride

TEVC: Two-electrode voltage clamp

Trp (W): Tryptophan

Tyr (Y): Tyrosine

TM: Transmembrane Protein domain

UNC: Uncoordinated phenotype

Ure: Urecholine (carbamyl- $\beta$ -methylcholine chloride)

VACHT: Vesicular acetylcholine transporter

*X. laevis*: *Xenopus laevis* (African clawed frog)

## Chapter I – Literature Review

### 1.1 *Phylum Nematoda*

The phylum Nematoda is among one of the most diverse groups of organisms worldwide, with a total number of species ranging from 100,000 to 1 million (Parkinson et al. 2004). The general shape of nematodes is a long slender worm body that is tapered at both ends, has bilateral symmetry, and a singular body cavity referred to as the pseudocoel. The exterior body of nematodes is covered by a cuticle layer, which is shed multiple times during nematode growth and maturation. Between the outer cuticle layer and inner pseudocoel cavity, is an inner tube extending the length of the nematode body containing pharyngeal muscle and intestine. The digestive system runs through the length of the nematode body with the mouth present at the anterior end, and the anus present at the posterior end. Many nematodes exhibit sexual dimorphism, with the female worms being significantly larger than males (Schmidt et al. 1977).

#### 1.1.1 The nervous system of nematodes

Nematodes have a relatively simple nervous system, making them an ideal point of research for many neuroscientists. There are two main centralizations of nerve elements in nematodes: one in the anterior esophageal region and the other in the anal region, both connected by longitudinal nerve trunks (Schmidt et al. 1977). The central nervous system (present in anterior esophageal region) contains a characteristic nerve ring, which is composed of a combination of nerve cells and supporting glial cells. The nerve trunk that runs through the body of nematodes contains both the ventral and dorsal nerve cords. The ventral nerve cord has regions that project into the nerve ring where they are involved in synaptic processes. Both the ventral and dorsal nerve cords are closely associated with the outer epidermis of nematodes (Schafer 2016). In addition, all nematodes contain two types of sensory organs, which are mechanosensory and chemosensory in nature. These sensory organs are located in the head region and are referred to as labial and cephalic sensilla, respectively. Finally, motor functions, such as egg laying and pharyngeal pumping for nematode feeding, are controlled by specialized motor neurons, whereas behaviors like nematode locomotion and mating are controlled by somatic muscles which run the length of the nematodes body (Schafer 2016).

### 1.1.2 Parasitic nematodes: *Haemonchus contortus*

The phylum Nematoda contains both free-living and parasitic nematodes. Specifically, parasitic nematodes have been of particular interest due to their ability to infect humans, animals, and plants. Parasitic nematodes differ from free-living nematodes, as they often require a secondary intermediate host, or vector, in order to propagate and develop to maturation. According to the World Health Organization, approximately 1.5 billion people are infected with soil-transmitted helminths worldwide (WHO, 2017). Similarly, parasitic nematodes cause an annual loss of food sources, including livestock, of about 12% in the United States alone (Barker et al. 1994). The success of parasitic nematodes can be attributed in part due to their ability to adapt to a range of environmental conditions, reduce their susceptibility to predators, and hide from their host's immune response (Harder 2016).

A parasitic nematode of particular interest, belonging to the trichostrongylidae family, is *Haemonchus contortus*, commonly referred to as the barber pole worm. *H. contortus* is a pathogenic nematode that infects the gastrointestinal tract of ruminant animals, including sheep, goats, and cattle. Specifically, *H. contortus* resides in the abomasum, or fourth stomach, of animals, which is why they primarily infect ruminants. The economic burden of *H. contortus* is significant, with hundreds of millions of sheep and goats infected globally, ultimately resulting in a loss of livestock production estimated to be tens of billions of dollars per year (Schwarz et al. 2013). The disease that results when an animal is infected with *H. contortus* is referred to as haemonchosis. Female *H. contortus* worms contain large white ovaries, which wrap around the intestine throughout the length of the worms body. As a result, when the parasite feeds on the blood of its host, the intestines become red in colour and the resulting pattern of ovaries wrapped around the red intestines gives rise to a "barber pole" visual effect, and ultimately the common name of barber pole worm (Schmidt et al. 1977).

The distribution of *H. contortus* is heavily dependent on the life-stage of the nematode as well as the various environmental requirements needed for survival. Specifically, the free-living stage of the nematode requires a warm and moist environment to thrive, and thus dictates the abundance of *H. contortus* based on seasonal variations (Besier et al. 2016). Although *H. contortus* originated in sub-Saharan Africa, the distribution of *H. contortus* is now high in many tropical and temperate climate zones. In fact, *H. contortus* has shown to be extremely adaptable to a variety of different environments, and as a result can be found in nearly all regions where host ruminants are present (Besier et al. 2016).

The life cycle of *H. contortus* was first described by Veglia in 1916. The life cycle can be broken down into two distinct phases, the free-living and the parasitic phases (Figure 1.1). The free-living portion of the life cycle begins when eggs are deposited from the adult female parasites in the abomasum of the ruminant hosts. One adult female can produce up to 10 000 eggs per day (Prichard 2001). The eggs are transported outside of the host through the feces. In the feces the eggs develop and hatch into first stage larvae (L1), develop and molt further into second stage larvae (L2), followed by the third stage larvae (L3). The parasitic portion of the life cycle takes roughly 15 days and begins when the grazing ruminants consume L3 larvae found in nearby grasses. L3 larvae maximize their likelihood of being consumed by grazing ruminant animals by travelling to the tips of blades of grass. Once consumed, the L3 travel to the abomasum of the host, undergo the second ecdysis, and reside in the stomach mucosa. Once the second cuticle is shed, the L3 are able to feed. The L3 have a well-developed mouth, which is surrounded by six cephalic papillae. The L3 undergo a third ecdysis, where they rid their final outer skin and become stage 4 larvae (L4). This stage results in the full formation of the mouth apparatus which is used for piercing the mucosa of the abomasum and allows for the feeding of blood (Veglia 1916). The L4 finally go through their fourth ecdysis into adult worms, which have a hooked tail that allows the parasite to attach to their surroundings in the fourth stomach and resume their parasitic nature. Each ruminant host can be infected with thousands of worms, which feed on roughly 12 $\mu$ l of blood each per day (Laing et al. 2013), causing severe anemia and resulting in poor growth, weight loss, and ultimately death (Schallig 2000).

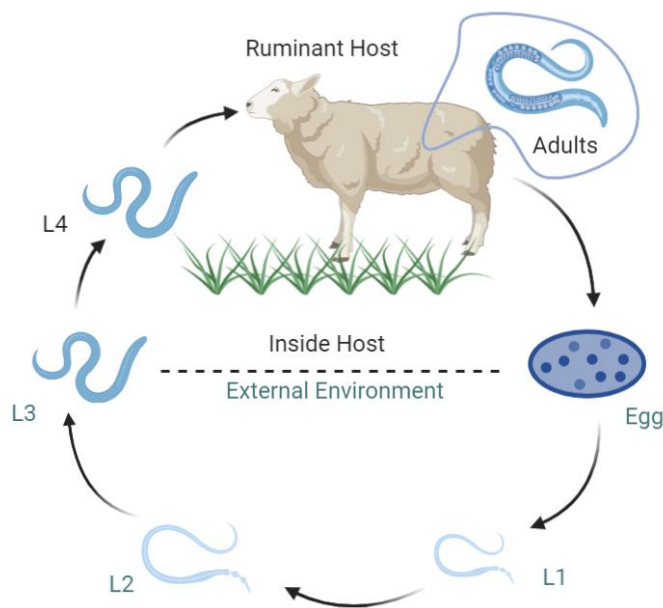


**Figure 1.1:** Life Cycle of *Haemonchus contortus*. Created with BioRender.com

## 1.2 Current Control Mechanisms

Currently, a variety of broad-spectrum anthelmintics are used for the treatment of animals infected with *H. contortus*. An anthelmintic is defined as an anti-parasitic pharmaceutical drug. Some major classes of anthelmintics include, piperazines, benzimidazoles, levamisole/pyrantel/morantel, paraherquamides, and macrocyclic lactones such as ivermectin. Anthelmintics are separated into these classes based on similarity in chemical structure and modes of action (Holden-Dye and Walker 2007). Of these, much research has focused on the role of benzimidazoles, ivermectin, and levamisole in anthelminthic action, as well as determining the mechanism of resistance of nematodes to each drug. The following sections will explore these different anthelmintics in relation to their mode of action in nematodes, and the mechanisms of resistance developed in populations of *H. contortus*.

## 1.3 Mechanisms of Resistance

The phenomenon of a population developing resistance to a certain drug can be simply explained as the survival of individuals who possess “resistance alleles”. Parasites that contain genes that allow them to be susceptible to a particular anthelmintic will not survive and therefore will be unable to pass on their genes to their offspring. Individuals containing anthelmintic resistant alleles will survive and pass on these characteristics to their offspring. Thus, those “resistance” genes are passed on through generations, resulting in a large population of parasites which are no longer affected by the particular anthelmintic. For *H. contortus*, it has been shown that there is a high amount of gene flow among populations, which is increased even more due to the commercial utilization of their host ruminants. The transport of sheep and goats all over the world contributes significantly to the genetic diversity among and between populations of *H. contortus* (Blouin et al. 1995). This high genetic variability in nematode DNA accounts for the increased resistance of parasitic nematodes to frequently used anthelmintics.

*H. contortus* is one of the most studied parasitic nematodes in relation to anthelmintic resistance because of its ability to develop resistance to all classes of anthelmintic drugs. Nematodes employ mechanisms of resistance in order to reduce their susceptibility to various anthelmintics. Resistance can develop as a result of a variety of molecular alterations including 1) genetic changes of a specific protein drug target, 2) changes in metabolism which promotes the removal of a drug/prevents drug activation, 3) changes in the abundance and relocation of a drug, and 4) overexpression of closely related drug targets which are

insensitive to the drug (Harder 2016). Much work focuses on the molecular changes developed within drug targets, which render drugs ineffective, as this accounts for the primary method of anthelmintic resistance in nematodes. Specific mechanisms of resistance related to each class of anthelmintic are described below.

### 1.3.1 Benzimidazoles

Thiabendazole, a member of the benzimidazole class, was the first drug developed to target parasitic nematodes in livestock (resulting in 95% removal) (Brown 1961). The mode of action of thiabendazole involves compromising the cytoskeleton of nematodes through its selective interactions with  $\beta$ -tubulin (Oxberry et al. 2001). However, it is very common for parasitic nematodes to develop resistance to anthelmintic drugs, and the resistance to benzimidazoles is one of the first examples of this. Thiabendazole resistance was first reported in field populations of *H. contortus* in the United States (Drudge et al. 1964), Australia (Le Jambre et al. 1976), and South Africa (Berger 1975). It was later found that a single point mutation of a phenylalanine (Phe) to a tyrosine (Tyr) residue at position 200 in the gene encoding  $\beta$ -tubulin was responsible for *H. contortus* resistance to benzimidazoles (Kwa et al. 1995). Similarly, another group later discovered that the same mutation of a Phe to a Tyr residue, this time at amino acid position 167, accounts for Benzimidazole resistance in populations of *H. contortus* (Prichard et al. 2000). Finally, it was found that a nearby point mutation of a glutamate (Glu) to an alanine (Ala) at amino acid position 198 also contributes to benzimidazole resistance in this parasite (Ghisi et al. 2007). These mutations appear to reduce the ability of benzimidazoles to bind to their target  $\beta$ -tubulin (Lacey and Prichard 1986).

### 1.3.2 Macrocyclic lactones

Many anthelmintics are designed to target the nervous system of nematodes, through the interaction with ligand-gated ion channel (LGIC) receptors, including glutamate receptors, gamma-aminobutyric acid (GABA) receptors, and nicotinic acetylcholine receptors (nAChRs). Ivermectin (IVM), belonging to the macrocyclic lactone class, was developed in 1981 in part due to the already wide spread nematode resistance to Benzimidazoles (Chabala et al. 1980). IVM elicits potent and persistent paralysis in nematodes through its interactions with glutamate-gated chloride channels (GluCl) (Cully et al. 1994). However, like Benzimidazoles, resistance to IVM in many parasite populations has developed. Resistance

to IVM has been reported in parasites which infect ruminant animals (Kaplan 2004), horses (Wolstenholme et al. 2004), domestic pets such as dogs (Bourguinat et al. 2015), and humans (Osei-Atweneboana et al. 2007). Specifically, early reports of IVM resistance were first identified in field populations of *H. contortus* located in South Africa (Carmichael et al. 1987), Brazil (Echevarria and Trindade 1989), the United States (Craig and Miller 1990), and Australia (Le Jambre 1993). Much of the research into the mechanism of IVM resistance in populations of *H. contortus* has focused on the role of p-glycoprotein drug efflux pumps. It has been found that polymorphisms in the p-glycoprotein genes from *H. contortus* is associated with IVM resistance (Blackhall et al. 1998).

### 1.3.3 nAChR agonists

Levamisole, pyrantel, and morantel comprise another class of potent anthelmintics that target nAChRs in nematodes. Cholinergic anthelmintics, such as levamisole, act as agonists of nAChRs located at neuromuscular junctions (NMJ), and results in the disruption of neuromuscular transmission (Aubry et al. 1970). Specifically, activation of these receptors by cholinergic anthelmintics causes spastic paralysis in the nematodes, resulting in their death (Wolstenholme et al. 2004). To date, there have been 5 levamisole-sensitive AChRs identified in *H. contortus*, including UNC-63, UNC-38, LEV-8, UNC-29, and LEV-1 (Boulin et al. 2011). However, similar to the other anthelmintics discussed, resistance to levamisole has developed among populations of *H. contortus*. The first reports of levamisole resistance in field populations of *H. contortus* in Australia was in 1981 (Green et al. 1981). Since these cholinergic anthelmintics all target nAChRs, resistance to levamisole appears to result in resistance to pyrantel and morantel as well (Wolstenholme et al. 2004). Levamisole-resistant populations of *H. contortus* have been linked to three different molecular changes found in these nematodes. The first molecular change involves the presence of truncated forms of two nAChR subunit genes, *unc-63* and *acr-8* (truncated versions annotated as *unc-63b* and *acr-8b*, respectively) (Neveu et al. 2007; Neveu et al. 2010; Martin et al. 2012). The second molecular change involves the reduced transcription of nAChR subunit genes in *H. contortus*, including *unc-29.3* and *unc-63* (Williamson et al. 2011). Further research showed many Levamisole resistant populations of *H. contortus* exhibit downregulation of multiple nAChR genes, including *unc-63a*, *unc-63b*, *unc-29.2*, *unc-29.4*, *unc-26*, and *acr-8a* (Sarai et al. 2014). The third molecular change in *H. contortus* linked to levamisole resistance is the downregulation and reduced expression of ancillary proteins involved in the assembly of nAChRs, including *unc-74*, *unc-50*, *ric-3.1*, and *ric-3.2* (Sarai et al. 2014).

#### 1.3.4 Amino-acetonitrile derivatives (ADDs)

In 2008 a new class of anthelmintics called amino-acetonitrile derivatives (ADDs) was discovered (Ducray et al. 2008). The new anthelmintic monepantel, a member belonging to the AAD class, came to the market in 2009 to mitigate parasitic infection in sheep. Monepantel acts as an agonist on the nAChR subunit ACR-23, causing hypertension of the body wall muscles of nematodes including *C. elegans* and *H. contortus* (Kaminsky and Rufener 2012). Unfortunately, the first incident of monepantel resistance in *H. contortus* species was found in Uruguay in 2014 only 5 years after the drug was introduced to the market (Mederos et al. 2014). Monepantel resistant *H. contortus* populations were later isolated from populations in the Netherlands (Van den Brom et al. 2015). The mechanism of monepantel resistance in field populations of *H. contortus* is still yet to be determined.

#### 1.4 Cys-loop Ligand-Gated Ion Channels

As mentioned earlier, many of the control mechanisms in place for the removal of parasite nematodes from host species involve the use of anthelmintics, which target LGICs. The Cys-loop (cysteine-loop) superfamily of LGICs are a major class of receptor-coupled ion channels. These channels contain five protein subunits, encoded by different subunit genes, all situated around a central aqueous pore. These protein subunits can all be of the same type, forming a homomeric channel, or they can be composed of different subunit types, forming a heteromeric channel. Each subunit contains an extracellular N-terminal domain, where two cysteine residues, situated 13 amino acid residues apart, form a disulfide bond. In addition, each subunit contains a ligand binding domain, four transmembrane domains (TM1-TM4), and extracellular C-terminus (Sine and Engel 2006) (Figure 1.2). The extracellular binding domain contains 6 binding loops, which are termed Loops A-F (Corringer et al. 2000).



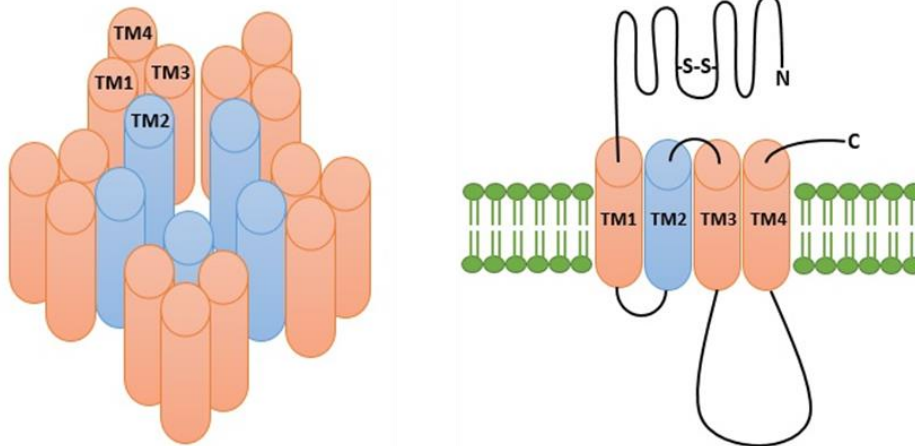


**Figure 1.2:** A) Outline of 5 receptor subunits coming together forming channel pore. B) Representation of one individual receptor subunit

Upon ligand binding, these channels elicit fast inhibitory or excitatory neurotransmission in the nematodes. In mammals, excitatory channels include nAChRs and the serotonin 5-hydroxytryptamine (5-HT<sub>3</sub>) receptors, and inhibitory channels include GABA and glycine receptors (Ortells and Lunt 1995). Excitatory channels allow for the flow of cations through the channel, whereas inhibitory channels allow for the flow of anions. Invertebrates, specifically parasitic and free-living nematodes, contain a variety of LGIC subunit types which are not found in vertebrates (Jones and Sattelle 2008). These channels have been shown to be gated by neurotransmitters including, GABA (Siddiqui et al. 2010), glutamate (Cully et al. 1994), tyramine (Pirri et al. 2009), acetylcholine (ACh) (Putrenko et al. 2005), and serotonin (Ranganathan et al. 2000).

#### 1.4.1 The Binding Site

The ligand binding site is located at the interface of two adjacent subunits which are termed the principle and complementary subunits. Specifically, the ligand binding region is between three polypeptide loops (loops A-C) on the principle subunit and three  $\beta$ -sheets (loops D-F) on the complementary subunit (Thompson et al. 2010). Each receptor has a different ligand-binding domain that contains various residues, which allow for the selection of different molecular agonists. Many neurotransmitters contain a cationic center that acts to stabilize the interaction between a cation (within the ligand) and the negative electrostatic potential on the face of the aromatic ring (within the binding pocket). These are known as

cation- $\pi$  interactions (Beene et al. 2002). It is understood that these cation-  $\pi$  interactions involve the aromatic amino acids present in the ligand binding region, including Phe, Tyr, and tryptophan (Trp) forming what is termed as the “aromatic box” (Dougherty 1996). When looking at 5-HT<sub>3A</sub> serotonin receptors, the Trp residue at position 183, which aligns with a similar Loop B Trp residue in the nAChR, binds the primary ammonium group on serotonin via cation-  $\pi$  interactions (Beene et al. 2002). In the *H. contortus* UNC-49 receptor, homology modelling suggests that there are two Tyr residues, Y166 (Loop B) and Y218 (Loop C), involved in  $\pi$ -cationic interactions with GABA (Accardi and Forrester 2011). Similarly, in the *Drosophila* RDL receptor the two aromatic residues that contribute to  $\pi$ -cationic interactions with GABA are F206 (Loop B) and Y254 (Loop C) (Lummis et al. 2011).

#### 1.4.2 The Channel Pore

The channel pore is created in the center of the five receptor subunits and is protected by a “gate” which opens to allow the flow of ions through the channel upon ligand binding. Each subunit is arranged with its M2  $\alpha$ -helices facing in toward the center of the pore (Miller and Smart 2010). In anion specific channels there is a proline-alanine-arginine (PAR) motif present at the beginning of the M2 domain, which allows for the selection of anions through the channel (Galzi et al. 1992). In order to confirm ion selectivity through a channel, a current-voltage test must be completed using two-electrode voltage clamp electrophysiology (TEVC). An anion channel, expressed in *Xenopus laevis* oocytes, in the presence of an external chloride concentration of 103.6 mM exhibits a reverse potential (Nernst potential) of -18.5 mV, assuming a 60 mM internal concentration of chloride in the oocyte (Kusano et al. 1982). When the external concentration of chloride is decreased to 62.5 mM, an anion channel exhibits a reverse potential (Nernst potential) which shifts to -5.7 mV. This rightward shift of potential is indicative of anion selectivity through the channel (Kusano et al. 1982).

### 1.5 Diversity of cys-loop ligand-gated chloride channel receptors in nematodes

There are many types of cys-loop receptors that have been identified in free-living and parasitic nematodes. In particular, the free-living nematode *C. elegans* possesses the most extensive number of cys-loop LGICs, which consists of 102 subunit-encoding genes (Jones and Sattelle 2008). These genes have been further divided into groups based on their sequence homology, including the groups EXP-1, AVR-14, UNC-49, GGR-1, GGR-3, LGC-45, MOD-1, and ACC-1 (Jones and Sattelle 2008). Currently, only some of the

subunits in these groups have been pharmacologically characterized, and thus sets the basis for my PhD work. Pharmacological characterization involves determining the ligands for each receptor group, and which concentration of the ligand is required for 50% of receptor activation ( $EC_{50}$ ).

The EXP-1 group consists of two genes, *exp-1* and *lgc-35*, which encode the protein subunits EXP-1 and LGC-35, respectively (Jones and Sattelle 2008). In *C. elegans*, the EXP-1 subunit forms a homomeric excitatory GABA-gated chloride channel that mediates muscle contraction in the gut. Specifically, the EXP-1 protein is localized to clusters at the neuromuscular junction (Beg and Jorgensen 2003). The LGC-35 subunit from *C. elegans* forms a homomeric excitatory GABA-gated chloride channel that mediates sphincter muscle contraction. LGC-35 localizes to a group of acetylcholine motor neurons in *C. elegans*, where it is involved in locomotor behavior in nematodes (Jobson et al. 2015). In regards to parasitic nematodes, homologues of both *exp-1* and *lgc-35* have been identified within the genome of *H. contortus* (Laing et al. 2013). However their localization and function in *H. contortus* is still unknown.

The AVR-14 group includes six genes, *avr-14*, *avr-15*, *glc-1*, *glc-2*, *lgc-3*, and *glc-4*, which encode glutamate-gated chloride channel receptor subunits AVR-14, -15, and GLC-1 – 4, respectively (Jones and Sattelle 2008). These channels have been shown to be the target of macrocyclic lactones, such as avermectin and milbemycin (Wolstenholme and Rogers 2006). The subunits AVR-15 and GLC-2 are located in pharyngeal muscle and are associated with pumping and feeding (Dent et al. 1997; Laughton et al. 1997). Similarly, AVR-14, -15, GLC-1 and -3 are involved in *C. elegans* locomotion (Cook et al. 2006). Homologues of all of the AVR-14 gene family members, with the absence of *glc-1*, have been identified in the parasitic nematode *H. contortus*. Interestingly, whole genome sequencing of *H. contortus*, identified two novel gene members, *hco-glc-5* and *hco-glc-6*, which are unique to *H. contortus*, and absent in *C. elegans* (Laing et al. 2013). Early research of the *avr-14* gene from *H. contortus* revealed that *avr-14* localizes to the nerve ring in nematodes and appears to be absent in pharyngeal and body wall muscle cells (Jagannathan et al. 1999).

The UNC-49 group consists of five receptor subunit genes, including *unc-49*, *lgc-36*, *lgc-37*, *lgc-38*, and *gab-1* (Jones and Sattelle 2008). Products of these genes form highly sensitive GABA-gated chloride channels (Bamber et al. 2003). Specifically, through alternative splicing the *unc-49* gene encodes three receptor subunits, UNC-49A, UNC-49B, and UNC-49C (Bamber et al. 1999). The UNC-49B and C subunits assemble to form a heteromeric channel that is highly sensitive to GABA. Similarly, these two subunits localize together at the neuromuscular junctions in *C. elegans*. Nematodes mediate inhibition of body wall muscle during locomotion through the action of UNC-49 GABA receptors (Bamber et al. 1999). This is why

the *unc-49* gene is termed after “uncoordinated” (UNC) behavior. Homologues of all five of the UNC-49 gene family members have been identified in the parasitic nematode *H. contortus* (Laing et al. 2013). Similar to what we see in *C. elegans*, the *unc-49* gene from *H. contortus* is alternatively spliced to form two unique UNC-49 receptors, UNC-49B and C (Siddiqui et al. 2010). Further characterization of the UNC-49 receptor from *H. contortus* has revealed a key difference between homologous receptors in *C. elegans*. Specifically, the UNC-49C receptor from *H. contortus* appears to be a positive modulator of GABA sensitivity in the UNC-49B/C heteromeric channel, whereas the UNC-49C receptor from *C. elegans* is a negative modulator of GABA sensitivity in the heteromeric channel (Bamber et al. 1999; Siddiqui et al. 2010).

The GGR-1 group consists of six subunit encoding genes, including *lgc-39*, *lgc-40*, *lgc-41*, *lgc-42*, *ggr-1*, and *ggr-2*, present in both *C. elegans* (Jones and Sattelle 2008) and *H. contortus* (Laing et al. 2013). Phylogenetic analysis suggests that members of the GGR-1 family are closely related to glycine and histamine receptors (Jones and Sattelle 2008). Of the members of the GGR-1 family, only LGC-40 has been partially characterized from *C. elegans*. LGC-40 forms a functional homomeric channel that responds to ligands choline, acetylcholine and serotonin, and is inhibited by nAChR antagonist d-tubocurarine (Ringstad et al. 2009). Apart from characterization of LGC-40 from *C. elegans*, very little is known about the other members of the GGR-1 family in free-living nematodes, and nothing is known in parasitic nematodes.

The GGR-3 group consists of six receptor subunits present in *C. elegans*, LGC-51, LGC-52, LGC-53, LGC-54, LGC-55, and GGR-3 (Jones and Sattelle 2008). Homologues to all of these gene family members, with the absence of LGC-54, have been identified in the parasitic nematode *H. contortus* (Laing et al. 2013). Sequence analysis of the GGR-3 family members from *C. elegans*, suggests that these subunits are likely to form anion-selective channels (Jones and Sattelle 2008). Initial characterization of LGC-53 and LGC-55 receptors from *C. elegans* revealed that they are activated by dopamine and tyramine, respectively (Ringstad et al. 2009; Pirri et al 2009). Finally, characterization of the GGR-3 subunit from *H. contortus* found that GGR-3 forms a homomeric channel, which is highly sensitive to the biogenic amine dopamine (Rao et al. 2009). Aside from this, little is known about other members of the GGR-3 family from *H. contortus*.

The MOD-1 family consists of two receptor subunit genes, including *mod-1* and *lgc-50* (Jones and Sattelle 2008). The *mod-1* gene encodes for a serotonin-gated chloride channel which is involved in locomotion in *C. elegans* (Ranganathan et al. 2000). Homologous genes of both *mod-1* and *lgc-50* have been identified

in the parasitic nematode *H. contortus* (Laing et al. 2013). Specifically, *mod-1* encodes a ligand-gated chloride channel. Molecular modelling and sequence analysis of the Hco-MOD-1 protein revealed that the Trp involved in  $\pi$ -cationic interactions with ligands is located in Loop C of the binding pocket (Beech et al. 2013). This is interesting because the  $\pi$ -cationic contributing Trp is present in Loop B of nAChRs and human 5HT<sub>3</sub> receptors (Beene et al. 2002). Pharmacological characterization of the MOD-1 protein from *H. contortus* has not yet been completed.

## 1.6 Cholinergic neurotransmission in nematodes

ACh is the major excitatory neurotransmitter present in the nervous systems of both free-living and parasitic nematodes (Seegerberg and Stretton 1993). ACh is located at the neuromuscular junctions in nematodes and is involved in motor functions (Duerr et al. 2008). Specifically, ACh is synthesized in organisms by the enzyme choline acetyltransferase (ChAT), and loaded into synaptic vesicles by the vesicular acetylcholine transporter (VAChT). ACh elicits a variety of biological responses through its interaction with nAChRs, G-protein linked muscarinic receptors (Lee et al. 1999; Lee et al. 2000), and ACh-gated chloride channels (Putrenko et al. 2005). The function of ACh in excitatory cholinergic neurotransmission is well understood, with two types existing. Rapid ACh-induced neurotransmission is mediated by nAChRs, whereas slow ACh-induced neurotransmission is mediated by muscarinic ACh receptors (Lee et al. 2000). It wasn't until early studies in the mollusk *Aplysia* (Kehoe and McIntosh 1998a), and subsequent research in the free-living nematode *C. elegans* (Putrenko et al. 2005), that a family of ACh-gated receptors that result in inhibitory neurotransmission were identified. These inhibitory ACh-gated chloride channels (ACCs) are only present in nematodes, and thus provide a prime target for anthelmintic development.

## 1.7 The ACC family

Until this work began, the only published reports of ACCs were from early studies from the mollusk *Aplysia*, which characterized these channels from neurons (Kehoe 1972a; Kehoe 1972b; Kehoe and McIntosh 1998a) and two studies from the Dent group of McGill University who identified these receptors in *C. elegans* (Putrenko et al. 2005; Wever et al 2015). Initial characterization in *Aplysia* neurons found a subset of ACh receptors that mediate inhibitory chloride-dependent cholinergic responses (Kehoe 1972b). The inhibitory ACh-induced response observed in *Aplysia* neurons is biphasic in nature, with both a short-

latency rapid response, and a long-latency slow response. In addition, the antagonists tubocurarine and strychnine inhibit the chloride-dependent inhibitory responses observed (Kehoe 1972a). Finally, further characterization using toxins that differentiate between types of nAChRs, indicated that two distinct Cl<sup>-</sup>-induced ACh receptors exist in *Aplysia* neurons, and the observed pharmacology suggests that one of these receptors strongly resembles the vertebrate  $\alpha$ -bungarotoxin-sensitive containing receptor (Kehoe and McIntosh 1998b).

Putrenko et al. (2005) went on to identify and characterize these inhibitory ACCs in nematodes. The ACC-1 family in *C. elegans* contains eight receptor subunit genes, *acc-1*, *-2*, *-3*, and *-4* and *lgc-46*, *-47*, *-48*, and *-49* (Putrenko et al. 2005; Jones and Sattelle 2008). Each gene encodes for a different protein receptor subunit. Of these, four subunits (ACC-1, -2, -3, and -4) have been characterized pharmacologically. The ACC-1, -2, and -3 receptors contain a PAR motif at the beginning of the TM2 domain, and thus indicate anion selectivity of these receptors. Moreover, current-voltage analysis of the ACC receptors proved that these channels allow for the passage of chloride ions upon activation (Putrenko et al. 2005). Pharmacological characterization of the ACC receptors from *C. elegans* showed that two receptor subunits, ACC-1 and ACC-2, form functional homomeric channels that are highly sensitive to ACh, with EC<sub>50</sub> values of 0.26 and 9.54  $\mu$ M respectively. The classic nAChR agonist, nicotine, is a poor agonist of the ACC channels, with less than 15% activation of the ACC-1 and ACC-2 channels observed when expressed in *X. laevis* oocytes. In addition, the human glycine receptor antagonist strychnine was shown to be an antagonist of the ACC-1 and ACC-2 channels, with IC<sub>50</sub> values of 4.6  $\mu$ M and 3.0  $\mu$ M, respectively. Similarly, atropine, an antagonist of nAChRs, also showed antagonism properties against the ACC-1 and ACC-2 receptors, with IC<sub>50</sub> values of 23  $\mu$ M and 6.6  $\mu$ M, respectively. Interestingly, atropine also proved to be an agonist of the ACC-2 channel, activating the receptor with an EC<sub>50</sub> of 873  $\mu$ M. However, atropine was unable to activate the ACC-1 receptor (Putrenko et al. 2005). This is interesting because this pharmacology shows us that the ACC receptors have a unique ligand binding site, unlike nAChRs.

Further pharmacological analysis revealed that the subunits ACC-3 and ACC-4 do not form homomeric channels. However, they are able to form heteromeric channels with ACC-1 and ACC-2. The heteromeric channel of ACC-1 and -3 is less sensitive to ACh, with an EC<sub>50</sub> value of 39.6  $\mu$ M (Putrenko et al. 2005). The co-expression of ACC-1 with ACC-4 does not appear to alter the maximal response of the ACC-1 receptor, indicating that these two receptors likely do not interact. In contrast, the presence of ACC-2 with either ACC-3 or ACC-4 appears to inhibit ACC-2 receptor function. Specifically, the co-expression of ACC-2 and ACC-3 resulted in a weakened response from the ACC-2 receptor, whereas the co-expression of ACC-2

with ACC-4 resulted in complete inhibition of ACC-2 receptor function. Inhibition of the ACC-2 receptor by ACC-3 or ACC-4 appears to be specific to ACC-2, as neither ACC-3 or ACC-4 showed inhibition of other receptors such as the GluCl AVR-15 (Putrenko et al. 2005).

Studies conducted by Wever and colleagues (2015) revealed that members of the ACC-1 family in *C. elegans*, ACC-1 and LGC-47, are strongly expressed in neurons innervating the ventral nerve cord. This is an important tissue involved in nematode locomotion, suggesting that these channels are good targets for anthelmintic development. Similarly, LGC-46 and ACC-4 are strongly expressed in cholinergic motor neurons, and specifically localize to presynaptic terminals on these neurons. Here, they are involved in synaptic vesicle release (Pereira et al. 2015; Takayanagi-Kiya et al. 2016). The localization of two ACC receptor subunits together, ACC-4 and LGC-46, suggests that these subunits may form unique heteromeric receptors in these nematodes. Electrophysiological characterization of combinations of subunits from the ACC-1 family could provide insight into which heteromers are likely to exist.

It is interesting to note that the sequence of the extracellular ligand binding site of the ACC's differs significantly from both nematode and vertebrate nAChRs. Specifically, the double cysteine residues in loop C of nAChRs, which are known to contribute to ligand binding, are absent in ACCs. This shows the ability for ACC receptors to bind ACh independently of the key nAChRs binding site residues. In addition, genes encoding ACC receptors appear to be absent in all vertebrate species, making them of particular interest to explore further (Putrenko et al. 2005).

To date, seven of the eight receptor subunit genes belonging to the ACC-1 family, with the absence of *lgc-48*, have been identified in *H. contortus* (Jones and Sattelle 2008; Laing et al. 2013), but have yet to be pharmacologically characterized. Further exploration into the ACC family in *H. contortus* could provide insight into inhibitory cholinergic neurotransmission in parasitic nematodes, and aid in the development of novel pharmaceuticals in the future. This sets the basis for my PhD research outlined to follow.

## 1.8 Goals and objectives

The overall goal of this thesis is to pharmacologically characterize the ACC-1 family of cys-loop receptors from the parasitic nematode *H. contortus*.

**Objective 1:** Clone the remaining members of the ACC-1 gene family: *acc-3*, *acc-4*, *lgc-46*, *lgc-47*, and *lgc-49*.

**Objective 2:** Conduct a comprehensive pharmacological characterization of the homomeric channels by expressing proteins in *Xenopus* oocytes and conducting two-electrode voltage clamp electrophysiology.

**Objective 3:** Determine and pharmacologically characterize unique heteromeric receptors by co-expressing various subunit combinations in *Xenopus* oocytes.

**Objective 4:** Characterize the binding site of the ACC receptors via site-directed mutagenesis and *in silico* homology modelling.



## Chapter II – Manuscript I

# Molecular and pharmacological characterization of an acetylcholine-gated chloride channel (ACC-2) from the parasitic nematode *Haemonchus contortus*

**Sarah A. Habibi**, Micah Callanan, and Sean G. Forrester

Published in:

International Journal for Parasitology: Drugs and Drug Resistance. 8(3): 518-525

DOI: [doi.org/10.1016/j.ijpddr.2018.09.004](https://doi.org/10.1016/j.ijpddr.2018.09.004)

## 2.0: Abstract

Nematode cys-loop ligand-gated ion channels (LGICs) have been shown to be attractive targets for the development of novel anti-parasitic drugs. The ACC-1 family of receptors are a unique group of acetylcholine-gated chloride channels present only in invertebrates, and sequence analysis suggests that they contain a novel binding site for acetylcholine. We have isolated a novel member of this family, Hco-ACC-2, from the parasitic nematode *Haemonchus contortus* and using site-directed mutagenesis, electrophysiology and molecular modelling examined how two aromatic amino acids in the binding site contributed to agonist recognition. It was found that instead of a tryptophan residue in binding loop B, which is essential for ligand binding in mammalian nAChRs, there is a phenylalanine (F200) in Hco-ACC-2. Amino acid changes at F200 to either a tyrosine or tryptophan were fairly well tolerated, where a F200Y mutation resulted in a channel hypersensitive to ACh and nicotine as well as other cholinergic agonists such as carbachol and methacholine. In addition, both pyrantel and levamisole were partial agonists at the wild-type receptor and like the other agonists showed an increase in sensitivity at F200Y. On the other hand, in Hco-ACC-2 there is a tryptophan residue at position 248 in loop C that appears to be essential for receptor function, as mutations to either phenylalanine or tyrosine resulted in a marked decrease in agonist sensitivity. Moreover, mutations that swapped the residues F200 and W248 (ie. F200W/W248F) produced non-functional receptors. Overall, Hco-ACC-2 appears to have a novel cholinergic binding site that could have implications for the design of specific anthelmintics that target this family of receptors in parasitic nematodes.

## 2.1: Introduction

The Cys-loop (cysteine-loop) superfamily of ligand-gated ion channels (LGICs) is a major class of receptor-coupled ion channels. These channels have been widely studied in invertebrate organisms for decades because they play key roles in the nervous system, making them prime targets for insecticides and nematocides (Del Castillo et al., 1963). The channel contains five protein subunits, encoded by the same or different subunit genes, all situated around a central aqueous pore. Each subunit contains an extracellular N-terminal ligand binding domain, where two cysteine residues, situated 13 amino acid residues apart, form a disulfide bond, as well as four transmembrane domains (TM1-TM4), and an

extracellular C-terminus. These subunits can assemble as homo-oligomers, containing one subunit type, or hetero-oligomers, containing multiple subunit types (Sine and Engel, 2006).

Upon ligand binding, these channels elicit fast inhibitory or excitatory neurotransmission. In mammals, excitatory channels include nicotinic acetylcholine receptors (nAChRs) and 5-hydroxytryptamine (5-HT<sub>3</sub>) serotonin receptors, and inhibitory channels include gamma-aminobutyric acid (GABA) and glycine receptors (Ortells and Lunt, 1995). Invertebrates, specifically parasitic and free-living nematodes, contain a variety of LGIC subunit types which are not found in vertebrates (Jones and Sattelle, 2008). These channels have been shown to be gated by neurotransmitters including GABA (Bamber et al., 1999; Siddiqui et al., 2010), glutamate (Cully et al., 1994), tyramine (Pirri et al., 2009), acetylcholine (ACh) (Putrenko et al., 2005), and serotonin (Ranganathan et al., 2000).

The ligand-binding site of cys-loop receptors is located at the interface of two adjacent subunits, which are loops A-C on the principal subunit and loops D-G on the complementary subunit (Hibbs and Gouaux, 2011). Each receptor has a different ligand-binding domain that contain various residues, which allows for the selection of different molecular agonists. There are key aromatic residues in the binding site of LGICs that have been shown to be involved in ligand binding (Beene et al., 2004). Many neurotransmitters contain a cationic center that acts to stabilize the interaction between a cation and the negative electrostatic potential on the face of the aromatic ring. This is known as cation- $\pi$  interactions (Beene et al., 2002). These cation- $\pi$  interactions involve aromatic amino acids (either phenylalanine, tyrosine, or tryptophan) in the ligand binding region (Dougherty, 1996). While the importance of aromatic residues for the function of the agonist binding pocket is widely shared across the phyla, there is variability across different receptors with respect to the type of aromatic residues that contribute to binding and their location within the binding loops (Lynagh and Pless, 2014). This highlights the promiscuous nature of neurotransmitter binding across a variety of receptors in animals.

Early studies from the mollusk, *Aplysia*, reported the presence of a unique class of acetylcholine receptors in neurons, the acetylcholine-gated chloride channels (ACCs) (Kehoe and McIntosh, 1998). Later, studies identified these receptors in the model nematode *Caenorhabditis elegans* (Putrenko et al., 2005; Wever et al., 2015). In *C. elegans* the ACC-1 family is made up of eight receptor subunit genes, *acc-1*, *-2*, *-3*, and *-4*, and *lgc-46*, *-47*, *-48*, and *-49* (Jones and Sattelle, 2008). The sheep parasite, *Haemonchus contortus*, contains homologues for seven of the ACC-1 gene members, with the absence of *lgc-48* (Laing et al., 2013).

As a whole, this family of receptors has potential to be novel antiparasitic drug targets. This is primarily due to the fact that they appear to be expressed in tissues that are sensitive to anthelmintic action, and as sequence analysis suggests, they are not present in mammals and exhibit a unique acetylcholine binding site (Putrenko et al., 2005; Wever et al., 2015). However, the structural components that are important for agonist recognition of this class of cholinergic receptors has not been explored.

Here we have isolated a novel member of the ACC-1 family (Hco-ACC-2) from the parasitic nematode *H. contortus* and investigated the binding site through site-directed mutagenesis and pharmacological analysis. Several introduced point mutations that changed key aromatic residues at the binding site revealed some interesting pharmacological properties. Molecular modelling was used to visualize the structure of the binding pocket and the interaction of key residues with a variety of agonists.

## 2.2: Methods

### 2.2.1: Isolation of *hco-acc-2*

*H. contortus* was received from Dr. Prichard (Institute of Parasitology, McGill University). Total RNA was extracted from adult male *H. contortus* using Trizol (Invitrogen, Carlsbad, USA). Complementary DNA (cDNA) was synthesized using the Quantitect Reverse Transcriptase kit from Qiagen (Dusseldorf, Germany), using a unique 3' oligo-dT anchor primer sequence (5'CCTCTGAAGGTTACGGATCCACATCTAGATTTTTTTTTTTTTTTTTVN3'); [where V is either A, C, or G and N is either A, C, G, or T] (Weston et al., 1999). Gene specific primers were generated based on a partial sequence provided by Dr. Robin Beech (McGill University) as part of the genome sequencing project for *H. contortus* (Laing et al., 2013). The original sequence appeared to contain the full 3' end of the gene but was missing the 5' region that would include the signal peptide cleavage site. The 5' end of the gene was isolated using the 5' rapid amplification of cDNA ends (RACE) protocol (Frohman et al., 1988). Two internal primers were used for the amplification of the 5' end along with a primer specific for the splice-leader 1 sequence (SL1-5'-GGTTTAATTACCCAAGTTTGAG-3') (Van Doren and Hirsh, 1988). The resulting amplicon of predicted size was isolated via a QIAquick Gel Extraction Kit (Qiagen, Dusseldorf, Germany) and sub-cloned into the pGEMT easy™ sequencing vector and was sequenced at Genome Quebec. Amplification of the complete *hco-acc-2* gene was carried out using primers specific to the 5' and 3' end of the gene

with the XbaI and BamHI restriction sites and was subsequently cloned into the pGEMHE *Xenopus* expression vector (Zhang et al., 2008). All sequence alignments were produced using ClustalW.

### 2.2.2: Site-directed mutagenesis

The coding sequence of Hco-ACC-2 was sub-cloned into the pGEMHE transcription vector (3022 bp). The introduction of mutations in the Hco-ACC-2 coding sequence was performed using the QuikChange® II Site-Directed Mutagenesis Kit (Agilent Technologies). The primers carrying the specific mutation were generated using QuikChange Primer Design software from Agilent Technologies (QuikChange Primer Design). Five ACC-2 mutants were generated: F200Y, F200W, W248Y, W248F, and F200W/W248F. Point-mutations were confirmed using sequence analysis (Genome Quebec).

### 2.2.3: Expression in *Xenopus laevis* oocytes

All animal procedures followed the University of Ontario Institute of Technology Animal Care Committee and the Canadian Council on Animal Care guidelines. Expression of channels in oocytes was conducted as outlined in Abdelmassih et al. (2018). Female *Xenopus laevis* frogs were supplied by Nasco (Fort Atkinson, WI, USA). All frogs were housed in a climate controlled room (18 °C) with constant light cycling. Frogs were fed and tanks were cleaned regularly. Frogs were anesthetized with 0.15% 3-aminobenzoic acid ethyl ester methanesulphonate salt (MS-222) buffered with NaHCO<sub>3</sub> to pH 7 (Sigma-Aldrich, Oakville, ON, CA). Surgical removal of a section of the ovary of the frog was performed, and the lobe was defolliculated with a calcium-free oocyte Ringer's solution (82 mM NaCl, 2 mM KCl, 1 mM MgCl<sub>2</sub>, 5 mM HEPES pH 7.5 (Sigma-Aldrich)) (OR-2) containing 2 mg·mL<sup>-1</sup> collagenase-II (Sigma-Aldrich). The oocytes in the defolliculation solution were incubated at room temperature for 2 h. Collagenase was washed from the oocytes with ND96 solution (1.8 mM CaCl<sub>2</sub>, 96 mM NaCl, 2 mM KCl, 1 mM MgCl<sub>2</sub>, 5 mM HEPES pH 7.5) and allowed one hour to recover at 18 °C in ND96 supplemented with 275 µg·mL<sup>-1</sup> pyruvic acid (Sigma-Aldrich) and 100 µg·mL<sup>-1</sup> of the antibiotic gentamycin (Sigma-Aldrich) (Supplemented ND96). Stage V and VI oocytes were selected for cytoplasmic injection of cRNA.

The pGEMHE vector containing the *hco-acc-2* coding sequence was linearized using the restriction enzyme PstI (New England Biolabs, USA), and used as template for an in vitro transcription reaction (T7 mMessage mMachine kit, Ambion, Austin, TX, USA) yielding *hco-acc-2* copy RNA. *X. laevis* oocytes were injected with

50 nl of *hco-acc-2* ( $0.5 \text{ ng}\cdot\text{nL}^{-1}$ ) using the Drummond (Broomall, PA, USA) Nanoject microinjector. The expression of *hco-acc-2* required the co-injection with the copy RNA encoding three accessory proteins, *unc-50*, *unc-74*, and *ric-3.1* (Boulin et al., 2011) which were gifts from Dr. Cédric Neveu (INRA). The injected oocytes were incubated at 18 °C in supplemented ND96 solution. Electrophysiological recordings of the oocytes were conducted between 48 and 72 h after cRNA injection.

#### 2.2.4: Electrophysiological recordings

Two-electrode voltage clamp electrophysiology was conducted using the Axoclamp 900A voltage clamp (Molecular Devices, Sunnyvale, CA, USA). Glass electrodes were produced using a P-97 Micropipette Puller (Sutter Instrument Co., Novato, CA, USA). The electrodes were backfilled with 3 M KCl and contained Ag|AgCl wires. The following molecules were first dissolved in ND96; Acetylcholine (ACh), Choline Chloride (Choline), Carbamoylcholine Chloride (Carbachol), Acetyl- $\beta$ -methylcholine Chloride (Methacholine), Carbamyl- $\beta$ -methylcholine chloride (Urecholine) [Sigma Aldrich], Levamisole Hydrochloride (Levamisole), and Pyrantel Citrate Salt (Pyrantel) [Santa Cruz Biotechnology]. These solutions were perfused over oocytes using the RC-1Z recording chamber (Warner Instruments Inc., Hamdan, CT, USA). Data was analyzed using Clampex Software v10.2 (Molecular Devices) and all graphs were generated using Graphpad Prism Software v5.0 (San Diego, CA, USA). EC<sub>50</sub> values were determined by dose response curves that had been fitted to the following equation:

$$I_{max} = \frac{1}{1 + \left(\frac{EC_{50}}{[D]}\right)^h}$$

Where  $I_{max}$  is the maximal response, EC<sub>50</sub> is the concentration of compound required to elicit 50% of the maximal response, [D] is compound concentration, and  $h$  is the Hill coefficient. Both EC<sub>50</sub> and  $h$  are free parameters, and the curves were normalized to the estimated  $I_{max}$  using 250  $\mu\text{M}$  ACh. Graphpad Prism used the equation to fit a sigmoidal curve of variable slopes to the data. Means were determined from at least 5 oocytes from at least two batches of frogs. Significant differences between EC<sub>50</sub> values comparing WT to mutants was performed using Student's T-test with the Bonferroni correction. P-values  $\leq 0.01$  were considered significant.

Current-voltage relationships were recorded by changing the holding potential from  $-60$  mV to  $40$  mV in  $20$  mV increments. At each step the oocyte was exposed to a  $250$   $\mu$ M concentration of ACh. For reduced  $\text{Cl}^-$  trials, NaCl was partially replaced by Na-gluconate (Sigma) in the ND96 buffer solution, for a final  $\text{Cl}^-$  concentration of  $62.5$  mM. Current-voltage graphs were generated using Graphpad Prism Software v5.0 (San Diego, CA, USA).

### 2.2.5: Homology modeling

The template used was the *Danio rerio* alpha-1 glycine receptor (3JAD) which showed the highest homology to Hco-ACC-2. The protein coding sequence of Hco-ACC-2 was aligned to template using SWISS-MODEL which was used in MODELLER v9.15 (Šali and Blundell, 1993) for the generation of the Hco-ACC-2 homodimer. The associated DOPE and molpdf scores determined the most energetically favorable model. The final model chosen was visually inspected to ensure the binding loops were in the proper positions. Visual inspection included assessing that non-aligned sequences were absent, binding loops were in the appropriate location compared to previously crystallized receptors, and four transmembrane domains were present. Preparation of the homodimer for agonist docking was carried out using AutoDock Tools. Ligands including ACh and all of the molecules mentioned were obtained from the Zinc database in their energy-reduced extended form. AutoDock Vina was used to simulate docking of each ligand to the homodimers (Trott and Olson, 2010). Pymol was used to visualize the protein homodimer with its associated ligands, and Chimera v1.6.1 (Pettersen et al., 2004) was used to determine the distance between amino acid residues and ligand.

## 2.3: Results

### 2.3.1: Isolation of *hco-acc-2*

The full-length coding sequence of the *hco-acc-2* gene consisted of  $1332$  nucleotides (GenBank Accession # KC918364.1). When viewed in the appropriate reading frame, the sequence encodes a protein containing  $443$  amino acids (AHM25234.1). The protein sequence contains a signal peptide cleavage site (Signal P; <http://www.cbs.dtu.dk/services/SignalP/>), all seven extracellular binding loops, four transmembrane domains, and the hallmark Cys-loop motif (Fig. 2.1). The Hco-ACC-2 protein sequences

shares 88% sequence similarity to the *Cel-ACC-2* protein (Fig. 2.1). The PAR motif present at the beginning of the transmembrane 2 domain indicates anion selectivity through the channel (Jensen et al., 2002).

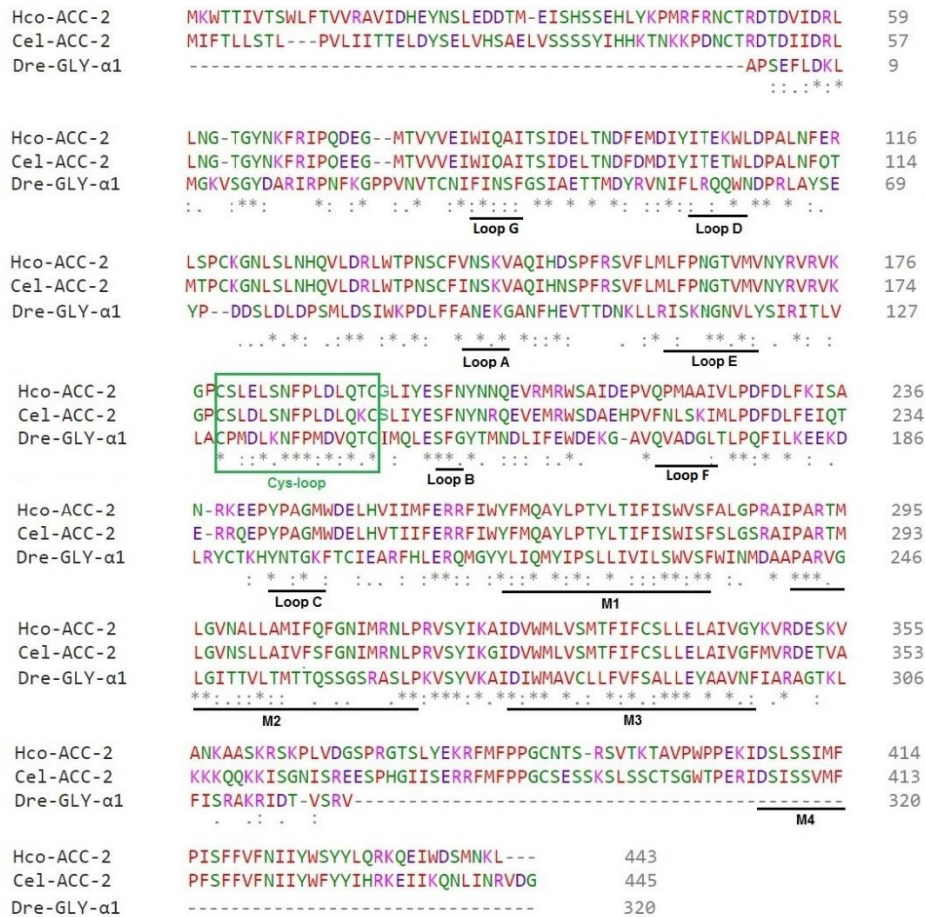


**Figure 2.1:** Protein sequence alignment of the *H. contortus* Hco-ACC-2 receptor with *C. elegans* Cel-ACC-2 and *D. rerio* Dre-GLY-α1 receptors. All seven binding loops (Loop A-G), the characteristic cysteine residues that form the “cys-loop”, and four transmembrane domains (M1-M4) and highlighted with underlines. (\*) indicates identity and (:) indicates similarity.

### 2.3.2: Expression of *hco-acc-2* in *Xenopus* oocytes

Injection of *hco-acc-2* cRNA alone did not result in ACh-sensitive channels. However, the injection of *X. laevis* oocytes with cRNA encoding *hco-acc-2*, and the accessory proteins, *hco-unc-74*, *hco-unc-50*, and



*hco-ric-3.1*, resulted in a homomeric ACC-2 channel that was highly sensitive to ACh. ACh currents were in  $\mu\text{A}$  range, dose-dependent and desensitizing and were consistent in multiple oocytes from several frogs (Fig. 2.2A and B). In addition, current-voltage analysis of the Hco-ACC-2 channel was conducted to confirm anion selectivity through the channel. A full  $\text{Cl}^-$  concentration of ND96 (103.6 mM  $\text{Cl}^-$ ) indicated a reverse potential of  $-17.44 \pm 5 \text{ mV}$  ( $n = 4$ ). This is consistent with the calculated Nernst potential for  $\text{Cl}^-$  of  $-18.5 \text{ mV}$ , when assuming an internal  $\text{Cl}^-$  concentration of 50 mM (Kusano et al., 1982). When NaCl was partially replaced with Na-gluconate (final  $\text{Cl}^-$  concentration of 62.5 mM) the reverse potential shifted to  $-3.4 \pm 2 \text{ mV}$  ( $n = 4$ ), which is also consistent with the assumed Nernst potential of  $-5.7 \text{ mV}$  (Fig. 2.2B).

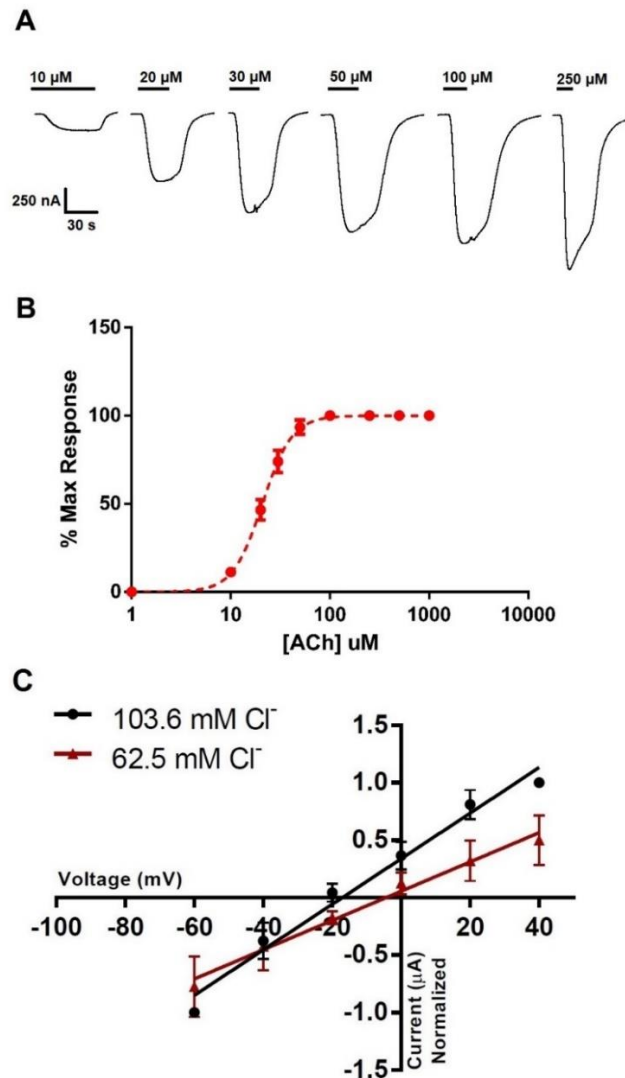


**Figure 2.2:** Hco-ACC-2 is an acetylcholine-gated chloride channel. (A) Electrophysiological response of Hco-ACC-2 to increasing concentrations of ACh. (B) Dose-response curve for acetylcholine on the Hco-ACC-2 channel. Standard errors are shown.  $n = 7$  oocytes (C) Current-voltage analysis of the Hco-ACC-2 channel using 103.6 mM  $\text{Cl}^-$  and 62.5 mM  $\text{Cl}^-$  in ND96 buffer solution. Acetylcholine response were generated using a maximum wild-type ligand saturation concentration of 250  $\mu\text{M}$ . Standard errors are shown.

### 2.3.3: Pharmacological analysis

Several cholinergic agonists and anthelmintics were examined. The EC<sub>50</sub> value for ACh was 21 ± 0.7 μM (n = 7). The ACh analogue carbachol had an EC<sub>50</sub> of 43 ± 3.6 μM (n = 6). Other ACh derivatives, including methacholine, urecholine, and choline also activated the channel with EC<sub>50</sub> values of 100 ± 2 μM (n = 6), 747 ± 22 μM (n = 10), and 1276 ± 35 μM (n = 7), respectively. Currently used anthelmintics such as pyrantel and levamisole were partial agonists for the receptor with EC<sub>50</sub> values of 72 ± 4 μM (n = 6) and 98 ± 4 μM (n = 6) respectively. All pharmacological data is represented in Fig. 2.3. The compounds that showed to be full agonists were ACh and methacholine. All other compounds tested appeared to be partial agonists of the channel (Fig. 2.3).

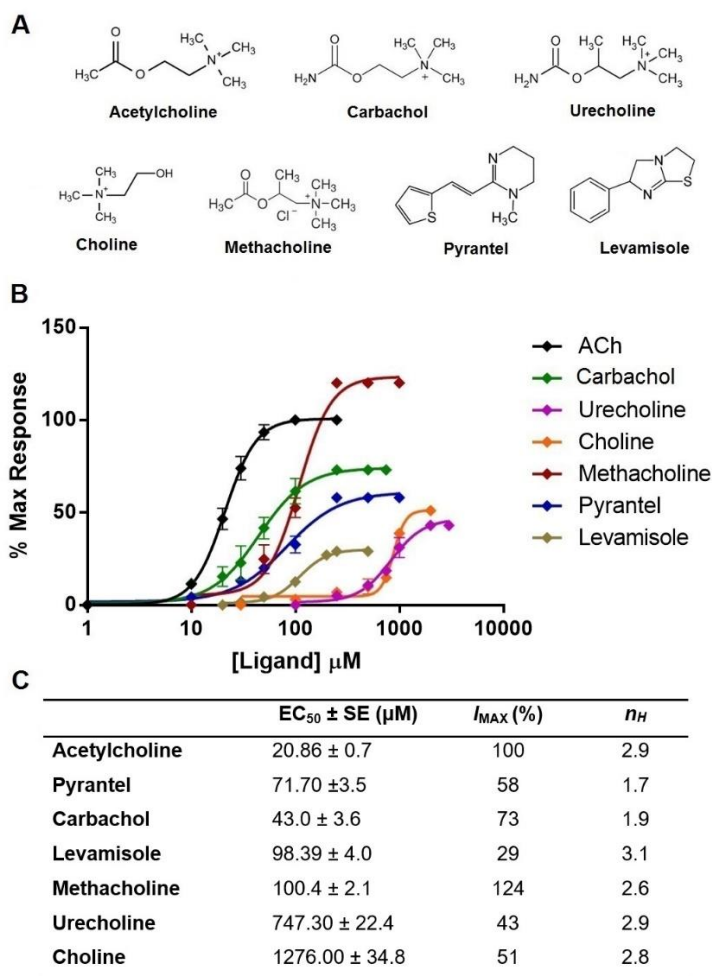
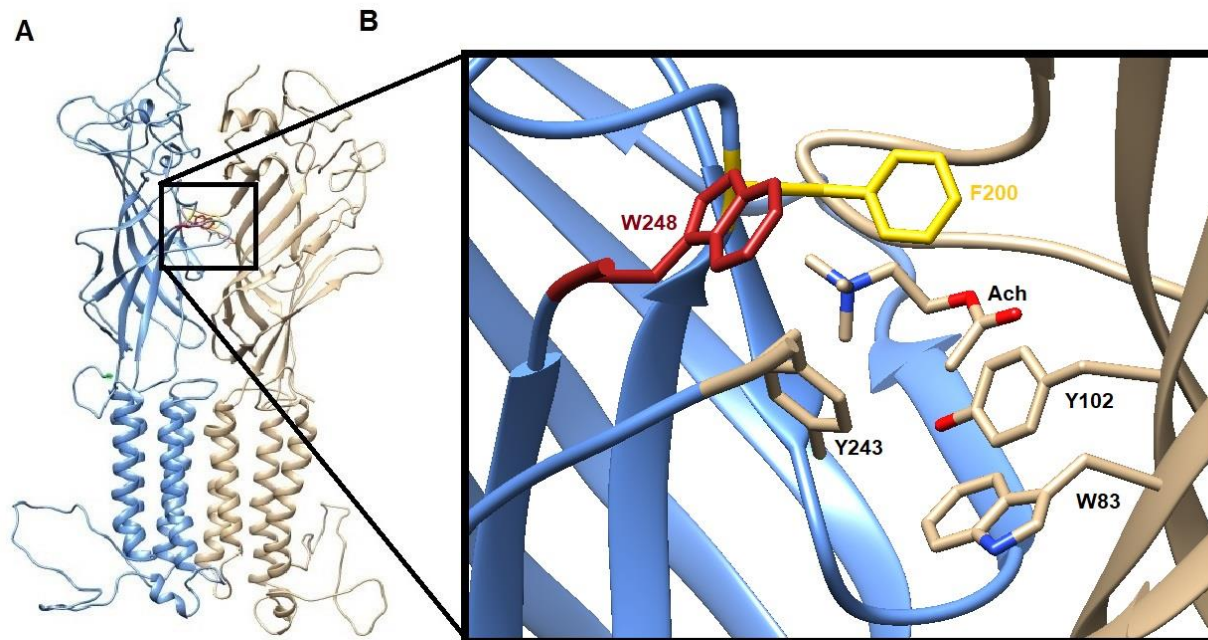


**Figure 2.3:** Pharmacology of Hco-ACC-2 (A) Chemical structures for the various molecular agonists used for the characterization of the Hco-ACC-2 binding site. (B) Dose-response curves for each of the listed compounds against the wild-type Hco-ACC-2 channel. Each curve is represented as a percent of the maximum acetylcholine response (250 μM). Partial agonists are those that have a maximum response lower than 100%. (C) Summary of the EC<sub>50</sub> values ± standard error for each compound listed from most sensitive to least. I<sub>max</sub> represents the maximal current response for each agonist.

### 2.3.4: Homology modelling

In order to visualize the interaction of agonists with residues in the binding pocket, a homology model was generated for the Hco-ACC-2 dimer using the *D. rerio* glycine receptor 3JAD as template which exhibited the highest sequence similarity with Hco-ACC-2. The model chosen, with the lowest DOPE score, is outlined in Fig. 2.4A. Cys-loop receptors are known to contain an aromatic box in the binding site. The binding site on the primary and complementary subunits appear to be composed of several aromatic residues. Based on sequence alignment of the Hco-ACC-2 protein with the mammalian nAChR, two aromatic residues in binding loops B and C appear to be swapped. The residues that appeared to interact with all agonists were phenylalanine 200 (F200) in loop B, and tryptophan 248 (W248) in loop C. The quaternary amine group in ACh was situated between 4.7 Å and 5.7 Å away from W248 and F200 respectively (Fig. 2.4, Fig. 2.5A). The quaternary amine of other molecules such as carbachol, methacholine and urecholine also docked at a similar distance from the two aromatic residues (Fig. 2.5B, C and D). Partial agonists such as carbachol and urecholine docked in a bent formation (Fig. 2.5C and D). The anthelmintics levamisole and pyrantel also docked with their quaternary amine close to W248 (Fig. 2.5E and F). In addition, an asparagine residue (N170) in loop E is also present within the binding pocket, and its hydroxyl group is located 3 Å from the carbonyl oxygen in ACh. The equivalent position in the nAChR is L121 ( $\beta$ 2 subunit) (Morales-Perez et al., 2016) which highlights another potential difference in the agonist binding site between ACCs and nAChRs. Methacholine which is also a full agonist docked in a similar orientation as ACh with its carbonyl oxygen within 3 Å from the NH<sub>2</sub> group of N170 (Fig. 2.5B). Since all agonists appear to dock with their quaternary amine between F200 and W248, these two residues were chosen for further analysis.



C	Loop B					Loop C				
			200					248		
Hco-Acc-2	E	S	<b>F</b>	N	Y	G	M	<b>W</b>	D	E
Cel-ACC-2	E	S	<b>F</b>	N	Y	G	M	<b>W</b>	D	E
Cel-Deg-3	S	S	<b>W</b>	T	N	E	P	<b>W</b>	V	I
nAChR (human)	G	S	<b>W</b>	T	Y	E	I	<b>Y</b>	P	D
			*					*		

**Figure 2.4:** (A) Homology model of Hco-ACC-2 homodimer. The principal and complementary subunits are represented by blue and beige respectively. (B) View of the Hco-ACC-2 binding pocket with acetylcholine docked. Key aromatic residues explored in this study, phenylalanine 200 (yellow) and tryptophan 248 (red) are highlighted. Other aromatic residues that may contribute to the binding site are also indicated. A portion of Loop C is removed from the image for clarity. (C) Protein alignment of the residues found in loop B and C of the Hco-ACC-2 with Cel-ACC-2, Cel-DEG-3 (GenBank accession # CAA98507.1), and the mammalian nAChR. \* indicates the residue position for mutational analysis. (For interpretation of the references to colour in this figure legend, the reader is referred to the Web version of this article.)

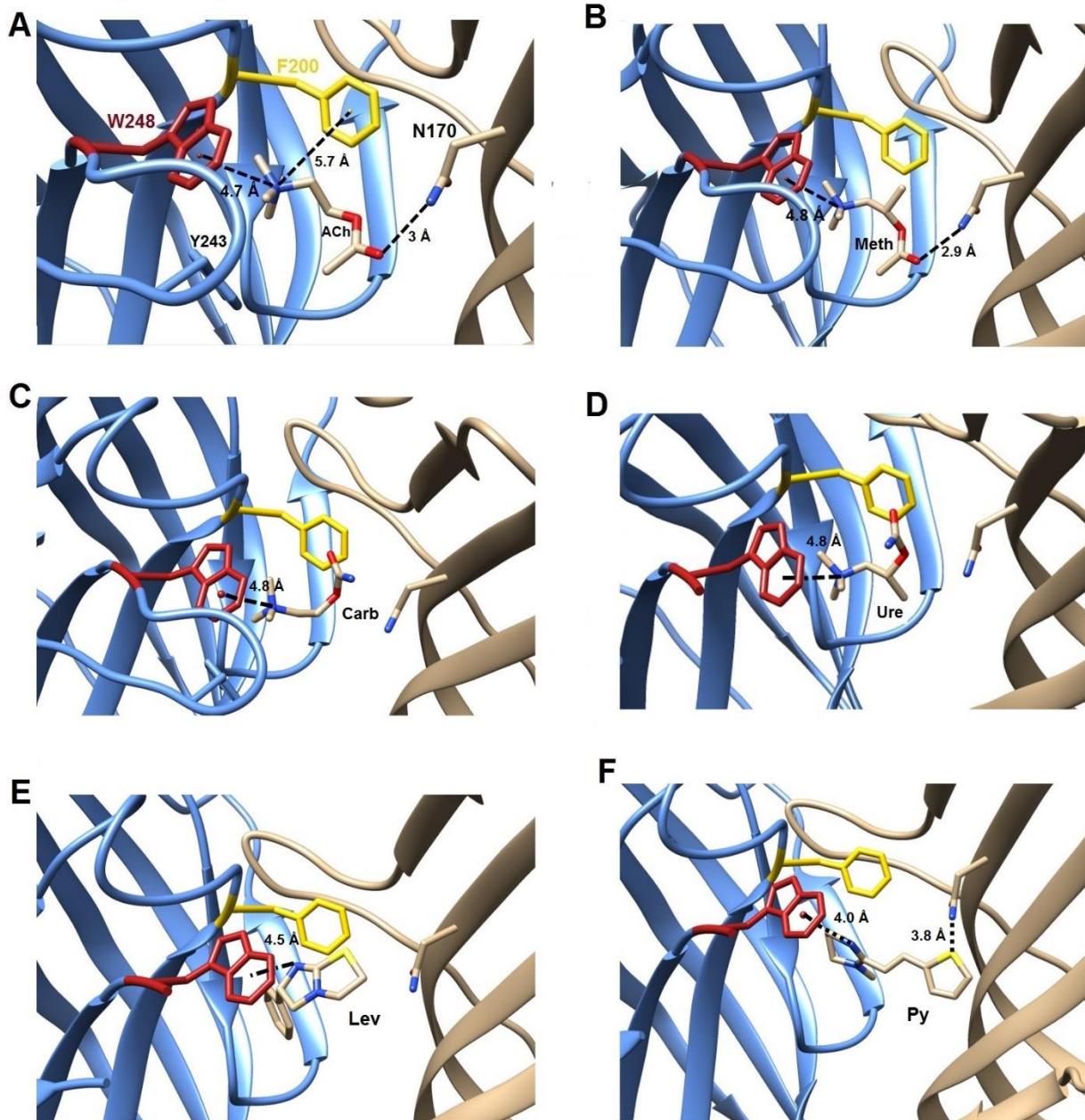


**Figure 2.5:** Homology models of Hco-ACC-2 with docked agonists. (A) Acetylcholine (ACh) docked in the binding pocket of the Hco-ACC-2 receptor. Distance between the quaternary amine in ACh with W248 (4.7 Å) and F200 (5.7 Å) are represented by a dotted line and measured in angstroms (Å). Distance between N170 in loop E to the carbonyl oxygen in ACh (3 Å) is also shown.

(B) Methacholine (Meth) docked in the Hco-ACC-2 binding pocket. W248 is 4.8 Å away from the quaternary amine of methacholine. N170 is 2.9 Å away from the carbonyl oxygen in methacholine. (C) Carbachol (Carb) docked in the Hco-ACC-2 binding pocket. W248 is 4.8 Å away from the quaternary amine in carbachol. (D) Urecholine (Ure) docked in the Hco-ACC-2 binding pocket. W248 is 4.8 Å away from the quaternary amine in urecholine. (E) Levamisole (Lev) docked in the Hco-ACC-2 binding pocket. (F) Pyrantel (Py) docked in the Hco-ACC-2 binding pocket.

### 2.3.5: Mutational analysis

Five Hco-ACC-2 mutants were generated, including F200Y, F200W, W248Y, W248F, and F200W/W248F swap. When the phenylalanine (Phe) at position 200 was replaced with a tyrosine (Tyr) residue, the resulting channel became significantly more sensitive to ACh compared to wild-type (Fig. 2.6A). The EC<sub>50</sub> of the F200Y channel was  $3 \pm 0.1 \mu\text{M}$  ( $n = 5$ ) (Fig. 2.6B). The mutation of the Phe in loop B to a tryptophan (Trp) resulted in a channel that was slightly less sensitive to ACh, with an EC<sub>50</sub> value of  $72 \pm 4 \mu\text{M}$  ( $n = 5$ ) (Fig. 2.6B). Replacement of Trp at position 248 had a much larger negative impact on the channel, with EC<sub>50</sub> values for ACh of  $7854 \pm 275 \mu\text{M}$  ( $n = 5$ ) and  $5600 \pm 1258 \mu\text{M}$  ( $n = 6$ ) for W248Y and W248F, respectively (Fig. 2.6B). These two mutants did not respond to any of the other compounds at the concentrations tested. The double swap mutation (F200W/W248F) resulted in a channel that was no longer responsive to ACh nor the other compounds (Table 2.1).

Both the F200Y and F200W single mutants were further characterized using the other agonists listed in Fig. 2.3A. The F200Y mutation was up to 9-fold more sensitive to all compounds listed, whereas the F200W mutation was up to 7-fold less sensitive (Fig. 2.7). It appears that both ACh and urecholine were most affected by the F200Y mutation whereas methacholine was most affected by F200W. On the other hand, the sensitivity of the anthelmintic pyrantel was only minimally affected by the two mutations. The resulting EC<sub>50</sub> values for each compound is outlined in Table 2.1. The two Trp mutants, W248Y and W248F, did not respond to any of the other agonists (Table 2.1). Similarly the double mutant F200W/W248F did not respond to any of the agonists tested (Table 2.1).

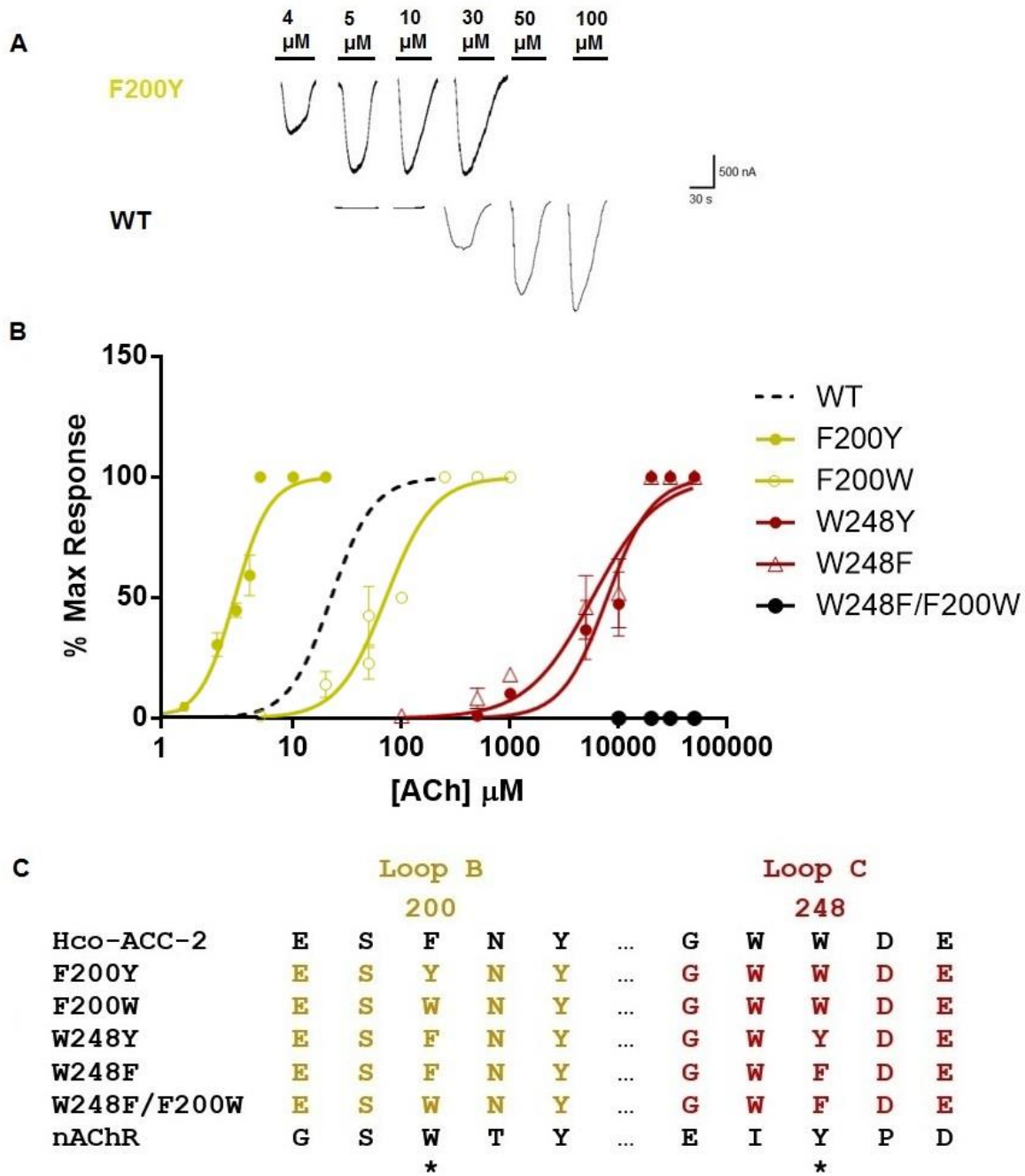


**Figure 2.6:** Impact of mutations at key aromatic residues (A) Electrophysiological traces of the F200Y mutant compared to Hco-ACC-2 wild-type. (B) Dose-response curves for the WT and each of the mutated channels with acetylcholine. Loop B and C mutants are represented by yellow and red respectively. (C) Protein alignment of Loop B and C in the Hco-ACC-2 receptor for each of the generated mutants. \* indicates the location of mutational analysis. (For interpretation of the references to colour in this figure legend, the reader is referred to the Web version of this article.)

**Table 2.1:** Summary of EC<sub>50</sub> values ± standard error for each channel with all of the compounds listed. N.R\*\* indicates the channel did not respond to concentrations of indicated compound at concentrations ≥1 mM which is a concentration that elicited a maximal response on the WT channel. N.R\* indicated that the channel did not respond to concentration up to 20 mM. n ≥ 5 oocytes. NR = no response; ND = not determined. \*indicates significant difference compared to WT (P < 0.01). \*\*indicates significant difference compared to WT (P < 0.001). NOTE: For each molecule (row), statistical analysis compared EC<sub>50</sub> values between WT and each mutant.

	EC <sub>50</sub> Value ± Standard Error (μM) [% MAX Response]					
	WT	F200Y	F200W	W248Y	W248F	SWAP
Acetylcholine	21 ± 0.7	2.9 ± 0.1	61 ± 4	7854 ± 275	5600 ± 1258	N.R*
Carbachol	50 ± 3.6	9.7 ± 0.5	67 ± 4	N.R**	N.R**	N.R*
Choline	1276 ± 35	650 ± 13	4771 ± 543	N.R**	N.R**	N.R*
Methacholine	100 ± 2	20 ± 0.6	644 ± 84	N.R**	N.R**	N.R*
Urecholine	747 ± 22	81 ± 3	2151 ± 215	N.R**	N.R**	N.R*
Levamisole	98 ± 4	39 ± 3	N.D	N.R**	N.R**	N.R*
Pyrantel	72 ± 4	44 ± 2	160 ± 20	N.R**	N.R**	N.R*

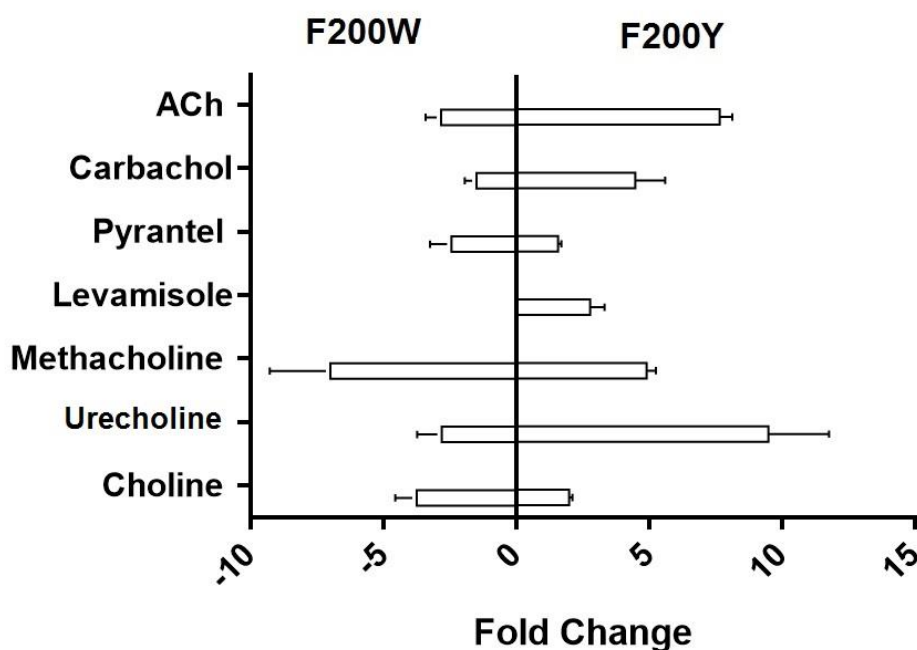


**Figure 2.7:** Mutations at F200 have varying effects on agonist sensitivity. Fold changes in EC<sub>50</sub> for the loop B mutants (F200Y and F200W) against all of the compounds listed. A positive fold change represents the channel becoming more sensitive to that compound, whereas a negative fold change represents the channel becoming less sensitive.



### 2.3.6: Nicotine activates Hco-ACC-2 F200Y

The Hco-ACC-2 WT channel responded to nicotine at concentrations above 500  $\mu\text{M}$ . It should be noted that some un-injected oocytes showed a small increase in current when exposed to 500  $\mu\text{M}$  nicotine (Data not shown). Therefore, while we believe that the WT channel does respond to high concentrations of nicotine we did not determine an  $\text{EC}_{50}$ . However, since the F200Y mutant responded to lower concentrations of nicotine we conducted dose response experiments which revealed an  $\text{EC}_{50}$  of  $277 \pm 8 \mu\text{M}$  ( $n = 5$ ) (Fig. 2.8B). Nicotine was docked in the binding pocket and its quaternary amine was situated 4  $\text{\AA}$  away from the center of the W248 benzene ring (Fig. 2.8A). The N2 quaternary amine in nicotine was 5.5  $\text{\AA}$  from the F200.

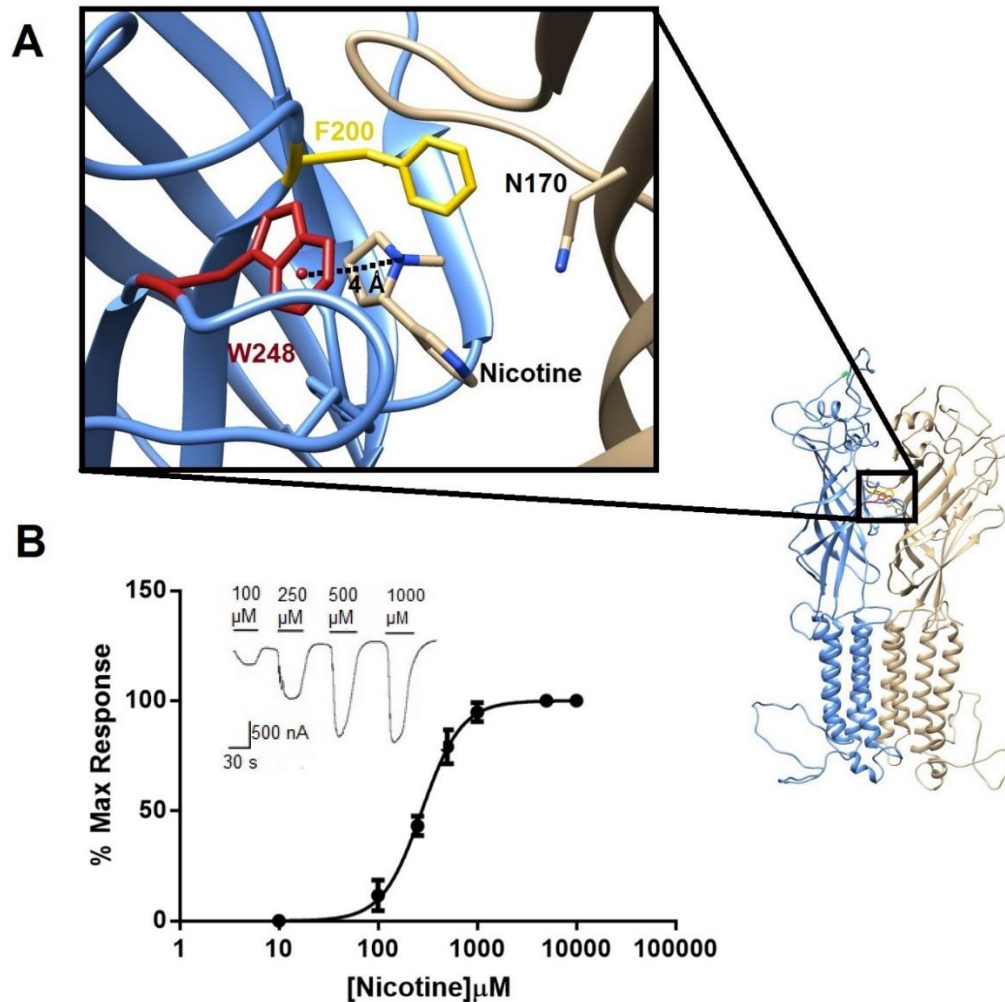


**Figure 2.8:** (A) Nicotine docked in the Hco-ACC-2 WT binding pocket. The quaternary amine of nicotine is located 4  $\text{\AA}$  away from W248. (B) Dose-response curve for the F200Y mutant with nicotine. INSET: Electrophysiological traces of nicotine activation of Hco-ACC-2.  $n = 5$  oocytes.

## 2.4: Discussion

We have identified a member of the ACC-1 family in the parasitic nematode *H. contortus* and investigated its binding site using site-directed mutagenesis, homology modelling and pharmacological analysis. This family of receptors appear to be unique to invertebrates and not present in mammals, making them attractive targets for novel nematocides. This has been validated by research demonstrating that this family of receptors are expressed in tissues that are sensitive to anthelmintic action (Wever et al., 2015). The research described here has examined in detail the structure of the ACC binding site which is important for future research focused on the discovery of novel therapeutics.

The pharmacology of the Hco-ACC-2 receptor can provide some valuable insight into the nature of the binding site. In our analysis, the receptor is least sensitive to choline. The low sensitivity of the receptor to choline is likely due to the molecules smaller size and lack of a carbonyl group which limits its interaction with residues. These features could explain why, compared to the other agonists, there was very little change in sensitivity of choline in the hypersensitive mutant F200Y. Moreover, the comparison between the sensitivities of ACh, carbachol, methacholine and urecholine along with the molecular docking results highlights some interesting trends. For example, all molecules docked with their quaternary amine close to W248. However, both ACh and methacholine, which exhibited maximum efficacy, appear to dock in a similar extended orientation, which places them within 3 Å of N170. On the other hand, carbachol and urecholine, which are both partial agonists, dock in a similar bent orientation, which is more pronounced in urecholine, and places them further away from N170.

One of the key features of ACh binding to mammalian nAChR is the presence of a tryptophan residue that participates in  $\pi$ -cationic interactions with the quaternary amine on ACh. In mammalian nAChRs this tryptophan residue is present in loop B (Beene et al., 2002). However, in ACC receptors there is no tryptophan residue in loop B. Instead, sequence analysis and homology modelling reveal a tryptophan residue present in loop C (W248). W248 is facing into the binding pocket and appears to be within 5 Å of the quaternary amine of the agonists that were docked in this study. While we did not confirm that W248 is participating in a  $\pi$ -cationic interaction with agonists, it is clear that it is essential for the function of Hco-ACC-2. Evidence for the importance of W248 in the function of ACC receptors is highlighted by mutational analysis, which showed that changing W248 to either W248Y or W248F resulted in a severely impacted receptor that did not respond to any agonists other than ACh. This could be partially explained

by the removal of the indole nitrogen which is found in tryptophan. The presence of an indole nitrogen causes a large negative electrostatic cloud around this residue, allowing for increased potential of  $\pi$ -cationic interactions (Mecozzi et al., 1996). Since this indole is not present in tyrosine or phenylalanine, it could explain why these mutations were detrimental to receptor function. In addition, the positioning of this tryptophan in loop C could be important in ACC receptor function, as swapping the residues from loop C to B (F200W/W248F) produced a non-functional channel. This phenomenon is reminiscent of the novel nematode 5-HT receptor MOD-1 which also has a tryptophan residue in loop C instead of loop B, as seen in 5-HT<sub>3</sub> receptors (Ranganathan et al., 2000). The loop C tryptophan in the MOD-1 receptor was shown to participate in the essential  $\pi$ -cationic interaction with serotonin which is key for receptor binding (Mu et al., 2003). Interestingly, this loop C tryptophan is not only present in ACC and MOD-1 receptors but other amine-gated chloride channels such as LGC-55 (tyramine) (Rao et al., 2010) and LGC-53 (dopamine) (Beech et al., 2013) as well as the nematode DEG-3 receptor. From an evolutionary perspective it appears that the presence of a tryptophan in loop C is an essential requirement for a diverse array of nematode cys-loop receptors, and their ability to bind to wide range of ligands.

Unlike mammalian nAChRs which exhibit a tryptophan in loop B, the Hco-ACC-2 receptor exhibits a phenylalanine (F200). Mutations at this position provided some additional insight into the structure of the ACC binding site. First, the introduction of a F200W change caused a reduced sensitivity to all agonists, albeit to varying degrees. Carbachol was the least affected by the change while methacholine was most affected. Methacholine is a full agonist for the ACC receptor and differs from ACh with the addition of a methyl group in the backbone, but both appear to bind in a similar orientation in the wildtype receptor. The addition of a bulky tryptophan residue may therefore cause the larger methacholine to shift orientation and reducing its ability to bind and activate the channel. Interestingly, the opposite was found with the F200Y mutation, which increased the sensitivity of all agonists (including nicotine) to varying degrees. Here, urecholine exhibited the highest increase in sensitivity. It is possible the hydroxyl group on tyrosine allows additional hydrogen-bond interactions with surrounding residues, thus changing the structure of the binding site and enhancing agonist (especially urecholine) binding. F200 may also have other roles such as participating in  $\pi$ -cationic interactions with agonists. However, future experiments would have to confirm.

The ACC receptor family appear to be attractive targets for the development of novel anthelmintics. With this in mind we also tested the activity of the anthelmintics levamisole and pyrantel which activate the

nematode nAChR (Martin and Robertson, 2007). We found both molecules were partial agonists for the Hco-ACC-2 receptor. However, we were surprised to observe that the mutations we introduced into the receptor minimally affected their activity. This may highlight the distinct manner at which these anthelmintics bind to the ACC receptors. Molecular models for docked pyrantel and levamisole place both molecules within 5 Å of W248. However, the overall positioning of levamisole and pyrantel within the ACC-2 binding site are clearly different (Fig. 2.5). How this relates to the differences in efficacy we observed between the two molecules requires further examination.

This study has described the isolation of a member of the ACC family from *H. contortus* and examined two residues in the binding site that are important for agonist recognition. Further research on the essential requirements for agonist recognition of ACC receptor can provide insight into the evolution of cholinergic neurotransmission and may possibly lead to the discovery of novel cholinergic anthelmintics.

## 2.5: Acknowledgements

This research was funded by grants from Natural Sciences and Engineering Research Council of Canada (Grant #210290) and the Canadian Foundation for Innovation to SGF. The authors declare no conflicts of interest.

## 2.6: References

Abdelmassih SA, Cochrane E, Forrester SG. 2018. Evaluating the longevity of surgically extracted *Xenopus laevis* oocytes for the study of nematode ligand-gated ion channels. *Invertebr. Neurosci.* 18:1.

Bamber BA, Beg AA, Twyman RE, Jorgensen EM. 1999. The *Caenorhabditis elegans* unc-49 locus encodes multiple subunits of a heteromultimeric GABA receptor. *J. Neurosci.* 19:5348–5359.

Beech RN, Callanan MK, Rao VTS, Dawe GB, Forrester SG. 2013. Characterization of cys-loop receptor genes involved in inhibitory amine neurotransmission in parasitic and free living nematodes. *Parasitol. Int.* 62:599–605.

Beene DL, Brandt GS, Zhong W, Zacharias NM, Lester HA, Dougherty DA. 2002. Cation- $\pi$  interactions in ligand recognition by serotonergic (5-HT<sub>3A</sub>) and nicotinic acetylcholine receptors: The anomalous binding properties of nicotine. *Biochemistry* 41:10262–10269.

Beene DL, Price KL, Lester HA, Dougherty DA, Lummis SCR. 2004. Tyrosine residues that control binding and gating in the 5-hydroxytryptamine<sub>3</sub> receptor revealed by unnatural amino acid mutagenesis. *J. Neurosci.* 24:9097–9104.

Boulin T, Fauvin A, Charvet CL, Cortet J, Cabaret J, Bessereau J, Neveu C. 2011. Functional reconstitution of *Haemonchus contortus* acetylcholine receptors in *Xenopus* oocytes provides mechanistic insights into levamisole resistance. *Br. J. Pharmacol.* 164:1421–1432.

Del Castillo J, Morales TA, Sanchez V. 1963. Action of piperazine on the neuromuscular system of *Ascaris lumbricoides*. *Nature* 200:706.

Cully DF, Vassilatis DK, Liu KK, Paress PS, Van der Ploeg LH, Schaeffer JM, et al. 1994. Cloning of an avermectin-sensitive glutamate-gated chloride channel from *Caenorhabditis elegans*. *Nature* 371:707.

Van Doren K, Hirsh D. 1988. Trans-spliced leader RNA exists as small nuclear ribonucleoprotein particles in *Caenorhabditis elegans*. *Nature* 335:556.

Dougherty DA. 1996. Cation- $\pi$  interactions in chemistry and biology: a new view of benzene, Phe, Tyr, and Trp. *Science* (80) 271:163.

Frohman MA, Dush MK, Martin GR. 1988. Rapid production of full-length cDNAs from rare transcripts: amplification using a single gene-specific oligonucleotide primer. *Proc. Natl. Acad. Sci.* 85:8998–9002.

Jensen ML, Timmermann DB, Johansen TH, Schousboe A, Varming T, Ahring PK. 2002. The  $\beta$  subunit determines the ion selectivity of the GABA<sub>A</sub> receptor. *J. Biol. Chem.* 277:41438–41447.

Jones AK, Sattelle DB. 2008. The cys-loop ligand-gated ion channel gene superfamily of the nematode, *Caenorhabditis elegans*. *Invertebr. Neurosci.* 8:41–47.

Kehoe J, McIntosh JM. 1998. Two Distinct Nicotinic Receptors, One Pharmacologically Similar to the Vertebrate  $\alpha$ 7-Containing Receptor, Mediate Cl Currents in *Aplysia* Neurons. *J. Neurosci.* 18:8198–8213.

Kusano K, Miledi R, Stinnakre J. 1982. Cholinergic and catecholaminergic receptors in the *Xenopus* oocyte membrane. *J. Physiol.* 328:143–170.

Laing R, Kikuchi T, Martinelli A, Tsai IJ, Beech RN, Redman E, et al. 2013. The genome and transcriptome of *Haemonchus contortus*, a key model parasite for drug and vaccine discovery. *Genome Biol.* 14:R88.

Lynagh T, Pless SA (2014) Principles of agonist recognition in Cys-loop receptors. *Front Physiol* 24;5:160

Martin RJ, Robertson AP. 2007. Mode of action of levamisole and pyrantel, anthelmintic resistance, E153 and Q57. *Parasitology* 134:1093–1104.

Morales-Perez CL, Noviello CM, Hibbs RE. 2016. X-ray structure of the human  $\alpha 4\beta 2$  nicotinic receptor. *Nature* 538:411.

Mu T-W, Lester HA, Dougherty DA. 2003. Different binding orientations for the same agonist at homologous receptors: a lock and key or a simple wedge? *J. Am. Chem. Soc.* 125:6850–6851.

Ortells MO, Lunt GG. 1995. Evolutionary history of the ligand-gated ion-channel superfamily of receptors. *Trends Neurosci.* 18:121–127.

Pettersen EF, Goddard TD, Huang CC, Couch GS, Greenblatt DM, Meng EC, et al. 2004. UCSF Chimera—a visualization system for exploratory research and analysis. *J. Comput. Chem.* 25:1605–1612.

Pirri JK, McPherson AD, Donnelly JL, Francis MM, Alkema MJ. 2009. A tyramine-gated chloride channel coordinates distinct motor programs of a *Caenorhabditis elegans* escape response. *Neuron* 62:526–538.

Putrenko I, Zakikhani M, Dent JA. 2005. *J. Biol. Chem.* 280:6392–6398.

Ranganathan R, Cannon SC, Horvitz HR. 2000. MOD-1 is a serotonin-gated chloride channel that modulates locomotory behaviour in *C. elegans*. *Nature* 408:470–475.

Rao VTS, Accardi M V, Siddiqui SZ, Beech RN, Prichard RK, Forrester SG. 2010. Characterization of a novel tyramine-gated chloride channel from *Haemonchus contortus*. *Mol. Biochem. Parasitol.* 173:64–68.

Šali A, Blundell TL. 1993. Comparative protein modelling by satisfaction of spatial restraints. *J. Mol. Biol.* 234:779–815.

Siddiqui SZ, Brown DDR, Rao VTS, Forrester SG. 2010. An UNC-49 GABA receptor subunit from the parasitic nematode *Haemonchus contortus* is associated with enhanced GABA sensitivity in nematode heteromeric channels. *J. Neurochem.* 113:1113–1122.

Sine SM, Engel AG. 2006. Recent advances in Cys-loop receptor structure and function. *Nature* 440:448–455.

Thompson AJ, Lester HA, Lummis SCR. 2010. The structural basis of function in Cys-loop receptors. *Q. Rev. Biophys.* 43:449–499.

Trott O, Olson, AJ (2010). AutoDock Vina: improving the speed and accuracy of docking with a new scoring function, efficient optimization, and multithreading. *J. Comput. Chem.* 31: 455-461

Weston D, Patel B, Van Voorhis WC. 1999. Virulence in *Trypanosoma cruzi* infection correlates with the expression of a distinct family of sialidase superfamily genes. *Mol. Biochem. Parasitol.* 98:105–116.

Wever CM, Farrington D, Dent JA. 2015. The validation of nematode-specific acetylcholine-gated chloride channels as potential anthelmintic drug targets. *PLoS One* 10:e0138804.

Zhang J, Xue F, Chang Y. 2008. Structural determinants for antagonist pharmacology that distinguish the  $\rho 1$  GABAC receptor from GABAA receptors. *Mol. Pharmacol.* 74:941–951.

## Connecting Statement I

Having pharmacologically characterized the first member of the ACC-1 family from *H. contortus* in Chapter II, Hco-ACC-2, and identifying key residues for cholinergic ligand binding in the binding pocket through sequence analysis and homology modeling, my thesis research moved forward to further characterize other members of the ACC-1 family. Prior research suggested that members of the ACC-1 family from *C. elegans* co-assemble into unique heteromeric channels. The following chapter explores another member of the ACC-1 family from *H. contortus*, Hco-ACC-1, and presents its unique pharmacology when co-expressed with Hco-ACC-2. We also highlight the exact location of the Hco-ACC-1 receptor in adult *H. contortus* and identify its role in parasite feeding.



## Chapter III – Manuscript II

### Investigating the function and possible biological role of an acetylcholine-gated chloride channel subunit (ACC-1) from the parasitic nematode *Haemonchus contortus*

**Sarah A. Habibi\***, Micah K. Callanan\*, Wen Jing Law, Kristen Nazareth, Richard L. Komuniecki, and Sean G. Forrester

**\*Joint first author**

Published in:

International Journal for Parasitology: Drugs and Drug Resistance. 8(3): 526-533

DOI: [doi.org/10.1016/j.ijpddr.2018.10.010](https://doi.org/10.1016/j.ijpddr.2018.10.010)

### 3.0: Abstract

The cys-loop superfamily of ligand-gated ion channels are well recognized as important drug targets for many invertebrate specific compounds. With the rise in resistance seen worldwide to existing anthelmintics, novel drug targets must be identified so new treatments can be developed. The acetylcholine-gated chloride channel (ACC) family is a unique family of cholinergic receptors that have been shown, using *Caenorhabditis elegans* as a model, to have potential as anti-parasitic drug targets. However, there is little known about the function of these receptors in parasitic nematodes. Here, we have identified an *acc* gene (*hco-acc-1*) from the sheep parasitic nematode *Haemonchus contortus*. While similar in sequence to the previously characterized *C. elegans* ACC-1 receptor, Hco-ACC-1 does not form a functional homomeric channel in *Xenopus* oocytes. Instead, co-expression of Hco-ACC-1 with a previously characterized subunit Hco-ACC-2 produced a functional heteromeric channel which was 3x more sensitive to acetylcholine compared to the Hco-ACC-2 homomeric channel. We have also found that Hco-ACC-1 can be functionally expressed in *C. elegans*. Overexpression of both *cel-acc-1* and *hco-acc-1* in both *C. elegans* N2 and *acc-1* null mutants decreased the time for worms to initiate reversal avoidance to octanol. Moreover, antibodies were generated against the Hco-ACC-1 protein for use in immunolocalization studies. Hco-ACC-1 consistently localized to the anterior half of the pharynx, specifically in pharyngeal muscle tissue in *H. contortus*. On the other hand, expression of Hco-ACC-1 in *C. elegans* was restricted to neuronal tissue. Overall, this research has provided new insight into the potential role of ACC receptors in parasitic nematodes.

### 3.1: Introduction

*Haemonchus contortus* is a pathogenic gastrointestinal parasitic nematode that causes severe livestock damage worldwide, particularly in the sheep industry. The disease, known as haemonchosis, leads to severe symptoms in host ruminants including anemia and death (Besier et al., 2016). Traditionally, *H. contortus* is controlled with broad spectrum anthelmintic chemotherapeutics that target different proteins within the parasite. There are multiple classes of these drugs that target cys-loop ligand-gated ion channels, including macrocyclic lactones which specifically target glutamate-gated chloride channels (GluCl<sub>s</sub>) (Forrester et al., 2003; McCavera et al., 2009; Glendinning et al., 2011) and nicotinic acetylcholine receptor (nAChR) agonists such as pyrantel and levamisole (Boulin et al., 2011; Duguet et al., 2016; Blanchard et al., 2018). Macrocyclic lactones have also been shown to interact with nematode cys-

loop GABA receptors (Accardi et al., 2012; Hernando and Bouzat, 2014). There is global concern about the increase in drug resistant populations of *H. contortus* in the field, including documented resistance to more recently developed drugs such as monepantel and derquantel (Raza et al., 2016). This information drives the need for the discovery of novel anthelmintic targets that could be used for the rational design or screening of new and effective anthelmintics.

The cys-loop ligand-gated chloride channel (LGCC) family of receptors is a very attractive group of proteins for drug-target discovery. Information from the *H. contortus* genome suggests that this family of receptors has approximately 35 genes that encode various subunits (Laing et al., 2013). However, approximately half of these potential channels have no confirmed ligand. In addition, many of these channels are either not present in mammals or are sufficiently divergent, suggesting the potential to develop highly specific drugs that will not target host receptors (Laing et al., 2013). However, of the 35 possible LGCC targets in the *H. contortus* genome it is likely that only a subset could be developed as targets for broad-spectrum anthelmintics. This is because the genomes of other parasitic nematodes, particularly human pathogens, appear to contain a significantly lower number of *lgcc* genes with some groups of channels being absent (Williamson et al., 2007; Beech et al., 2013). In addition, several LGCCs are likely to have functions that have no real consequence to the parasite if targeted. Therefore, the most attractive LGCCs from an anthelmintic discovery point of view are those present in a broad range of parasitic nematodes, that have a function in the parasitic stage that if bound by an anthelmintic would lead to death or expulsion of the parasite and are not similar to host receptors (Wever et al., 2015). The latter point can be achieved by either targeting unique nematode-specific families of receptors or similar receptors that exhibit unique binding sites for potential drugs.

Previous research has suggested that the acetylcholine-gated chloride channels (ACCs) in *Caenorhabditis elegans* (Putrenko et al., 2005) exhibit the characteristics of promising drug targets. The genes that encode the various subunits of this family are present across the nematode phylum and appear to have fairly broad function in the nematode nervous system (Wever et al., 2015). One of the channels, Cel-ACC-1 exhibits a pharmacology distinct from mammalian cys-loop acetylcholine channels and appears in *C. elegans* to be localized to ventral cord and extrapharyngeal neurons (Wever et al., 2015). Due to their broad role in the *C. elegans* nervous system, the ACC family of receptors appear to be promising targets for effective anthelmintic action against parasitic nematodes (Wever et al., 2015). However, directly extrapolating results from *C. elegans* to parasitic nematodes should be done with caution since the

expression patterns of individual LGCCs have been shown in some cases to be different (Portillo et al., 2003).

Here we have isolated a member of the ACC family (Hco-ACC-1) from the parasitic nematode *H. contortus*. Electrophysiological examination revealed that while Hco-ACC-1 does not form a functional homomeric channel in *Xenopus* oocytes, co-expression with a previously characterized subunit (Hco-ACC-2) can form a channel highly sensitive to acetylcholine and carbachol. The ACC-1/2 heteromeric channel was 3x more sensitive to acetylcholine compared to the ACC-2 homomeric channel. When expressed in *C. elegans*, *hco-acc-1*, localizes to pharyngeal neurons and enhances reversal avoidance to octanol demonstrating that *hco-acc-1* can function *in vivo*. In *H. contortus*, ACC-1 may play an essential role in the pharynx as immunolocalization revealed expression in a specific region of the pharyngeal muscle. Overall, this research has provided some novel insight into the possible role of ACC receptors in parasitic nematodes.

## 3.2: Materials and Methods

### 3.2.1: RNA/cDNA

Total RNA was isolated using Trizol (Invitrogen, Carlsbad, USA) from adult *H. contortus* strain PF23. cDNA was synthesized using the Quantitect Reverse Transcription kit from Qiagen (Dusseldorf, Germany) using a unique 3' anchor sequence primer (5'CCTCTGAAGGTTACGGATCCACATCTAGATTTTTTTTTTTTTTTTTVN3'); [where V is either A, C, or G and N is either A, C, G, or T] (Weston et al., 1999). The partial *H. contortus* sequence of *acc-1* was initially identified by the Sanger Institute (Cambridge, UK) and used for the creation of gene specific primers. These primers were used in the 5' and 3' rapid amplification of cDNA ends (RACE) protocol (Frohman et al., 1988).

### 3.2.2: Isolation of *hco-acc-1* and sequence analysis

The 5' end of the *hco-acc-1* gene was amplified using two internal *hco-acc-1* specific antisense primers [NESTED PRIMER 5' GTTGTTCCAAACGCACCTGTGG 3'] and a primer specific for splice leader – 1 sequence (SL1-5'GGTTTAATTACCCAAGTTTGAG3') (Van Doren and Hirsh, 1988) in a PCR using the PTC-100 Programmable Thermal Controller (MJ Research, Inc, Waltham, MA, USA). For the 3' end, two *hco-acc-*

1 gene specific primers [NESTED PRIMER – 5'GTGACTTACTGGAGCTACTAC 3'] and two primers specific for the 3' oligo-dT anchor sequence were used in a nested PCR reaction. Each amplicon of a predicted size was isolated via gel extraction and subcloned into the pGEMT easy™ vector and sequenced. Amplification of the complete *hco-acc-1* gene was conducted using primers designed targeting 5' and 3' untranslated region. This amplicon was subcloned and sequenced to achieve a consensus sequence. Sequence alignments were produced using ClustalW.

For phylogenetic analysis of the nematode ACC subunit family, the most highly conserved regions of the ligand-binding domain and membrane-spanning regions 1–3 (144 amino acids) were aligned using ClustalW and imputed into PhyML 3.0 to create a rooted phylogenetic tree with 100 bootstrap repetitions. The final formatted tree was produced using FigTree v1.4.3.

### 3.2.3: Expression in *Xenopus* oocytes

All animal procedures followed the University of Ontario Institute of Technology Animal Care Committee and the Canadian Council on Animal Care guidelines and according to methods outlined in Abdelmassih et al., (2018). *Xenopus laevis* frogs (all female) were supplied by Nasco (Fort Atkinson, WI, USA). The frogs were housed in a room, which was climate controlled, light cycled, and stored in tanks which were regularly cleaned. Frogs were anesthetized with 0.15% 3-aminobenzoic acid ethyl ester methanesulphonate salt (MS-222) buffered with NaHCO<sub>3</sub> to pH 7 (Sigma-Aldrich, Oakville, ON, CA). Surgical removal of a section of the ovary of the frog was performed, and the lobe was defolliculated with a calcium-free oocyte Ringer's solution (82 mM NaCl, 2 mM KCl, 1 mM MgCl<sub>2</sub>, 5 mM HEPES pH 7.5 (Sigma-Aldrich)) (OR-2) containing 2 mg/mL collagenase-II (Sigma-Aldrich). The oocytes in the defolliculation solution were incubated at room temperature for 2 h. Collagenase was washed from the oocytes with ND96 solution (1.8 mM CaCl<sub>2</sub>, 96 mM NaCl, 2 mM KCl, 1 mM MgCl<sub>2</sub>, 5 mM HEPES pH 7.5) and allowed 1 h to recover at 18 °C in ND96 supplemented with 275 µg mL<sup>-1</sup> pyruvic acid (Sigma-Aldrich) and 100 µg mL<sup>-1</sup> of the antibiotic gentamycin (Sigma-Aldrich). Stage V and VI oocytes were selected for cytoplasmic injection of cRNA.

The coding sequence of *hco-acc-1* and *hco-acc-2* (Habibi et al., 2018) was subcloned into the *X. laevis* expression vector pGEMHE (Zhang et al., 2008). The vector was linearized using the restriction enzyme *Pst*I (New England Biolabs, USA), and used as template for an *in vitro* transcription reaction (T7

mMessage mMachine kit, Ambion, Austin, TX, USA) yielding *hco-acc-1* and *hco-acc-2* copy RNA. *X. laevis* oocytes were injected with 50 nl of *hco-acc-1* (0.5 ng/nL), *hco-acc-2* (0.5 ng/nL) or *hco-acc-1/2* (0.25 ng/nl each) using the Drummond (Broomall, PA, USA) Nanoject microinjector. Oocytes were also co-injected with the copy RNA encoding three accessory proteins, *hco-unc-50*, *hco-unc-74*, and *hco-ric-3.1* (Boulin et al., 2011) which were gifts from Dr. Cédric Neveu (INRA). The injected oocytes were incubated at 18 °C in ND96 (96 mM NaCl, 2 mM KCl, 1 mM MgCl<sub>2</sub>, 1.8 mM CaCl<sub>2</sub>, 5 mM HEPES pH 7.5) supplemented with 0.275 µg/mL pyruvate and 50 µg/mL gentamycin. Electrophysiological recordings of the oocytes were conducted between 48 and 72 h after cRNA injection.

### 3.2.4: Electrophysiology recordings

The Axoclamp 900A voltage clamp (Molecular Devices, Sunnyvale, CA, USA) was used to conduct two electrode voltage clamp electrophysiology. Glass electrodes were produced using a P-97 Micropipette Puller (Sutter Instrument Co., Novato, CA, USA). The electrodes were backfilled with 3M KCl and contained Ag|AgCl wires, and electrodes with resistances of 1–8 MΩ were selected for recordings. All oocytes were clamped at –60 mV for the entirety of the experiments. Acetylcholine and carbamylcholine (Sigma-Aldrich) were first dissolved in ND96. The resultant solutions were perfused over oocytes using the RC-1Z recording chamber (Warner Instruments Inc., Hamdan, CT, USA). Data was subsequently analyzed using Clampex Software v10.2 (Molecular Devices) and all graphs were generated using Graphpad Prism Software v5.0 (San Diego, CA, USA). Acetylcholine and carbamylcholine (carbachol) EC<sub>50</sub> values were determined by dose response curves which had been fitted to the equation:

$$I_{max} = \frac{1}{1 + \left(\frac{EC_{50}}{[D]}\right)^h}$$

Where  $I_{max}$  is the maximal response, EC<sub>50</sub> is the concentration of compound required to elicit 50% of the maximal response, [D] is compound concentration, and  $h$  is the Hill coefficient. Both EC<sub>50</sub> and  $h$  are free parameters, and the curves were normalized to the estimated  $I_{max}$ . Graphpad prism used the equation to fit a sigmoidal curve of variable slopes to the data. Dose-response curves comparing Hco-ACC-2 and Hco-ACC-1/2 were conducted in the same week and with the same batch of eggs. Means were determined from at least 4 oocytes from at least two batches of oocytes.

### 3.2.5: *In silico* modelling

The protein sequences of Hco-ACC-1 and 2 were aligned to the recently crystalized alpha-1 glycine receptor (3jad) from *Danio rerio* for use in MODELLER v9.15 (Sali and Blundell, 1993) for the generation of the hypothetical Hco-ACC-1/2 heteromeric dimer. The associated DOPE score determined the most energetically favorable model. Preparation of the heteromer for agonist docking was carried out using AutoDock Tools (Morris et al., 2009). ACh and carbachol were obtained from the Zinc database in their energy-reduced form (Irwin et al., 2012). AutoDock Vina (Trott and Olson, 2010) was used to simulate docking of each ligand to the Hco-ACC-1/2 heteromer. Pymol was used to visualize the protein heterodimer with its associated ligand docking, and Chimera v1.6.1 (Pettersen et al., 2004) was used to determine the distance between amino acid residues and ligands.

### 3.2.6: Immunolocalization in *H. contortus*

Two peptides specific for a portion of the N-terminal region of the Hco-ACC-1 protein (ACC-1.1- YNKHYIPSHPTQVRVDM and ACC-1.2- YQPVQRSRPERNLLSAIRKW) were synthesized commercially and used to immunize two rabbits (21st Century Biochemicals, Marlboro, MA, USA). Peptides were conjugated to the carrier protein ovalbumin and its sequence was initially BLASTed against the *H. contortus* genome database and the NCBI general database to ensure specificity. Whole sera was collected from the animals and subjected to affinity purification using separate columns for each peptide to isolate and purify each antibody separately. Whole antisera was tested for specificity and titer against the immunogenic peptide by ELISA. For immunolocalization two strains of *H. contortus* were used, PF23 and MOF23. Both strains were derived from the same parental strain. However, the PF23 strain was generated by passage through sheep over 23 generations without anthelmintic treatment whereas MOF23 was generated by passage through sheep over 23 generations with increasing dosage of moxidectin at each generation. Further details of the strains can be found in Urdaneta-Marquez et al., (2014). Adult female *H. contortus* worms (strains PF23 and MOF23) were fixed, permeabilized and subsequently digested as previously described (Rao et al., 2009). Worms were subsequently washed 3 times with PBS, and incubated at 4 °C for 72 h with a 1/150 dilution of primary antibody diluted in 0.1% w/v BSA, 0.5% Triton X-100, and 0.05% sodium azide (Sigma) under slight shaking. The removal of unbound antibodies was conducted by 4 washes of the worms with PBS and a final wash with PBS with 0.1% (v/v) Triton X-100 (PBST). Worms were then incubated at 4 °C with a 1/2000 dilution of Alexa Fluor 448<sup>®</sup> goat anti-rabbit IgG (H + L) secondary antibody

for 24 h. Alexa Fluor 488<sup>®</sup> was used due its photostability and sensitivity to detect potentially low abundance proteins such as cys-loop LGCCs. Unbound secondary antibody was removed by 4 washes of the worms with PBS, and a final PBST wash. Worms were mounted on slides using Fluoromount™ Aqueous Mounting Medium (Sigma) and examined. Slides were examined using a Zeiss LSM710 confocal microscope (Carl Zeiss Inc., Canada) equipped with the Zeiss Zen 2010 software package. The lasers used for image acquisition were an Argon 488 nm, with the filter sets adjusted to minimize bleed-through due to spectral overlap.

Several controls were conducted including the omission of primary antibody, a pre-immune control (where 1/50 dilutions of pre-immune serum from experimental rabbits were applied instead of the purified primary antibody), and a peptide absorbed control, where an excess of peptide (50 µg/ml) was added to the primary antibody dilution and incubated for 24 h at 4 °C before immunolocalization.

### 3.2.7: Expression of *acc-1* in *C. elegans*

All transgenic constructs were made by overlap fusion PCR (Hobert, 2002). *H. contortus* and *C. elegans acc-1* cDNAs were fused to *C. elegans acc-1* (5.3 kb) promoter. All transgenes contain sequence encoding a GFP marker (with an *unc-54* 3'-UTR) at the 3'-end of receptor cDNA. PCR products from multiple reactions were pooled and co-injected with coelomocyte-RFP as a screening marker into the appropriate backgrounds (Mello and Fire, 1995). Multiple transgenic lines from each construct were examined. Localization of GFP expression was performed using confocal microscopy.

Well-fed hermaphrodite fourth-stage *C. elegans* larvae carrying a coelomocyte RFP screening marker were picked 24 h prior to assay and incubated overnight at 20 °C. Fresh nematode growth medium (NGM) plates were prepared on the day of assay. Aversive responses were examined off food as described in Chao et al. (2004) and are presented as the time taken to initiate backward locomotion after the presentation of 30% 1-octanol on a hair in front of a forward moving animal.



### 3.3: Results

#### 3.3.1: Hco-ACC-1 isolation and polypeptide analysis

The final consensus nucleotide product obtained through the RACE procedure was sequenced and shown to consist of 1380 nucleotides and assigned the GenBank accession number AHM25233.1. When translated in the appropriate reading frame, the sequence encodes a protein containing 459 amino acids with the hallmark Cys-loop motif (Fig. 3.1A). Additionally, 4 hydrophobic transmembrane domains were identified along with a signal peptide cleavage site (Signal P; <http://www.cbs.dtu.dk/services/SignalP/>). The PAR motif (residues 266–268) was noted in the M2 transmembrane portion of the peptide, indicative of chloride ion selectivity (Jensen et al., 2005). The Hco-ACC-1 peptide shares 89% sequence similarity with the *C. elegans* ACC-1 subunit. A few key amino acid differences were noted in the major binding loops. Firstly, in ligand binding loop B, a tyrosine (Y178) was identified in the Hco-ACC-1 protein where a phenylalanine (F179) is seen in the analogous position in Cel-ACC-1. Secondly, there are two differences seen in binding loop F. In Hco-ACC-1 two positions P199 and Q201 align to R200 and E201 in Cel-ACC-1 (Fig. 3.1A). The functional consequences of these differences are not known. In addition, the amino acid sequence of Hco-ACC-1 is identical (except for amino acid 448) to an unnamed protein (CDJ86191.1) deposited to GenBank as part of the *H. contortus* genome sequencing project (Laing et al., 2013).

Using the crystal structure of the *Danio rerio* glycine receptor (PDB 3JAD), a homology model of the ACC receptor (dimer) was generated. This crystal structure was selected as template as it shares the highest sequence similarity with ACC-1 and 2 of the crystal structures currently in the protein database. A hypothetical heteromer was generated where Hco-ACC-1 was designated the primary subunit and Hco-ACC-2 the complementary subunit. Fig. 3.1B displays the best model (ie. with lowest DOPE and molpdf scores out of 50 possibilities). Acetylcholine was docked in a 30 × 30 × 30 Å box centered between the primary and complementary subunits (between loops A, B and C of the primary and adjacent to loops D, E and F of the complementary subunit).

End-point PCR indicates that *hco-acc-1* is expressed in both the adult male and L3 stage (Fig. 3.1C) and phylogenetic analysis indicated that Hco-ACC-1 groups with other nematode ACC-1 subunits (Fig. 3.1D).

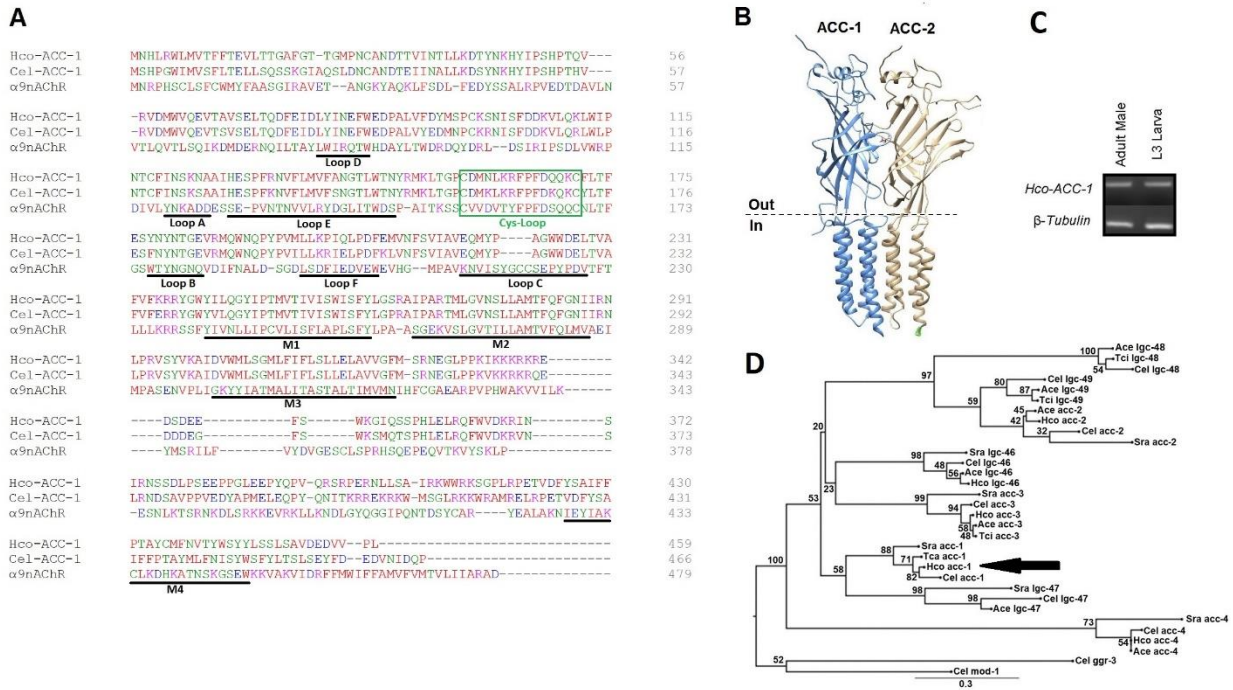


**Figure 3.1:** Isolation of *hco-acc-1* and protein sequence analysis. A. Protein sequence alignment of *H. contortus* and *C. elegans* ACC-1 with the nAChR. Stars indicate regions of amino acid identity. Dashes represent no alignment between sequences while colons indicate similar amino acids. The 6 ligand binding loops (Loops A-F), 4 transmembrane regions (M1-M4) and the cys-loop are indicated. B. Homology model of a hypothetical receptor showing a dimer of Hco-ACC-1 and Hco-ACC-2 that was used for ligand-docking. C. End point PCR analysis of the *hco-acc-1* cDNA in the adult male and L3 larval stages of *H. contortus*. PCR reactions were simultaneously performed on the housekeeping gene  $\beta$ -tubulin. Replicate experiments showed a similar trend. No PCR products were detected in negative controls (including negative RT control). D. Phylogenetic analysis of the ACC family from various nematodes. Cel - *Caenorhabditis elegans* Hco - *Haemonchus contortus*; Tci - *Teladorsagia circumcincta*; Ace - *Ancylostoma ceylanicum*; Sra - *Strongyloides ratti*; Tca - *Toxocara canis*. Hco-ACC-1 is indicated by arrow.

### 3.3.2: Functional Characterization of Hco-ACC-1

Oocytes injected with *hco-acc-1* cRNA alone did not respond to up to 1 mM ACh or carbachol. However, the same batches of oocytes injected with *hco-acc-2* cRNA responded readily to both ACh and carbachol (Fig. 3.2A and B) with EC<sub>50</sub> values similar to those reported in Habibi et al. (2018) of 19 ± 1 μM (n = 5) and 46 ± 2 μM (n = 5), respectively (Fig. 3.2B). However, co-expression of *hco-acc-1* and 2 produced a channel significantly more sensitive to both ACh and carbachol with EC<sub>50</sub> values of 5.9 ± 1 μM ( $p < 0.001$ ) (n = 6) and 32.5 ± 3 μM ( $p = 0.04$ ) (n = 4), respectively. Both the ACC-2 and ACC1/2 channels produced currents that were in the microamp range and desensitized. These responses were observed repeatedly in oocytes from different frogs, but was not seen in eggs injected with water. Current-voltage analysis of the Hco-ACC-1/2 heteromeric channel using full Cl<sup>-</sup> ND96 (final concentration 103.6 mM Cl<sup>-</sup>) indicated a reversal

potential of  $-17.7 \pm 5$  mV ( $n = 4$ ) (Fig. 3.2C) consistent with the calculated Nernst potential for  $\text{Cl}^-$  of  $-18.5$  mV, assuming 50 mM internal Cl (Kusano et al., 1982). When NaCl was partially replaced with Na-gluconate in the ND96, the reversal potential shifted to  $-2.1 \pm 1$  mV ( $n = 3$ ), consistent with the predicted Nernst potential of  $-5.7$  mV.

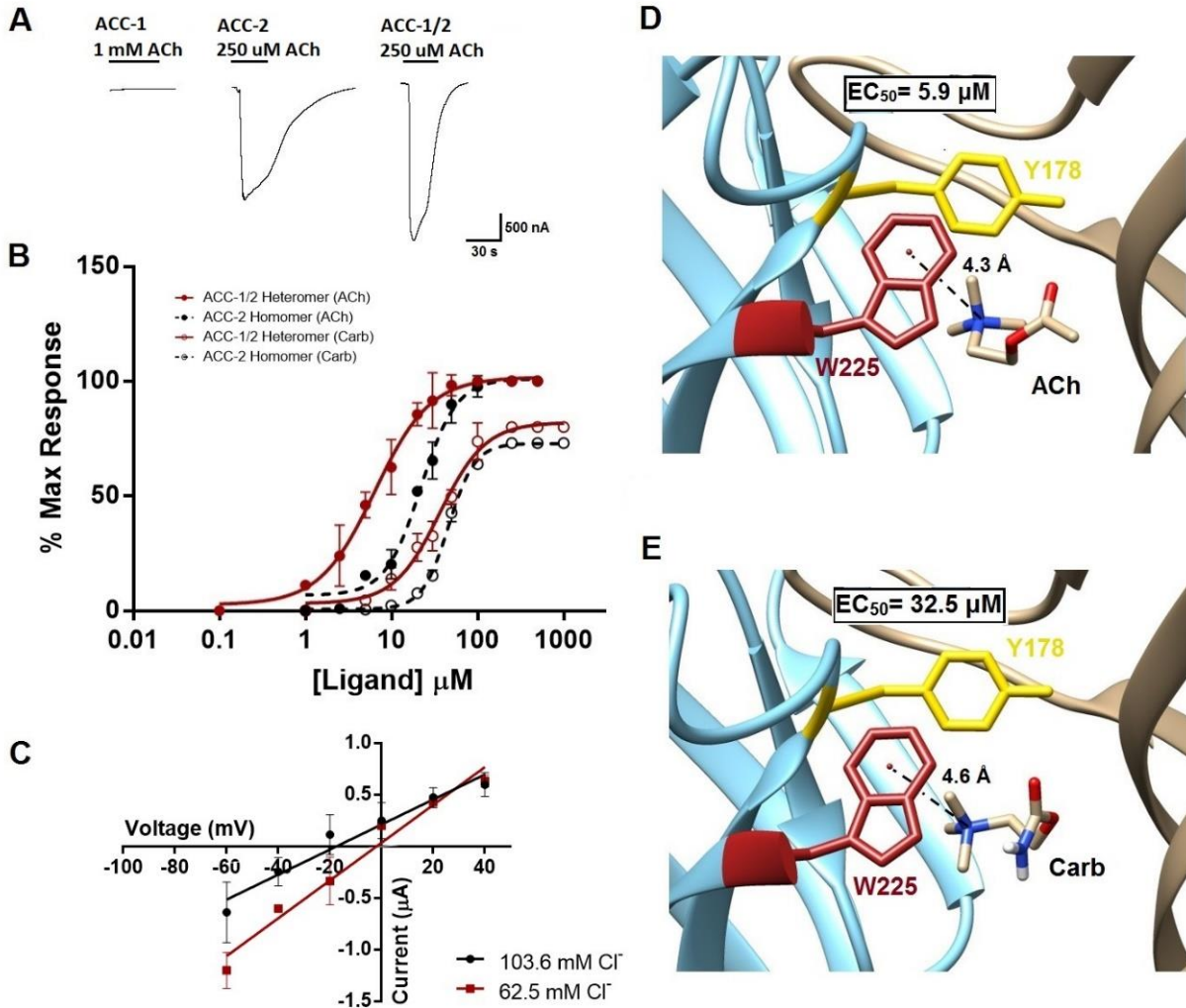


**Figure 3.2:** Hco-ACC-1 and Hco-ACC-2 form a functional heteromeric receptor. A. Representative electrophysiological traces of the acetylcholine responses to oocytes expressing Hco-ACC-1 alone, Hco-ACC-2 alone and Hco-ACC-1 + 2. B. Dose response curves comparing the sensitivities of the Hco-ACC-2 channel and the Hco-ACC-1/2 channel to acetylcholine and carbachol. Each data point is a mean  $\pm$  SEM with  $n \geq 4$ . C. Current/Voltage relationship of the Hco-ACC-1/2 channel comparing full  $\text{Cl}^-$  ND96 (103.6 mM) partial  $\text{Cl}^-$  ND96 (62.5 mM). D. Ligand docking of acetylcholine to the Hco-ACC1/2 receptor shown the distance of the ligand to W225. E. Ligand docking of carbachol to the Hco-ACC-1/2 receptor shown the distance of the ligand to W225.

### 3.3.3: Ligand docking analysis

Docking results clustered all 10 acetylcholine binding poses to the predicted binding location. The dock with the highest affinity (-5.4 kcal) is shown in Fig. 3.2D. The acetylcholine quaternary amine group was located directly between W225 (loop C) and Y178 (loop B). This quaternary amine was 4.3 Å away from the center of the W225 aromatic ring suggesting the formation of single pi-cation bond with W225. Similarly, carbachol docked at a similar pose and its quaternary amine was 4.6 Å away from W225 (Fig. 3.2E).

### 3.3.4: Immunolocalization

The application of anti-Hco-ACC-1 antibodies was performed on adult female *H. contortus* worms to determine the tissue expression of the ACC-1 protein. Worms from both the PF23 and MOF23 strains were successfully stained, with repeated staining over multiple batches of collected worms. The signal was identified consistently in pharyngeal muscle cells, in the anterior half of the pharynx in both strains (Fig. 3.3A–D). There were no obvious differences in the signal between *H. contortus* strains. The observed signal was robust and reconstructed stacks of slicing through the Z axis shows the triradiate organization of nematode pharyngeal muscle (supplemental movies 1 and 2). Peptide absorbed controls, pre-immune serum controls and no primary antibody controls displayed no signal beyond background (Fig. 3.3F and G). In addition, no autofluorescence was detected.

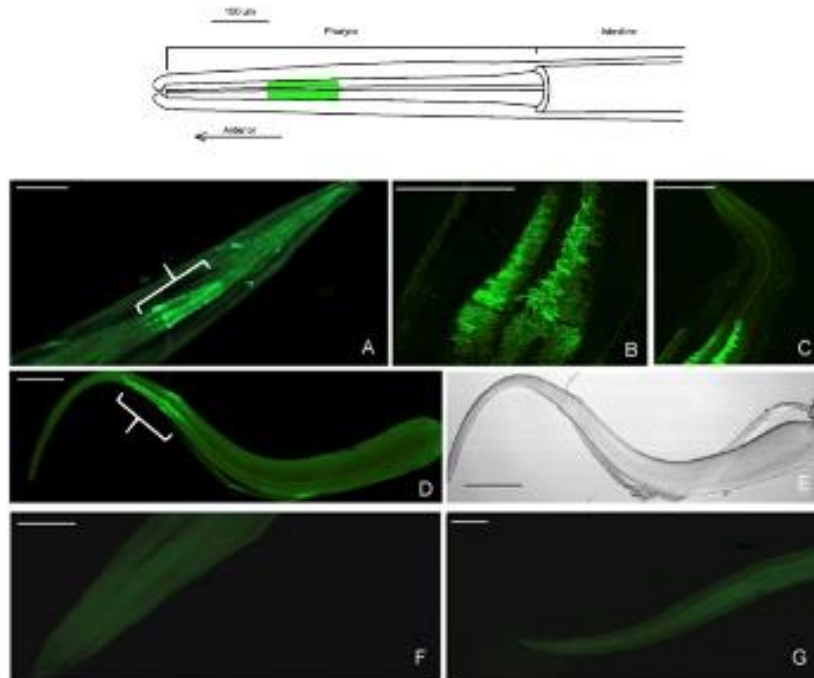


**Figure 3.3:** Immunolocalization of Hco-ACC-1 in adult female *H. contortus* worms. A cartoon schematic of the anterior end of the female *H. contortus* adult nematode is shown at the top. Green denotes detected signal in the anterior half of the pharynx seen during immunolocalization experiments. A. 25x magnification of the anterior end of *H. contortus* PF23 strain. B. 40X magnification stack of 25 of 5  $\mu\text{m}$  confocal slices of *H. contortus* PF23 focused on the anterior half of the pharyngeal muscle tissue. C. 25x magnification of a female adult *H. contortus* MOF23 parasite focusing on the anterior end of the worm. D. 25x magnification of isolated pharynx from a female *H. contortus* MOF23 adult worm. E. 25x magnification light micrograph of D. F. Pre-immune serum negative control of *H. contortus* PF23, 25x magnification focusing on anterior end of the worm. G. Peptide-absorbed control of *H. contortus* MOF23 at 10x magnification focusing on the anterior end of the worm. Lines denote 100  $\mu\text{m}$ . (For interpretation of the references to colour in this figure legend, the reader is referred to the Web version of this article.)

### 3.3.5: Expression of *hco-acc-1* in *C. elegans*

To determine whether *hco-acc-1* could function *in vivo* we expressed the gene in *C. elegans*. Aversive responses to 1-octanol have been studied extensively in *C. elegans* and are modulated by a complex locomotory circuit involving an array of sensory and interneurons (Komuniecki et al., 2012, 2014). Both *C. elegans* wild-type and *acc-1* null animals initiate aversive responses to 1-octanol in about 10 s, but the overexpression of either the *C. elegans* or *H. contortus acc-1* genes in wild type-animals, driven by 5.2 kb of the predicted *C. elegans acc-1* promoter, significantly decreased the time taken to initiate an aversive response (Fig. 3.4). Overexpression of the *H. contortus acc-1* in an *acc-1* null background yielded a similar result, confirming the putative orthology of the two proteins. Fluorescence from an *H. contortus acc-1::gfp* transgene, driven by the same *C. elegans acc-1* promoter was exclusively neuronal and limited to a

small number of neurons in both the anterior (Fig. 3.5) and the posterior (supplemental Figure 1) ends of the worm, similar to published reports for the *C. elegans acc-1* (Pereira et al., 2015).

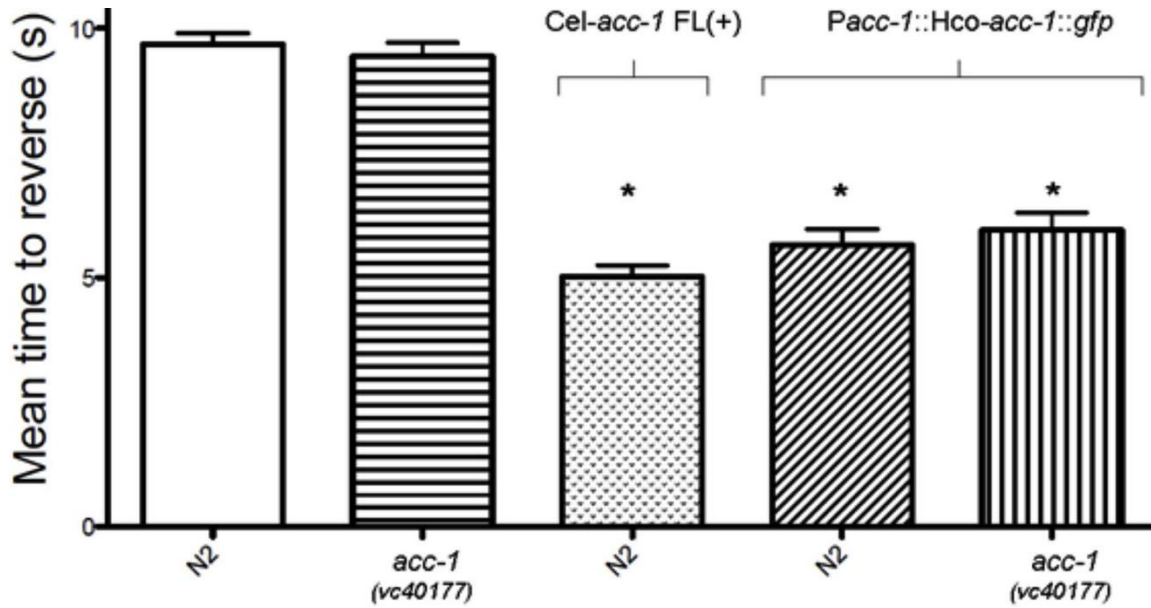


**Figure 3.4:** Mean time to reverse of *C. elegans* in the presence of 30% octanol. N2, wild type; ACC-1 vc40177, Cel-ACC-1 knockout strain. PACC-1::ACC-1 FL(+) – overexpression of Cel-ACC-1 in N2 WT. PACC-1::Hco-ACC-1::GFP expression of Hco-ACC-1 in the wild type N2 *C. elegans* strain and the ACC-1 vc40177 (Cel-ACC-1 knockout) strains. Stars denote significant difference ( $P < 0.0005$ ) compared to N2.

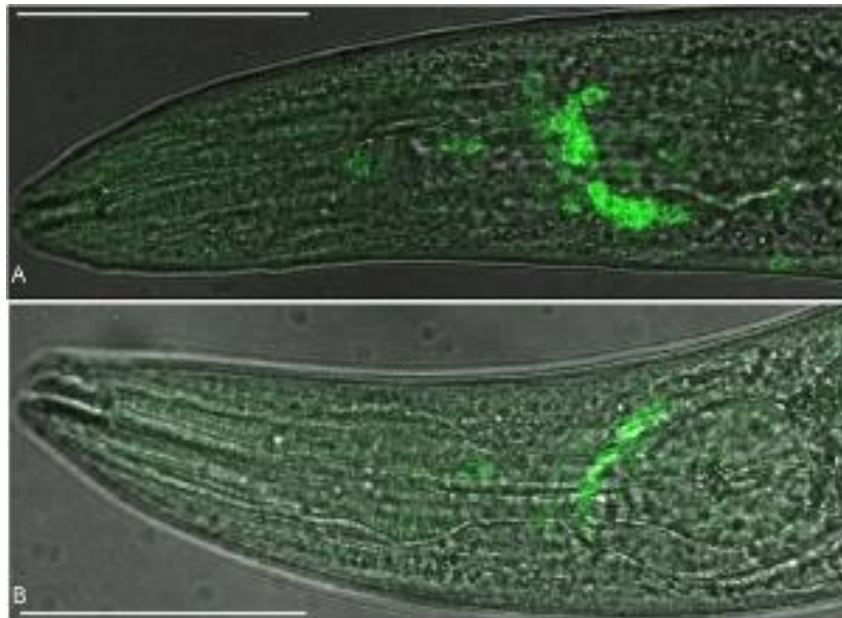


**Figure 3.5:** Confocal image of N2 *Caenorhabditis elegans* worms expressing *hco-acc-1* under control of the *cel-acc-1* wild type promoter. Images A and B both show the expression of the construct in neurons near the posterior (terminal bulb) of the pharynx. Line represents 100  $\mu$ m.

### 3.4: Discussion

Here we report the isolation and characterization of an acetylcholine-gated chloride channel from a parasitic nematode. Recently, Wever et al. (2015) provided evidence that the ACC family of receptors were potentially good anthelmintic targets in *C. elegans*. Here *avr-15* (encoding a GluCl subunit) under the control of *acc* promoters exhibited high level of sensitivity to ivermectin demonstrating that the ACC family of receptors function in what was referred to as “essential” tissues. In this case one of the essential tissues was extrapharyngeal neurons (Wever et al., 2015). Interestingly, while we did not observe the localization of Hco-ACC-1 in any neurons in *H. contortus* we consistently found this receptor in pharyngeal muscle tissue. It appears therefore that although ACC-1 localizes to different tissues in *H. contortus* compared to *C. elegans* though they both appear to function in tissues that would be considered essential from the point of view of anthelmintic action.

The difference in the localization of ACC receptors between *C. elegans* and *H. contortus* resembles the situation observed with the ivermectin target, the GluCl channel. In *C. elegans*, GluCl channel subunits have been localized to pharyngeal muscle and various neurons (Dent et al., 1997, 2000; Laughton et al., 1997), but in *H. contortus*, the GluCl receptors localized thus far were found to be exclusively neuronal (Portillo et al., 2003). However, both nematodes are still very sensitive to ivermectin with respect to both locomotion and pharyngeal pumping (Dent et al., 1997; Wolstenholme, 2012). Here, we have found that Hco-ACC-1 localizes to pharyngeal muscle tissue in *H. contortus* but localizes to pharyngeal neurons in *C. elegans*. It is tempting to speculate that like the GluCls, the ACCs family of receptors show different expression patterns but have some overlapping function between *H. contortus* and *C. elegans*. We are in the process of characterizing all additional ACC subunits from *H. contortus* to provide better insight into how conserved the function is between free-living and parasitic nematodes.

An additional difference in ACC-1 between *H. contortus* and *C. elegans* comes from the oocyte expression experiments. Here we found that unlike Cel-ACC-1 that was reported to form a functional homomeric channel (Putrenko et al., 2005), Hco-ACC-1 does not. However, we have observed that in general the *hco-acc* genes do not express in oocytes as readily as other cys-loop receptors we have examined in our laboratory. However, co-expression of Hco-ACC-1 and 2 yielded a channel 3x more sensitive to ACh (EC<sub>50</sub> 5.9 μM) compared to the Hco-ACC-2 homomeric channel. Differences in sensitivities between nematode homomeric and heteromeric channels have also been observed in the UNC-49 GABA receptor

(Bamber et al., 1999; Siddiqui et al., 2010) and the GluCl (Cully et al., 1994). Interestingly, we have found that changing loop B phenylalanine to a tyrosine in Hco-ACC-2 produced a hypersensitive channel with an  $EC_{50}$  of 2.9  $\mu$ M (Habibi et al., 2018). In Hco-ACC-1 there is a naturally occurring tyrosine (Y178) at the analogous position which may partially explain why the ACC-1/2 heteromeric channel was more sensitive to ACh compared to the ACC-2 homomeric channel. The significance of this naturally occurring tyrosine in Hco-ACC-1 to the *in vivo* function of the receptor is unknown. Moreover, we are still uncertain whether Hco-ACC-1 requires co-expression with additional subunits *in vivo* and while we have found that ACC-1 can co-express with ACC-2 in oocytes we have been unsuccessful, thus far, in determining the tissue location of ACC-2. Thus, we do not know at this time whether Hco-ACC-1 and 2 assemble to form a functional channel *in vivo*. The oocyte experiments merely suggest that the assembly of ACC-1 and ACC-2 is possible.

Examination of the Hco-ACC-1 binding site using *in silico* modelling has also highlighted some unique features of this receptor family. Aside from the fact that ACCs are not present in mammals, they also appear to have a unique agonist binding site. The most striking difference between Hco-ACC-1 and both alpha and non-alpha nAChRs is absence of the signature cys-cys motif in binding loop C (see Fig. 3.1A). Second, the tryptophan residue that has been shown in nAChRs to contribute to a pi-cationic interaction with the quaternary amine of acetylcholine (and carbachol) is still present in ACC-1, but is located in loop C (W225) rather than in the traditional loop B seen in nicotinic receptors and the AChBP (Beene et al., 2002; Celie et al., 2004). Recently, we have shown that this loop C tryptophan is crucial for receptor function in the Hco-ACC-2 receptor (Habibi et al., 2018). Interestingly, a similar shifting of this key tryptophan residue from loop B to C is also seen when we compare serotonin 5-HT<sub>3</sub> and nematode MOD-1 receptors (Mu et al., 2003). A loop C tryptophan is also present in tyramine and dopamine-gated chloride channels (Beech et al., 2013), suggesting that it may be important for the ability of nematode cys-loop receptors to respond to a diverse array of molecules. However, it is important to note that the binding site for ACh on the Hco-ACC-1/2 channel could also be on the interface of two ACC-1 or ACC-2 subunits (Habibi et al., 2018) or an ACC-2/1 heterodimer. Further research will be important to determine the subunit stoichiometry and variation in binding-sites of the ACC family of receptors.

While traditionally characterized as a muscarinic receptor agonist used primarily for the treatment of glaucoma, we have shown that carbachol (carbamylcholine) is an effective agonist at the nematode ACC-1/2 receptor with an  $EC_{50}$  about 2-fold higher than acetylcholine. Carbachol is also an agonist for muscle



nicotinic receptors but with an EC<sub>50</sub> over 10 -fold higher compared to acetylcholine (Akk and Auerbach, 1999). Perhaps the structural differences between nAChRs and ACC receptors as outlined above can explain the relatively high sensitivity of carbachol observed in our study. Nevertheless, it is clear that further study of the molecular pharmacology of ACC receptors can provide an excellent opportunity for the study of current AChR agonists and the possible discovery of novel agonists.

In conclusion, this study provides the first investigation of role of ACC receptors in parasitic nematodes. While research using *C. elegans* to evaluate anthelmintic targets is an excellent tool to provide relevant information, research on similar targets in parasitic nematodes can provide key information on whether a rational drug design approach might be worthwhile. While there is still much more to be learned about the role of ACC receptors in parasitic nematodes it is clear that comparing the function of the LGCC family in free-living and parasitic nematodes can potentially lead to the discovery of future anthelmintic targets and a better understanding of the evolution of parasitism.

### 3.5: Acknowledgements

Research was funded by the Natural Science and Engineering Council of Canada (NSERC) (Grant #210290) SGF. The funding body played no role in the design or execution of the study. The authors declare no conflict of interest. We thank Paula Ribeiro, McGill University, for the antibodies used in this study and the many years of mentorship and contribution to the field of helminth neurochemistry.

### 3.6: References

Abdelmassih SA, Cochrane E, and Forrester SG (2018) Evaluating the longevity of surgically extracted *Xenopus laevis* oocytes for the study of nematode ligand-gated ion channels. *Invertebr. Neurosci.* 18, 1

Accardi MV, Forrester SG (2011) The *Haemonchus contortus* UNC-49B subunit possesses the residues required for GABA sensitivity in homomeric and heteromeric channels. *Mol Biochem Parasitol* 178(1-2):15-22

Akk G, Auerbach A (1999) Activation of muscle nicotinic acetylcholine receptor channels by nicotinic and muscarinic agonists. *Br J Pharmacol* 128(7):1467-76

Beech R, Callanan M, Rao V, Dawe G, and Forrester S. (2013) Characterization of cys-loop receptor genes involved in inhibitory amine neurotransmission in parasitic and free living nematodes. *Para. Int.* 62: 599-605

Boulin T, Fauvin A, Charvet CL, Cortet J, Cabaret J, Bessereau J, Neveu C. 2011. Functional reconstitution of *Haemonchus contortus* acetylcholine receptors in *Xenopus* oocytes provides mechanistic insights into levamisole resistance. *Br. J. Pharmacol.* 164:1421–1432.

Chao M, Komatsu H, Fukuto H, Dionne H, and Hart A. (2004). Feeding status and serotonin rapidly and reversibly modulate a *Caenorhabditis elegans* chemosensory circuit. *Proc Natl Acad Sci* 101:15512–15517

Frohman M. A., Dush M. K. and Martin G. R. (1988) Rapid production of full-length cDNAs from rare transcripts: amplification using a single gene-specific oligonucleotide primer. *Proc. Natl Acad. Sci. USA* 85:8998–9002.

Hobert O. (2002). PCR fusion-based approach to create reporter gene constructs for expression analysis in transgenic *C. elegans*. *Biotechniques.* 32:728-30.

Irwin JJ, Sterling T, Mysinger MM, Bolstad ES, Coleman RG. (2012) ZINC: a free tool to discover chemistry for biology. *J Chem Inf Model* 23;52(7):1757-68

Jones A, and Sattelle D. (2008). The cys-loop ligand-gated ion channel gene superfamily of the nematode, *Caenorhabditis elegans*. *Invert Neurosci.* 8(1):41-47

Jensen ML, Pedersen LN, Timmermann DB, Schousboe A, Ahring PK. (2005) Mutational studies using a cation-conducting GABA<sub>A</sub> receptor reveal the selectivity determinants of the Cys-loop family of ligand-gated ion channels. *J Neurochem* 92(4):962-72

Kusano K, Miledi R and Stinnakre J (1982) Cholinergic and catecholaminergic receptors in the *Xenopus* oocyte membrane. *J. Physiol. (Lond.)* 328, 143–170.

Köhler P. (2001) The biochemical basis of anthelmintic action and resistance. *Int. J. Parasitol.* 31(4): 336–345.

Komuniecki R, Hapiak V, Harris G, Bamber B (2014) Context-dependent modulation reconfigures interactive sensory-mediated microcircuits in *Caenorhabditis elegans*. *Curr Opin Neurobiol.* 29:17-24. doi: 10.1016.

Komuniecki R, Harris G, Hapiak V, Wragg R, Bamber B (2012) Monoamines activate neuropeptide signaling cascades to modulate nociception in *C. elegans*: a useful model for the modulation of chronic pain? *Invert Neurosci.* 12(1):53-61. doi: 10.1007/s10158-011-0127-0.

Laskowski R, MacArthur M, Moss D, and Thornton J. (1993). PROCHECK - a program to check the stereochemical quality of protein structures. *J. App. Cryst.* 26: 283-291.

McCavera S, Rogers AT, Yates DM, Woods DJ, Wolstenholme AJ (2009) An ivermectin-sensitive glutamate-gated chloride channel from the parasitic nematode *Haemonchus contortus*. *Mol Pharmacol* 75(6):1347-55

Mehlhorn H. (2008) *Encyclopedia of Parasitology* (3rd edn). Springer, Berlin Heidelberg.

Mello C, and Fire A (1995). DNA Transformation. *Methods Cell Biol.* 48: 451-82.

Morris GM, Huey R, Lindstrom W, Sanner MF, Belew RK, Goodsell DS, Olson AJ. (2009) AutoDock4 and AutoDockTools4: Automated docking with selective receptor flexibility. *J Comput Chem* 30(16):2785-91

Pereira L, Kratsios P, Serrano-Saiz E, Sheftel H, Hobert O *et al.* (2015) A cellular and regulatory map of the cholinergic nervous system of *C. elegans*. *Elife.* pii: e12432. doi: 10.7554/eLife.12432.

Pettersen EF, Goddard TD, Huang CC, Couch GS, Greenblatt DM, Meng EC, Ferrin TE. (2004) UCSF Chimera - a visualization system for exploratory research and analysis. *J Comput Chem* 25(13):1605-12

Rao V, Siddiqui S, Prichard R, and Forrester S. (2009). A dopamine-gated ion channel (HcGGR3\*) from *Haemonchus contortus* is expressed in the cervical papillae and is associated with macrocyclic lactone resistance. *Mol Biochem Parasitol.* 166(1):54-61

Raza A, Lamb J, Chambers M, Hunt P, and Kotze A. (2016). Larval development assay reveal the presence of sub-populations showing high- and low-level resistance in a monepantel (Zolvix®)-resistant isolate of *Haemonchus contortus*. *Vet Parasitol.* 220:77-82

Sarai R, Kopp S, Knox M, Coleman G, Kotze A. (2015). In vitro levamisole selection pressure on larval stages of *Haemonchus contortus* over nine generations gives rise to drug resistance and target site gene expression changes specific to the early larval stages only. *Vet Parasitol.* 211(1-2):45-53

Siddiqui SZ, Brown DD, Rao VT, Forrester SG (2010) An UNC-49 GABA receptor subunit from the parasitic nematode *Haemonchus contortus* is associated with enhanced GABA sensitivity in nematode heteromeric channels. *J Neurochem* 113(5):1113-22

Trott O, Olson AJ. (2010) AutoDock Vina: improving the speed and accuracy of docking with a new scoring function, efficient optimization, and multithreading. *J Comput Chem* 30;31(2):455-61

Urdaneta-Marquez L, Bae SH, Janukavicius P, Beech R, Dent J, Prichard R. (2014) A dyf-7 haplotype causes sensory neuron defects and is associated with macrocyclic lactone resistance worldwide in the nematode parasite *Haemonchus contortus*. *Int J Parasitol* 44(14):1063-71

Van Doren K, Hirsh D. (1988) Trans-spliced leader RNA exists as small nuclear ribonucleoprotein particles in *Caenorhabditis elegans*. *Nature* 6;335(6190):556-9

Weston D., Patel B. and Van Voorhis W. C. (1999) Virulence in *Trypanosoma cruzi* infection correlates with the expression of a distinct family of sialidase superfamily genes. *Mol. Biochem. Parasit.* 98:105–116.

Wever C, Farrington D, and Dent J. (2015). The Validation of Nematode-Specific Acetylcholine-Gated Chloride Channels as Potential Anthelmintic Drug Targets. *PLoS One.* 2210(9)

Zhang J, Xue F, Chang Y. (2008) Structural determinants for antagonist pharmacology that distinguish the rho1 GABA<sub>C</sub> receptor from GABA<sub>A</sub> receptors. *Mol Pharmacol* 74(4):941-51

## Connecting Statement II

The work outlined in Chapter III highlights the ability for members of the ACC-1 family to co-assemble with one another when expressed in *Xenopus* oocytes. Specifically, I observed that although Hco-ACC-1 does not form a functional homomeric channel, it does associate with Hco-ACC-2 to form a heteromeric receptors which exhibits increased sensitivity to ACh compared to the Hco-ACC-2 homomeric receptor. This led me to hypothesize that Hco-ACC-1 may have the ability to co-assemble with other members of the ACC-1 family. In the following chapter, I introduce two previously uncharacterized ACC-1 family members, Hco-LGC-46 and Hco-ACC-4. This is the first pharmacological characterization of the LGC-46 receptor from *H. contortus*. The following chapter demonstrates that, similar to Hco-ACC-2, Hco-LGC-46 also forms a heteromeric receptor with Hco-ACC-1, which is significantly more sensitive to cholinergic ligands compared to the Hco-LGC-46 homomeric receptor. In addition, this chapter describes the potential role Hco-ACC-4 plays in inhibiting function of the ACC-1 family of receptors.

## Chapter IV – Manuscript III

Isolation and characterization of a novel member of the ACC ligand-gated chloride channel family, Hco-LCG-46, from the parasitic nematode *Haemonchus contortus*.

**Sarah A. Habibi**, Stephen M. Blazie, Yishi Jin and Sean G. Forrester

Published in:

Molecular Biochemical Parasitology. 237(111276)

DOI: [10.1016/j.molbiopara.2020.111276](https://doi.org/10.1016/j.molbiopara.2020.111276)

## 4.0: Abstract

The ACC-1 family of cys-loop receptors are ligand-gated chloride channels sensitive to acetylcholine (ACh), and are only present in invertebrates. Studies of this family of inhibitory receptors has provided insight into how they bind and respond to ACh in a manner vastly different from nicotinic acetylcholine receptors and appear to be present in tissues that are relevant to anthelmintic action. Here, we have identified two members of the ACC-1 family from the parasitic nematode *Haemonchus contortus*, Hco-LGC-46 and Hco-ACC-4. Hco-LGC-46 is an ACC subunit that has never been previously expressed and pharmacologically characterized. We found that Hco-LGC-46 when expressed in *Xenopus laevis* oocytes forms a functional homomeric channel that is responsive to the cholinergic agonists ACh and methylcholine. *hco-lgc-46* expressed in a *C. elegans lgc-46* null strain (*ok2900*) suppressed hypersensitivity to aldicarb in a manner similar to *cel-lgc-46*. It was also found that Hco-LGC-46 assembles with Hco-ACC-1 and produces a receptor that is over 5-fold more sensitive to ACh and responds to the cholinergic agonists methychole and carbachol. In contrast, the co-expression of Hco-LGC-46 with Hco-ACC-4 resulted in non-functional channels in oocytes. Hco-ACC-4 also appears to form heteromeric channels with a previously characterized subunit, Hco-ACC-2. Co-expression of Hco-ACC-4 with Hco-ACC-2 resulted in a functional heteromeric channel with an EC<sub>50</sub> value similar to that of the Hco-ACC-2 homomeric channel. However, the maximum currents generated in the ACC-4/ACC-2 channel were significantly ( $p < 0.005$ ) lower than those from the ACC-2 homomeric channel. Overall, this is the first report confirming that *lgc-46* encodes an acetylcholine-gated chloride channel which when co-expressed with *acc-4* results in reduced receptor function or trafficking in oocytes.

## 4.1: Introduction

Ion channels have been extensively studied, due to the role they play in fast synaptic neurotransmission in the nervous system of vertebrate and invertebrate organisms. The cys-loop (cysteine-loop) superfamily of ligand-gated ion channels are a major class of receptor-coupled ion channels that play a significant role in the nervous system of invertebrates, making them prime targets for nematocides (Del Castillo et al. 1963). These channels have been shown to be gated by neurotransmitters such as gamma-aminobutyric acid (GABA) (Bamber et al. 1999; Siddiqui et al. 2010), glutamate (Cully et al. 1994), tyramine (Pirri et al. 2009), serotonin (Ranganathan et al. 2000), and acetylcholine (Putrenko et al. 2005).

Cholinergic neurotransmission is mediated by ACh receptors including nicotinic ACh receptors (nAChRs), which are cation-selective channels that result in neuro-excitation in the presence of agonists. However, early studies of the mollusk, *Aplysia*, revealed a population of receptors that resulted in neuro-inhibition in the presence of ACh (Kehoe and McIntosh 1998b). Further investigation in the free-living nematode *Caenorhabditis elegans* led to the identification of the inhibitory acetylcholine-gated chloride channel (ACC-1) family of cys-loop receptors (Putrenko et al. 2005; Wever et al. 2015). The entire family is encoded by eight receptor subunit genes, named *acc-1*, *-2*, *-3*, and *-4*, and *lgc-46*, *-47*, *-48*, and *-49* (Jones and Sattelle 2008). Of these eight genes, 7 have been identified in the sheep parasite *Haemonchus contortus*, with the absence of *lgc-48* (Laing et al. 2013). The ACC-1 family is of interest since they are nematode specific receptors that do not contain homologs in mammalian species (Putrenko et al. 2005). In addition, they are shown to be present in anthelmintic relevant tissues, such as pharyngeal neurons in *C. elegans* (Wever et al. 2015) and pharyngeal muscle in *H. contortus* (Callanan et al. 2018), making them prime candidates for the development of novel pharmaceuticals.

Recent work by our group identified and pharmacologically characterized two members of the ACC-1 family, ACC-1 and ACC-2, from *H. contortus*. We found that Hco-ACC-2 forms a functional homomeric channel when expressed in *Xenopus laevis* oocytes (Habibi et al. 2018). Although Hco-ACC-1 does not form a function homomeric receptor on its own, it does associate with Hco-ACC-2 to form a heteromeric receptor which exhibits increased sensitivity to acetylcholine compared to the ACC-2 homomeric channel (Callanan et al. 2018). Immunolocalization of Hco-ACC-1 revealed specific expression in the anterior part of the pharynx of adult *H. contortus*, revealing a potential role in parasite feeding (Callanan et al. 2018).

Aside from ACC-1 through -4, very little is known about the other members of the ACC-1 family. However, it has been shown that in *C. elegans* LGC-46 and ACC-4 are strongly expressed in cholinergic motor neurons (Pereira et al. 2015; Takayanagi-Kiya et al. 2016). Specifically they are localized to presynaptic terminals on these neurons and are involved in synaptic vesicle release (Takayanagi-Kiya et al. 2016). This suggests the possibility that LGC-46, ACC-4, and other members of the ACC-1 family have the ability to form heteromeric channels. However, to date only ACC-1 through -4 have been expressed and functionally characterized in *Xenopus* oocytes (Putrenko et al. 2005; Callanan et al. 2018; Habibi et al. 2018) so it is unknown whether other members, such as LGC-46, can form ACh-gated chloride channels.



Here, we report the first pharmacological characterization of the LGC-46 receptor from the parasitic nematode *H. contortus*. We found that LGC-46 forms a functional homomeric receptor which is sensitive to acetylcholine and other cholinergic ligands. In addition, the co-expression of LGC-46 with ACC-1 results in an acetylcholine receptor that is 5x more sensitive to ACh compared to the LGC-46 homomeric channel. In contrast, the co-expression of ACC-4 with LGC-46 inhibited receptor function in *Xenopus* oocytes. Our data suggests that that LGC-46 interacts with both ACC-2 and ACC-4 in oocytes, but only the LGC-46/ACC-2 channel is functional.

## 4.2: Methods

### 4.2.1: Isolation of *hco-lgc-46* and *hco-acc-4*

Whole adult *H. contortus* were received from Dr. Prichard (Institute of Parasitology, McGill University). Total RNA was extracted from adult male *H. contortus* worms using Trizol (Invitrogen, Carlsbad, USA). Complementary DNA (cDNA) was synthesized using the Quantitect Reverse Transcriptase kit from Qiagen (Dusseldorf, Germany), using a unique 3' oligo-dT anchor primer sequence (5'CCTCTGAAGGTTACGGATCCACATCTAGATTTTTTTTTTTTTTTTTTVN3'); [where V is either A, C, or G and N is either A, C, G, or T] (Weston et al. 1999). Gene specific primers were generated based on a full sequence provided by Dr. Robin Beech (McGill University) as part of the genome sequencing project for *H. contortus* (Laing et al. 2013). Amplification of the complete *hco-lgc-46* and *hco-acc-4* genes was carried out using primers specific to the 5' and 3' end of the gene with XbaI and XmaI restrictions sites. *hco-lgc-46* and *hco-acc-4* were subcloned into the *X. laevis* expression vector pGEMHE (Zhang et al. 2008).

### 4.2.2: Expression in *Xenopus laevis* oocytes

All animal procedures followed the University of Ontario Institute of Technology Animal Care Committee and the Canadian Council on Animal Care guidelines. Channels were expressed in *X. laevis* oocytes according to (Abdelmassih et al. 2018). Female *X. laevis* frogs were supplied by Nasco (Fort Atkinson, WI, USA). Animals were fed and tanks were cleaned regularly. Frogs were housed in a climate-controlled room (18°C) with continuous light cycling. Frogs were anesthetized with 0.15% 3-aminobenzoic acid ethyl ester methanesulphonate salt (MS-222) buffered with NaHCO<sub>3</sub> to pH 7 (Sigma-Aldrich, Oakville, ON, CA). Surgical removal of a section of the ovary of the frog was performed, and the lobe was defolliculated with

a calcium-free oocyte Ringer's solution (82 mM NaCl, 2 mM KCl, 1 mM MgCl<sub>2</sub>, 5 mM HEPES pH 7.5 (Sigma-Aldrich) (OR-2) containing 2 mg/mL collagenase-II (Sigma-Aldrich). The oocytes in the defolliculation solution were incubated at room temperature for 2h. Collagenase was washed from the oocytes with ND96 solution (1.8 mM CaCl<sub>2</sub>, 96 mM NaCl, 2 mM KCl, 1 mM MgCl<sub>2</sub>, 5 mM HEPES pH 7.5) and allowed one hour to recover at 18°C in ND96 supplemented with 275 µg/mL pyruvic acid (Sigma-Aldrich) and 100 µg/mL of the antibiotic gentamycin (Sigma-Aldrich) (Supplemented ND96). Stage V and VI oocytes were selected for cytoplasmic injection of cRNA.

The pGEMHE vector containing the *hco-lgc-46*, *hco-acc-1*, *hco-acc-2*, and *hco-acc-4* coding sequences were linearized using Sph1 or NheI (New England Biolabs, USA), and used as templates for an *in vitro* transcription reaction (T7 mMessage mMachine kit, Ambion, Austin, TX, USA) yielding copy RNA corresponding to each gene. *X. laevis* oocytes were injected with 50 nl of each subunit gene (0.5 ng/µL) alone or in combination (0.25 ng/µL each) using the Drummond (Broomall, PA, USA) Nanoject microinjector. Oocytes were also co-injected with the *H. contortus* genes *unc-50*, *unc-74*, and *ric-3.1* (Boulin et al. 2011). The injected oocytes were incubated at 18°C in supplemented ND96 solution. Electrophysiological recordings of the oocytes were conducted between 48 and 72 hours after cRNA injection.

#### 4.2.3: Electrophysiological recordings

Two-electrode voltage clamp electrophysiology was conducted using the Axoclamp 900A voltage clamp (Molecular Devices, Sunnyvale, CA, USA). Glass electrodes were produced using a P-97 Micropipette Puller (Sutter Instrument Co., Novato, CA, USA). The electrodes were backfilled with 3M KCl and contained Ag|AgCl wires. The following molecules were first dissolved in ND96; Acetylcholine (ACh), Carbamoylcholine Chloride (Carbachol), Acetyl-β-methylcholine Chloride (Methacholine), Levamisole Hydrochloride (Levamisole), and Pyrantel Citrate Salt (Pyrantel) [Santa Cruz Biotechnology]. These solutions were perfused over oocytes using the RC-1Z recording chamber (Warner Instruments Inc., Hamdan, CT, USA). Data was analyzed using Clampex Software v10.2 (Molecular Devices) and all graphs were generated using Graphpad Prism Software v5.0 (San Diego, CA, USA). EC<sub>50</sub> values were determined by dose response curves that had been fitted to the following equation:

$$I_{max} = 1 / \left[ 1 + \left( \frac{EC_{50}}{[D]} \right)^h \right]$$

Where  $I_{max}$  is the maximal response,  $EC_{50}$  is the concentration of compound required to elicit 50% of the maximal response,  $[D]$  is compound concentration, and  $h$  is the Hill coefficient. Both  $EC_{50}$  and  $h$  are free parameters, and the curves were normalized to the estimated  $I_{max}$ . Graphpad Prism used the equation to fit a sigmoidal curve of variable slopes to the data. Means were determined from at least 7 oocytes from at least three batches of frogs.

Current-voltage relationships were recorded by changing the holding potential from -60 mV to 40 mV in 20 mV increments. At each step the oocyte was exposed to either a 1 or 10 mM concentration of ACh. For reduced  $Cl^-$  trials, NaCl was partially replaced by Na-gluconate (Sigma) in the ND96 buffer solution, for a final  $Cl^-$  concentration of 62.5 mM. Current-voltage graphs were generated using Graphpad Prism Software v5.0 (San Diego, CA, USA).

#### 4.2.4: *In silico* modelling

The protein coding sequences of Hco-LGC-46 and Hco-ACC-1 were aligned with the *Danio rerio* alpha-1 glycine receptor (3JAD). MODELLER v9.21 software (Šali and Blundell 1993) was used for the generation of the Hco-LGC-46 homodimer and Hco-ACC-1/Hco-LGC-46 heterodimer. Both homodimer and heterodimers were prepared for agonist docking using AutoDock Tools. Ligands were obtained from PubChem in their energy-reduced form. AutoDock Vina was used to simulate docking of each ligand to the homo- or hetero-dimers. Pymol was used to visualize the protein models with their associated ligands, and Chimera v1.6.1 (Pettersen et al. 2004) was used for the generation of figures.

#### 4.2.5: Expression of Hco-LGC-46 in *C. elegans*

The *C. elegans* strain (*ok2900*) is a knockout strain for *lgc-46* and the mutant worms are hypersensitive to aldicarb (Takayanagi-Kiya et al. 2016), an inhibitor of acetylcholine esterase, compared to WT. To generate *Punc-17βhco-lgc-46*, we amplified *hco-lgc-46* cDNA from pGEM *hco-lgc-46* using the primers YJ12412 and YJ12414 (Supplementary data T1). We used Gibson Assembly (NEB, Ipswich, MA) to clone the resulting amplicon downstream of the *Punc-17β* promoter sequence within expression vector pCZGY1091

(Takayanagi-Kiya et al. 2016), which was amplified using primers YJ12416 and YJ12417. *Punc-17 $\beta$*  is the sequence 498 bp upstream of the annotated (WS220) *C. elegans unc-17 $\beta$*  start codon and is active only in *C. elegans* cholinergic motor neurons (Charlie et al. 2006). Two independent transgenic lines expressing *Punc-17 $\beta$  hco-lgc-46* from transmitting extrachromosomal arrays were generated by injecting *Punc-17 $\beta$  hco-lgc-46* (15 ng/ $\mu$ l), *Pmyo-2::mCherry* (pCFJ90) co-injection marker (2.5 ng/ $\mu$ l), and 100bp DNA ladder (82.5 ng/ $\mu$ l) into the *lgc-46(ok2900)* background using standard *C. elegans* microinjection procedure (Mello et al. 1991). The *lgc-46(ok2900)* + empty vector transgenic line included as a control in our aldicarb assay was generated by injecting the empty pCZGY1091 plasmid (15 ng/ $\mu$ l), which contains *Punc-17 $\beta$*  and not the *hco-lgc-46* cDNA, along with *Pmyo-2::mCherry* (pCFJ90, 2.5 ng/ $\mu$ l), and 100 bp DNA ladder (82.5 ng/ $\mu$ l) into the *lgc-46(ok2900)* background. Construction of the extrachromosomal array line expressing *Punc-17 $\beta$  cel-lgc-46* was reported previously (Takayanagi-Kiya et al. 2016). In transgenic animals with *Pmyo-2* co-injection marker, no toxicity was observed. Aldicarb response was assessed using one-day old young adults on NGM plates seeded with OP50, containing 500  $\mu$ M aldicarb. Paralysis was defined as absence of movement in response to touch three times with a platinum wire pick and was assessed over a 5 hr period. Two independent trials involving n=15 worms per line were performed on different days. For each trial, the proportion of non-paralyzed worms at each time point was averaged and these results are reported in Figure 4.6.

### 4.3: Results

#### 4.3.1: Isolation of *hco-lgc-46* and *hco-acc-4*

The full-length cDNA of the *hco-lgc-46* gene consisted of 1569 nucleotides (GenBank Accession # MN402460). The sequence encodes a protein containing 522 amino acids. The full-length coding sequence of the *hco-acc-4* gene consisted of 1239 nucleotides (GenBank Accession # AHM25235.1) and encodes a protein containing 412 amino acids (KC918365.1). Both protein sequences contain all seven extracellular binding loops, four transmembrane domains, and the Cys-loop motif (Figure 4.1). The Hco-LGC-46 protein sequence shares 74% sequence similarity to the Cel-LGC-46 protein (Figure 4.1). The Hco-ACC-4 protein sequence shares 86% similarity with Cel-ACC-4. The PAR motif present at the beginning of the transmembrane 2 domain is indicative of anion selectivity (Jensen et al. 2002).

Hco-ACC-4 MYFGN~~FLLVFP~~---LLAD---A~~FEA~~---FE--EQNCPY~~GVC~~---SEAPPN~~LTIAPFG~~ 44  
 Cel-ACC-4 --MRLIILVIS---ILISNAGS~~LLRS~~---LEDDSN~~ECMFNCP~~---K---RARNV~~SVPH~~T 45  
 Hco-LGC-46 MY~~YITF~~LL~~LLLVFVGC~~S~~CNARRSVYRRNS~~RT~~LRRLSR~~N~~YDWEVDEHGGLRPI~~I~~INPAK~~~~VERA~~ 60  
 Cel-LGC-46 M~~QYLQ~~~~FLSLV~~-VLL~~IM~~CH~~ARKSVYRRNS~~PS~~LRRL~~~~TRNYDWEVDEHGGLKPI~~I~~INPAK~~~~VERA~~ 59  
 Dre-GLY- $\alpha$ 1 ----- 0

Hco-ACC-4 SGLCTGDDV~~IIEHI~~---LHD~~YNKLEL~~--PGGGH~~VKVSVEI~~W~~VQEVSKIIEITSEFELDIY~~ 99  
 Cel-ACC-4 E~~KTCMGDDAIIAQI~~---LDG~~YNKLDL~~--PGGGH~~VVVSIEI~~W~~VQEVSKIIEITSEFELDIY~~ 100  
 Hco-LGC-46 T~~KECANDSYILSAI~~---MHN~~YNRHKI~~--PGG-~~QVEVKEV~~W~~VQVEITTI~~SD~~ITSD~~FD~~IQLDIY~~ 114  
 Cel-LGC-46 T~~KNCANDS~~FIL~~GTI~~---MSN~~YNRHKI~~--PGG-~~QVDVEV~~W~~VQVEITTI~~SD~~ITSD~~FD~~IQLDIY~~ 113  
 Dre-GLY- $\alpha$ 1 -----APSE~~FLDKLMGKVSGYDARI~~PN~~FKGPPVNVTCNIFINSFGSIAET~~TM~~DYRVNIF~~ 55  
 . : : : : \* : \* \* \* : : : : . \* : \* : : : : \*

Hco-ACC-4 VTERW~~TDPNLAYAHLN~~PCKS~~IMSV~~DG~~R~~TI~~IERIWNPHACFVNSKLANIHTSPFKNI~~FL~~QI~~ 159  
 Cel-ACC-4 VTERW~~TDP~~S~~LAYSHLN~~PCKS~~NMSV~~DGAT~~ILNKIWNPHACFVNSKLANIHES~~SP~~FKNIFLQI~~ 160  
 Hco-LGC-46 ISEM~~WLPALDY~~SALN~~PCKYNLSLNS~~-V~~LEK~~L~~WT~~PN~~SCFIN~~SK~~TADLHKS~~PF~~PNI~~FL~~LI~~ 173  
 Cel-LGC-46 IY~~ETWYDPALNYAFMN~~PCK~~YNLSLNS~~-V~~LEK~~L~~WT~~PN~~SCFIN~~SK~~TADLHKS~~PF~~PNI~~FL~~MI~~ 172  
 Dre-GLY- $\alpha$ 1 LR~~QQW~~ND~~PRLAYSEY~~P~~DDSL~~--DL~~DP~~-S~~MLDS~~I~~WK~~PD~~LFFAN~~E~~KANF~~H~~EV~~T~~TDN~~K~~LLRI~~ 112  
 : : \* \* \* \* : . : : : : \* \* \* \* \* : : \* \* \* \* : : \* \* \*

Hco-ACC-4 Loop D Loop A YSNGS~~I~~W~~YNYRIKLTG~~PCS~~N~~TL~~R~~TF~~PI~~D~~QQRCMLFYES~~FT~~H~~N~~H~~D~~QVEMEWID~~TV~~PPITIM~~ 219  
 Cel-ACC-4 YSNGS~~I~~W~~YNYRIKLTG~~PCS~~N~~TL~~R~~TF~~PI~~D~~QQRCMLFYES~~FT~~H~~N~~H~~D~~QVEMEWIT~~TV~~PPITIL~~ 220  
 Hco-LGC-46 YAN~~G~~S~~V~~W~~T~~N~~YRLK~~L~~Q~~G~~PC~~EM~~DL~~TR~~FP~~FD~~N~~V~~TC~~SL~~T~~FE~~S~~F~~N~~Y~~N~~T~~DE~~V~~Q~~M~~SW~~TP--S~~G~~V~~S~~K~~M~~ 231  
 Cel-LGC-46 YAN~~G~~TV~~WT~~N~~YRLK~~L~~Q~~G~~PC~~IM~~DL~~T~~K~~FP~~FD~~N~~V~~TC~~SL~~T~~FE~~S~~F~~N~~Y~~N~~T~~DE~~V~~K~~M~~D~~W~~SV--N~~G~~V~~Q~~K~~M~~ 230  
 Dre-GLY- $\alpha$ 1 SK~~NG~~N~~V~~L~~YSIRI~~TL~~V~~L~~AC~~PM~~DL~~KN~~FP~~MD~~V~~Q~~TC~~IM~~Q~~LES~~F~~G~~Y~~TM~~N~~DL~~I~~FE~~W~~DE--K~~G~~A~~V~~Q~~V~~ 170  
 \* \* : . \* : \* \* \* \* \* : : \* \* \* : : : : : \*

Hco-ACC-4 Loop E Loop B KGNI~~TLPDYV~~L~~VDF~~S~~ASS~~-EL~~R~~L~~Y~~PP~~GI~~F~~NELIAT~~TF~~FQRLYGFYILQVYVPAYISV~~F~~IS~~ 278  
 Cel-ACC-4 KGNI~~TLPDYV~~L~~VDF~~S~~SSS~~-EL~~R~~L~~Y~~PP~~GI~~F~~NELIAT~~TF~~FQRLYGFYILQVYVPAYISV~~F~~IS~~ 279  
 Hco-LGC-46 R~~K~~M~~E~~L~~A~~D~~YEL~~V~~D~~I~~K~~N~~V~~R-N~~V~~E~~P~~Y~~PAGY~~W~~HEL~~T~~M~~M~~F~~H~~F~~K~~R~~R~~A~~G~~WYILQAYLP~~TY~~L~~T~~I~~C~~IS~~ 290  
 Cel-LGC-46 R~~K~~M~~E~~L~~A~~D~~YEL~~V~~D~~I~~H~~K~~I~~R-T~~T~~E~~E~~Y~~PAGY~~W~~HEL~~T~~M~~S~~F~~E~~F~~K~~R~~R~~A~~G~~WYILQAYLP~~TY~~L~~T~~I~~C~~IS~~ 289  
 Dre-GLY- $\alpha$ 1 A~~D~~G~~L~~T~~P~~Q~~FIL~~KE~~E~~K~~D~~L~~R~~Y~~CTK~~H~~Y~~N~~T~~G~~K~~F~~T~~C~~I~~E~~A~~R~~F~~H~~L~~E~~R~~Q~~M~~G~~Y~~L~~I~~Q~~M~~Y~~I~~P~~S~~L~~L~~I~~V~~I~~L~~S 230  
 . : \* : : \* : . \* \* \* \* : : \* : : \* \* \* \* : : : : \*

Hco-ACC-4 Loop F Loop C TM1 WVS~~F~~Y~~L~~G~~A~~E~~QIP~~S~~R~~T~~T~~V~~GVNS~~L~~L~~A~~L~~T~~FQ~~F~~G~~S~~V~~V~~N~~N~~L~~P~~K~~T~~S~~D~~V~~K~~A~~I~~D~~V~~W~~I~~L~~S~~S~~M~~A~~F~~I~~F~~A~~S~~L~~ 338  
 Cel-ACC-4 WVS~~F~~T~~L~~G~~A~~E~~QIP~~S~~R~~T~~T~~V~~GVNS~~L~~L~~A~~L~~T~~FQ~~F~~G~~A~~V~~N~~N~~L~~P~~K~~T~~S~~D~~V~~K~~A~~I~~D~~V~~W~~I~~L~~S~~S~~M~~A~~F~~I~~F~~A~~S~~L 339  
 Hco-LGC-46 W~~I~~S~~F~~A~~L~~G~~S~~K~~A~~I~~P~~A~~R~~T~~M~~L~~GVNS~~L~~L~~A~~M~~T~~FQ~~F~~G~~N~~I~~R~~N~~L~~P~~R~~V~~S~~Y~~V~~K~~A~~I~~D~~V~~W~~M~~L~~S~~C~~M~~T~~F~~V~~F~~C~~S~~L 350  
 Cel-LGC-46 W~~I~~S~~F~~A~~L~~G~~S~~K~~A~~I~~P~~A~~R~~T~~M~~L~~GVNS~~L~~L~~A~~M~~T~~FQ~~F~~G~~N~~I~~R~~N~~L~~P~~R~~V~~S~~Y~~V~~K~~A~~I~~D~~V~~W~~M~~L~~S~~C~~M~~T~~F~~V~~F~~C~~S~~L 349  
 Dre-GLY- $\alpha$ 1 W~~V~~S~~F~~W~~I~~N~~M~~D~~A~~A~~P~~A~~R~~V~~G~~I~~T~~V~~L~~T~~M~~T~~Q~~S~~S~~G~~S~~R~~A~~S~~L~~P~~K~~V~~S~~Y~~V~~K~~A~~I~~D~~I~~M~~A~~V~~C~~L~~L~~F~~V~~F~~S~~A~~L 290  
 \* : \* \* : . \* : \* : \* : \* : \* : \* : \* : \* : \* : \* : \* : \* : \* : \* : \* : \* : \*

Hco-ACC-4 TM2 TM3 IEL~~AV~~V~~G~~Y~~L~~TR~~NG~~N~~H~~A~~S~~I~~K~~CH~~C~~SW~~L~~----- 363  
 Cel-ACC-4 IEL~~AV~~V~~G~~Y~~L~~SR~~D~~Q~~H~~G~~S~~I~~K~~C~~R~~C~~SW~~L----- 364  
 Hco-LGC-46 IEL~~AW~~V~~G~~Y~~L~~S~~R~~E~~D~~E~~S~~P~~ST~~PP~~P~~ST~~P~~AL~~PS~~K~~SL~~P~~P~~L~~T~~LN~~K~~T~~T~~P~~V~~A~~P~~P~~T~~PS~~L~~Q~~V~~H~~S~~A~~S~~ST~~L~~ 410  
 Cel-LGC-46 IEL~~AW~~V~~G~~Y~~L~~S~~R~~E~~E~~E~~P~~T~~S~~A~~K~~L~~Q~~P-----SA~~Q~~V~~A~~P~~K~~P~~C~~H~~PP~~V~~Q~~Q~~N~~A~~N~~N~~S~~S~~V~~H~~R~~ 397  
 Dre-GLY- $\alpha$ 1 LE~~Y~~A~~A~~V~~N~~F~~I~~A~~R~~A~~G~~T~~K~~L~~F~~I----- 308  
 : \* \* \* . : : \*

Hco-ACC-4 ----- 363  
 Cel-ACC-4 ----- 364  
 Hco-LGC-46 H~~R~~R~~N~~P~~A~~N~~E~~E~~E~~S~~A~~L~~L~~S~~L~~R~~N~~D~~Y~~G~~I~~PP~~G~~F~~L~~NG~~N~~I~~A~~S~~A~~M~~R~~S~~F~~G~~A~~R~~C~~S~~C~~D~~P~~H~~Q~~S~~Y~~Q~~T~~E~~V~~D~~D~~V 470  
 Cel-LGC-46 R~~Q~~K~~Q~~P~~K~~N~~E~~E~~S~~A~~L~~L~~S~~L~~R~~N~~D~~Y~~G~~I~~PP~~G~~F~~L~~NG~~N~~V~~A~~N~~A~~M~~K~~S~~F~~S~~S~~C~~S~~C~~E~~P~~T~~N~~V~~V~~N~~L~~M~~L~~D~~E~~A 457  
 Dre-GLY- $\alpha$ 1 ----- 308

Hco-ACC-4 -----C~~I~~R~~C~~R~~D~~W~~T~~A~~A~~K~~L~~D~~K~~A~~S~~S~~V~~I~~F~~P~~T~~C~~F~~L~~F~~F~~N~~I~~W~~Y~~W~~F~~V~~L~~GN~~L~~L~~A~~A~~P~~G~~M~~K~~I~~R~~ 411  
 Cel-ACC-4 -----C~~M~~N~~K~~D~~W~~T~~A~~L~~K~~I~~D~~Q~~M~~S~~S~~I~~V~~F~~P~~V~~S~~F~~L~~A~~F~~N~~I~~W~~Y~~W~~F~~I~~FL~~G~~K~~L~~L~~V~~R~~T~~I~~----- 408  
 Hco-LGC-46 H~~P~~P~~E~~H~~V~~S~~Q~~T~~F~~S~~S~~R~~H~~Q~~R~~E~~R~~L~~A~~K~~R~~I~~D~~T~~L~~S~~A~~I~~L~~F~~P~~S~~L~~F~~S~~L~~F~~N~~I~~A~~Y~~W~~S~~H~~Y~~L~~R~~S~~D~~G----- 522  
 Cel-LGC-46 E~~T~~I~~P~~T~~S~~T~~S~~S~~S~~L~~S~~R~~K~~Q~~R~~E~~I~~L~~A~~H~~K~~I~~D~~S~~V~~S~~V~~F~~M~~F~~P~~F~~L~~V~~L~~F~~N~~I~~A~~Y~~W~~Q~~H~~Y~~L~~R~~G~~Y----- 508  
 Dre-GLY- $\alpha$ 1 -----S~~R~~A~~K~~R~~I~~D~~T~~V~~S~~R~~V~~A~~F~~P~~L~~V~~L~~I~~F~~N~~I~~F~~Y~~W~~I~~T~~Y~~K~~L~~V~~P~~R----- 342  
 \* : \* \* \* \* \* \* \* \* \* \* \* \* \* \* \*

Hco-ACC-4 R 412 TM4  
 Cel-ACC-4 - 408  
 Hco-LGC-46 - 522  
 Cel-LGC-46 - 508  
 Dre-GLY- $\alpha$ 1 - 342

**Figure 4.1:** Protein sequence alignment of the *H. contortus* Hco-LGC-46 and Hco-ACC-4 receptors with *C. elegans* Cel-LGC-46 and Cel-ACC-4 and *D. rerio* Dre-GLY- $\alpha$ 1 receptors. All five binding loops (Loop A-E), the characteristic cysteine residues that form the “cys-loop”, and four transmembrane domains (M1-M4) and highlighted with underlines. (\*) indicates identity and (:;) indicates similarity.

#### 4.3.2: Expression of *hco-lgc-46* and *hco-acc-1* in *Xenopus* oocytes

Upon injection of *X. laevis* oocytes with cRNA encoding Hco-LGC-46, along with the accessory proteins Hco-UNC-74, Hco-UNC-50, and Hco-RIC-3.1, a homomeric LGC-46 channel is formed (Figure 4.2A). The EC<sub>50</sub> value for the Hco-LGC-46 homomeric channel in response to ACh was 893 ± 200 μM (Figure 4.2C). The Hco-LGC-46 channel also responded to ACh derivative, methacholine, with an EC<sub>50</sub> value of 7348 ± 900 μM (Figure 4.2A and C). However, the Hco-LGC-46 channel did not respond to 20 μM carbachol. The Hco-ACC-1/Hco-LGC-46 channel was more sensitive to ACh compared to the Hco-LGC-46 homomeric channel (Figure 4.2A and B). The EC<sub>50</sub> value for the Hco-ACC-1/Hco-LGC-46 heteromeric channel in response to ACh was 166 ± 4 μM (Figure 4.2C). The heteromeric channel also responded to derivatives, carbachol and methacholine, with EC<sub>50</sub> values of 1680 ± 70 μM and 3990 ± 600 μM, respectively (Figure 4.2C). Carbachol was a partial agonist of the heteromeric channel, whereas for both the Hco-LGC-46 and Hco-LGC-46/ACC-1 channel, methacholine was a weak partial agonist. Neither the Hco-LGC-46 homomeric channel nor the Hco-ACC-1/Hco-LGC-46 heteromeric channel respond to the cholinergic anthelmintics 20 μM levamisole or 20 μM pyrantel.

Current-voltage analysis of the Hco-LGC-46 channel was conducted to confirm anion selectivity (Figure 4.3A). A full Cl<sup>-</sup> concentration of ND96 (103.6 mM Cl<sup>-</sup>) indicated a reverse potential of -17.44 ± 5 mV (n=5). This is consistent with the calculated Nernst potential for Cl<sup>-</sup> of -24.5 mV, when assuming an internal Cl<sup>-</sup> concentration of 50 mM (Kusano et al. 1982). When NaCl was partially replaced with Na-gluconate (final Cl<sup>-</sup> concentration of 62.5 mM) the reverse potential shifted to -3.4 ± 2 mV (n=5), which is also consistent with the assumed Nernst potential of -5.7 mV (Figure 4.3A). Current-voltage analysis of the Hco-ACC-1/LGC-46 channel indicated reverse potentials of -27.7 mV and -1.1 mV when recorded in full and partial chloride concentrations respectively (Figure 4.3B).

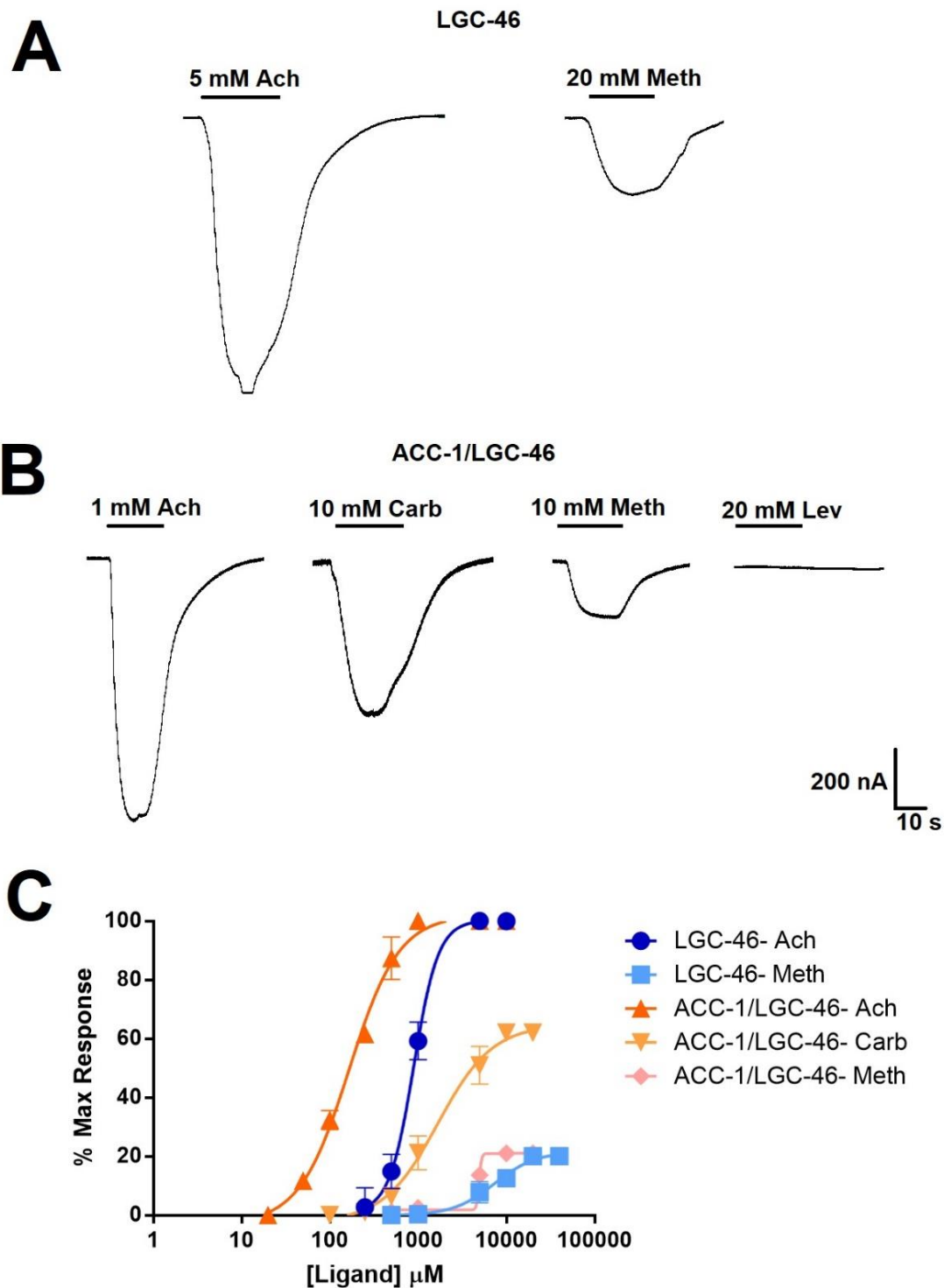


**Figure 4.2:** (A) Maximal electrophysiological response of the Hco-LGC-46 receptor in response to acetylcholine and methacholine. (B) Maximal electrophysiological response of the Hco-ACC-1/Hco-LGC-46 heteromeric receptor in the presence of acetylcholine, carbachol, methacholine, and levamisole. (C) Dose-response curves of the Hco-LGC-46 and Hco-ACC-1/Hco-LGC-46 receptors in the presence of ligands shown. Standard errors are shown.  $n \geq 7$  oocytes. Each curve is represented as a percent of the maximum acetylcholine response. Partial agonists are those that have a maximum response lower than 100%.

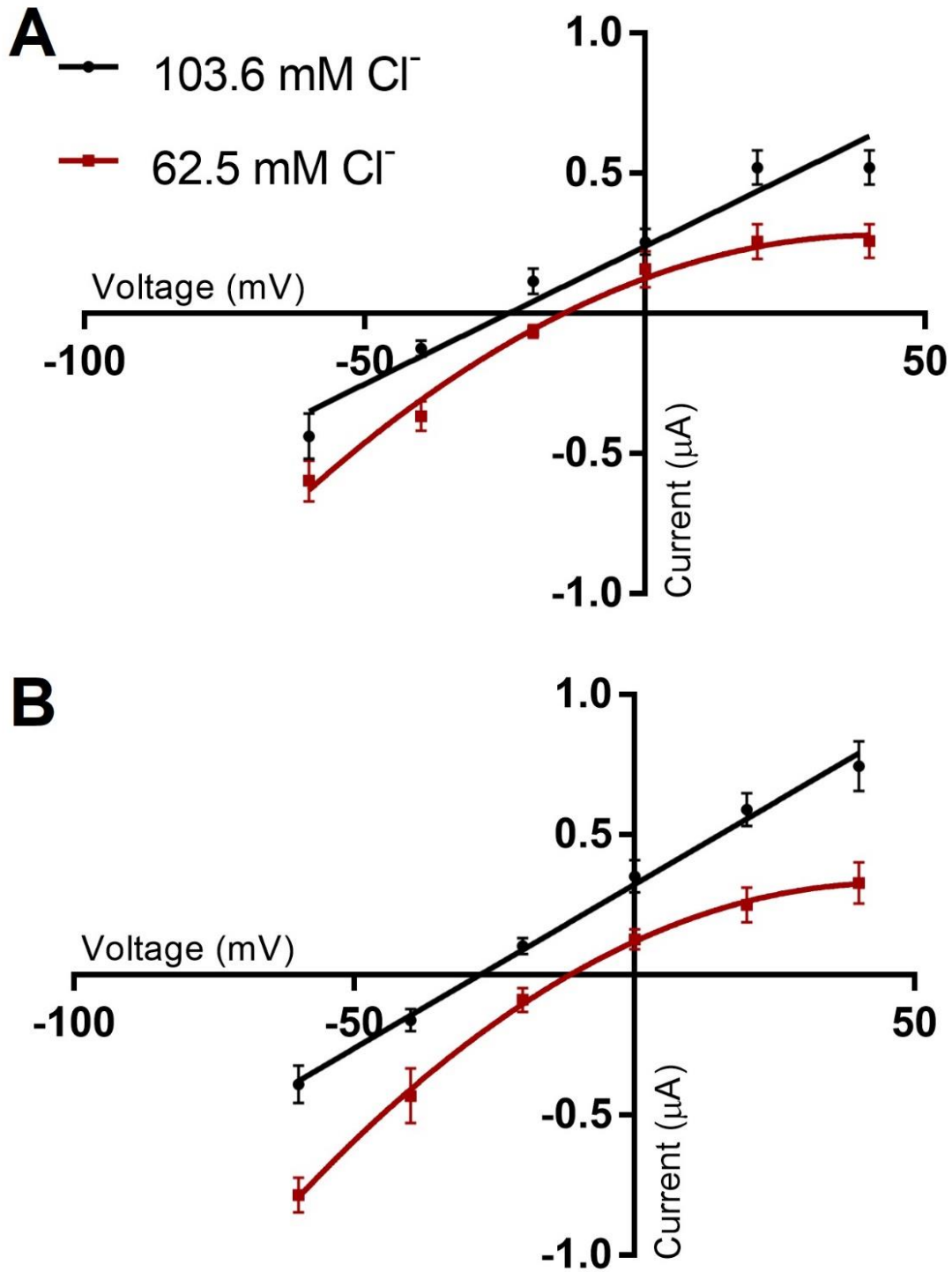


**Figure 4.3:** (A) Current-voltage analysis of the Hco-LGC-46 channel using 103.6 mM Cl<sup>-</sup> and 62.5 mM Cl<sup>-</sup> buffer solutions. Acetylcholine response was generated using a maximum concentration. The indicated reverse potentials were -17.44 mV and -3.4 mV when recorded in full and partial chloride concentrations respectively. Standard errors are shown. (B) Current-voltage analysis of the Hco-LGC-46/ACC-1 channel using 103.6 mM Cl<sup>-</sup> and 62.5 mM Cl<sup>-</sup> buffer solutions. Acetylcholine response was generated using a maximum concentration. The indicated reverse potentials were -27.7 mV and -1.1 mV when recorded in full and partial chloride concentrations respectively.



### 4.3.3: Homology modelling

To aid in understanding how the agonists sit in the binding pocket, homology models were generated. The Hco-LGC-46 homodimer and a Hco-ACC-1/Hco-LGC-46 heterodimer were produced using the *D. rerio* glycine receptor 3JAD as template. This template was chosen as it contained the highest sequence similarity with the ACC-1 family of receptors. The model for the Hco-LGC-46 homodimer is outlined in Figure 4.4A. The binding site appears to be composed of several aromatic residues. Docking of channel activators, ACh and methacholine, is outlined in Figures 4.4B and C. The quaternary amine on ACh is located 5.6 Å from W259. The asparagine (N182) in loop E is located 3.3 Å away from the carbonyl oxygen in ACh, allowing for potential hydrogen bond interactions to occur. Both ACh and Meth dock in an extended orientation in the LGC-46 binding pocket. However, the quaternary amine of methacholine is shifted away from W259. The model for the Hco-ACC-1/Hco-LGC-46 heteromeric channel is outlined in Figure 4.5A. Similar to the homomeric model, the binding site of the heteromeric channel is composed of many aromatic residues. Docking of agonists, ACh, carbachol, and methacholine, is shown in Figure 4.5B, C, and D. The quaternary amine on ACh and carbachol is located 5.2 Å from W225, whereas this amine in methacholine is located 5.6 Å away from W225. The Y178 residue in loop B is 2.7 Å from N179 allowing for an increase in potential hydrogen bonding in the binding pocket. When looking at how each molecule docks in the binding pocket, we can see a similar extended orientation for each.

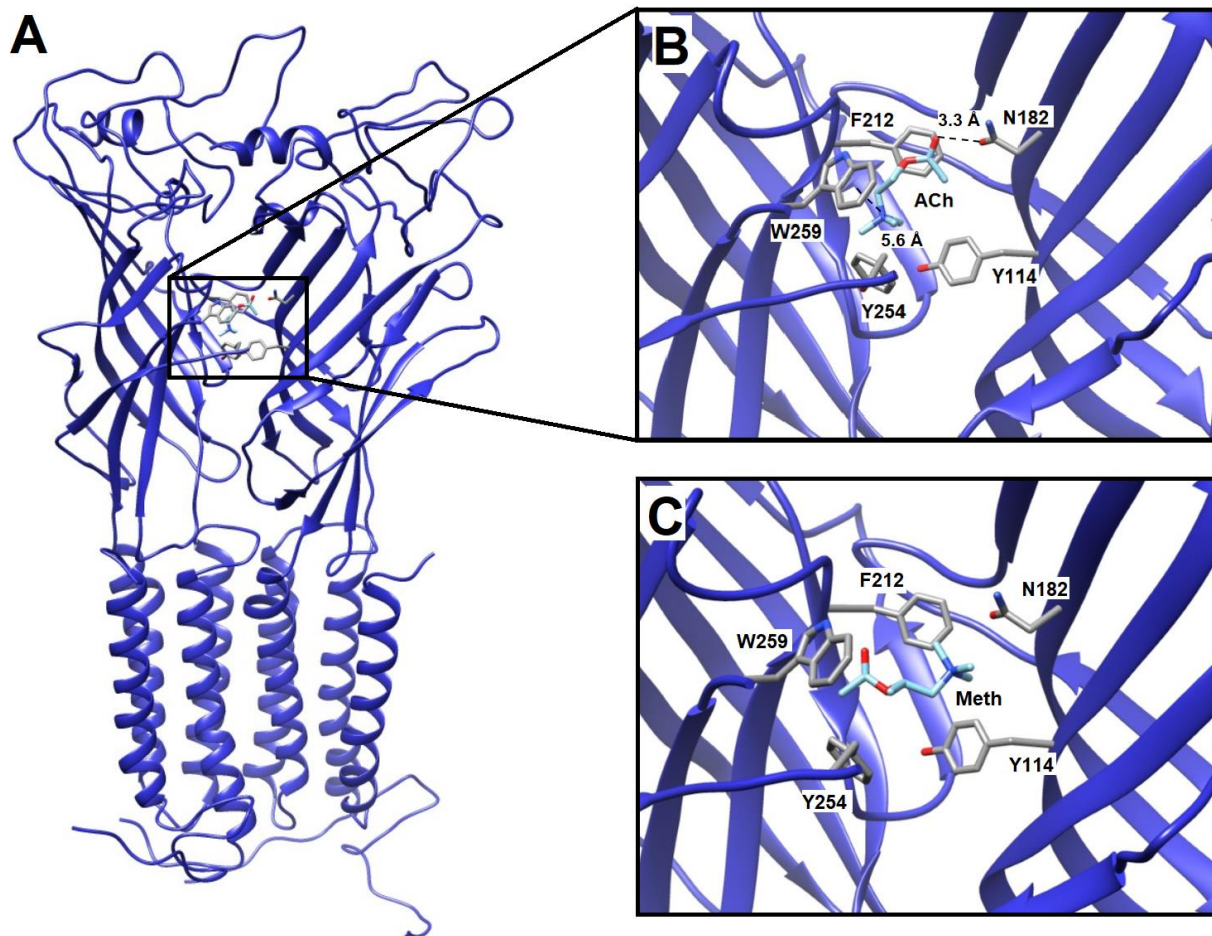


**Figure 4.4:** (A) Homology model of Hco-LGC-46 homodimer. The principal and complementary subunits are represented by the colour blue. (B) View of the Hco-LGC-46 binding pocket with acetylcholine docked. Key aromatic residues in binding pocket are highlighted and distances to tryptophan (W259) and asparagine (N182) are shown. (C) View of the Hco-LGC-46 binding pocket with methacholine docked. \*A portion of Loop C is removed from the images for clarity.

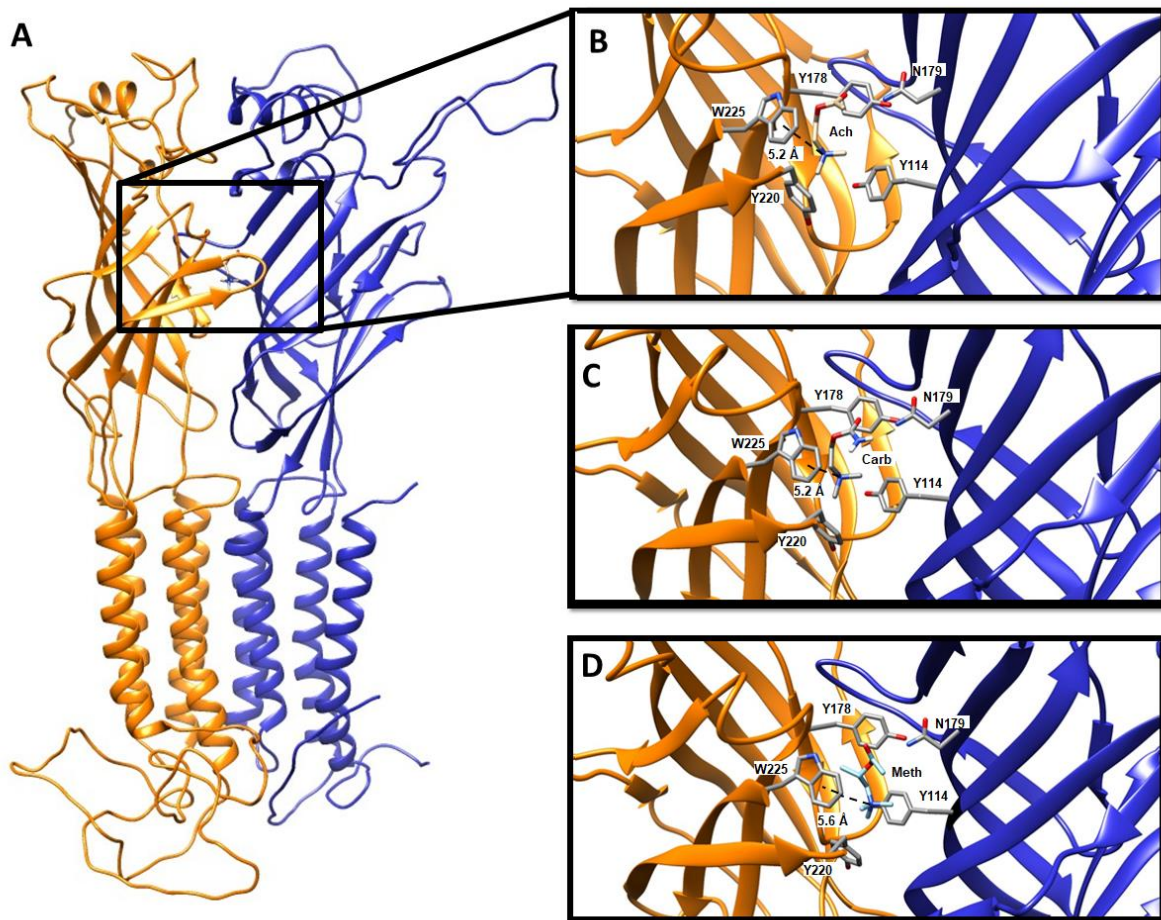


**Figure 4.5:** (A) Homology model of Hco-ACC-1/ Hco-LGC-46 heterodimer. Hco-ACC-1 and LGC-46 are the principal and complimentary subunits, and are represented by the colours orange and blue, respectively. (B) View of the Hco-ACC-1/Hco-LGC-46 binding pocket with acetylcholine docked. (C) View of the Hco-ACC-1/Hco-LGC-46 binding pocket with carbachol docked. (D) Methacholine docked in binding pocket. Key aromatic residues in binding pocket are highlighted and distance to tryptophan (W225) is shown. \*A portion of Loop C is removed from the images for clarity

#### 4.3.4: Expression of *hco-lgc-46* in *C. elegans*

To assess whether *hco-lgc-46* can function *in vivo* we took advantage of a *lgc-46* null strain *ok2900* which is hypersensitive to aldicarb, an acetylcholine esterase inhibitor that causes paralysis over time (Takayanagi-Kiya et al. 2016). Compared to WT, *lgc-46(ok2900)* animals were much more sensitive to 500  $\mu$ M aldicarb assessed over 5hrs (Figure 4.6). Expressing *cel-lgc-46* or *hco-lgc-46* specifically in the cholinergic motor neurons (*Punc-17 $\beta$* ) was sufficient to partially suppress aldicarb hypersensitivity. While we did not observe complete suppression, the level is similar to that reported in Takayanagi-Kiya et al. 2016 (Figure 4.6).

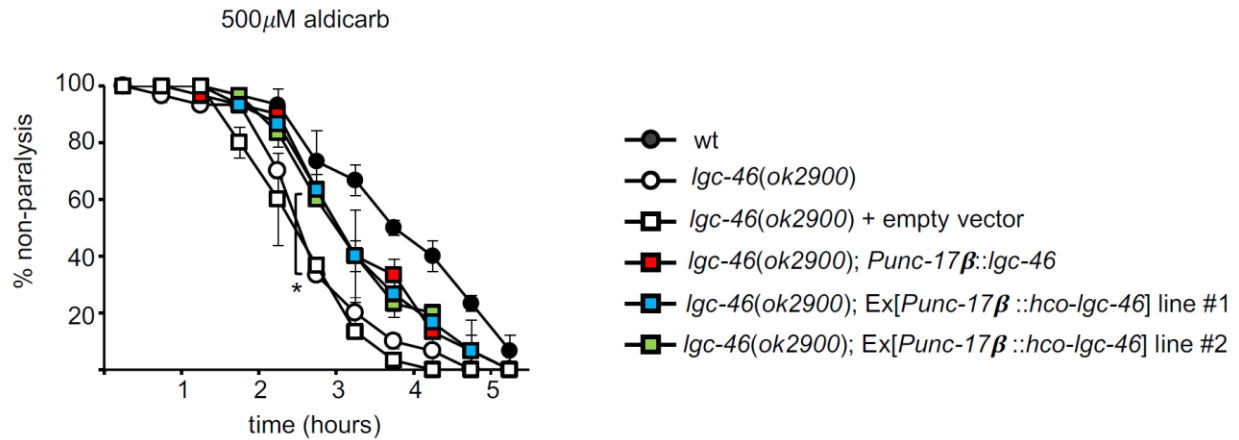


**Figure 4.6:** Expression of Hco-LGC-46 partially rescues aldicarb hypersensitivity of *C. elegans lgc-46(ok2900)*. Results show the comparison between one extrachromosomal array line expressing *C. elegans* LGC-46 and two independent lines expressing Hco-LGC-46 and under a cholinergic motor neuron specific promoter (*Punc-17β*). When restored to this subset of the nervous system, both *C. elegans* and Hco-LGC-46 partially rescue aldicarb hypersensitivity in the *lgc-46* genetic null (*ok2900*) background. The empty vector control line carries a plasmid containing *Punc-17β* without the *hco-lgc-46* cDNA insert in the *lgc-46(ok2900)* transgenic background. All transgenic lines express co-injection marker *Pmyo-2::mCherry*. Results are from two independent experiments of n=15 worms per group, performed on different days. Each data point is the mean % non-paralysis ± SEM. \*: p<0.05 by two-way ANOVA and Bonferroni post-hoc test.

#### 4.3.5: Expression of Hco-ACC-4 in oocytes

Similar to the *C. elegans* version of *acc-4* (Putrenko et al. 2005), injection of *hco-acc-4* cRNA alone in oocytes did not result in a functional ACh-sensitive channel. In addition, the co-injection of cRNA encoding *hco-lgc-46* with *hco-acc-4* did not result in the expression of a sensitive heteromeric channel (Figure 4.7). The co-injection of *hco-acc-4* with *hco-acc-2* resulted in a channel that was sensitive to ACh. The resulting ACC-4/ACC-2 receptor had an EC<sub>50</sub> value of 25 ± 0.3 μM which is similar to the ACC-2 homomeric channel 21 ± 0.7 μM (Habibi et al. 2018). However, the maximum current produced by the channel in the presence of ACC-4/ACC-2 channel was significantly lower (p<0.005) when compared to ACC-2 alone (Figure 4.7). This is consistent with results obtained for the *C. elegans* ACC-4/ACC-2 subunits expressed in oocytes (Putrenko et al. 2005).

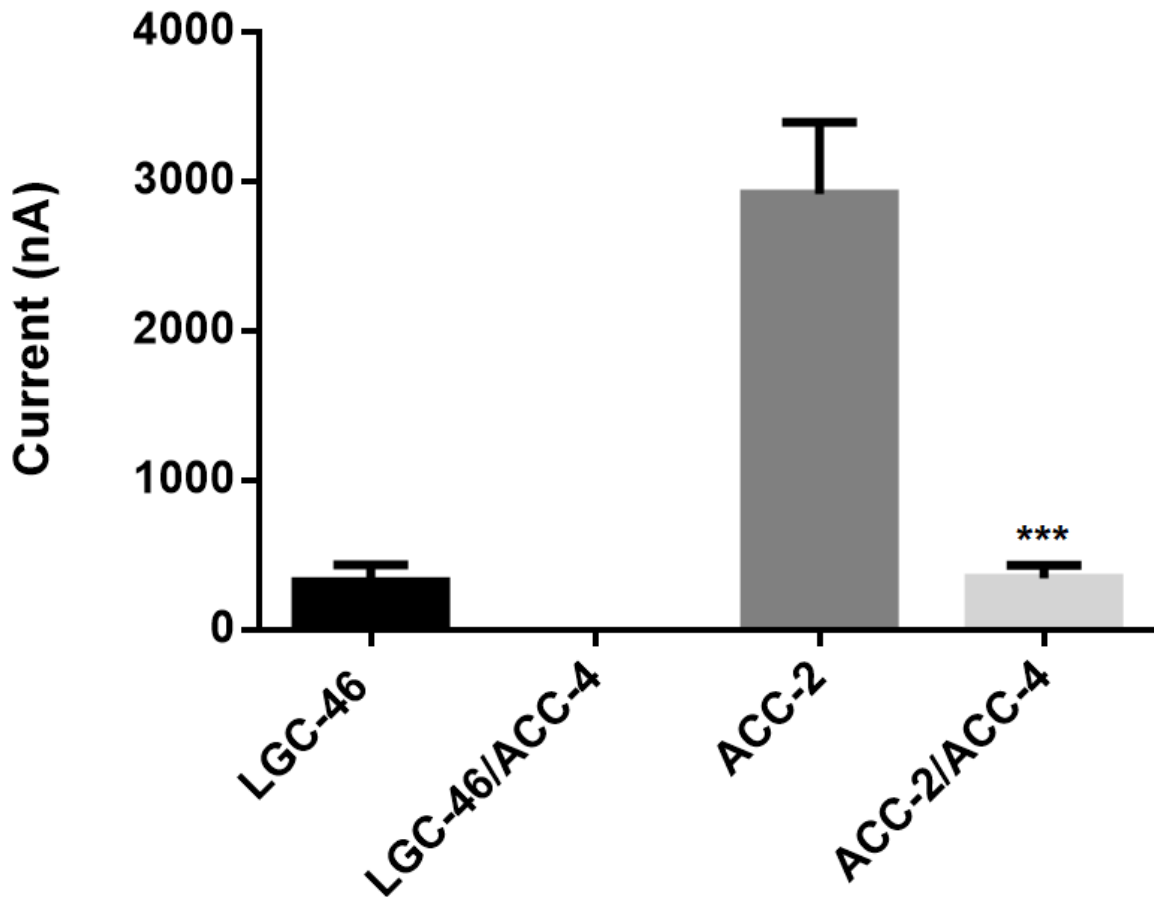


**Figure 4.7:** Average maximal currents shown for the Hco-LGC-46 and Hco-ACC-2 receptors in comparison to the heteromeric channels with Hco-ACC-4 present. Standard errors are shown, n=5). \*\*\* indicates significant difference between ACC-2 and ACC-2/ACC-4 currents ( $P < 0.005$ )

**Table 4.1:** Pharmacological summary of ACC-1 family of receptors from *H. contortus* in response to various cholinergic ligands and nAChR anthelmintics. Pharmacological responses are represented by  $EC_{50} \pm SE$ . N.R refers to no observed response of receptor to 20 mM concentration of ligand.

	ACC-2*	ACC-1/ACC-2**	LGC-46	ACC-1/LGC-46	LGC-46/ACC-4
<b>Acetylcholine</b>	20.86 ± 0.7 μM	5.9 ± 1 μM	893 ± 200 μM	166 ± 4 μM	N.R
<b>Carbachol</b>	43.0 ± 3.6 μM	32.5 ± 3 μM	N.R	1680 ± 70 μM	N.R
<b>Methacholine</b>	100.4 ± 2.1 μM	--	7348 ± 900 μM	3990 ± 600 μM	N.R
<b>Levamisole</b>	98.39 ± 4.0 μM	--	N.R	N.R	N.R
<b>Pyrantel</b>	71.7 ± 3.5 μM	--	N.R	N.R	N.R

\* Data retrieved from Habibi et al. 2018

\*\* Data retrieved from Callanan et al. 2018

#### 4.4: Discussion

We have identified and cloned the *Hco-lgc-46* gene from the parasitic nematode *H. contortus*, which encodes a member of the ACC-1 family of cys-loop ligand-gated chloride channels in nematodes. This unique family of inhibitory receptors is only present in nematode species, and thus provides an opportunity for exploration as new potential anthelmintic targets. In addition, phylogenetic analysis has revealed members of the ACC-1 family are present in a vast number of parasitic nematode species (Callanan et al. 2018). Previously it has been shown that members of this family from *H. contortus* combine to form homomeric and heteromeric channels that are highly sensitive to acetylcholine (Callanan et al. 2018; Habibi et al. 2018). Here, we report that Hco-LGC-46 expressed in *Xenopus* oocytes can form a homomeric channel and a heteromeric channel with Hco-ACC-1 (Callanan et al. 2018), that responds to cholinergic agonists, albeit at much higher concentrations than previously reported for other members of this family. Hco-LGC-46 when expressed in *C. elegans* cholinergic motor neurons partially suppresses aldicarb hypersensitivity in a similar manner to Cel-LGC-46, confirming that Hco-LGC-46 can function *in vivo*. Whether Hco-LGC-46 functions in a similar manner in *H. contortus* is unknown at this time. We have found previously that ACC-1 is expressed in different tissues in *C. elegans* vs *H. contortus* (Callanan et al. 2018), so it is possible that there are differences in LGC-46 function between nematodes.

The pharmacology of Hco-LGC-46 and Hco-LGC-46/Hco-ACC-1 receptors, provide insight into the nature of the binding site. The Hco-LGC-46 receptor is minimally sensitive to the partial agonist methacholine (Meth). When referring to the model, Meth can be seen docked in an extended orientation surrounded by aromatic residues in the binding pocket. In mammalian nAChRs a tryptophan residue in loop B has been shown to be a key player in ACh binding where it forms a cationic pi interaction with the quaternary amine of ACh (Beene et al. 2002). In nematode ACCs however, this key tryptophan residue is found in loop C (Habibi et al. 2018). In the Hco-LGC-46 receptor we see Meth docking with its quaternary amine directed away from this tryptophan residue, W259, possibly explaining its lower sensitivity on the receptor. On the other hand, the Hco-LGC-46 receptor appears to be more sensitive to ACh. In the LGC-46 homodimer model ACh docks with its quaternary amine 5.6 Å from the tryptophan residue (W259) in loop C which would allow essential cation pi interactions to occur.

When Hco-LGC-46 was co-expressed with Hco-ACC-1 we generate a receptor that is over 5-fold more sensitive to ACh. Interestingly, when other members of the ACC-1 family are co-expressed with Hco-ACC-

1, increased receptor sensitivity is also observed (Callanan et al. 2018). A pharmacological summary of the ACC-1 family of receptors in response to the cholinergic ligands and anthelmintics can be found in Table 4.1. Upon analysis of sequence alignments, it is noted that Hco-ACC-1 contains a tyrosine residue (Y178) in binding loop B, whereas the Hco-LGC-46 receptor contains a phenylalanine (F212) in the equivalent position. The presence of a tyrosine residue in loop B has been shown to contribute to hypersensitivity of these receptors when expressed in *Xenopus* oocytes (Habibi et al. 2018). The addition of the hydroxyl group in the ACC-1/LGC-46 channel places the tyrosine residue (Y178) within 2.7 Å of the amine group found on nearby asparagine (N179), allowing for hydrogen bond interactions to occur and provides a possible reason for increased channel activation. If Hco-ACC-1 is responsible for this increased receptor sensitivity it may indicate that it is playing the role of the principle subunit in pentamer formation (ie contributing this loop B tyrosine). Similarly, the Hco-ACC-1/Hco-LGC-46 receptor was 2-fold more sensitive to Meth, compared to Hco-LGC-46 homomer, and was responsive to ACh derivative carbachol. Both methacholine and carbachol were partial agonists of the ACC-1/LGC-46 receptor. Finally, neither the Hco-LGC-46 nor the Hco-ACC-1/Hco-LGC-46 receptors responded to nAChR anthelmintics pyrantel or levamisole, which have shown to have some activity at the Hco-ACC-2 channel. This could indicate differences in the agonist binding site even within members of the ACC-1 family of receptors.

When Hco-LGC-46 was co-expressed with Hco-ACC-4 we observed no receptor functionality. It is unknown at this time whether the presence of ACC-4 is preventing the expression of LGC-46 in oocytes, or if it is forming a unique heteromeric receptor which is no longer sensitive to cholinergic ligands. Interestingly, nematodes that possess LGC-46 also possess ACC-4, and those lacking one also lack the other (Wever et al. 2015). When analyzing the sequence alignments of these two subunits we see that in loop C of the ACC-4 receptor, the key tryptophan residue that has been shown to form essential cation pi interactions in other nematode cys-loop receptors (Mu et al. 2003) is missing, and instead there is a phenylalanine. Prior research from our group has shown that the substitution of this tryptophan residue for a phenylalanine severely impacts the function of the resulting receptor that is over 200 times less sensitive to ACh compared to wild-type (Habibi et al. 2018). If LGC-46 and ACC-4 were forming a heteromeric channel where the binding site is at the interface of the two subunits, this could possibly explain the reason for the inhibited function. In *C. elegans* ACC-4 and LGC-46 have been shown to function together in pre-synaptic cholinergic neurons by regulating synaptic vesicle release. Specifically, *lgc-46* gain-of function mutants showed suppressed activity in the *acc-4* knock-outs, indicating the role of ACC-4 in LGC-46 function (Takayanagi-Kiya et al. 2016). However, while our results provide evidence for an

interaction between ACC-4 and LGC-46 in oocytes the interaction appears to negatively affect channel function. Since there are no detectable currents in the ACC-4/LGC-46 receptor, we are unable to conclude whether the result is due to expression of receptor, or changes made to the binding site.

In *C. elegans*, ACC-4 has been shown to negatively impact the function of other ACC-1 family members such as ACC-2, where no currents were detected from the channel (Putrenko et al. 2005). During our investigation we saw a similar observation with ACC-2 and ACC-4, where the presence of ACC-4 significantly ( $p < 0.005$ ) reduced the current flowing through the channel in the presence of ACh with little change in the  $EC_{50}$ . This suggests that ACC-4 is negatively impacting expression and not necessarily the agonist binding site in the ACC-4/ACC-2 channel.

#### 4.5: Acknowledgements

This study was funded by a grant from the Natural Science and Engineering Research Council of Canada to SGF and an NIH NS grant (NS R37 035546) to YJ.

#### 4.7: References

Abdelmassih SA, Cochrane E, Forrester SG. 2018. Evaluating the longevity of surgically extracted *Xenopus laevis* oocytes for the study of nematode ligand-gated ion channels. *Invertebr Neurosci*. 18(1):1.

Bamber BA, Beg AA, Twyman RE, Jorgensen EM. 1999. The *Caenorhabditis elegans* unc-49 locus encodes multiple subunits of a heteromultimeric GABA receptor. *J Neurosci*. 19(13):5348–5359.

Beene DL, Brandt GS, Zhong W, Zacharias NM, Lester HA, Dougherty DA. 2002. Cation- $\pi$  interactions in ligand recognition by serotonergic (5-HT<sub>3A</sub>) and nicotinic acetylcholine receptors: The anomalous binding properties of nicotine. *Biochemistry*. 41(32):10262–10269.

Boulin T, Fauvin A, Charvet CL, Cortet J, Cabaret J, Bessereau J, Neveu C. 2011. Functional reconstitution of *Haemonchus contortus* acetylcholine receptors in *Xenopus* oocytes provides mechanistic insights into levamisole resistance. *Br J Pharmacol*. 164(5):1421–1432.



- Callanan MK, Habibi SA, Law WJ, Nazareth K, Komuniecki RL, Forrester SG. 2018. Investigating the function and possible biological role of an acetylcholine-gated chloride channel subunit (ACC-1) from the parasitic nematode *Haemonchus contortus*. *Int J Parasitol Drugs Drug Resist*. 8(3):526–533.
- Del Castillo J, Morales TA, Sanchez V. 1963. Action of piperazine on the neuromuscular system of *Ascaris lumbricoides*. *Nature*. 200(4907):706.
- Charlie NK, Schade MA, Thomure AM, Miller KG. 2006. Presynaptic UNC-31 (CAPS) is required to activate the G $\alpha$ s pathway of the *Caenorhabditis elegans* synaptic signaling network. *Genetics*. 172(2):943–961.
- Cully DF, Vassilatis DK, Liu KK, Paress PS, Van der Ploeg LH, Schaeffer JM, Arena JP. 1994. Cloning of an avermectin-sensitive glutamate-gated chloride channel from *Caenorhabditis elegans*. *Nature*. 371(6499):707.
- Habibi SA, Callanan M, Forrester SG. 2018. Molecular and pharmacological characterization of an acetylcholine-gated chloride channel (ACC-2) from the parasitic nematode *Haemonchus contortus*. *Int J Parasitol Drugs Drug Resist*. 8(3):518–525.
- Jensen ML, Timmermann DB, Johansen TH, Schousboe A, Varming T, Ahring PK. 2002. The  $\beta$  subunit determines the ion selectivity of the GABA $_A$  receptor. *J Biol Chem*. 277(44):41438–41447.
- Jones AK, Sattelle DB. 2008. The cys-loop ligand-gated ion channel gene superfamily of the nematode, *Caenorhabditis elegans*. *Invertebr Neurosci*. 8(1):41–47.
- Kehoe J, McIntosh JM. 1998. Two Distinct Nicotinic Receptors, One Pharmacologically Similar to the Vertebrate  $\alpha$ 7-Containing Receptor, Mediate Cl Currents in *Aplysia* Neurons. *J Neurosci*. 18(20):8198–8213.
- Kusano K, Miledi R, Stinnakre J. 1982. Cholinergic and catecholaminergic receptors in the *Xenopus* oocyte membrane. *J Physiol*. 328(1):143–170.
- Laing R, Kikuchi T, Martinelli A, Tsai IJ, Beech RN, Redman E, Holroyd N, Bartley DJ, Beasley H, Britton C. 2013. The genome and transcriptome of *Haemonchus contortus*, a key model parasite for drug and vaccine discovery. *Genome Biol*. 14(8):R88.

Mello CC, Kramer JM, Stinchcomb D, Ambros V. 1991. Efficient gene transfer in *C. elegans*: extrachromosomal maintenance and integration of transforming sequences. *EMBO J.* 10(12):3959–3970.

Mu T-W, Lester HA, Dougherty DA. 2003. Different binding orientations for the same agonist at homologous receptors: a lock and key or a simple wedge? *J Am Chem Soc.* 125(23):6850–6851.

Pereira L, Kratsios P, Serrano-Saiz E, Sheftel H, Mayo AE, Hall DH, White JG, LeBoeuf B, Garcia LR, Alon U. 2015. A cellular and regulatory map of the cholinergic nervous system of *C. elegans*. *Elife.* 4:e12432.

Pettersen EF, Goddard TD, Huang CC, Couch GS, Greenblatt DM, Meng EC, Ferrin TE. 2004. UCSF Chimera—a visualization system for exploratory research and analysis. *J Comput Chem.* 25(13):1605–1612.

Pirri JK, McPherson AD, Donnelly JL, Francis MM, Alkema MJ. 2009. A tyramine-gated chloride channel coordinates distinct motor programs of a *Caenorhabditis elegans* escape response. *Neuron.* 62(4):526–538.

Putrenko I, Zakikhani M, Dent JA. 2005. A family of acetylcholine-gated chloride channel subunits in *Caenorhabditis elegans*. *J Biol Chem.* 280(8):6392–6398.

Ranganathan R, Cannon SC, Horvitz HR. 2000. MOD-1 is a serotonin-gated chloride channel that modulates locomotory behaviour in *C. elegans*. *Nature.* 408(6811):470–475.

Šali A, Blundell TL. 1993. Comparative protein modelling by satisfaction of spatial restraints. *J Mol Biol.* 234(3):779–815.

Siddiqui SZ, Brown DDR, Rao VTS, Forrester SG. 2010. An UNC-49 GABA receptor subunit from the parasitic nematode *Haemonchus contortus* is associated with enhanced GABA sensitivity in nematode heteromeric channels. *J Neurochem.* 113(5):1113–1122.

Takayanagi-Kiya S, Zhou K, Jin Y. 2016. Release-dependent feedback inhibition by a presynaptically localized ligand-gated anion channel. *Elife.* 5:e21734.

Weston D, Patel B, Van Voorhis WC. 1999. Virulence in *Trypanosoma cruzi* infection correlates with the expression of a distinct family of sialidase superfamily genes. *Mol Biochem Parasitol.* 98(1):105–116.

Wever CM, Farrington D, Dent JA. 2015. The validation of nematode-specific acetylcholine-gated chloride channels as potential anthelmintic drug targets. *PLoS One*. 10(9):e0138804.

Zhang J, Xue F, Chang Y. 2008. Structural determinants for antagonist pharmacology that distinguish the  $\rho 1$  GABA<sub>C</sub> receptor from GABA<sub>A</sub> receptors. *Mol Pharmacol*. 74(4):941–951.

## Connecting Statement III

After confirming that Hco-ACC-1 associates with a variety of members from the ACC-1 family to form highly sensitive ACh receptors, my research focused on further assessing the role Hco-ACC-1 plays in cholinergic neurotransmission in *H. contortus*. The main goal of this chapter was to determine whether members of another family of potential cholinergic receptors, the GGR-1 family, can associate with ACC-receptors to form functional channels. It was shown by a previous student in the Forrester lab that LGC-39 and 40 are potential cholinergic receptors. The following chapter confirms that both Hco-LGC-39 and Hco-LGC-40 form homomeric receptors, which respond to cholinergic ligands, and they associate with Hco-ACC-1 to form unique heteromeric receptors, which also respond to cholinergic ligands. The chapter also describes the characterization of agonist responses of classical cholinergic antagonists to ACh-gated chloride channels.

## Chapter V – Manuscript IV

Investigation of subunit co-assembly of members of the ACC family with other cys-loop receptors

**Sarah A. Habibi**

## 5.1: Introduction

Cholinergic neurotransmission has been extensively studied for decades now for its role in neuro-excitation in vertebrate and invertebrate organisms (Changeux 2012). This type of neuro-excitation is mediated by the neurotransmitter acetylcholine (ACh) acting on cation-sensitive nicotinic acetylcholine receptors (nAChRs). nAChRs are pentameric ionotropic receptors which belong to the superfamily of Cysteine (Cys) loop ligand-gated ion channels (LGICs). These LGICs are understood to play a role in the nervous system of nematodes, and have been used as a primary target for anthelmintic action. In nematodes, these channels have been shown to be activated by neurotransmitters including serotonin (Ranganathan et al. 2000), gamma-aminobutyric acid (GABA) (Bamber et al. 1999; Siddiqui et al. 2010), and glutamate (Cully et al. 1994). Pentameric LGICs can exist as either homomeric or heteromeric receptors with varying affinity to different ligands (Ortells and Lunt 1995).

Research on cholinergic neurotransmission in invertebrates suggest that in addition to nAChRs these animals contain inhibitory cholinergic cys-loop receptors. In particular, early studies in the mollusk, *Aplysia*, revealed that a group of receptors were involved in neuro-inhibition in the presence of ACh (Kehoe and McIntosh 1998a). Exploration of these receptors further in the free-living nematode and model organism, *C. elegans*, revealed a novel family of inhibitory ACh-gated chloride channels. These inhibitory channels make up the ACC-1 family, which belong to the superfamily of cys-loop receptors (Putrenko et al. 2005; Wever et al. 2015). Eight receptor subunit genes encode the ACC-1 family in *C. elegans* (Jones and Sattelle 2008). Further investigation in the parasitic sheep nematode *Haemonchus contortus* revealed the presence of 7 homologues genes, named *acc-1*, *-2*, *-3*, and *-4*, and *lgc-46*, *-47*, and *-49* (Laing et al. 2013). *In vivo* studies performed by Wever and colleagues in 2015 and our group in 2018 (Callanan et al. 2018) show the presence of the ACC-1 family in tissues involved in nematode feeding, suggesting they would make effective targets for anthelmintic action.

Our group has extensively studied 4 members of the ACC-1 family, ACC-1, ACC-2, ACC-4, and LGC-46 in the parasitic nematode *H. contortus*. We have found that both ACC-2 and LGC-46 form functional homomeric channels when expressed in *Xenopus laevis* oocytes (Habibi et al. 2018; Habibi et al. 2020). Both receptors respond and activate in the presence of various cholinergic ligands and nAChR anthelmintics. Although Hco-ACC-1 does not form a functional homomeric channel, it can associate with Hco-ACC-2 or Hco-LGC-46 to form a heteromeric channel. In both instances, subunits that associated with

Hco-ACC-1 resulted in receptors which were significantly more sensitive to ACh when compared to homomeric counterparts (Callanan et al. 2018; Habibi et al. 2020).

Jones and Sattelle (2008) identified a novel family of cys-loop LGICs in *C. elegans* through phylogenetic analysis, named GGR-1. The GGR-1 family consists of six subunit encoding genes, including *lgc-39*, *lgc-40*, *lgc-41*, *lgc-42*, *ggr-1*, and *ggr-2*, present in both *C. elegans* (Jones and Sattelle 2008) and *H. contortus* (Laing et al. 2013). However, the only study to date on members of this clade was (Ringstad et al. 2009) where they determined that LGC-40 was activated by serotonin, ACh and choline and inhibited by the nAChR antagonist *d*-tubocurarine (Ringstad et al. 2009). Apart from characterization of LGC-40 in *C. elegans*, very little is known about the GGR-1 family in nematodes. Since Cel-LGC-40 responds to cholinergic ligands, we hypothesize that members of the GGR-1 family from *H. contortus* may form unique cholinergic receptors, which have the potential to associate with members of the ACC-1 family to form novel heteromeric receptors.

This study extends the initial characterization of members of the GGR-1 family by Kristen Nazareth (MSc Thesis, Nazareth 2019) and describes the functional characterization of Hco-LGC-39 and Hco-LGC-40 as functional homomeric receptors, and functional heteromeric channels with Hco-ACC-1. Other members of the GGR-1 family, LGC-41 and GGR-2, did not respond to cholinergic ligands when expressed in *X. laevis* oocytes on their own or in combination with Hco-ACC-1. In addition, members of the ACC-1 and GGR-1 families were activated in response to common LGIC antagonists atropine (Atro) and strychnine (Strya), suggesting a functional difference between family members from free-living and parasitic nematodes.

## 5.2: Methods

### 5.2.1: Expression in *Xenopus laevis* oocytes

All animal procedures followed the Ontario Tech University Animal Care Committee and the Canadian Council on Animal Care guidelines. Channels were expressed in *Xenopus laevis* oocytes according to (Abdelmassih et al. 2018). *X.laevis* frogs were supplied by Nasco (Fort Atkinson, WI, USA). The frogs were kept in a climate controlled, light cycled room, where they were fed and had the tanks cleaned regularly. *X. laevis* were anesthetized with 0.15% 3-aminobenzoic acid ethyl ester methanesulphonate salt (MS-222) buffered with NaHCO<sub>3</sub> to pH 7 (Sigma-Aldrich, Oakville, ON, CA). During surgery, a section of the frog ovary

was removed and the lobe was defolliculated with OR-2, calcium-free oocyte Ringer's solution [82 mM NaCl, 2 mM KCl, 1 mM MgCl<sub>2</sub>, 5 mM HEPES pH 7.5 (Sigma-Aldrich)] and 2 mg/mL collagenase-II (Sigma-Aldrich). The oocytes were incubated in the defolliculation solution for 2 hours at room temperature under agitation. Collagenase was washed from the oocytes with ND-96 solution (96 mM NaCl, 2mM KCl, 1 mM MgCl<sub>2</sub>, 1.8 mM CaCl<sub>2</sub>) and oocytes were incubated in ND96 supplemented with 0.275 µg/mL pyruvate and 50 µg/ mL gentamycin for one hour at 18°C prior to injection. Stage V and VI oocytes were selected for cytoplasmic injection of cRNA.

Kristen Nazareth carried out cloning for the *hco-lgc-39* and *hco-lgc-40* genes into the *Xenopus laevis* expression vector and conducting the initial pharmacological characterization. The pGEMHE vector containing the *hco-lgc-39* and *hco-lgc-40* coding sequences were linearized using NheI (New England Biolabs, USA). Linear plasmids were used for an *in vitro* transcription reaction (T7 mMessage mMachine kit, Ambion, Austin, TX, USA) yielding copy RNA corresponding to each gene. *X. laevis* oocytes were injected with 50 nl of each subunit gene (0.5 ng/µL) alone or in combination (0.25 ng/µL each) using the Drummond (Broomall, PA, USA) Nanoject microinjector. Each oocyte was co-injected with the *H. contortus* genes *unc-50*, *unc-74*, and *ric-3.1*, which encode accessory proteins (Boulin et al. 2011). Injected oocytes were incubated at 18°C in supplemented ND96 solution. Electrophysiological recordings of the oocytes were conducted between 48 and 72 hours after cRNA injection.

### 5.2.2: Electrophysiological recordings

Two-electrode voltage clamp electrophysiology was conducted using the Axoclamp 900A voltage clamp (Molecular Devices, Sunnyvale, CA, USA). Glass electrodes were produced using a P-97 Micropipette Puller (Sutter Instrument Co., Novato, CA, USA). The electrodes were backfilled with 3M KCl and contained Ag|AgCl wires. The following molecules were first dissolved in ND96; Acetylcholine (ACh), Carbamoylcholine Chloride (Carbachol), Acetyl-β-methylcholine Chloride (Methacholine), Levamisole Hydrochloride (Levamisole), Pyrantel Citrate Salt (Pyrantel), Atropine Hydrochloride (Atro), and Strychnine Hydrochloride (Strya) [Sigma]. These solutions were perfused over oocytes using the RC-1Z recording chamber (Warner Instruments Inc., Hamdan, CT, USA). Data was analyzed using Clampex Software v10.2 (Molecular Devices) and all graphs were generated using Graphpad Prism Software v5.0 (San Diego, CA, USA). EC<sub>50</sub> values were determined by dose response curves that had been fitted to the following equation:



$$I_{max} = \frac{1}{1 + \left(\frac{EC_{50}}{[D]}\right)^h}$$

In this equation,  $I_{max}$  is the maximal response,  $EC_{50}$  is the concentration of the ligand required to produce 50% of the maximal response,  $[D]$  is the ligand concentration, and  $h$  is the hill coefficient. The hill coefficient provides a measure of cooperative binding. Both  $EC_{50}$  and  $h$  are free parameters, and the curves were normalized to the estimated  $I_{max}$ . Graphpad Prism used the equation to fit a sigmoidal curve of variable slopes to the data. Means were determined from at least 5 oocytes from at least two batches of frogs.

### 5.2.3: *In silico* modelling

The protein coding sequences of Hco-LGC-39, Hco-LGC-40 and Hco-ACC-1 were aligned with the *Danio rerio* alpha-1 glycine receptor (3JAD). MODELLER v9.21 software (Šali and Blundell 1993) was used for the generation of the Hco-LGC-39 and Hco-LGC-40 homodimers and the Hco-LGC-39/Hco-ACC-1 and Hco-LGC-40/Hco-ACC-1 heterodimers and as described in Habibi et al 2018. Both homodimers and heterodimers were prepared for ligand docking using AutoDock Tools (Morris et al. 2009). Ligands were obtained from PubChem in their energy-reduced form. AutoDock Vina was used to simulate docking of each ligand to the homo- or hetero-dimers (Trott and Olson 2010). Pymol was used to visualize the protein models with their associated ligands. Chimera v1.6.1 (Pettersen et al. 2004) was used to determine the distance between the amino acid residues and the docked ligands and for the generation of figures.

## 5.3: Results

### 5.3.1: Expression in *Xenopus* oocytes

Alignment of the Hco-ACC-1, Hco-ACC-2, Hco-LGC-39, and Hco-LGC-40 proteins is shown in Figure 5.1. The injection of *X. laevis* oocytes with cRNA encoding *hco-igc-39*, and the accessory proteins, *hco-unc-74*, *hco-unc-50*, and *hco-ric-3.1*, resulted in a homomeric LGC-39 channel that was sensitive to cholinergic ligands (Figure 5.2A) similar to described in Nazareth 2019.

The injection of *X. laevis* oocytes with cRNA encoding either *hco-lgc-39* or *hco-lgc-40* with cRNA encoding Hco-ACC-1, resulted in unique heteromeric channels which were sensitive to cholinergic ligands at varying degrees compared to their homomeric counterparts (Figures 5.2B and 5.3A).

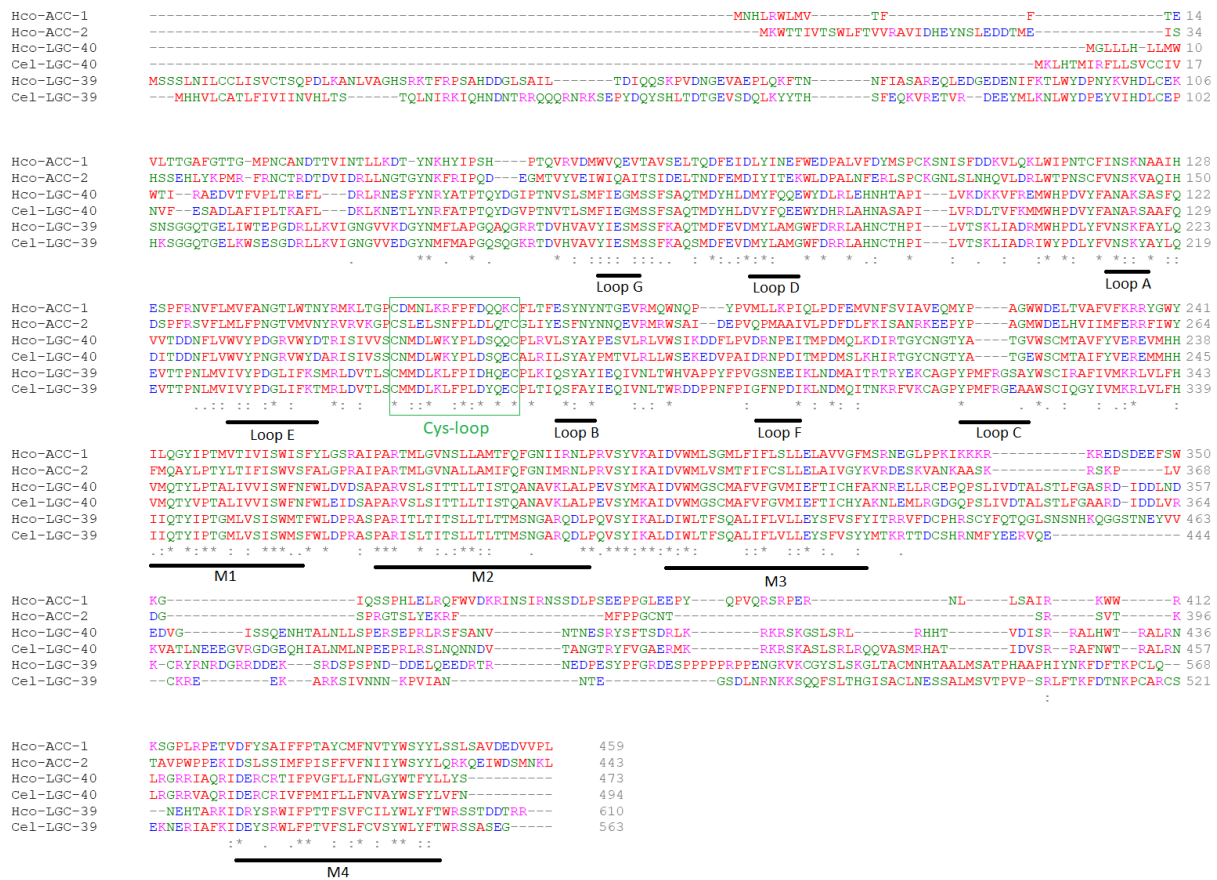


**Figure 5.1:** Protein sequence alignment of the *H. contortus* Hco-ACC-1, Hco-ACC-2, Hco-LGC-39, and Hco-LGC-40 receptors with *C. elegans* Cel-LGC-39 and Cel-LGC-40 receptors. All six binding loops (Loop A-F), the characteristic cysteine residues that form the “cys-loop”, and four transmembrane domains (M1-M4) and highlighted with underlines. (\*) indicates identity and (:) indicates similarity.

### 5.3.2: Pharmacological analysis of homomeric and heteromeric channels

The homomeric Hco-LGC-39 receptor responded to ACh and methacholine with  $EC_{50}$  values of  $1087 \pm 92 \mu\text{M}$  ( $n=5$ ) and  $465.3 \pm 32.4 \mu\text{M}$  ( $n=5$ ) respectively (Figure 5.2C) similar to Nazareth 2019. Methacholine proved to be a full agonist of the channel, whereas ACh was a strong partial agonist (Figure 5.2A). The heteromeric Hco-LGC-39/Hco-ACC-1 receptor was significantly more sensitive to ACh ( $p<0.05$ ) compared to the LGC-39 homomer, with an  $EC_{50}$  value of  $782.5 \pm 47 \mu\text{M}$ . Hco-LGC-39/Hco-ACC-1 was also sensitive to methacholine and urecholine, with  $EC_{50}$  values of  $327.9 \pm 25 \mu\text{M}$  and  $1150 \pm 167 \mu\text{M}$  respectively (Figure 5.2C). Methacholine was a full agonist of the heteromeric channel, whereas ACh and urecholine were both strong partial agonists, activating the channel at 80% (Figure 5.2C). Neither the Hco-LGC-39 nor the Hco-LGC-39/Hco-ACC-1 receptors responded to 100  $\mu\text{M}$  of carbachol, levamisole, pyrantel, tyramine, serotonin, GABA, or nicotine. A summary of all pharmacological response data is outlined in Table 5.1.

The heteromeric Hco-LGC-40/Hco-ACC-1 receptor was 5-fold less sensitive to ACh compared to the LGC-40 homomer ( $EC_{50} = 4.8 \pm 0.2 \mu\text{M}$ ), with an  $EC_{50}$  value of  $24.72 \pm 1.9 \mu\text{M}$ . Hco-LGC-40/Hco-ACC-1 responded to methacholine with an  $EC_{50}$  value of  $380 \pm 15 \mu\text{M}$  (Figure 5.3B). Neither the Hco-LGC-40 nor the Hco-LGC-40/Hco-ACC-1 receptors responded to 100  $\mu\text{M}$  of levamisole, pyrantel, tyramine, serotonin, GABA, or nicotine.

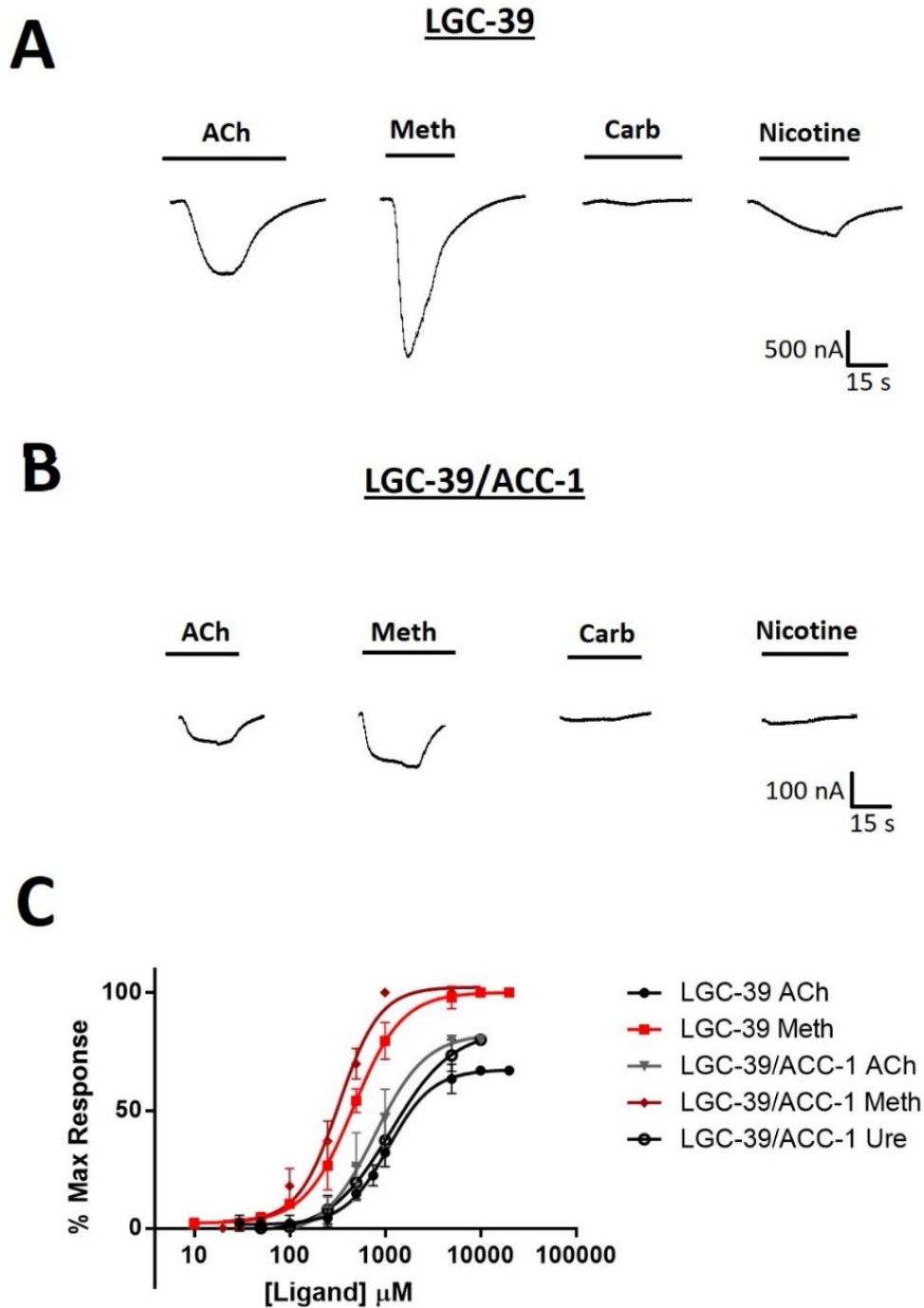


**Figure 5.2:** (A) Electrophysiological response of the Hco-LGC-39 receptor in the presence of 100  $\mu\text{M}$  of acetylcholine (ACh), methacholine (Meth), carbachol (Carb), and nicotine. (B) Electrophysiological response of the Hco-LGC-39/Hco-ACC-1 receptor in the presence of 100  $\mu\text{M}$  of acetylcholine (ACh), methacholine (Meth), carbachol (Carb), and nicotine. (C) Dose-response curves of the Hco-LGC-39 and Hco-LGC-39/Hco-ACC-1 receptors in the presence of ligands shown. Standard errors are shown.  $n \geq 5$  oocytes. Each curve is represented as a percent of the maximum methacholine response. Partial agonists are those that have a maximum response lower than 100%.

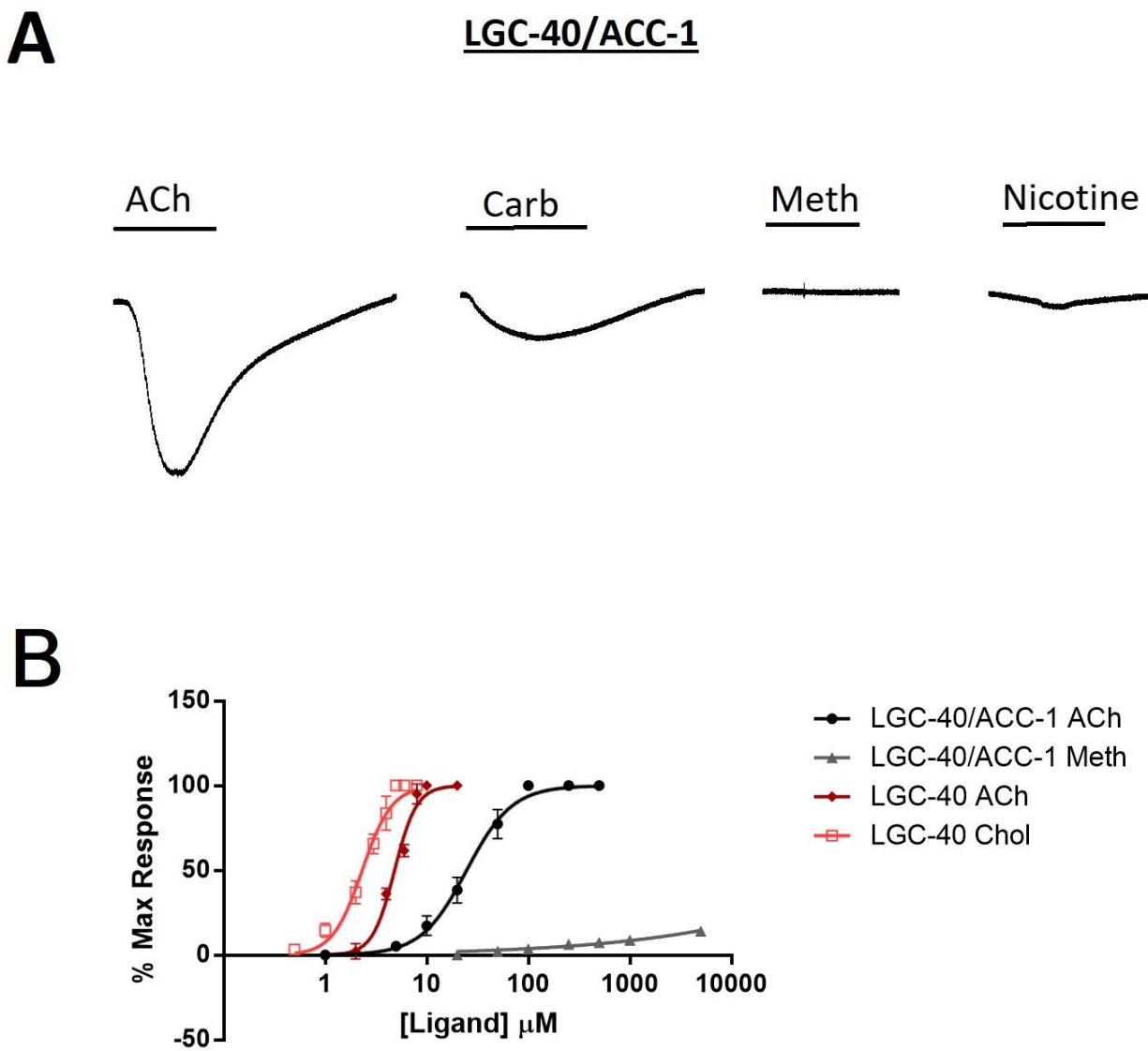


**Figure 5.3: (A)** Electrophysiological response of the Hco-LGC-40/Hco-ACC-1 receptor in the presence of 100  $\mu\text{M}$  of acetylcholine (ACh), carbachol (Carb), methacholine (Meth), and nicotine. **(B)** Dose-response curves of the Hco-LGC-40 and Hco-LGC-40/Hco-ACC-1 receptors in the presence of ligands shown. Standard errors are shown.  $n \geq 5$  oocytes. Both ACh and Chol act as full agonists for the receptors. Partial agonists (methacholine) are those that have a maximum response lower than 100%.

### 5.3.3: Action of antagonist on members of the ACC-1 and GGR-1 family

To further assess the pharmacology of each of the homomeric and heteromeric channels we measured their activity in the presence of common antagonists. We analyzed the following 5 antagonists, atropine (Atro), strychnine (Strya), mecamlamine (Meca), tubocurarine (Turbo), and betaine. At 100  $\mu\text{M}$  of ligand, Atro acted as an agonist for the Hco-LGC-39 and Hco-LGC-39/Hco-ACC-1 receptors (Figure 5.4). Neither of these channels were activated in the presence of 100  $\mu\text{M}$  of the other antagonists (Figure 5.4A). Atropine activated the Hco-LGC-39 and Hco-LGC-39/Hco-ACC-1 channels with  $\text{EC}_{50}$  values of  $2.4 \pm 0.05 \mu\text{M}$  and  $3.1 \pm 0.06 \mu\text{M}$  respectively (Figure 5.4B).

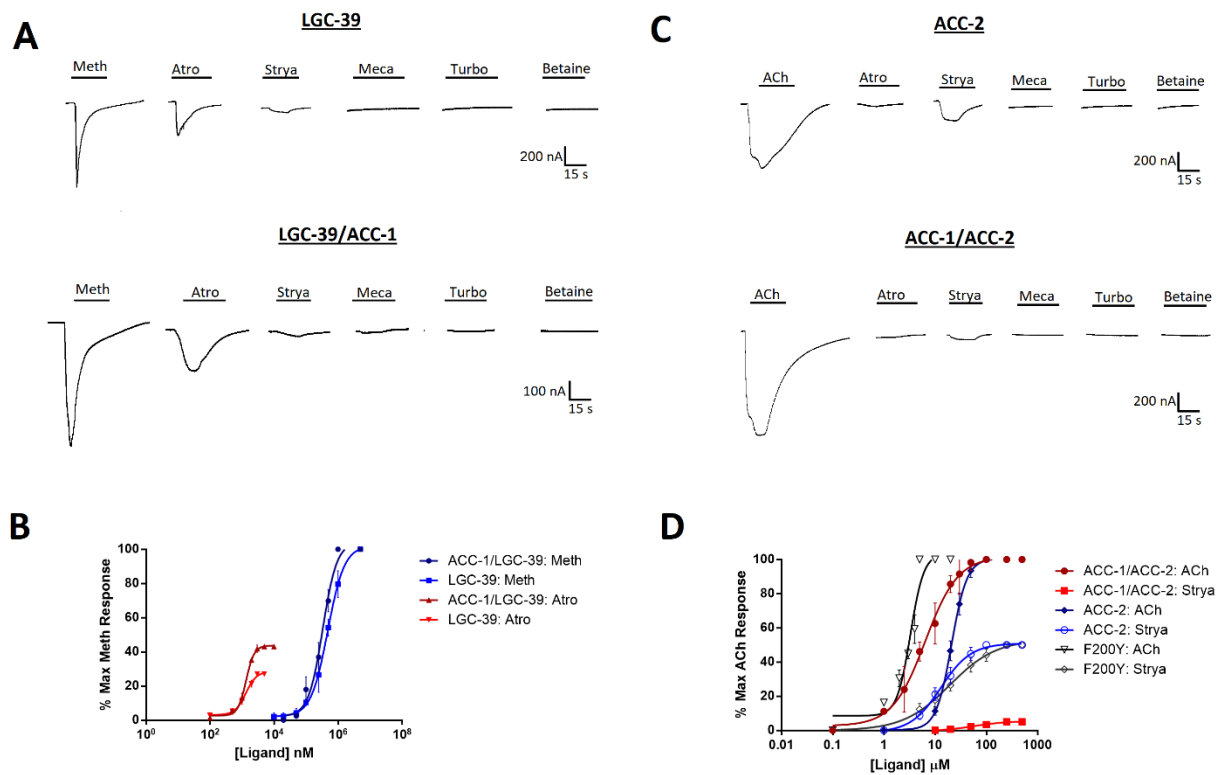


**Figure 5.4:** (A) Electrophysiological response of the Hco-LGC-39 and Hco-LGC-39/Hco-ACC-1 receptors in the presence of 100  $\mu\text{M}$  of the antagonists atropine (Atro), strychnine (Strya), mecamlamine (Meca), tubocurarine (Turbo), and betaine. (B) Dose-response curves of the Hco-LGC-39 and Hco-LGC-39/Hco-ACC-1 receptors in the presence of atropine compared to methacholine. Atropine is shown as a partial agonist of both receptors. (C) Electrophysiological response of the Hco-ACC-2, Hco-ACC-1/Hco-ACC-2, and Hco-ACC-2 F200Y receptors in the presence of 100  $\mu\text{M}$  of the antagonists atropine (Atro), strychnine (Strya), mecamlamine (Meca), tubocurarine (Turbo), and betaine. (D) Dose-response curves of the Hco-ACC-2, Hco-ACC-1/Hco-ACC-2, and Hco-ACC-2 F200Y receptors in the presence of strychnine compared to acetylcholine. Strychnine is shown as a partial agonist of each receptor.

To assess the ability of other heteromeric channels containing Hco-ACC-1 to respond to antagonists, we tested the Hco-ACC-1/Hco-ACC-2 heteromer previously characterized by our group (Callanan et al. 2018). Both the Hco-ACC-2 homomer and Hco-ACC-1/Hco-ACC-2 heteromer were activated in the presence of the antagonist strychnine, with EC<sub>50</sub> values of 12.9 ± 1.5 μM and 56.2 ± 3.3 μM, respectively (Figure 5.4C). The Hco-ACC-2 F200Y mutation previously characterized by our group (Habibi et al. 2018), which mimics the Hco-ACC-1 side of the binding pocket also responded to Strya with an EC<sub>50</sub> value of 16.6 ± 1.9 μM. Neither of these channels were activated in the presence of 100 μM Atro, Meca, Turbo, or Betaine (Figure 5.4C). A summary of all pharmacological response data is outlined in Table 5.1.

Table 5.1: Pharmacological summary of the various ACC receptors from *H. contortus* in response to various cholinergic ligands, nAChR anthelmintics, and classic antagonists. Pharmacological responses are represented by EC<sub>50</sub> ± SEM. Maximal responses of the receptors to each ligand is outlined in the square brackets []. N.R\* indicates the channel is unresponsive to 100 μM of ligand (n > 7). † Indicates the data is retrieved from Habibi et al. 2018. \*\*Indicates the data is retrieved from Callanan & Habibi et al. 2018. ND: not determined.

	EC <sub>50</sub> ± SEM (μM) [% Max response]						
	ACC-2	ACC-1/ ACC-2	F200Y	ACC-1/ LGC-39	LGC-39	ACC-1/ LGC-40	LGC-40
Acetylcholine	20 ± 0.5 [100]	6.4 ± 0.7 [100]	3.3 ± 0.2 [100]	782 ± 47 [80]	1087 ± 92 [67]	25 ± 2 [100]	4.8 ± 0.2 [100]
Methacholine	100 ± 2 [124] <sup>†</sup>	ND	20 ± 1 [108] <sup>†</sup>	328 ± 25 [100]	465 ± 32 [100]	380 ± 15 [14]	ND
Urecholine	747 ± 22 [43] <sup>†</sup>	ND	81 ± 3 [96] <sup>†</sup>	1150 ± 167 [80]	ND	ND	ND
Carbachol	43 ± 4 [73] <sup>†</sup>	32 ± 3 [80] <sup>**</sup>	9.7 ± 0.5 [79] <sup>†</sup>	ND	ND	ND	ND
Choline	1276 ± 35 [51] <sup>†</sup>	ND	650 ± 13 [59] <sup>†</sup>	ND	ND	ND	2.3 ± 0.1 [100]
Levamisole	98 ± 4 [29] <sup>†</sup>	ND	39 ± 3 [25] <sup>†</sup>	N.R*	N.R*	N.R*	N.R*
Pyrantel	72 ± 3.5 [58] <sup>†</sup>	ND	44 ± 2 [60] <sup>†</sup>	N.R*	N.R*	N.R*	N.R*
Tyramine	N.R*	N.R*	N.R*	N.R*	N.R*	N.R*	N.R*
Serotonin	N.R*	N.R*	N.R*	N.R*	N.R*	N.R*	N.R*
GABA	N.R*	N.R*	N.R*	N.R*	N.R*	N.R*	N.R*
Nicotine	N.R*	N.R*	N.R*	N.R*	N.R*	N.R*	N.R*
Strychnine	56 ± 3.3 [50]	13 ± 1.5 [5]	17 ± 2 [50]	N.R**	N.R**	N.R*	N.R*
Atropine	N.R*	N.R*	N.R*	3.1 ± 0.06 [43]	2.4 ± 0.05 [27]	N.R*	N.R*
Mecamylamine	N.R*	N.R*	N.R*	N.R*	N.R*	N.R*	N.R*
Tubocurarine	N.R*	N.R*	N.R*	N.R*	N.R*	N.R*	N.R*
Betaine	N.R*	N.R*	N.R*	N.R*	N.R*	N.R*	N.R*

### 5.3.4: Homology modelling

In order to visualize the interaction of the agonists and antagonist with residues in the binding pocket of these unique receptors, homology models were generated for the Hco-LGC-39 and Hco-LGC-40 homodimers and the Hco-LGC-39/Hco-ACC-1 and Hco-LGC-40/Hco-ACC-1 heterodimers using the *D. rerio* alpha-1 glycine receptor (3JAD) as a template. Hco-LGC-39, Hco-LGC-40 and Hco-ACC-1 share 33%, 38%, and 30% sequence identity with 3JAD respectively. The model for the Hco-LGC-39 homodimer is outlined in Figure 5.5A. Docking of channel activators, ACh, Meth, and Atro is outlined in Figures 5.5A I, II, and III. ACh docks in an extended orientation in the Hco-LGC-39 binding pocket (Figure 5.5A I). The quaternary amine on ACh is located 4.4 Å from W327. The serine (S243) in loop E is located 4.6 Å from the carbonyl oxygen in ACh, allowing for potential hydrogen bond interactions to occur. In contrast to ACh, Meth docks in a bent orientation in the Hco-LGC-39 binding pocket (Figure 5.5A II). The quaternary amine of Meth is located 4.7 Å from W327. This bent orientation of Meth places the carbonyl oxygen in 2.6 Å from S243. Atro is a much bulkier molecule compared to ACh and Meth; however it docks in a similar bent orientation in the Hco-LGC-39 binding pocket (Figure 5.5A III). The positively charged amine in Atro is located 4.5 Å from W327, whereas the carbonyl oxygen is located 3.6 Å from S243.

The model for the Hco-LGC-39/Hco-ACC-1 heterodimer is outlined in Figure 5.5B. Here, Hco-LGC-39 is positioned as the primary subunit (Blue), contributing loops A, B and C to the binding pocket, and Hco-ACC-1 is positioned as the complementary subunit (Orange), contributing loops D, E and F to the binding pocket (Figure 5.5B). Docking of agonists ACh, Meth, and Ure, and antagonist Atro, is outlined in Figure 5.5B I, II, III, and IV. ACh docked in an extended orientation in the Hco-LGC-39/Hco-ACC-1 binding pocket (Figure 5B I). Unlike what we see in the Hco-LGC-39 homomer, ACh is oriented with its quaternary amine pointed away from the loop C W327, at a distance of 7.0 Å. The tyrosine residue (Y273) is located 4.0 Å from the carbonyl oxygen in ACh. Similar to ACh, Meth docks in an extended orientation in the Hco-LGC-39/Hco-ACC-1 binding pocket with its quaternary amine pointed away from W327, at a distance of 8.0 Å (Figure 5.5B II). The asparagine (N148) in loop E is located 3.4 Å and 4.2 Å from Y273 and the carbonyl oxygen on Meth respectively, allowing for potential hydrogen bond interactions to occur and further stabilization of the binding pocket. Ure docks in an extended orientation in the Hco-LGC-39/Hco-ACC-1 binding pocket, with its quaternary amine pointed away from W327, at a distance of 7.2 Å (Figure 5.5B III). The carbonyl oxygen on Ure is located 3.2 Å from N148, allowing for potential hydrogen bond

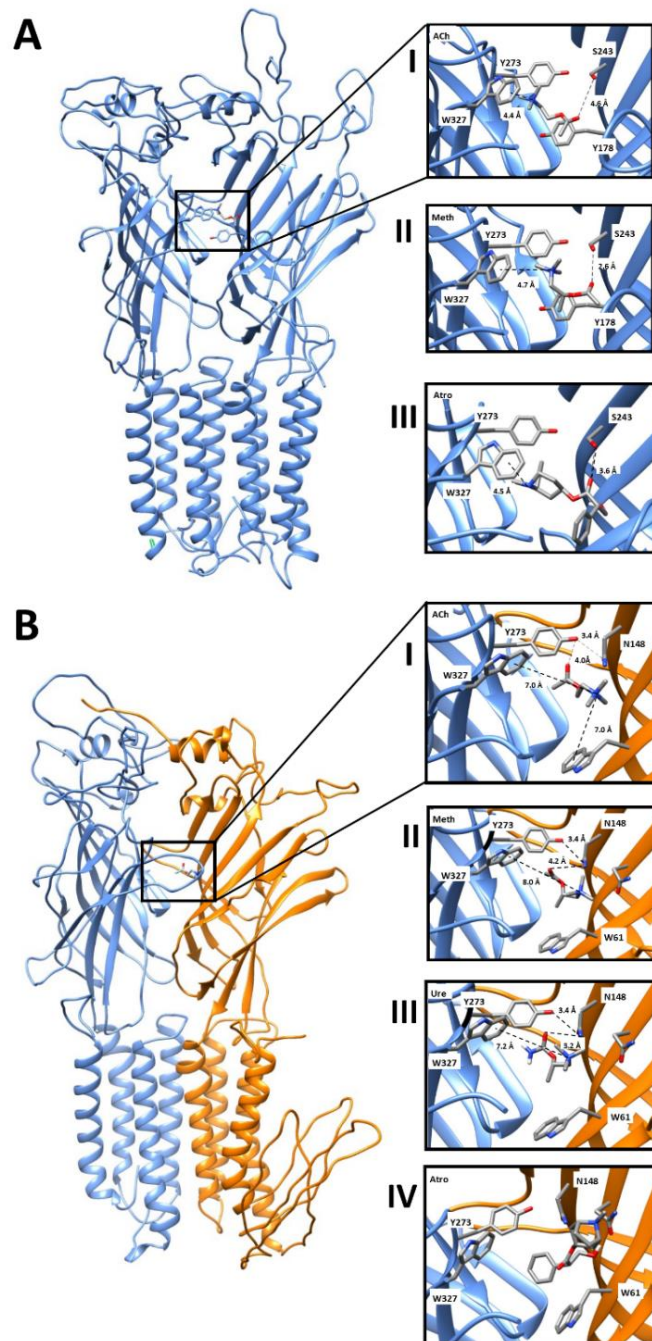


interactions to occur. Atro is docked in the Hco-LGC-39/Hco-ACC-1 binding pocket with its positively charged amine pointed away (12.7 Å) from W237 (Figure 5.5B IV).

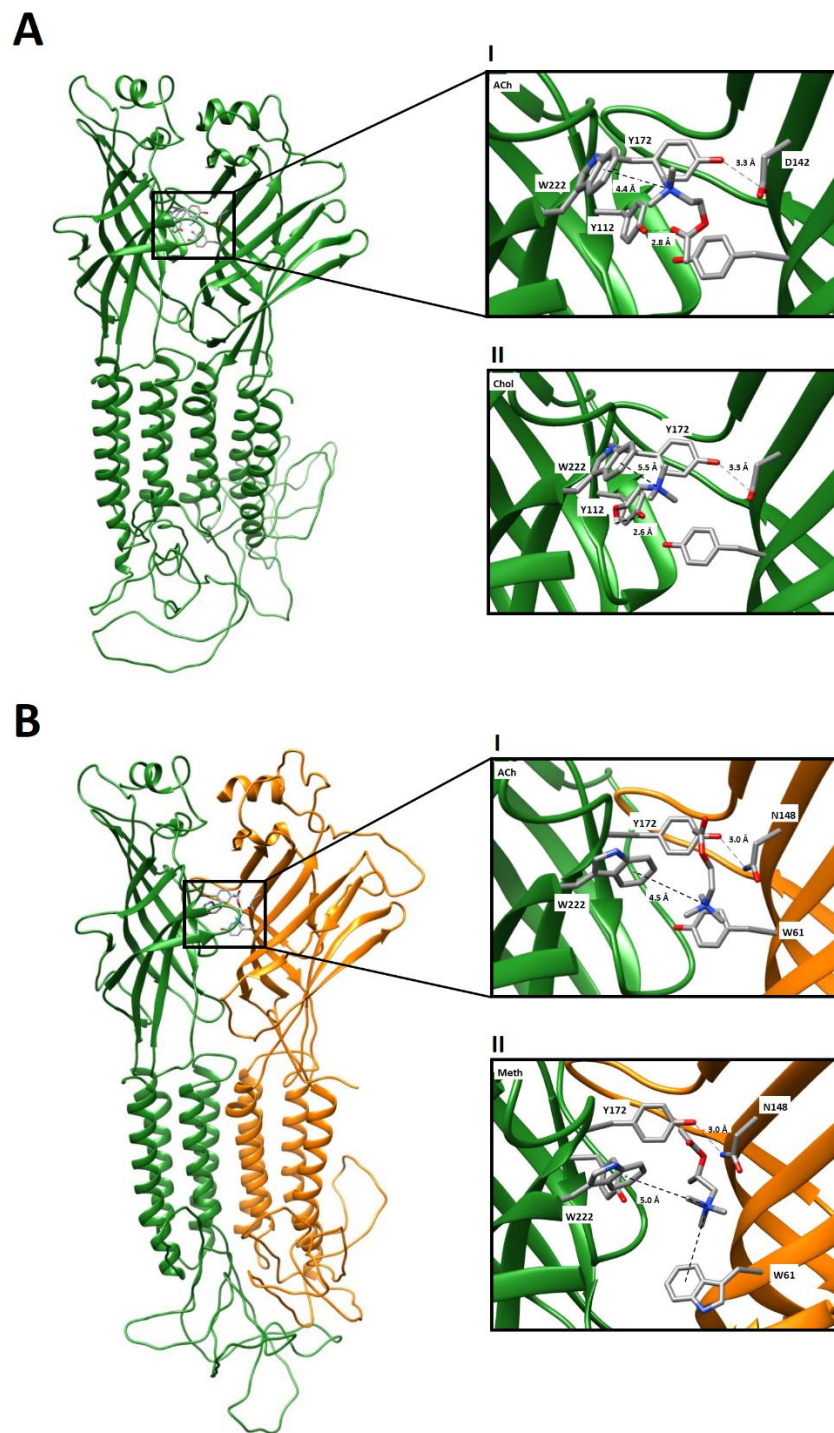
The model for the Hco-LGC-40 homodimer is outlined in Figure 5.6A. Again, the binding site appears to be composed of several aromatic residues. Docking of channel activators, ACh and Choline is outlined in Figure 5.6A I and II. ACh is docked in a bent formation in the Hco-LGC-40 binding pocket with its quaternary amine located 4.4 Å from W222 (Figure 5.6A I). The carbonyl oxygen is bent towards the tyrosine residue (Y112) in Loop A at a distance of 2.8 Å, allowing for potential hydrogen bond interactions to occur. The aspartic acid (D142) in loop E is located 3.3 Å from Y172, allowing for additional stabilization of the Hco-LGC-40 binding pocket through potential hydrogen bonding. In contrast, choline docks in an extended orientation in the Hco-LGC-40 binding pocket, with its quaternary amine located 5.5 Å from W222 (Figure 5.6A II). Similarly, the hydroxyl group on choline is located 2.6 Å from Y112.

The model for the Hco-LGC-40/Hco-ACC-1 heterodimer is outlined in Figure 5.6B. Here, Hco-LGC-40 is positioned as the primary subunit (Green), whereas Hco-ACC-1 is positioned as the complementary subunit (Orange). Docking of agonists ACh and Meth is outlined in Figure 5.6B I and II. ACh is docked in an extended orientation with its quaternary amine located 4.5 Å from W222 (Figure 5.6B I). The asparagine (N148) in loop E is located 3.0 Å from Y172, allowing for potential hydrogen bond interactions to occur and further stabilization of the binding pocket. Meth is docked in a similar extended orientation in the Hco-LGC-40/Hco-ACC-1 binding pocket, with its quaternary amine located 5.0 Å from W222 (Figure 5.6B II).

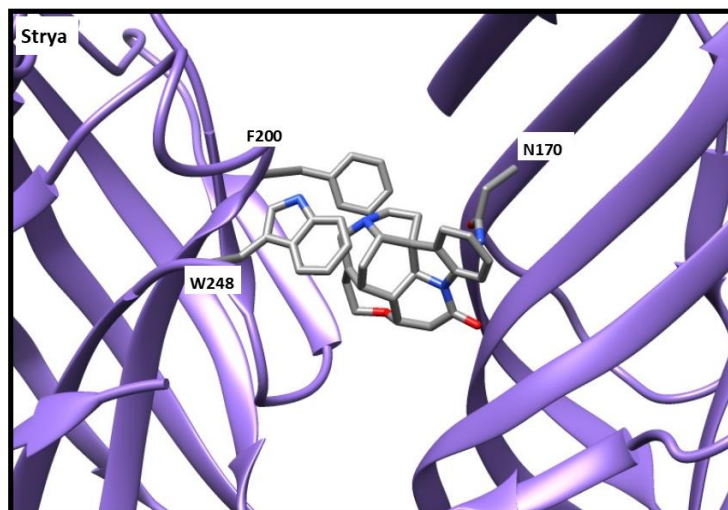
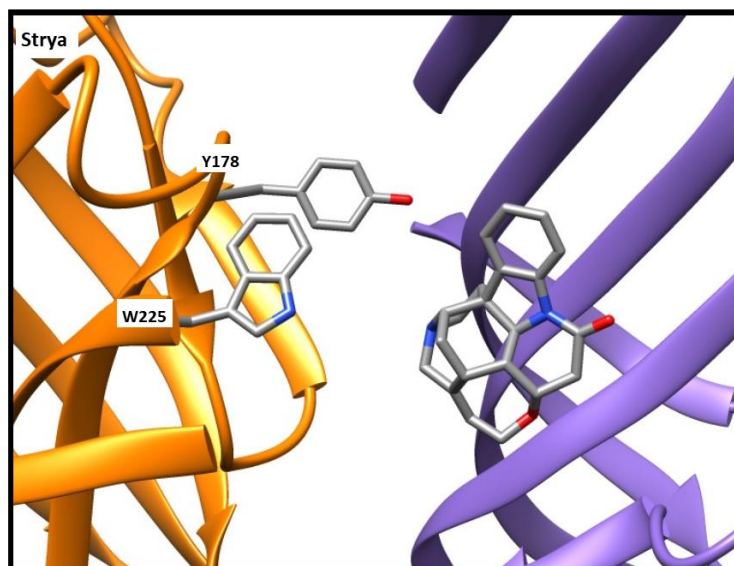
The models for the Hco-ACC-2 and Hco-ACC-1/Hco-ACC-2 receptors with strychnine bound in the binding pocket are outlined in (Figure 5.7 A and B). Stry sits in the Hco-ACC-2 binding pocket with its  $\gamma$ -sulfur atom on C188 oriented towards W248 (Figure 5.7A). However in the Hco-ACC-1/Hco-ACC-2 model, the  $\gamma$ -sulfur atom in Strya is oriented away from this crucial tryptophan (W225) residue in loop C (Figure 5.7B).



**Figure 5.5:** (A) Homology model of Hco-LGC-39 homodimer. The principle and complimentary subunits are represented by the colour blue. **I:** View of the Hco-LGC-39 binding pocket with acetylcholine docked. **II:** View of the Hco-LGC-39 binding pocket with methacholine docked. **III:** View of the Hco-LGC-39 binding pocket with atropine docked. (B) Homology model of Hco-LGC-39/Hco-ACC-1 heterodimer. Hco-LGC-39 and ACC-1 are the principal and complimentary subunits, and are represented by the colours blue and orange, respectively. **I:** View of the Hco-LGC-39/ACC-1 binding pocket with acetylcholine docked. **II:** View of the Hco-LGC-39/ACC-1 binding pocket with methacholine docked. **III:** View of the Hco-LGC-39/ACC-1 binding pocket with urecholine docked. **IV:** View of the Hco-LGC-39/ACC-1 binding pocket with atropine docked. Key aromatic residues in binding pocket are highlighted and distance to tryptophan (W327) is shown. \*A portion of Loop C is removed from the images for clarity.



**Figure 5.6:** (A) Homology model of Hco-LGC-40 homodimer. The principle and complimentary subunits are represented by the colour green. I: View of the Hco-LGC-40 binding pocket with acetylcholine docked. II: View of the Hco-LGC-40 binding pocket with choline docked. (B) Homology model of Hco-LGC-40/Hco-ACC-1 heterodimer. Hco-LGC-40 and ACC-1 are the principal and complimentary subunits, and are represented by the colours green and orange, respectively. I: View of the Hco-LGC-40/ACC-1 binding pocket with acetylcholine docked. II: View of the Hco-LGC-40/ACC-1 binding pocket with methacholine docked. Key aromatic residues in binding pocket are highlighted and distance to tryptophan (W327) is shown. \*A portion of Loop C is removed from the images for clarity.

**A****B**

**Figure 5.7:** **(A)** View of the Hco-ACC-2 homodimer binding pocket with strychnine docked. **(B)** View of the Hco-ACC-1/ACC-2 binding pocket with strychnine docked. ACC-1 and ACC-2 proteins are represented by the colours orange and purple, respectively. Key aromatic residues in binding pocket are highlighted and distance to tryptophan (W248 and W225) are shown.

\*A portion of Loop C is removed from the images for clarity.

## 5.4: Discussion

This study describes an investigation into the GGR-1 family of receptors in the parasitic nematode *H. contortus*. Hco-LGC-39 and Hco-LGC-40 appear to be cholinergic receptors that form functional channels on their own and in association with other members of the ACC-1 family. The ACC-1 family represents a unique group of inhibitory receptors that are only present in nematodes (Putrenko et al. 2005). Although the function of the GGR-1 family is unknown, prior research suggests that it is unique to invertebrate species (Jones and Sattelle 2008). The work done in this study outlines the first pharmacological characterization of these novel cholinergic receptors and provides insight into the binding pockets through homology modelling. Members of the GGR-1 family have been shown to form unique heteromeric channels with ACC-1 when expressed in *Xenopus* oocytes.

The pharmacology of the Hco-LGC-39 receptor and subsequent homology modelling provides insight into the nature of the Hco-LGC-39 homomeric binding site. The Hco-LGC-39 receptor is sensitive to the cholinergic ligands, ACh and meth, and is minimally sensitive to GABA and biogenic amines. This is interesting because prior characterization of the GGR-1 family in *C. elegans*, through phylogenetic analysis, suggested that members were closely related to glycine and histamine receptors (Jones and Sattelle 2008). When comparing EC<sub>50</sub> values of ACh and Meth, it appears that the Hco-LGC-39 receptor is slightly more sensitive to Meth, with Meth activating the channel to a larger degree compared to ACh. This suggests that Meth is a full agonist of the Hco-LGC-39 receptor, while ACh is a partial agonist, which is similar to observations of Nazareth 2019. When comparing the structure of the two ligands, the only notable difference is the presence of a  $\beta$ -methyl group. The presence of this methyl group appears to dock the molecule in a more structurally favorable manner, where the carbonyl oxygen is bent towards the polar serine (S243) in loop E, potentially contributing to the stability of the molecule in the binding pocket. When referring to the Hco-LGC-39 model, we can see the binding pocket is made up of many aromatic residues. Of these, the most notable aromatic residue is tryptophan, as it has been shown in mammalian nAChRs that this tryptophan residue in loop B contributes to cationic pi interaction with the quaternary amine of ACh (Beene et al. 2002). However, we have previously shown that in nematode ACCs this key tryptophan is found in loop C (Callanan et al. 2018). Similar to the ACCs, this crucial tryptophan (W327) residue is located in loop C of the Hco-LGC-39 receptor. Both ACh and Meth can be seen docking in the Hco-LGC-39 binding pocket with their quaternary amine directed towards W327.

When assessing the pharmacology of the Hco-LGC-40 receptor we found that when expressed in *Xenopus* oocytes, it produces a homomeric receptor that is sensitive to the cholinergic ligands choline and ACh in

a similar manner as observed by Nazareth 2019. When compared to the homologous protein in *C. elegans*, the *H. contortus* LGC-40 receptor was similarly sensitive to choline but 18-fold more sensitive to ACh (Ringstad et al. 2009). Differences in sensitivity between homologous receptors in *H. contortus* and *C. elegans* have been observed in other members of the cys-loop LGICs, including the ACC-1 family and UNC-49 family (Siddiqui et al. 2010; Callanan et al. 2018; Habibi et al. 2020). Similar to Hco-LGC-39 and other members of the ACC-1 family, the Hco-LGC-40 binding pocket is made up of several aromatic residues, with the crucial tryptophan residue (W222) present in loop C. Both ACh and Chol dock in the binding pocket with their quaternary amine located within an appropriate distance from W222, allowing for participation in cationic- $\pi$  interaction.

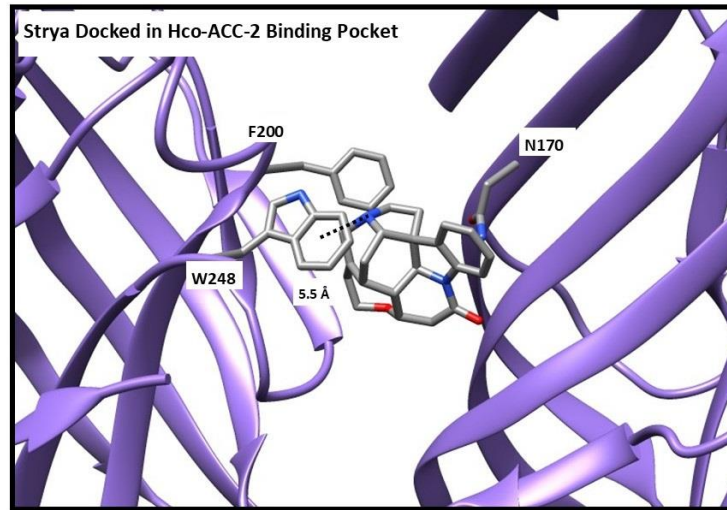
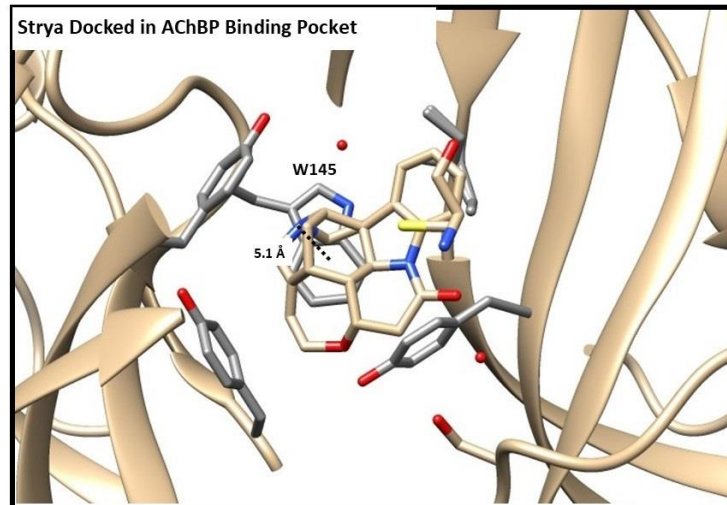
Since members of the GGR-1 family are activated by cholinergic ligands, it was hypothesized that Hco-LGC-39 and Hco-LGC-40 may have the ability to co-assemble with members of the ACC-1 family. When Hco-LGC-39 is co-expressed with Hco-ACC-1, a unique heteromeric channel is generated which is significantly more sensitive to ACh. We have previously observed this trend of increased receptor sensitivity when ACC-1 is present with other members of the ACC-1 family, such as ACC-2 and LGC-46 (Callanan et al. 2018; Habibi et al. 2020). In contrast, when Hco-LGC-40 is co-expressed with Hco-ACC-1 a unique heteromeric channel is generated which is less sensitive to Meth. When looking at how ACh and Meth dock in the Hco-LGC-40/Hco-ACC-1 binding pocket, we notice the carbonyl oxygen groups are oriented away from the tyrosine (Y112) residue found in loop A. This could potentially decrease the ability for ACh and Meth to stabilize in the binding pocket by removing that hydrogen bond interaction with Y112. In contrast, the Trp residue, which is typically involved in cationic- $\pi$  interaction with ACh and Meth, is located at a similar distance from docked ligands in both the LGC-40 homomeric and LGC-40/ACC-1 heteromeric receptors, suggesting that this is not a factor contributing to the heteromeric channel being less sensitive to ligands.

Of notable significance in this study, we observe that classical antagonists activate members of the GGR-1 and ACC-1 receptor families. Strychnine is an antagonist of the human glycine receptor (Curtis et al. 1971), whereas atropine is an antagonist of neuronal nAChRs (Phillis and York 1968). Here, we observed that strychnine activates the Hco-ACC-2 and Hco-ACC-1/Hco-ACC-2 receptors when expressed in *Xenopus* oocytes. Early research has shown that the strychnine-binding subunit of the human glycine receptor closely resembles nAChRs in both amino-acid sequence and structural organization (Grenningloh et al. 1987), and since then strychnine has been widely used for understanding the function of nAChRs. This could possibly provide insight into this phenomenon in nematode ACC receptors. The X-ray crystal

structure of the *Aplysia* acetylcholine binding protein (AChBP) with Strya bound shows a  $\gamma$ -sulfur atom in Strya is oriented towards the carbonyl oxygen of tryptophan (W145) in Loop B, resulting in stabilization in the binding pocket (Figure 5.8). This W145 also takes part in pi-cationic interactions with other aromatic in the binding pocket (Brams et al. 2011). In nematodes, this key tryptophan residue is located in loop C (Callanan et al. 2018; Habibi et al. 2018). Our models of the Hco-ACC-2 and Hco-ACC-1/Hco-ACC-2 receptors with Strya bound show that the  $\gamma$ -sulfur atom on Strya is oriented towards this tryptophan (W248 and W225) residue in loop C. Since this tryptophan residue is important in Strya binding to AChBP, it is possible this interaction in the ACC binding pockets provides a possible explanation for how Strya binds to this family of receptors.

Here, we observed that atropine activates the Hco-LGC-39 and Hco-LGC-39/Hco-ACC-1 receptors expressed in *Xenopus* oocytes. Atropine is a common muscarinic and neuronal nicotinic acetylcholine receptor antagonist (Phillis and York 1968; Parker et al. 2003). However, early research has shown that atropine can also act at the ACh binding site of  $\alpha 4$  subunit-containing receptors to cause neuronal potentiation in the presence of low concentrations of ACh (Zwart and Vijverberg 1997). It was later found that potentiation of nAChRs by atropine is specifically achieved over a narrow concentration range between 0.3-3  $\mu$ M, where higher concentrations result in receptor inhibition (Parker et al. 2003). Although our results do not show receptor potentiation in the presence of ACh and atropine, we do show that activation of both the Hco-LGC-39 and Hco-LGC-39/Hco-ACC-1 receptors was achieved with concentrations of atropine less than 3  $\mu$ M. Future research into how atropine also inhibits ACh elicited responses through receptor antagonism would be of interest. Although the mechanism of Atropine acting as an agonist of the ACC receptor is unknown, these results provide further insight into cholinergic neurotransmission in parasitic nematodes.

This study has found that unlike prior characterization using phylogenetic analysis, LGC-39 and 40 appear to be receptors that are cholinergic in nature and co-assemble with members of the ACC-1 family. Further research into the location and levels of expression of the GGR-1 family in *H. contortus* could provide insight into their potential use for future anthelmintic development.

**A****B**

**Figure 5.8:** (A) View of the Hco-ACC-2 homodimer binding pocket with strychnine docked. (B) View of the crystal structure of the *Aplysia* AChBP binding pocket with strychnine bound. PDB model (2xys) retrieved from Brams et al. 2011.

#### 5.4: Acknowledgements

Thank you Kristen Nazareth for cloning Hco-LGC-39 and Hco-LGC-40 and conducting the initial pharmacological characterization of the homomeric receptors.



## Chapter VI – General Discussion

The work presented in this thesis provides an in-depth look at inhibitory cholinergic neurotransmission in the parasitic nematode *H. contortus*. Through sequence analysis, pharmacological characterization using two-electrode voltage clamp electrophysiology, site-directed mutagenesis, and *in silico* homology modelling, we have been able to further understand the function of inhibitory ACh receptors in nematodes, and how they differ from nAChRs.

The ACC-1 family consists of 7 receptor subunit genes, of which I have cloned two members, Hco-LGC-46 and Hco-ACC-4. I conducted an extensive pharmacological characterization of four unique ACC-1 family members, Hco-ACC-2, Hco-ACC-1/Aco-ACC-2, Hco-LGC-46, and Hco-ACC-1/Hco-LGC-46. In addition, I characterized two members of the GGR-1 family of LGICs, Hco-LGC-39 and Hco-LGC-40, and explored the pharmacology of two unique heteromeric receptors, Hco-LGC-39/Hco-ACC-1 and Hco-LGC-40/Hco-ACC-1. To complement each pharmacological characterization, I generated homology models of each receptor and assessed how various cholinergic ligands, anthelmintics, and inhibitors interact in the binding pockets.

Through sequence analysis of the ACC receptors, I found key residues within the binding pocket that would be of importance for ligand docking. Specifically, the binding pocket of many cys-loop ligand gated ion channels is composed of aromatic residues (Dougherty 1996). Two binding loops that we placed particular focus on were loops B and C, since this is where we noticed differences between ACC receptors and nAChRs. In nAChRs, loop B contains a tryptophan residue that is involved in pi-cationic interactions with the cationic center of ligands (Beene et al. 2002). I found that in nematode ACC receptors (ACC-2, ACC-1, and LGC-46), this tryptophan residue (W225, W248, and W259, respectively) is located in loop C. The ACC-2 and LGC-46 receptors contain a phenylalanine residue in loop B (F200 and F212 respectively), whereas the ACC-1 receptor contains a tyrosine residue (Y178). Of the receptors examined in this thesis, ACC-4 is the only one that does not contain a tryptophan residue in loop C, and instead contains a phenylalanine residue. In addition to identifying residues of importance in the ACC binding pockets, analysis of the ACC receptor sequences revealed the PAR motif at the beginning of the transmembrane 2 domain, which is indicative of anion selectivity (Jensen et al. 2002). I performed current-voltage analysis on all of the receptors analyzed (ACC-2, ACC-1/ACC-2, LGC-46, and ACC-1/LGC-46) and confirmed that chloride ions flow through the channels when activated.

Hco-ACC-2 and Hco-LGC-46 both form functional homomeric ligand-gated chloride channels (Manuscript I: Habibi et al. 2018; Manuscript III: Habibi et al. 2020), whereas Hco-ACC-1 and Hco-ACC-4 do not form

functional homomeric ligand-gated chloride channels. The ACC-2 receptor is sensitive to ACh, ACh derivatives (carbachol, methacholine, urecholine, and choline), and nAChR anthelmintics (pyrantel and levamisole). The LGC-46 receptor is sensitive to ACh and Methacholine. Site-directed mutagenesis of aromatic residues in the ACC-2 receptor binding pocket revealed residues of significant importance. Specifically, mutation of the tryptophan residue (W248) in loop C to either a tyrosine or phenylalanine residue resulted in a receptor that was significantly less sensitive to ACh and ACh derivatives. When the loop C tryptophan and loop B phenylalanine are swapped in position, functionality of the receptor is inhibited. This shows the importance of the presence and location of the loop B tryptophan in ligand binding and channel activation. When we mutated the phenylalanine residue in loop B to a tyrosine residue, to mimic the ACC-1 receptor binding pocket, the resulting receptor was hypersensitive to ACh and ACh derivatives. Thus, the introduction of a hydroxyl group into the ACC-2 binding pocket enhances ligand binding and channel activation.

When expressed in *X. laevis* oocytes, ACC-2 co-assembles with ACC-1 to form a unique heteromeric receptor, which is highly sensitive to both ACh and carbachol (Manuscript II: Callanan et al. 2018). Similarly, LGC-46 also co-assembles with ACC-1 to form a unique heteromeric channel that is significantly more sensitive to ACh, carbachol, and methacholine, compared to the LGC-46 homomeric receptor. The expression of ACC-1 alone in *X. laevis* oocytes does not result in a functional homomeric channel. This differs from *C. elegans* homologues, where Cel-ACC-1 does form a functional homomeric ligand-gated ion channel on its own (Putrenko et al. 2005). When analyzing the sequence of ACC-1, we see that it contains a tyrosine residue in loop B. Based on the mutagenesis results we obtained with the ACC-2 receptor, it appears that the naturally occurring tyrosine residue in the ACC-1/ACC-2 and ACC-1/LGC-46 heteromeric receptors causes the hypersensitivity of the channels that we observe. When ACC-2 is expressed with ACC-4, we observe a decrease in current flowing through the channel. Interestingly, although the maximum current is reduced, the EC<sub>50</sub> of the channel in the presence of ACh remained unaffected. This suggested that ACC-4 plays a regulatory role through negatively affecting expression of the receptor (Manuscript III: Habibi et al. 2020). In *C. elegans*, the presence of ACC-4 also negatively impacts the function of ACC-2, with co-expression of ACC-4 with ACC-2 completely abolishing function of the ACC-2 receptor (Putrenko et al. 2005). The co-expression of ACC-4 with LGC-46 resulted in a non-functional LGC-46 receptor. Thus, ACC-4 appears to negatively influence the expression of both the ACC-2 and LGC-46 receptors. One possible explanation for this decrease in receptor expression in the presence of ACC-4 is the fact that ACC-4 does not contain a tryptophan residue in loop C, which stabilizes ligands for channel activation. Instead, ACC-4 contains a phenylalanine residue. My prior mutagenesis study showed that the

presence of a phenylalanine residue in place of the loop C tryptophan, severely impacts the ACC receptors and thus could explain why we see a decrease of ACC receptor functionality in the presence of ACC-4.

To supplement the pharmacological characterization of the ACC-1 family of receptors, I used homology modelling and associated ligand docking, to further investigate how these channels are activated. When looking at the binding pockets of the ACC-2 and LGC-46 homomeric receptors we see that all cholinergic ligands dock with their quaternary amine functional groups oriented towards the tryptophan residue in loop C. In addition, the quaternary amine groups are located at a distance from the loop C tryptophan residue to allow for cationic- $\pi$  interactions to occur. Similarly, both ACC-2 and LGC-46 contain a phenylalanine residue (F200 and F212 respectively) in loop B, which faces into the binding pocket. Both receptors also contain an asparagine residue (N170 and N182 respectively) in loop E of the complementary subunit located at an appropriate distance to participate in hydrogen bond interactions with the carbonyl oxygen of ligands. I see that both ACh and Meth dock in the ACC-2 and LGC-46 binding pockets with their carbonyl oxygen's oriented towards the loop E asparagine residues, possibly explaining why both of these molecules activate the ACC receptors with full efficacy.

To further the scope of my analysis of cholinergic receptors in nematodes, I moved forward to characterize novel cholinergic cys-loop ligand-gated ion channels from other families and clades. Since many families of LGICs have yet to be pharmacologically characterized, I was interested in exploring their role in the nervous system of nematodes. This would provide insight into their relevance for anthelmintic action. Prior work completed by Kristen Nazareth identified two members of the GGR-1 family from *H. contortus*, Hco-LGC-39 and Hco-LGC-40. Since these receptors respond to cholinergic ligands when expressed in *X. laevis* oocytes, I hypothesized that they could co-assemble with members of the ACC-1 family. I found that both LGC-39 and LGC-40 co-assemble with Hco-ACC-1 to form unique heteromeric channels, which are activated in the presence of cholinergic ligands. I also observed that when expressed in *X. laevis* oocytes, some receptors are activated in the presence of classical cholinergic antagonists. Specifically, atropine, an antagonist of neuronal nAChR's (Phillis and York 1968), activates the Hco-LGC-39 and Hco-LGC-39/Hco-ACC-1 receptors at very low concentrations. Strychnine, an antagonist of the human glycine receptor (Curtis et al. 1971), activates the Hco-ACC-2 and Hco-ACC-1/Hco-ACC-2 receptors. Together these results reveal that unlike mammalian nAChRs and glycine receptors, some nematode cys-loop LGICs are activated in the presence of antagonists, rather than being inhibited.

Together the research I have conducted over the course of my PhD has provided an in-depth examination of inhibitory cholinergic cys-loop receptors from the parasitic nematode *H. contortus*. I have identified

unique heteromeric LGCs both within the ACC-1 family and between clades with the GGR-1 family. This research provides insight into the nervous system of nematodes and how these systems differ from mammalian systems. In addition, the supplementation with computational homology modelling, allows us to paint a more detailed picture of how ligands bind in binding pockets of these receptors. Together these findings provide us with an in depth understanding of receptor protein-ligand interactions, which could be used in the future to inform chemists for pharmaceutical development.

Future work for this project will aim to confirm the nature of subunit association when co-expression of receptors takes place. Specifically I would be interested in determining whether altering the ratio of different subunit RNAs injected into *Xenopus* oocytes effects the subunit combinations of the pentamer being formed. This will also help determine whether or not a pentamer is indeed forming and not responsive to ligands present. The experiment that will provide answers to these questions is the Blue-Native Page. In general, the technique involves the injection of cRNA encoding receptor subunits into *Xenopus* oocytes, the subsequent metabolic labelling of injected oocytes with L-[<sup>35</sup>S]-methionine, the extraction of receptor proteins after expression, and the visualization of protein associations (based on molecular weight) once run on a blue-native page gel (Nicke et al. 1999). This method allows us to analyze the assembly of distinct combinations of homomeric and heteromeric receptor subunits. This will also provide insight into whether the ACC-1 protein is forming a pentameric channel that is unresponsive to ligands, or if it does not readily form a pentameric homomeric channel. Together, this work will provide a more in depth look at the assembly of the ACC-1 family of receptors in *Xenopus* oocytes, and provide suggestions for what may be taking place in whole *H. contortus* parasites.

## Chapter VII – References

- Abdelmassih SA, Cochrane E, Forrester SG. 2018. Evaluating the longevity of surgically extracted *Xenopus laevis* oocytes for the study of nematode ligand-gated ion channels. *Invertebr Neurosci.* 18(1):1.
- Accardi M V, Forrester SG. 2011. The *Haemonchus contortus* UNC-49B subunit possesses the residues required for GABA sensitivity in homomeric and heteromeric channels. *Mol Biochem Parasitol.* 178(1–2):15–22.
- Aubry ML, Cowell P, Davey MJ, Shevde S. 1970. Aspects of the pharmacology of a new anthelmintic: pyrantel. *Br J Pharmacol.* 38(2):332–344.
- Bamber BA, Beg AA, Twyman RE, Jorgensen EM. 1999. The *Caenorhabditis elegans* unc-49 locus encodes multiple subunits of a heteromultimeric GABA receptor. *J Neurosci.* 19(13):5348–5359.
- Bamber BA, Twyman RE, Jorgensen EM. 2003. Pharmacological characterization of the homomeric and heteromeric UNC-49 GABA receptors in *C. elegans*. *Br J Pharmacol.* 138(5):883–893.
- Barker KR, Hussey RS, Krusberg LR, Bird GW, Dunn RA, Ferris H, Ferris VR, Freckman DW, Gabriel CJ, Grewal PS. 1994. Plant and soil nematodes: societal impact and focus for the future. *J Nematol.* 26(2):127.
- Beech RN, Callanan MK, Rao VTS, Dawe GB, Forrester SG. 2013. Characterization of cys-loop receptor genes involved in inhibitory amine neurotransmission in parasitic and free living nematodes. *Parasitol Int.* 62(6):599–605.
- Beene DL, Brandt GS, Zhong W, Zacharias NM, Lester HA, Dougherty DA. 2002. Cation- $\pi$  interactions in ligand recognition by serotonergic (5-HT<sub>3A</sub>) and nicotinic acetylcholine receptors: The anomalous binding properties of nicotine. *Biochemistry.* 41(32):10262–10269.
- Beg AA, Jorgensen EM. 2003. EXP-1 is an excitatory GABA-gated cation channel. *Nat Neurosci.* 6(11):1145.
- Berger J. 1975. The resistance of a field strain of *Haemonchus contortus* to five benzimidazole anthelmintics in current use. *J S Afr Vet Assoc.* 46(4):369.
- Besier RB, Kahn LP, Sargison ND, Van Wyk JA. 2016. The pathophysiology, ecology and epidemiology of *Haemonchus contortus* infection in small ruminants. In: *Advances in parasitology.* Vol. 93. Elsevier. p. 95–

143.

Bianchi L, Driscoll M. 2006. Heterologous expression of *C. elegans* ion channels in *Xenopus* oocytes.

Blackhall WJ, Liu HY, Xu M, Prichard RK, Beech RN. 1998. Selection at a P-glycoprotein gene in ivermectin- and moxidectin-selected strains of *Haemonchus contortus*. *Mol Biochem Parasitol*. 95(2):193–201.

Blouin MS, Yowell CA, Courtney CH, Dame JB. 1995. Host movement and the genetic structure of populations of parasitic nematodes. *Genetics*. 141(3):1007–1014.

Boulin T, Fauvin A, Charvet CL, Cortet J, Cabaret J, Bessereau J, Neveu C. 2011. Functional reconstitution of *Haemonchus contortus* acetylcholine receptors in *Xenopus* oocytes provides mechanistic insights into levamisole resistance. *Br J Pharmacol*. 164(5):1421–1432.

Bourguinat C, Lee ACY, Lizundia R, Blagburn BL, Liotta JL, Kraus MS, Keller K, Epe C, Letourneau L, Kleinman CL. 2015. Macrocyclic lactone resistance in *Dirofilaria immitis*: failure of heartworm preventives and investigation of genetic markers for resistance. *Vet Parasitol*. 210(3–4):167–178.

Brams M, Pandya A, Kuzmin D, Van Elk R, Krijnen L, Yakel JL, Tsetlin V, Smit AB, Ulens C. 2011. A structural and mutagenic blueprint for molecular recognition of strychnine and d-tubocurarine by different cys-loop receptors. *PLoS Biol*. 9(3).

Van den Brom R, Moll L, Kappert C, Vellema P. 2015. *Haemonchus contortus* resistance to monepantel in sheep. *Vet Parasitol*. 209(3):278–280.

Brown HD. 1961. Antiparasitic Brown HD. 1961. Antiparasitic drugs. IV. 2-(4-thiazolyl)-benzimidazole, a new anthelmintic. *J. Am. Chem. Soc.* 83:1764–1765. drugs. IV. 2-(4-thiazolyl)-benzimidazole, a new anthelmintic. *J Am Chem Soc.* 83(7):1764–1765.

Callanan MK, Habibi SA, Law WJ, Nazareth K, Komuniecki RL, Forrester SG. 2018. Investigating the function and possible biological role of an acetylcholine-gated chloride channel subunit (ACC-1) from the parasitic nematode *Haemonchus contortus*. *Int J Parasitol Drugs Drug Resist*. 8(3):526–533.

Carmichael I, Visser R, Schneider D, Soll M. 1987. *Haemonchus contortus* resistance to ivermectin. *J S Afr Vet Assoc*. 58(2):93.

Del Castillo J, Morales TA, Sanchez V. 1963. Action of piperazine on the neuromuscular system of *Ascaris lumbricoides*. *Nature*. 200(4907):706.

Chabala JC, Mrozik H, Tolman RL, Eskola P, Lusi A, Peterson LH, Woods MF, Fisher MH, Campbell WC, Egerton JR and. 1980. Ivermectin, a new broad-spectrum antiparasitic agent. *J Med Chem*. 23(10):1134–1136.

Changeux J-P. 2012. The nicotinic acetylcholine receptor: the founding father of the pentameric ligand-gated ion channel superfamily. *J Biol Chem*. 287(48):40207–40215.

Charlie NK, Schade MA, Thomure AM, Miller KG. 2006. Presynaptic UNC-31 (CAPS) is required to activate the  $G\alpha s$  pathway of the *Caenorhabditis elegans* synaptic signaling network. *Genetics*. 172(2):943–961.

Cook A, Aptel N, Portillo V, Siney E, Sihota R, Holden-Dye L, Wolstenholme A. 2006. *Caenorhabditis elegans* ivermectin receptors regulate locomotor behaviour and are functional orthologues of *Haemonchus contortus* receptors. *Mol Biochem Parasitol*. 147(1):118–125.

Corringier P-J, Novère N Le, Changeux J-P. 2000. Nicotinic receptors at the amino acid level. *Annu Rev Pharmacol Toxicol*. 40(1):431–458.

Craig TM, Miller DK. 1990. Resistance by *Haemonchus contortus* to ivermectin in angora goats. *Vet Rec*. 126(23).

Cully DF, Vassilatis DK, Liu KK, Paresse PS, Van der Ploeg LH, Schaeffer JM, Arena JP. 1994. Cloning of an avermectin-sensitive glutamate-gated chloride channel from *Caenorhabditis elegans*. *Nature*. 371(6499):707.

Curtis DR, Duggan AW, Johnston GAR. 1971. The specificity of strychnine as a glycine antagonist in the mammalian spinal cord. *Exp Brain Res*. 12(5):547–565.

Dent JA, Davis MW, Avery L. 1997. *avr-15* encodes a chloride channel subunit that mediates inhibitory glutamatergic neurotransmission and ivermectin sensitivity in *Caenorhabditis elegans*. *EMBO J*. 16(19):5867–5879.

Dougherty DA. 1996. Cation- $\pi$  interactions in chemistry and biology: a new view of benzene, Phe, Tyr, and Trp. *Science* (80- ). 271(5246):163.

Drudge JH, Szanto J, Wyant ZN, Elam G. 1964. Field studies on parasite control in sheep: comparison of thia-bendazole, ruelene, and phenothiazine. *Am J Vet Res.* 25(108):1512–1518.

Ducray P, Gauvry N, Pautrat F, Goebel T, Fruechtel J, Desaulles Y, Weber SS, Bouvier J, Wagner T, Froelich O. 2008. Discovery of amino-acetonitrile derivatives, a new class of synthetic anthelmintic compounds. *Bioorg Med Chem Lett.* 18(9):2935–2938.

Duerr JS, Han H, Fields SD, Rand JB. 2008. Identification of major classes of cholinergic neurons in the nematode *Caenorhabditis elegans*. *J Comp Neurol.* 506(3):398–408.

Echevarria FA, Trindade GN. 1989. Anthelmintic resistance by *Haemonchus contortus* to ivermectin in Brazil: a preliminary report. *Vet Rec.* 124(6):147–148.

Galzi J-L, Devillers-Thierry A, Hussy N, Bertrand S, Changeux J-P, Bertrand D. 1992. Mutations in the channel domain of a neuronal nicotinic receptor convert ion selectivity from cationic to anionic. *Nature.* 359(6395):500–505.

Ghisi M, Kaminsky R, Mäser P. 2007. Phenotyping and genotyping of *Haemonchus contortus* isolates reveals a new putative candidate mutation for benzimidazole resistance in nematodes. *Vet Parasitol.* 144(3):313–320.

Green PE, Forsyth BA, Rowan KJ, Payne G. 1981. The isolation of a field strain of *Haemonchus contortus* in Queensland showing multiple anthelmintic resistance. *Aust Vet J.* 57(2):79–84.

Grenningloh G, Rienitz A, Schmitt B, Methfessel C, Zensen M, Beyreuther K, Gundelfinger ED, Betz H. 1987. The strychnine-binding subunit of the glycine receptor shows homology with nicotinic acetylcholine receptors. *Nature.* 328(6127):215–220.

Gurdon JB, Lane CD, Woodland HR, Marbaix G. 1971. Use of frog eggs and oocytes for the study of messenger RNA and its translation in living cells. *Nature.* 233(5316):177–182.

Habibi SA, Blazie SM, Jin Y, Forrester SG. 2020. Isolation and characterization of a novel member of the ACC ligand-gated chloride channel family, Hco-LCG-46, from the parasitic nematode *Haemonchus contortus*. *Mol Biochem Parasitol.*:111276.

Habibi SA, Callanan M, Forrester SG. 2018. Molecular and pharmacological characterization of an



- acetylcholine-gated chloride channel (ACC-2) from the parasitic nematode *Haemonchus contortus*. *Int J Parasitol Drugs Drug Resist.* 8(3):518–525.
- Harder A. 2016. The biochemistry of *Haemonchus contortus* and other parasitic nematodes. In: *Advances in parasitology*. Vol. 93. Elsevier. p. 69–94.
- Holden-Dye L, Walker RJ. 2007. Anthelmintic drugs. *WormBook*. 2:1–13.
- Jagannathan S, Laughton DL, Critten CL, Skinner TM, Horoszok L, Wolstenholme AJ. 1999. Ligand-gated chloride channel subunits encoded by the *Haemonchus contortus* and *Ascaris suum* orthologues of the *Caenorhabditis elegans* gbr-2 (avr-14) gene. *Mol Biochem Parasitol.* 103(2):129–140.
- Le Jambre LF. 1993. Ivermectin-resistant *Haemonchus contortus* in Australia. *Aust Vet J.* 70(9):357.
- Le Jambre LF, Southcott WH, Dash KM. 1976. Resistance of selected lines of *Haemonchus contortus* to thiabendazole, morantel tartrate and levamisole. *Int J Parasitol.* 6(3):217–222.
- Jensen ML, Timmermann DB, Johansen TH, Schousboe A, Varming T, Ahring PK. 2002. The  $\beta$  subunit determines the ion selectivity of the GABA<sub>A</sub> receptor. *J Biol Chem.* 277(44):41438–41447.
- Jobson MA, Valdez CM, Gardner J, Garcia LR, Jorgensen EM, Beg AA. 2015. Spillover transmission is mediated by the excitatory GABA receptor LGC-35 in *C. elegans*. *J Neurosci.* 35(6):2803–2816.
- Jones AK, Sattelle DB. 2008. The cys-loop ligand-gated ion channel gene superfamily of the nematode, *Caenorhabditis elegans*. *Invertebr Neurosci.* 8(1):41–47.
- Kaminsky R, Rufener L. 2012. Monepantel: from discovery to mode of action. *Parasit Helminths Targets, Screens, Drugs Vaccines.*:283–296.
- Kaplan RM. 2004. Drug resistance in nematodes of veterinary importance: a status report. *Trends Parasitol.* 20(10):477–481.
- Kehoe J. 1972a. Three acetylcholine receptors in *Aplysia* neurones. *J Physiol.* 225(1):115–146.
- Kehoe J. 1972b. Ionic mechanism of a two-component cholinergic inhibition in *Aplysia* neurones. *J Physiol.* 225(1):85–114.

- Kehoe J, McIntosh JM. 1998a. Two Distinct Nicotinic Receptors, One Pharmacologically Similar to the Vertebrate  $\alpha 7$ -Containing Receptor, Mediate Cl Currents in *Aplysia* Neurons. *J Neurosci*. 18(20):8198–8213.
- Kehoe J, McIntosh JM. 1998b. Two Distinct Nicotinic Receptors, One Pharmacologically Similar to the Vertebrate  $\alpha 7$ -Containing Receptor, Mediate Cl Currents in *Aplysia* Neurons. *J Neurosci*. 18(20):8198–8213.
- Kusano K, Miledi R, Stinnakre J. 1982. Cholinergic and catecholaminergic receptors in the *Xenopus* oocyte membrane. *J Physiol*. 328(1):143–170.
- Kwa MSG, Veenstra JG, Van Dijk M, Roos MH. 1995.  $\beta$ -Tubulin Genes from the Parasitic Nematode *Haemonchus contortus* Modulate Drug Resistance in *Caenorhabditis elegans*. *J Mol Biol*. 246(4):500–510.
- Lacey E, Prichard RK. 1986. Interactions of benzimidazoles (BZ) with tubulin from BZ-sensitive and BZ-resistant isolates of *Haemonchus contortus*. *Mol Biochem Parasitol*. 19(2):171–181.
- Laing R, Kikuchi T, Martinelli A, Tsai IJ, Beech RN, Redman E, Holroyd N, Bartley DJ, Beasley H, Britton C. 2013. The genome and transcriptome of *Haemonchus contortus*, a key model parasite for drug and vaccine discovery. *Genome Biol*. 14(8):R88.
- Laughton DL, Lunt GG, Wolstenholme AJ. 1997. Reporter gene constructs suggest that the *Caenorhabditis elegans* avermectin receptor beta-subunit is expressed solely in the pharynx. *J Exp Biol*. 200(10):1509–1514.
- Lee Y, Park Y, Chang D, Hwang JM, Min CK, Kaang B, Cho NJ. 1999. Cloning and expression of a G protein-linked acetylcholine receptor from *Caenorhabditis elegans*. *J Neurochem*. 72(1):58–65.
- Lee Y, Park Y, Nam S, Suh S, Lee J, Kaang B, Cho NJ. 2000. Characterization of GAR-2, a novel G protein-linked acetylcholine receptor from *Caenorhabditis elegans*. *J Neurochem*. 75(5):1800–1809.
- Lummis SCR, McGonigle I, Ashby JA, Dougherty DA. 2011. Two amino acid residues contribute to a cation- $\pi$  binding interaction in the binding site of an insect GABA receptor. *J Neurosci*. 31(34):12371–12376.
- Martin RJ, Robertson AP, Buxton SK, Beech RN, Charvet CL, Neveu C. 2012. Levamisole receptors: a second awakening. *Trends Parasitol*. 28(7):289–296.

- Mederos AE, Ramos Z, Banchero GE. 2014. First report of monepantel *Haemonchus contortus* resistance on sheep farms in Uruguay. *Parasit Vectors*. 7(1):598.
- Mello CC, Kramer JM, Stinchcomb D, Ambros V. 1991. Efficient gene transfer in *C. elegans*: extrachromosomal maintenance and integration of transforming sequences. *EMBO J*. 10(12):3959–3970.
- Miller PS, Smart TG. 2010. Binding, activation and modulation of Cys-loop receptors. *Trends Pharmacol Sci*. 31(4):161–174.
- Morris GM, Huey R, Lindstrom W, Sanner MF, Belew RK, Goodsell DS, Olson AJ. 2009. AutoDock4 and AutoDockTools4: Automated docking with selective receptor flexibility. *J Comput Chem*. 30(16):2785–2791.
- Mu T-W, Lester HA, Dougherty DA. 2003. Different binding orientations for the same agonist at homologous receptors: a lock and key or a simple wedge? *J Am Chem Soc*. 125(23):6850–6851.
- Nazareth K. 2019. Isolation and partial characterization of three members of the GGR-1 family in the parasitic nematode *Haemonchus contortus*. M.Sc. Thesis, Ontario Tech University.
- Neveu C, Charvet C, Fauvin A, Cortet J, Castagnone-Sereno P, Cabaret J. 2007. Identification of levamisole resistance markers in the parasitic nematode *Haemonchus contortus* using a cDNA-AFLP approach. *Parasitology*. 134(8):1105.
- Neveu C, Charvet CL, Fauvin A, Cortet J, Beech RN, Cabaret J. 2010. Genetic diversity of levamisole receptor subunits in parasitic nematode species and abbreviated transcripts associated with resistance. *Pharmacogenet Genomics*. 20(7):414–425.
- Nicke A, Rettinger J, Mutschler E, Schmalzing G. 1999. Blue native PAGE as a useful method for the analysis of the assembly of distinct combinations of nicotinic acetylcholine receptor subunits. *J Recept Signal Transduct*. 19(1–4):493–507.
- Ortells MO, Lunt GG. 1995. Evolutionary history of the ligand-gated ion-channel superfamily of receptors. *Trends Neurosci*. 18(3):121–127.
- Osei-Atweneboana MY, Eng JKL, Boakye DA, Gyapong JO, Prichard RK. 2007. Prevalence and intensity of *Onchocerca volvulus* infection and efficacy of ivermectin in endemic communities in Ghana: a two-phase

epidemiological study. *Lancet*. 369(9578):2021–2029.

Oxberry ME, Geary TG, Prichard RK. 2001. Assessment of benzimidazole binding to individual recombinant tubulin isotypes from *Haemonchus contortus*. *Parasitology*. 122(6):683–687.

Parker JC, Sarkar D, Quick MW, Lester RAJ. 2003. Interactions of atropine with heterologously expressed and native  $\alpha 3$  subunit-containing nicotinic acetylcholine receptors. *Br J Pharmacol*. 138(5):801–810.

Parkinson J, Mitreva M, Whitton C, Thomson M, Daub J, Martin J, Schmid R, Hall N, Barrell B, Waterston RH. 2004. A transcriptomic analysis of the phylum Nematoda. *Nat Genet*. 36(12):1259.

Pereira L, Kratsios P, Serrano-Saiz E, Sheftel H, Mayo AE, Hall DH, White JG, LeBoeuf B, Garcia LR, Alon U. 2015. A cellular and regulatory map of the cholinergic nervous system of *C. elegans*. *Elife*. 4:e12432.

Pettersen EF, Goddard TD, Huang CC, Couch GS, Greenblatt DM, Meng EC, Ferrin TE. 2004. UCSF Chimera—a visualization system for exploratory research and analysis. *J Comput Chem*. 25(13):1605–1612.

Phillis JW, York DH. 1968. Pharmacological studies on a cholinergic inhibition in the cerebral cortex. *Brain Res*. 10(3):297–306.

Pirri JK, McPherson AD, Donnelly JL, Francis MM, Alkema MJ. 2009. A tyramine-gated chloride channel coordinates distinct motor programs of a *Caenorhabditis elegans* escape response. *Neuron*. 62(4):526–538.

Prichard R. 2001. Genetic variability following selection of *Haemonchus contortus* with anthelmintics. *Trends Parasitol*. 17(9):445–453.

Prichard R, Oxberry M, Bounhas Y, Sharma S, Lubega G, Geary T. 2000. Polymerisation and benzimidazole binding assays with recombinant  $\alpha$ - and  $\beta$ -tubulins from *Haemonchus contortus*. In: American Association of Veterinary Parasitologists, Forty-fifth Annual Meeting.

Putrenko I, Zakikhani M, Dent JA. 2005. A family of acetylcholine-gated chloride channel subunits in *Caenorhabditis elegans*. *J Biol Chem*. 280(8):6392–6398.

Ranganathan R, Cannon SC, Horvitz HR. 2000. MOD-1 is a serotonin-gated chloride channel that

modulates locomotory behaviour in *C. elegans*. *Nature*. 408(6811):470–475.

Rao VTS, Siddiqui SZ, Prichard RK, Forrester SG. 2009. A dopamine-gated ion channel (HcGGR3\*) from *Haemonchus contortus* is expressed in the cervical papillae and is associated with macrocyclic lactone resistance. *Mol Biochem Parasitol*. 166(1):54–61.

Ringstad N, Abe N, Horvitz HR. 2009. Ligand-gated chloride channels are receptors for biogenic amines in *C. elegans*. *Science* (80- ). 325(5936):96–100.

Šali A, Blundell TL. 1993. Comparative protein modelling by satisfaction of spatial restraints. *J Mol Biol*. 234(3):779–815.

Sarai RS, Kopp SR, Coleman GT, Kotze AC. 2014. Drug-efflux and target-site gene expression patterns in *Haemonchus contortus* larvae able to survive increasing concentrations of levamisole *in vitro*. *Int J Parasitol Drugs Drug Resist*. 4(2):77–84.

Schafer W. 2016. Nematode nervous systems. *Curr Biol*. 26(20):R955–R959.

Schallig H. 2000. Immunological responses of sheep to *Haemonchus contortus*. *Parasitology*. 120(07):63–72.

Schmidt GD, Roberts LS, Janovy J. 1977. *Foundations of parasitology*. Mosby Saint Louis.

Schwarz EM, Korhonen PK, Campbell BE, Young ND, Jex AR, Jabbar A, Hall RS, Mondal A, Howe AC, Pell J. 2013. The genome and developmental transcriptome of the strongylid nematode *Haemonchus contortus*. *Genome Biol*. 14(8):R89.

Segeberg MA, Stretton AO. 1993. Actions of cholinergic drugs in the nematode *Ascaris suum*. Complex pharmacology of muscle and motorneurons. *J Gen Physiol*. 101(2):271–296.

Siddiqui SZ, Brown DDR, Rao VTS, Forrester SG. 2010. An UNC-49 GABA receptor subunit from the parasitic nematode *Haemonchus contortus* is associated with enhanced GABA sensitivity in nematode heteromeric channels. *J Neurochem*. 113(5):1113–1122.

Sine SM, Engel AG. 2006. Recent advances in Cys-loop receptor structure and function. *Nature*. 440(7083):448–455.

- Stühmer W, Parekh AB. 1995. Electrophysiological recordings from *Xenopus* oocytes. In: Single-channel recording. Springer. p. 341–356.
- Takayanagi-Kiya S, Zhou K, Jin Y. 2016. Release-dependent feedback inhibition by a presynaptically localized ligand-gated anion channel. *Elife*. 5:e21734.
- Thompson AJ, Lester HA, Lummis SCR. 2010. The structural basis of function in Cys-loop receptors. *Q Rev Biophys*. 43(04):449–499.
- Trott O, Olson AJ. 2010. AutoDock Vina: improving the speed and accuracy of docking with a new scoring function, efficient optimization, and multithreading. *J Comput Chem*. 31(2):455–461.
- Veglia F. 1916. The anatomy and life-history of *Haemonchus contortus* (Rud.). Pretoria: Government Printer and Stationery Office.
- Weber W-M. 1999. Ion currents of *Xenopus laevis* oocytes: state of the art. *Biochim Biophys Acta (BBA)- Biomembranes*. 1421(2):213–233.
- Weston D, Patel B, Van Voorhis WC. 1999. Virulence in *Trypanosoma cruzi* infection correlates with the expression of a distinct family of sialidase superfamily genes. *Mol Biochem Parasitol*. 98(1):105–116.
- Wever CM, Farrington D, Dent JA. 2015. The validation of nematode-specific acetylcholine-gated chloride channels as potential anthelmintic drug targets. *PLoS One*. 10(9):e0138804.
- Williamson SM, Storey B, Howell S, Harper KM, Kaplan RM, Wolstenholme AJ. 2011. Candidate anthelmintic resistance-associated gene expression and sequence polymorphisms in a triple-resistant field isolate of *Haemonchus contortus*. *Mol Biochem Parasitol*. 180(2):99–105.
- Wolstenholme AJ, Fairweather I, Prichard R, von Samson-Himmelstjerna G, Sangster NC. 2004. Drug resistance in veterinary helminths. *Trends Parasitol*. 20(10):469–476.
- Wolstenholme AJ, Rogers AT. 2006. Glutamate-gated chloride channels and the mode of action of the avermectin/milbemycin anthelmintics. *Parasitology*. 131(supplement 1):S85–S95.
- Zhang J, Xue F, Chang Y. 2008. Structural determinants for antagonist pharmacology that distinguish the  $\rho 1$  GABA<sub>C</sub> receptor from GABA<sub>A</sub> receptors. *Mol Pharmacol*. 74(4):941–951.

Zwart R, Vijverberg HPM. 1997. Potentiation and inhibition of neuronal nicotinic receptors by atropine: competitive and noncompetitive effects. *Mol Pharmacol.* 52(5):886–895.

## Appendix 1 – Technical Manuscript V

Evaluating the longevity of surgically extracted *Xenopus laevis* oocytes for the study of nematode ligand-gated ion channels.

**Sarah A. Habibi**, Everett Cochrane, and Sean G. Forrester

Published in: *Invertebrate Neuroscience*. 18(1): 1-6

DOI: 10.1007/s10158-017-0205-z



## A1.0: Abstract

*Xenopus laevis* oocytes have been extensively used as a heterologous expression system for the study of ion-channels. While used successfully worldwide as tool for expressing and characterizing ion channels from a wide range of species, the limited longevity of oocytes once removed from the animal can pose significant challenges. In this study, we evaluate a simple and useful method that extends the longevity of *Xenopus* oocytes after removal from the animal and quantitatively assessed the reliability of the electrophysiological data obtained. The receptor used for this study was the UNC-49 receptor originally isolated from the sheep parasite, *Haemonchus contortus*. Overall, we found that immediate storage of the ovary in supplemented ND96 storage buffer at 4°C could extend their use for up to 17 days with almost 80% providing reliable electrophysiological data. This means that a single extraction can provide at least three weeks of experiments. In addition, we examined 24 day old oocytes (week 4) extracted from a single frog and also obtained reliable data using the same approach. However, 50% of these oocytes were usable for full dose-response experiments. Overall, we did find that this method has the potential to significantly extend the use of single oocyte extractions for 2-electrode voltage clamp electrophysiology.

## A1.1: Introduction

Oocytes from the African-clawed frog, *Xenopus laevis*, have been extensively used for the study of ion channels for decades. Oocytes were first shown to translate mRNA into functional proteins as early as 1971 (Gurdon et al. 1971). Subsequently, Sumikawa et al. (1981) and Miledi et al. (1983) demonstrated that this system could readily express functional ion channel receptors for use in electrophysiological applications. Since then, *Xenopus* oocytes have been widely used for the study of both mammalian and invertebrate ion channels, particularly Cys-loop ligand-gated ion channels (Cys-loop LGIC) (for early reviews see Snutch 1988; Dascal 1987). The use of oocytes as a surrogate system to functionally express a single population of receptors has been pivotal for understanding the neurobiology of both free-living and parasitic nematodes and particularly important for the characterization of receptors where the ligand is not known. For example, expression cloning techniques using *Xenopus* oocytes led to the discovery of the first glutamate-gated chloride channel, the target for the nematocide ivermectin (Cully et al. 1994). This system was also central to the characterization of the first Cys-loop GABA receptor isolated from *C. elegans* (Bamber et al. 1999). In addition to Cys-loop LGICs, *Xenopus* oocytes have been used to study voltage-gated ion channels (Kulke et al. 2014) and G-protein coupled receptors (GPCRs) (Lee et al. 1999). *Xenopus* oocytes are particularly useful for the study of ion channels because of their large diameter (1-

1.2 mm) which allows easy penetration of electrodes for long-term electrophysiological recordings. They also express a low number of endogenous membrane receptors (Bianchi and Driscoll 2006) and various protocols state that they survive for up to two weeks *in vitro* after microinjection (Stühmer and Parekh 1995).

The standard method for the expression of ion channels in *Xenopus* oocytes involves the microinjection of complementary RNA, which has been transcribed *in vitro*, into the cytoplasm of the oocyte. Up to 48 hours is generally required for the oocytes to translate the cRNA and express the channels on the membrane. Expression can also be achieved by injecting cDNA into the nucleus (Smart and Krishek 1995). Both approaches require a small portion of the ovary to be surgically removed and oocytes to be separated from the surrounding follicle. Individual microinjected oocytes can then be used for electrophysiological recordings. A common type of recording involves the use of a two-electrode voltage clamp.

Although the use of oocytes for the study of ion channels has many benefits, it also presents some challenges. First, the initial cost and maintenance of *Xenopus* has become quite expensive for some laboratories particularly for international shipping and the surgical extraction of oocytes is invasive. Thus many laboratories have developed ways in which they can increase the use of a single extraction. From our perspective, the most common suggestion that seems to have resonated successfully is to store oocytes injected with cRNA at 4°C to keep them viable for electrophysiological recordings for several weeks (Smart and Krishek 1995). However, it is uncertain whether this approach can be used for all ion channels and Cys-loop LGICs, particularly those that express very highly. For example, we have not had particularly good success with the viability of oocytes injected with the *unc-49* GABA receptor cRNA from the parasitic nematode *Haemonchus contortus* and can normally only conduct electrophysiological recordings for about 3-5 days post injection even when placed at 4°C to suspend expression. We anticipate this is due to the very high expression of this receptor when injected with a standard 50 ng of cRNA. These difficulties have led to initiatives to evaluate other methods to extend the use of a single oocyte extraction for the study of the UNC-49 receptor.

An alternative approach that does not appear to have been presented in the literature is the long-term storage of surgically extracted intact ovaries (ie before defolliculation via collagenase). One advantage of this approach is that small portions of ovaries can be removed from storage at any time and used for cRNA injection and electrophysiology analysis. Here, we present an evaluation of both the success of this method and the consistency of the electrophysiological results. We found that by using this method almost 80% of 17 day oocytes provided successful electrophysiological recordings. Similarly, we have

initial evidence that 24 day old oocytes can also provide reliable data. This means that a single oocyte extraction can provide 4 weeks of electrophysiological recordings. We anticipate that the approach presented here could be further modified for even better success.

## A1.2: Methods

### A1.2.1: Oocyte extraction and preparation

All animal procedures followed the University of Ontario Institute of Technology Animal Care Committee and the Canadian Council on Animal Care guidelines. Female *Xenopus laevis* frogs were supplied by Nasco (Fort Atkinson, WI, USA). The frogs were stored in groups of 3 in individual tanks that were housed in a climate and light controlled room. The frogs were fed twice per week and tanks were regularly cleaned. All frog surgeries used in this study were terminal which provide a sufficient number of oocytes for this study and our regular investigations in the laboratory. Surgical removal of a section of the ovary of the frog was performed and a portion was used immediately for defolliculation. The remaining lobe was separated into a larger portion (~9 g) and a smaller portion (~0.5 g). The larger and smaller lobes were stored in a standard petri dish with 60 mL of ND96 (96 mM NaCl, 2 mM KCl, 1 mM MgCl<sub>2</sub>, 1.8 mM CaCl<sub>2</sub>, 5 mM HEPES pH 7.5) supplemented with 0.275 µg/mL pyruvate and 50 µg/mL gentamycin at 4°C. The storage media for the ovary was not changed when stored at 4°C. Oocytes were defolliculated with a calcium-free oocyte Ringer's solution (82 mM NaCl, 2 mM KCl, 1 mM MgCl<sub>2</sub>, 5 mM HEPES pH 7.5 (Sigma-Aldrich) (OR-2) containing 2 mg/mL collagenase-II (Sigma-Aldrich) under constant shaking conditions at room temperature for 2 hours. Collagenase was washed from the oocytes with ND96 solution and stored at 18°C in ND96 supplemented with 0.275 µg/mL pyruvic acid (Sigma-Aldrich) and 50 µg/mL gentamycin (Sigma-Aldrich). Stage V and VI oocytes were selected for cytoplasmic injection of cRNA.

### A1.2.2: cRNA injection

The cDNA of *hco-unc-49b* and *c* were already sub-cloned into the *X. laevis* expression vector pT7Ts which encode the UNC-49B and C subunits of the *H. contorts* UNC-49 GABA receptor (Siddiqui et al. 2010). The vector was linearized using XbaI restriction enzyme (New England Bio Labs), and used as a template for an *in vitro* transcription reaction (T7 mMessage mMachine kit, Ambion, Austin, TX, USA), producing *hco-unc-49b* and *c* cRNA. *X. laevis* oocytes were injected with a total of 55.2 nl of *hco-unc-49b* and *c* (0.45 and 0.3 ng/nl respectively) (~27 nl of each subunit) using the Drummond (Broomall, PA, USA) Nanoject microinjector. We injected some oocytes with cRNA on the day of surgical extraction (Day 1). The

remaining oocytes from ovaries that were incubated at 4°C were injected on day 7 and 14. Once injected with cRNA the oocytes were incubated at 18°C in supplemented ND96. Supplemented ND96 solution was changed once a day during incubation period. The number of oocytes that were visibly alive immediately after injection and 1 and 2 days post injection was monitored. Criteria for visual assessment of health include, spherical shape of oocyte (not irregular in shape), distinct boundary between white vegetal pole and black animal pole, absence of leaking cellular components, and a solid black/brown colour of animal pole (not spotty). Electrophysiological recordings of the oocytes were conducted 48 hrs after cRNA injection. Therefore, for the presentation of the data we refer to these oocytes as 3 day, 10 day and 17 day old oocytes. Only oocytes that were deemed alive and healthy (via visual inspection) were selected for electrophysiological recordings.

#### A1.2.3: Electrophysiological recordings

The Axoclamp 900A voltage clamp (Molecular Devices, Sunnyvale, CA, USA) was used to conduct two electrode voltage clamp electrophysiology. Glass electrodes were produced using a P-97 Micropipette Puller (Sutter Instrument Co., Novato, CA, USA). The electrodes were backfilled with 3M KCl and contained Ag|AgCl wires. All oocytes were clamped at a resting membrane potential of -60 mV for the entirety of the experiments. Gamma-Aminobutyric acid (GABA) (Sigma-Aldrich) was first dissolved in non-supplemented ND96. Concentrations above and below the known EC<sub>50</sub> value were washed over the oocytes using the RC-1Z recording chamber (Warner Instruments Inc., Hamdan, CT, USA). All data was analyzed using Clampex Software v10.2 (Molecular Devices) and all graphs were generated using Graphpad Prism Software v5.0 (San Diego, CA, USA). GABA EC<sub>50</sub> values were determined by dose response curve which were fitted to the following equation:

$$I_{max} = \frac{1}{1 + \left(\frac{EC_{50}}{[D]}\right)^h}$$

Where  $I_{max}$  is the maximal response, EC<sub>50</sub> is the concentration of compound required to elicit 50% of the maximal response, [D] is the compound concentration, and h is the Hill coefficient. Both EC<sub>50</sub> and h are free parameters, and the curves were normalized to the estimated  $I_{max}$ . Graphpad prism used the equation to fit a sigmoidal curve of variable slope to the data. Means were determined for at least 7 oocytes from 4 different frogs.

### A1.3: Results

*Xenopus* oocytes were evaluated for their longevity and percent that were useable for complete electrophysiological experiments after long-term storage. This was defined as an oocyte that was clamped at a resting current between -60 and -200 nA, provided channel activation currents in the 100-1000+ nA range when 4 increasing concentrations of GABA (50, 100, 250, and 500  $\mu$ M) were applied, returned to the original resting current when wash buffer was applied, and maintained a -60 mV holding membrane potential during the entire experiment. Using this criteria, it was found that 81% of 3 day old oocytes survived and were useable for complete experiments (Fig. A1.1, Table A1.1). This percentage appeared to decrease as the age of the oocyte increased. 76% of 10 day old oocytes retrieved from the 9 g lobe were useable for complete experiments; this number dropped to 53% in 17 day old oocytes. However, 77% of 17 days old oocytes that were stored as a 0.5 g lobe survived and were useable for complete experiments (Table A1.1). The long-term storage of the oocytes in a smaller portion of the ovary appeared to increase the longevity of oocytes.

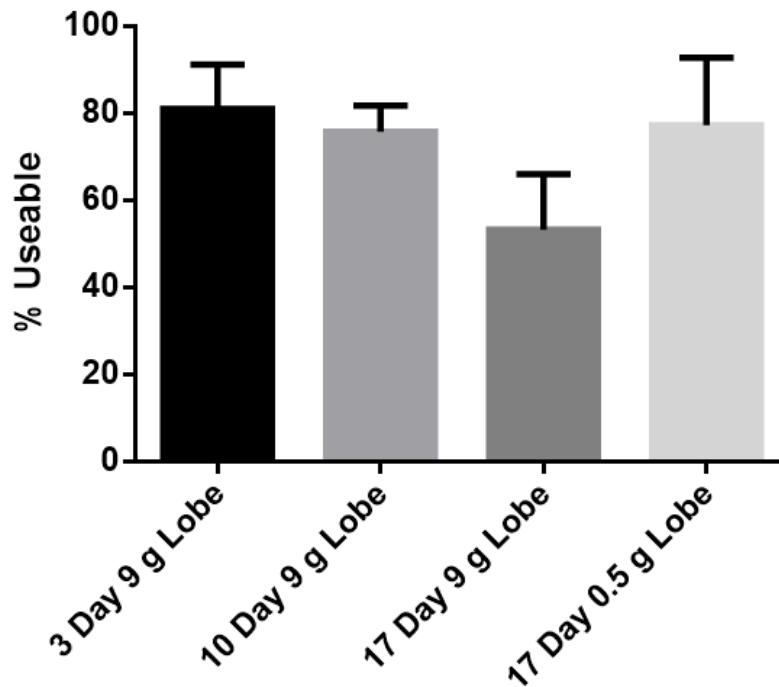


**Figure A1.1:** Analysis of the longevity of *Xenopus* oocytes stored as intact ovaries. Mean percentage ( $\pm$  SE) of 3, 10, and 17 day old oocytes stored at 4°C in supplemented ND96 as a 9 g or 0.5 g lobe that survived and were useable for electrophysiological recording ( $n \geq 7$ ). All oocytes were analyzed 48 hrs post cRNA injection.

**Table A1.1:** Summary of electrophysiological recording parameters and results from oocytes of various ages

Oocyte age post-surgical removal	Resting current amplitude (nA) range after clamping	Current amplitude (nA) range at EC <sub>50</sub> GABA	Average current amplitude (nA) at EC <sub>50</sub> GABA	% survival*
3 Day (9 g Lobe) (n=11)	-60-200 nA	300-4100 nA	1474 ± 293 nA	81
10 Day (9 g Lobe) (n=7)	-60-200 nA	300-1400 nA	628 ± 179 nA	76
17 Day (9 g Lobe) (n=7)	-60-200 nA	250-1050 nA	513 ± 108 nA	53
17 Day (0.5 g Lobe) (n=9)	-60-200 nA	110-1250 nA	419 ± 280 nA	77

The average EC<sub>50</sub> of the Hco-UNC-49 receptor observed from 3 and 10 day old *Xenopus* oocytes were  $96 \pm 7.6$  and  $98 \pm 11.4 \mu\text{M}$  respectively. Similarly, 17 day old oocytes stored initially as either a 0.5 g lobe or a 9 g lobe produced average EC<sub>50</sub> values of  $111 \pm 5.5$  and  $107 \pm 7.8 \mu\text{M}$  respectively. All EC<sub>50</sub> values are not statistically different ( $p > 0.05$ ) for the four groups analyzed. Fig. A1.2a outlines the dose-response curves representative of 3, 10 and 17 day oocytes. The average current observed when 3 day old oocytes were tested using an EC<sub>50</sub> concentration of GABA (100  $\mu\text{M}$ ) was 1474 nA which decreased to 628 and 513 nA in 10 and 17 day old oocytes respectively (Fig. A1.2b). Moreover, 24 day oocytes, extracted from a single frog and stored as a 0.5 g lobe, were also tested to determine their ability to provide consistent EC<sub>50</sub> values, compared to 3, 10, and 17 day oocytes. The average EC<sub>50</sub> observed from these oocytes was  $102 \pm 3.9 \mu\text{M}$  with 50% that survived and were useable for experiments. Fig. 3 shows a representative trace and dose-response curve for 24 day *Xenopus* oocytes.

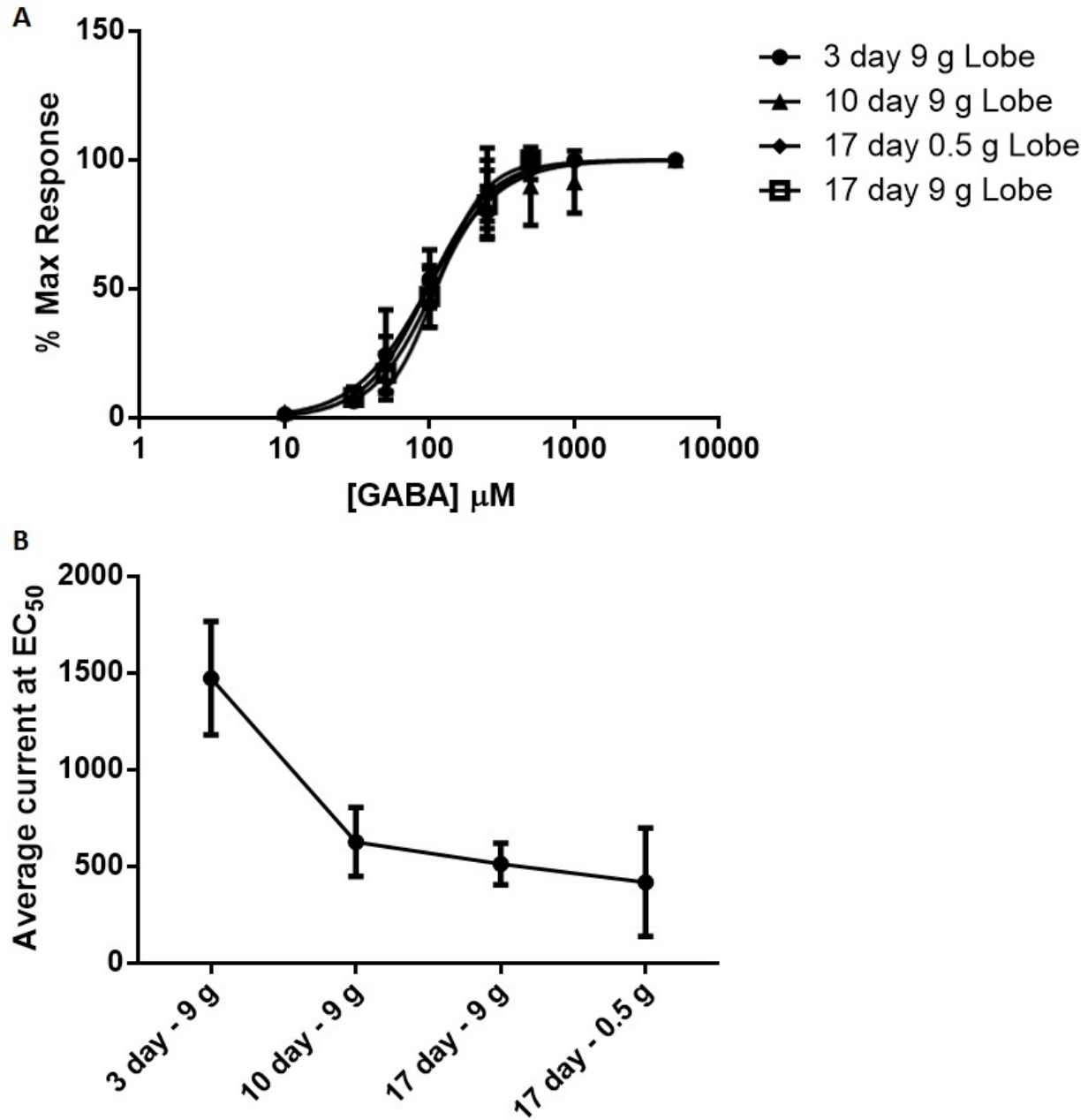


**Figure A1.2** Quality of electrophysiological data obtained from oocytes at various ages a) GABA dose –response curves for the Hco-UNC-49 channel expressed in 3, 10, and 17 day old *Xenopus* oocytes initially stored at 4°C as a 9 g or 0.5 g lobe. Data is expressed as means  $\pm$  SE. ( $n \geq 7$ ). b) Average current amplitude (nA) from 3, 10, and 17 day old *Xenopus* oocytes initially stored at 4°C as a 9 g or 0.5 g lobe and expressing the Hco-UNC-49 receptor. All oocytes were tested using the  $EC_{50}$  concentration for GABA (100  $\mu$ M). Data is expressed as mean  $\pm$  SE ( $n \geq 7$ ).

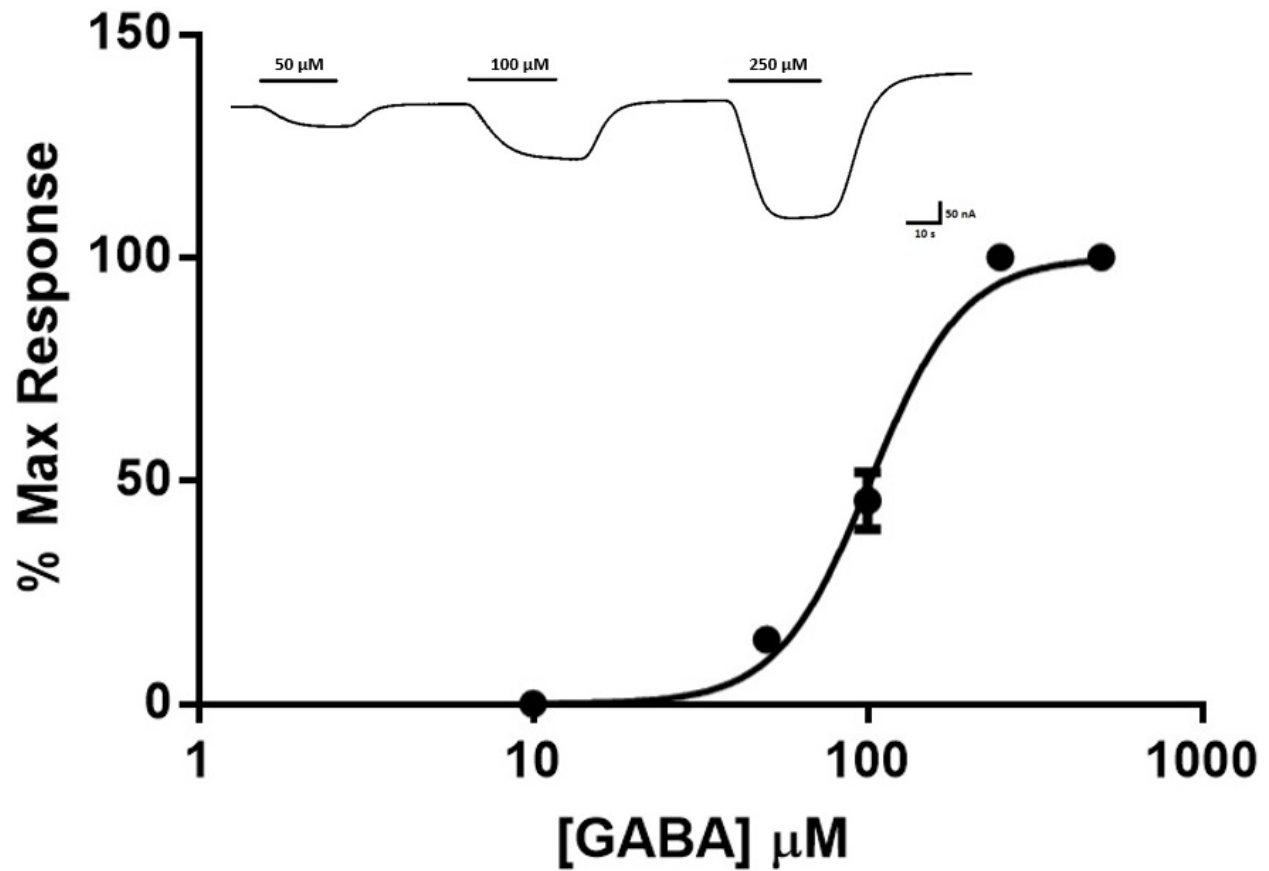


**Figure A1.3:** GABA dose–response curves for the Hco-UNC-49 channel expressed in 24 day old *Xenopus* oocytes stored at 4°C as a 0.5 g lobe. Data is expressed as means ± SE (n = 3). Inset: representative electrophysiological tracings using 3 increasing concentrations of GABA.

#### A1.4: Discussion

The purpose of this study was to evaluate one approach to increase the longevity of the *X. laevis* oocyte for the use in electrophysiology applications. *Xenopus* oocytes have been used for the study of ion channels for over 30 years. However, aside from some useful anecdotal information from various research laboratories, there are no studies evaluating the long term storage of the surgically extracted ovaries. The results of this study provide evidence that this approach can be routinely used to extend the use of surgically extracted oocytes and could be further refined for improved success.

In our study, we showed that a single ovary extraction could be stored for 3 weeks at 4°C and provide reliable results. We found that EC<sub>50</sub> values collected from 3, 10, and 17 day post-extraction oocytes were statistically the same ( $p > 0.05$ ). Consistent results were also obtained after 3 weeks using another type



of nematode Cys-loop LGIC, an acetylcholine-gated chloride channel (data not shown). In addition, we found that 50% of oocytes stored for 24 days could produce consistent electrophysiological responses. The average current obtained from activation of the Hco-UNC-49 receptor appeared to decrease substantially between 3 and 10 day old oocytes followed by a slight decrease between 10 and 17 day old oocytes.

We did see a clear difference in success when we stored the ovary as a 9 g vs 0.5 g lobe, where the small lobe produced much better results. This could be due to the increased availability of nutrients to the oocytes and a decrease in the concentration of harmful waste products when stored in smaller pieces. *Xenopus* oocytes have been shown to produce NH<sub>3</sub> waste products (Fort and Rogers 2005). Ammonia is a toxic waste product that when released can cause harm to surrounding oocytes. Therefore, the separation of the ovary into smaller sections could reduce the amount of ammonia available to surrounding oocytes.

When working with *Xenopus* oocytes many laboratories have explored different methods of storage to increase their survival rate. Some laboratories find separating oocytes into individual wells of a 24-well plate improves survival and once the oocytes have expressed the receptor of interest they can be stored in the refrigerator in order to extend their viability for recordings (Buckingham et al. 2006). Other researchers indicate that if stored correctly, *Xenopus* oocytes can survive up to 10-15 days (Weber 1999). Our results indicate that sectioning off a small portion of the ovary into its own petri dish improves the success rate of the oocyte after storage for 17 days (Table A1.1) which can be extended to 24 days or longer with further improvements to the protocol. This has been particularly useful in our laboratory where different receptors are expressed from week to week by several personnel. We intend to further refine this approach in an effort to further extend the use of *Xenopus* oocytes for electrophysiological recordings. However, overall we were able to obtain 4 weeks of electrophysiological recordings from a single oocyte extraction.

The defolliculation of the ovary each week could also have an impact on the viability of the oocytes. In our study we defolliculated roughly 2 mL of ovary using 10 mg/ml collagenase solution for 2 hours. Other protocols have recommended using 1-6 mg/ml of collagenase solution for 1-3 hours (Dascal 1987; Stuhmer 1995). Therefore, there is variability in how much and for how long collagenase treatment is performed. Evaluating the optimal concentration of collagenase and length of time for defolliculation could further improve the health and viability of the oocytes.

It should be noted that in our protocol once the ovary was sectioned off and stored in at 4°C, the media was not changed. However, once injected with cRNA and stored at 18°C the oocyte storage media was changed once per day. Frequent renewal of the storage media could perhaps increase the health of the oocytes during long-term storage.

Other factors have been shown to affect the viability of *Xenopus* oocytes, including the water temperature in which the frogs are stored. Frogs that are stored in 17°C water generally produce oocytes that are firm and perfect for microinjection, whereas warmer water causes oocytes to soften (Stühmer and Parekh 1995). Our laboratory stores the frogs in a temperature controlled room (18-20°C) with consistent full-spectrum lighting which could contribute the success rate that we noted.

From an animal welfare perspective these results have helped contribute to our progress with respect to the three “R’s” (Replacement, Reduction and Refinement) of good animal practice. This has also contributed greatly to reducing the overall cost of using *Xenopus* for ion channel research. In addition, since *Xenopus* can be susceptible to a variety of diseases (Smart and Krishek 1995) this approach has reduced the stress on the animals by increasing the time between surgeries and thus their potential susceptibility to infection. We also anticipate that the approach presented here can be further refined with better results.

#### A1.5: Acknowledgements

This research was funded by grants from National Science and Engineering Research Council (NSERC) and the Canadian Foundation for Innovation to SGF.

#### A1.5: Compliance with ethical standards

All animal procedures followed the University of Ontario Institute of Technology Animal Care Committee and the Canadian Council on Animal Care guidelines.

## A1.6: List of Figures

**Figure A1.1** Analysis of the longevity of *Xenopus* oocytes stored as intact ovaries.

**Figure A1.2** Quality of electrophysiological data obtained from oocytes at various ages.

**Figure A1.3** GABA dose –response curves for the Hco-UNC-49 channel expressed in 24 day old *Xenopus* oocytes stored at 4°C as a 0.5 g lobe.

## A1.7: List of Tables

**Table A1.1:** Summary of electrophysiological recording parameters and results from oocytes of various ages

## A1.8: References

Bamber, B. A., Beg, A. A., Twyman, R. E., & Jorgensen, E. M. (1999) The *Caenorhabditis elegans* unc-49 locus encodes multiple subunits of a heteromultimeric GABA receptor. *J Neurosci*, 19: 5348-59.

Bianchi, L. & Driscoll, M. (2006) Heterologous expression of *C. elegans* ion channels in *Xenopus* oocytes. In *WormBook* (pp. 1-16). The *C. elegans* Research Community: Piscataway.

Buckingham, S. D., Pym, L. & Sattelle, D. B. (2006) Oocytes as an expression system for studying receptor/channel targets of drugs and pesticides. *Meth Mol Biol*, 322: 331-345.

Cully, D. F., Vassilatis, D. K., Liu, K. K., Paress, P. S., Van der Ploeg, L. H., Schaeffer, J. M., & Arena, J. P. (1994) Cloning of an avermectin-sensitive glutamate-gated chloride channel from *Caenorhabditis elegans*. *Nature*, 371: 707-11.

Dascal, N. (1987) The use of *Xenopus* oocytes for the study of ion channels. *CRC Crit Rev Biochem*, 22: 317-87.

Fort, D. J. & Rogers, R. L. (2005) Enhanced frog embryo teratogenesis assay: *Xenopus* model using *Xenopus tropicalis*. In *Techniques in Aquatic Toxicology* (pp. 50-65). Boca Raton: CRC Press.

- Gurdon, J. B., Lane, C. D., Woodland, H. R., & Marbaix, G. (1971). Use of frog eggs and oocytes for the study of messenger RNA and its translation in living cells. *Nature*, 233: 177–182.
- Kulke, D., von Samson-Himmelstjerna, G., Miltsch, S. M., Wolstenholme, A. J., Jex, A. R., Gasser, R. B., et al. (2014) Characterization of the Ca<sup>2+</sup>-gated and voltage-dependent K<sup>+</sup>-channel Slo-1 of nematodes and its interaction with emodepside. *PLoS Negl Trop Dis*, 8(12): e3401.
- Lee, Y. S., Park, Y. S., Chang, D. J., Hwang, J. M., Min, C. K., Kaang, B. K., & Cho, N. J. (1999) Cloning and expression of a G protein-linked acetylcholine receptor from *Caenorhabditis elegans*. *J Neurochem*, 72: 58-65.
- Miledi, R., Parker, I. & Sumikawa, K. (1983). Recording of single  $\gamma$ -aminobutyrate- and acetylcholine-activated receptor channels translated by exogenous mRNA in *Xenopus* oocytes. *Proc. R. Soc. Lond*, 218: 481-484.
- Siddiqui, S. Z., Brown, D. D. R., Rao, V. T. S., & Forrester, S. G. (2010) An UNC-49 GABA receptor subunit from the parasitic nematode *Haemonchus contortus* is associated with enhanced GABA sensitivity in nematode heteromeric channels. *J Neurochem*, 113: 1113–1122.
- Smart, T. G. & Krishek, B. J. (1995) *Xenopus* Oocyte Microinjection and Ion-Channel Expression. In Boulton A. A., Baker G. B., Walz W. (eds) *Patch-Clamp Applications and Protocols* (pp. 259-305). Totowa: Humana Press.
- Snutch, T. P. (1988) The use of *Xenopus* oocytes to probe synaptic communication. *Trends Neurosci*, 11: 250-6.
- Stühmer, W. & Parekh, A. B. (1995). Electrophysiological recordings from *Xenopus* oocytes. In *Single-channel recording*. (pp. 341-356). New York: Springer.
- Sumikawa, K., Houghton, M., Emtage, J. S., Richards, B. M., & Barnard, E. A. (1981) Active multi-subunit ACh receptor assembled by translation of heterologous mRNA in *Xenopus* oocytes. *Nature*, 292: 862-864.
- Weber, W. M. (1999). Ion currents of *Xenopus laevis* oocytes: state of the art. *Biochim. Biophys. Acta (BBA)-Biomembranes*, 1421: 213–233.

## A1.9. Manuscript V



# Evaluating the longevity of surgically extracted *Xenopus laevis* oocytes for the study of nematode ligand-gated ion channels

Sarah A. Abdelmassih<sup>1</sup> · Everett Cochrane<sup>1</sup> · Sean G. Forrester<sup>1</sup>

Received: 4 October 2017 / Accepted: 18 November 2017  
© Springer-Verlag GmbH Germany, part of Springer Nature 2017

## Abstract

*Xenopus laevis* oocytes have been extensively used as a heterologous expression system for the study of ion channels. While used successfully worldwide as tool for expressing and characterizing ion channels from a wide range of species, the limited longevity of oocytes once removed from the animal can pose significant challenges. In this study, we evaluate a simple and useful method that extends the longevity of *Xenopus* oocytes after removal from the animal and quantitatively assessed the reliability of the electrophysiological data obtained. The receptor used for this study was the UNC-49 receptor originally isolated from the sheep parasite, *Haemonchus contortus*. Overall, we found that immediate storage of the ovary in supplemented ND96 storage buffer at 4 °C could extend their use for up to 17 days with almost 80% providing reliable electrophysiological data. This means that a single extraction can provide at least 3 weeks of experiments. In addition, we examined 24-day-old oocytes (week 4) extracted from a single frog and also obtained reliable data using the same approach. However, 50% of these oocytes were usable for full dose–response experiments. Overall, we did find that this method has the potential to significantly extend the use of single oocyte extractions for two-electrode voltage clamp electrophysiology.

**Keywords** Oocyte · *Xenopus* · Two-electrode voltage clamp · Longevity · Electrophysiological recordings · UNC-49 · *Caenorhabditis elegans* · *Haemonchus contortus*

## List of symbols

GABA  $\gamma$ -Aminobutyric acid  
Hco *Haemonchus contortus*

## Introduction

Oocytes from the African clawed frog, *Xenopus laevis*, have been extensively used for the study of ion channels for decades. Oocytes were first shown to translate mRNA into functional proteins as early as 1971 (Gurdon et al. 1971). Subsequently, Sumikawa et al. (1981) and Miledi et al. (1983) demonstrated that this system could readily express functional ion channel receptors for use in electrophysiological applications. Since then, *Xenopus* oocytes have been widely used for the study of both mammalian and invertebrate ion channels, particularly Cys-loop ligand-gated ion channels

(Cys-loop LGIC) (for early reviews see Snutch 1988; Dascal 1987). The use of oocytes as a surrogate system to functionally express a single population of receptors has been pivotal for understanding the neurobiology of both free-living and parasitic nematodes and particularly important for the characterization of receptors where the ligand is not known. For example, expression cloning techniques using *Xenopus* oocytes led to the discovery of the first glutamate-gated chloride channel, the target for the nematocide ivermectin (Cully et al. 1994). This system was also central to the characterization of the first Cys-loop GABA receptor isolated from *Caenorhabditis elegans* (Bamber et al. 1999). In addition to Cys-loop LGICs, *Xenopus* oocytes have been used to study voltage-gated ion channels (Kulke et al. 2014) and G-protein coupled receptors (GPCRs) (Lee et al. 1999). *Xenopus* oocytes are particularly useful for the study of ion channels because of their large diameter (1–1.2 mm) which allows easy penetration of electrodes for long-term electrophysiological recordings. They also express a low number of endogenous membrane receptors (Bianchi and Driscoll 2006), and various protocols state that they survive for up to 2 weeks in vitro after microinjection (Stühmer and Parekh 1995).

✉ Sean G. Forrester  
sean.forrester@uoit.ca

<sup>1</sup> Applied Bioscience Graduate Program, Faculty of Science, University of Ontario Institute of Technology, 2000 Simcoe Street North, Oshawa, ON L1H 7K4, Canada

The standard method for the expression of ion channels in *Xenopus* oocytes involves the microinjection of complementary RNA, which has been transcribed in vitro, into the cytoplasm of the oocyte. Up to 48 h is generally required for the oocytes to translate the cRNA and express the channels on the membrane. Expression can also be achieved by injecting cDNA into the nucleus (Smart and Krishek 1995). Both approaches require a small portion of the ovary to be surgically removed and oocytes to be separated from the surrounding follicle. Individual microinjected oocytes can then be used for electrophysiological recordings. A common type of recording involves the use of a two-electrode voltage clamp.

Although the use of oocytes for the study of ion channels has many benefits, it also presents some challenges. First, the initial cost and maintenance of *Xenopus* have become quite expensive for some laboratories particularly for international shipping, and the surgical extraction of oocytes is invasive. Thus, many laboratories have developed ways in which they can increase the use of a single extraction. From our perspective, the most common suggestion that seems to have resonated successfully is to store oocytes injected with cRNA at 4 °C to keep them viable for electrophysiological recordings for several weeks (Smart and Krishek 1995). However, it is uncertain whether this approach can be used for all ion channels and Cys-loop LGICs, particularly those that express very highly. For example, we have not had particularly good success with the viability of oocytes injected with the *unc-49* GABA receptor cRNA from the parasitic nematode *Haemonchus contortus* and can normally only conduct electrophysiological recordings for about 3–5 days post-injection even when placed at 4 °C to suspend expression. We anticipate this is due to the very high expression of this receptor when injected with a standard 50 ng of cRNA. These difficulties have led to initiatives to evaluate other methods to extend the use of a single oocyte extraction for the study of the UNC-49 receptor.

An alternative approach that does not appear to have been presented in the literature is the long-term storage of surgically extracted intact ovaries (i.e., before defolliculation via collagenase). One advantage of this approach is that small portions of ovaries can be removed from storage at any time and used for cRNA injection and electrophysiology analysis. Here, we present an evaluation of both the success of this method and the consistency of the electrophysiological results. We found that by using this method almost 80% of 17-day-old oocytes provided successful electrophysiological recordings. Similarly, we have initial evidence that 24-day-old oocytes can also provide reliable data. This means that a single oocyte extraction can provide 4 weeks of electrophysiological recordings. We anticipate that the approach presented here could be further modified for even better success.

## Methods

### Oocyte extraction and preparation

All animal procedures followed the University of Ontario Institute of Technology Animal Care Committee and the Canadian Council on Animal Care guidelines. Female *Xenopus laevis* frogs were supplied by Nasco (Fort Atkinson, WI, USA). The frogs were stored in groups of three in individual tanks that were housed in a climate and light controlled room. The frogs were fed twice per week, and tanks were regularly cleaned. All frog surgeries used in this study were terminal which provide a sufficient number of oocytes for this study and our regular investigations in the laboratory. Surgical removal of a section of the ovary was preformed, and a portion was used immediately for defolliculation. The remaining lobe was separated into a larger portion (~ 9 g) and a smaller portion (~ 0.5 g). The larger and smaller lobes were stored in a standard Petri dish with 60 mL of ND96 (96 mM NaCl, 2 mM KCl, 1 mM MgCl<sub>2</sub>, 1.8 mM CaCl<sub>2</sub>, 5 mM HEPES pH 7.5) supplemented with 0.275 µg/mL pyruvate and 50 µg/mL gentamycin at 4 °C. The storage media for the ovary was not changed when stored at 4 °C. Oocytes were defolliculated with a calcium-free oocyte Ringer's solution (82 mM NaCl, 2 mM KCl, 1 mM MgCl<sub>2</sub>), 5 mM HEPES pH 7.5 (Sigma-Aldrich) (OR-2) containing 2 mg/mL collagenase-II (Sigma-Aldrich) under constant shaking conditions for 2 h at room temperature. Collagenase was washed from the oocytes with ND96 solution and stored at 18 °C in ND96 supplemented with 0.275 µg/mL pyruvic acid (Sigma-Aldrich) and 50 µg/mL gentamycin (Sigma-Aldrich). Stage V and VI oocytes were selected for cytoplasmic injection of cRNA.

### cRNA injection

The cDNA of *hco-unc-49b* and *c* was already subcloned into the *X. laevis* expression vector pT7Ts which encode the UNC-49B and C subunits of the *H. contortus* UNC-49 GABA receptor (Siddiqui et al. 2010). The vector was linearized using XbaI restriction enzyme (New England Bio Labs), and used as a template for an in vitro transcription reaction (T7 mMessage mMachine kit, Ambion, Austin, TX, USA), producing *hco-unc-49b* and *c* cRNA. *X. laevis* oocytes were injected with a total of 55.2 nl of *hco-unc-49b* and *c* (0.45 and 0.3 ng/nl, respectively) (~ 27 nl of each subunit) using the Drummond (Broomall, PA, USA) Nanoject microinjector. We injected some oocytes with cRNA on the day of surgical extraction (day 1). The remaining oocytes from ovaries that were

incubated at 4 °C were injected on day 7 and 14. Once injected with cRNA, the oocytes were incubated at 18 °C in supplemented ND96. Supplemented ND96 solution was changed once a day during incubation period. The number of oocytes that were visibly alive immediately after injection and 1 and 2 days post-injection was monitored. Criteria for visual assessment of health include, spherical shape of oocyte (not irregular in shape), distinct boundary between white vegetal pole and black animal pole, absence of leaking cellular components, and a solid black/brown color of animal pole (not spotty). Electrophysiological recordings of the oocytes were conducted 48 h after cRNA injection. Therefore, for the presentation of the data we refer to these oocytes as 3-, 10-, and 17-day-old oocytes. Only oocytes that were deemed alive and healthy (via visual inspection) were selected for electrophysiological recordings.

### Electrophysiological recordings

The Axoclamp 900 A voltage clamp (Molecular Devices, Sunnyvale, CA, USA) was used to conduct two-electrode voltage clamp electrophysiology. Glass electrodes were produced using a P-97 Micropipette Puller (Sutter Instrument Co., Novato, CA, USA). The electrodes were back-filled with 3 M KCl and contained Ag/AgCl wires. All oocytes were clamped at a resting membrane potential of – 60 mV for the entirety of the experiments. Gamma-aminobutyric acid (GABA) (Sigma-Aldrich) was first dissolved in non-supplemented ND96. Concentrations above and below the known  $EC_{50}$  value were washed over the oocytes using the RC-1Z recording chamber (Warner Instruments Inc., Hamden, CT, USA). All data were analyzed using Clampex Software v10.2 (Molecular Devices), and all graphs were generated using GraphPad Prism Software v5.0 (San Diego, CA, USA). GABA  $EC_{50}$  values were determined by dose–response curve which was fitted to the following equation:

$$I_{\max} = 1 / \left[ 1 + \left( \frac{EC_{50}}{[D]} \right)^h \right]$$

where  $I_{\max}$  is the maximal response,  $EC_{50}$  is the concentration of compound required to elicit 50% of the maximal response,  $[D]$  is the compound concentration, and  $h$  is the Hill coefficient. Both  $EC_{50}$  and  $h$  are free parameters, and the curves were normalized to the estimated  $I_{\max}$ . GraphPad prism used the equation to fit a sigmoidal curve of variable slope to the data. Means were determined for at least seven oocytes from four different frogs.

### Results

*Xenopus* oocytes were evaluated for their longevity and percent that were usable for complete electrophysiological experiments after long-term storage. This was defined as an oocyte that was clamped at a resting current between – 60 and – 200 nA, provided channel activation currents in the 100–1000+ nA range when four increasing concentrations of GABA (50, 100, 250, and 500  $\mu$ M) were applied, returned to the original resting current when wash buffer was applied, and maintained a – 60 mV holding membrane potential during the entire experiment. Using these criteria, it was found that 81% of 3-day-old oocytes survived and were usable for complete experiments (Fig. 1, Table 1). This percentage appeared to decrease as the age of the oocyte increased. Seventy-six of 10-day-old oocytes retrieved from the 9-g lobe were usable for complete experiments; this number dropped to 53% in 17-day-old oocytes. However, 77% of 17-day-old oocytes that were stored as a 0.5-g lobe survived and were usable for complete experiments (Table 1). The long-term storage of the oocytes in a smaller portion of the ovary appeared to increase the longevity of oocytes.

The average  $EC_{50}$  of the Hco-UNC-49 receptor observed from 3- to 10-day-old *Xenopus* oocytes were  $96 \pm 7.6$  and  $98 \pm 11.4$   $\mu$ M, respectively. Similarly, 17-day-old oocytes stored initially as either a 0.5-g lobe or a 9-g lobe produced average  $EC_{50}$  values of  $111 \pm 5.5$  and  $107 \pm 7.8$   $\mu$ M, respectively. All  $EC_{50}$  values are not statistically different ( $p > 0.05$ ) for the four groups analyzed. Figure 2a outlines the dose–response curves representative of 3-, 10-, and 17-day oocytes. The average current observed when

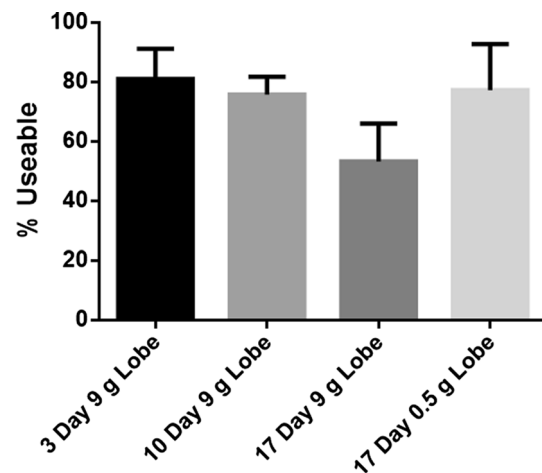


**Fig. 1** Analysis of the longevity of *Xenopus* oocytes stored as intact ovaries. Mean percentage ( $\pm$  SE) of 3-, 10-, and 17-day-old oocytes stored at 4 °C in supplemented ND96 as a 9- or 0.5-g lobe that survived and were usable for electrophysiological recording ( $n \geq 7$ ). All oocytes were analyzed 48 h post-cRNA injection



**Table 1** Summary of electrophysiological recording parameters and results from oocytes of various ages

Oocyte age postsurgical removal	Resting current amplitude (nA) range after clamping	Current amplitude (nA) range at EC <sub>50</sub> GABA	Average current amplitude (nA) at EC <sub>50</sub> GABA	% survival <sup>a</sup>
3 day (9-g lobe) (n = 11)	- 60 to 200	300–4100	1474 ± 293	81
10 day (9-g lobe) (n = 7)	- 60 to 200	300–1400	628 ± 179	76
17 day (9-g lobe) (n = 7)	- 60 to 200	250–1050	513 ± 108	53
17 day (0.5-g lobe) (n = 9)	- 60 to 200	110–1250	419 ± 280	77

<sup>a</sup>% survival refers to oocytes that survived and were usable for complete electrophysiological experiments

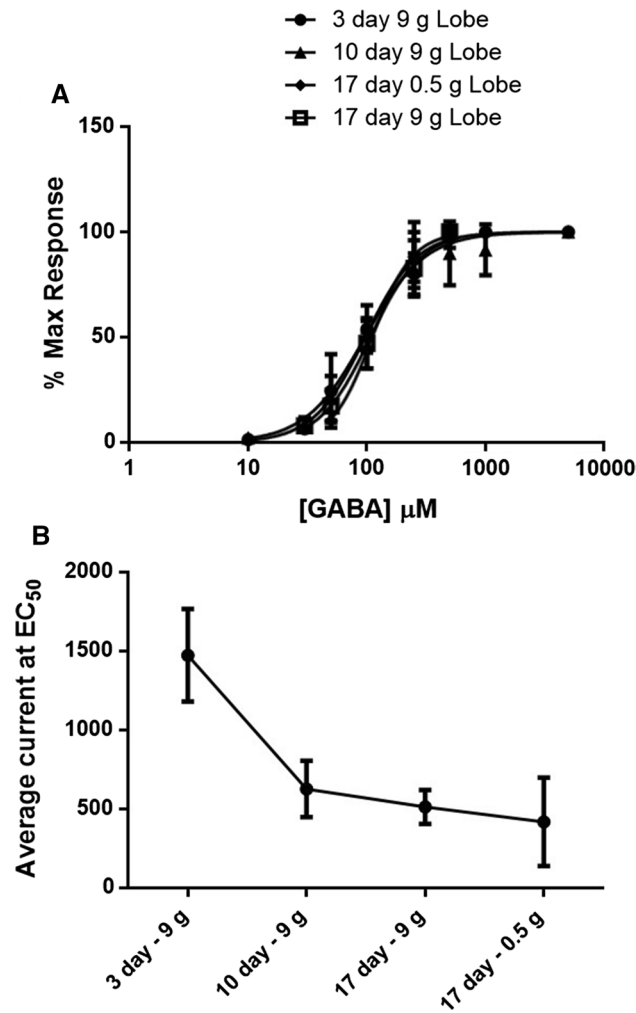


**Fig. 2** Quality of electrophysiological data obtained from oocytes at various ages **a** GABA dose–response curves for the Hco-UNC-49 receptor expressed in 3-, 10-, and 17-day-old *Xenopus* oocytes initially stored at 4 °C as a 9- or 0.5-g lobe. Data are expressed as mean ± SE (n ≥ 7). **b** Average current amplitude (nA) from 3-, 10-, and 17-day-old *Xenopus* oocytes initially stored at 4 °C as a 9- or 0.5-g lobe and expressing the Hco-UNC-49 receptor. All oocytes were tested using the EC<sub>50</sub> concentration for GABA (100 μM). Data are expressed as mean ± SE (n ≥ 7)

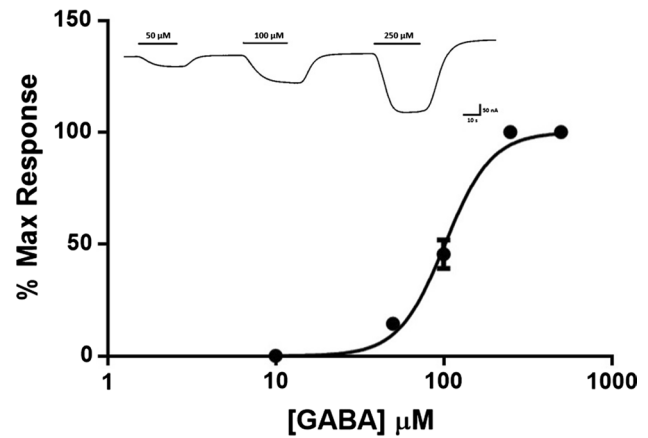


**Fig. 3** GABA dose–response curves for the Hco-UNC-49 channel expressed in 24-day-old *Xenopus* oocytes stored at 4 °C as a 0.5-g lobe. Data are expressed as mean ± SE (n = 3). Inset: representative electrophysiological tracings using three increasing concentrations of GABA

3-day-old oocytes were tested using an EC<sub>50</sub> concentration of GABA (100 μM) was 1474 nA which decreased to 628 and 513 nA in 10- and 17-day-old oocytes, respectively (Fig. 2b). Moreover, 24-day oocytes, extracted from a single frog and stored as a 0.5-g lobe, were also tested to determine their ability to provide consistent EC<sub>50</sub> values, compared to 3-, 10-, and 17-day oocytes. The average EC<sub>50</sub> observed from these oocytes was 102 ± 3.9 μM with 50% that survived and were usable for experiments. Figure 3 shows a representative electrophysiological trace and dose–response curve for 24-day *Xenopus* oocytes.

## Discussion

The purpose of this study was to evaluate one approach to increase the longevity of the *X. laevis* oocyte for the use in electrophysiology applications. *Xenopus* oocytes have been used for the study of ion channels for over 30 years. However, aside from some useful anecdotal information from various research laboratories, there are no studies evaluating the long-term storage of surgically extracted ovaries. The

results of this study provide evidence that this approach can be routinely used to extend the use of surgically extracted oocytes and could be further refined for improved success.

In our study, we showed that a single ovary extraction could be stored for 3 weeks at 4 °C and provide reliable results. We found that EC<sub>50</sub> values collected from 3, 10, and 17 day post-extraction oocytes were statistically the same ( $p > 0.05$ ). Consistent results were also obtained after 3 weeks using another type of nematode Cys-loop LGIC, an acetylcholine-gated chloride channel (data not shown). In addition, we found that 50% of oocytes stored for 24 days could produce consistent electrophysiological responses. The average current obtained from activation of the Hco-UNC-49 receptor appeared to decrease substantially between 3- and 10-day-old oocytes followed by a slight decrease between 10- and 17-day-old oocytes.

We did see a clear difference in success when we stored the ovary as a 9 versus 0.5-g lobe, where the small lobe produced much better results. This could be due to the increased availability of nutrients to the oocytes and a decrease in the concentration of harmful waste products when stored in smaller pieces. *Xenopus* oocytes have been shown to produce NH<sub>3</sub> waste products (Fort and Rogers 2005). Ammonia is a toxic waste product that when released can cause harm to surrounding oocytes. Therefore, the separation of the ovary into smaller sections could reduce the amount of ammonia available to surrounding oocytes.

When working with *Xenopus* oocytes many laboratories have explored different methods of storage to increase their survival rate. Some laboratories find separating oocytes into individual wells of a 24-well plate improves survival and once the oocytes have expressed the receptor of interest they can be stored in the refrigerator in order to extend their viability for recordings (Buckingham et al. 2006). Other researchers indicate that if stored correctly, *Xenopus* oocytes can survive up to 10–15 days (Weber 1999). Our results indicate that sectioning off a small portion of the ovary into its own Petri dish improves the success rate of the oocyte after storage for 17 days (Table 1) which can be extended to 24 days or longer with further improvements to the protocol. This has been particularly useful in our laboratory where different receptors are expressed from week to week by several personnel. We intend to further refine this approach in an effort to further extend the use of *Xenopus* oocytes for electrophysiological recordings. However, overall we were able to obtain 4 weeks of electrophysiological recordings from a single oocyte extraction.

The defolliculation of the ovary each week could also have an impact on the viability of the oocytes. In our study, we defolliculated roughly 2 mL of ovary using 10 mg/mL collagenase solution for 2 h. Other protocols have recommended using 1–6 mg/mL of collagenase solution for 1–3 h (Dascal 1987; Stühmer and Parekh 1995). Therefore, there

is variability in how much and for how long collagenase treatment is performed. Evaluating the optimal concentration of collagenase and length of time for defolliculation could further improve the health and viability of the oocytes.

It should be noted that in our protocol once the ovary was sectioned off and stored at 4 °C, the media was not changed. However, once injected with cRNA and stored at 18 °C, the oocyte storage media was changed once per day. Frequent renewal of the storage media could perhaps increase the health of the oocytes during long-term storage.

Other factors have been shown to effect the viability of *Xenopus* oocytes, including the water temperature in which the frogs are stored. Frogs that are stored in 17 °C water generally produce oocytes that are firm and perfect for microinjection, whereas warmer water causes oocytes to soften (Stühmer and Parekh 1995). Our laboratory stores the frogs in a temperature-controlled room (18–20 °C) with consistent full-spectrum lighting which could contribute to the success rate that we noted.

From an animal welfare perspective, these results have helped contribute to our progress with respect to the three “R’s” (replacement, reduction, and refinement) of more ethical use of animals. This has also contributed greatly to reducing the overall cost of using *Xenopus* for ion channel research. In addition, since *Xenopus* can be susceptible to a variety of diseases (Smart and Krishek 1995), this approach has reduced the stress on the animals by increasing the time between surgeries and thus their potential susceptibility to infection. We also anticipate that the approach presented here can be further refined with better results.

**Acknowledgements** This research was funded by grants from National Science and Engineering Research Council (NSERC) and the Canadian Foundation for Innovation to SGF.

## Compliance with ethical standards

**Conflict of interest** The authors declare that they have no conflict of interest.

**Human and animal rights** All animal procedures followed the University of Ontario Institute of Technology Animal Care Committee and the Canadian Council on Animal Care guidelines.

## References

- Bamber BA, Beg AA, Twyman RE, Jorgensen EM (1999) The *Caenorhabditis elegans* unc-49 locus encodes multiple subunits of a heteromultimeric GABA receptor. *J Neurosci* 19:5348–5359
- Bianchi L, Driscoll M (2006) Heterologous expression of *C. elegans* ion channels in *Xenopus* oocytes. In: Mano I, George AL Jr. (eds) *WormBook*. The *C. elegans* Research Community, Piscataway, pp 1–16

- Buckingham SD, Pym L, Sattelle DB (2006) Oocytes as an expression system for studying receptor/channel targets of drugs and pesticides. *Methods Mol Biol* 322:331–345
- Cully DF, Vassilatis DK, Liu KK, Pareess PS, Van der Ploeg LH, Schaeffer JM, Arena JP (1994) Cloning of an avermectin-sensitive glutamate-gated chloride channel from *Caenorhabditis elegans*. *Nature* 371:707–711
- Dascal N (1987) The use of *Xenopus* oocytes for the study of ion channels. *CRC Crit Rev Biochem* 22:317–387
- Fort DJ, Rogers RL (2005) Enhanced frog embryo teratogenesis assay: *Xenopus* model using *Xenopus tropicalis*. In: Ostrander GK (ed) *Techniques in aquatic toxicology*. CRC Press, Boca Raton, pp 50–65
- Gurdon JB, Lane CD, Woodland HR, Marbaix G (1971) Use of frog eggs and oocytes for the study of messenger RNA and its translation in living cells. *Nature* 233:177–182
- Kulke D, von Samson-Himmelstjerna G, Miltsch SM, Wolstenholme AJ, Jex AR, Gasser RB et al (2014) Characterization of the Ca<sup>2+</sup>-gated and voltage-dependent K<sup>+</sup>-channel Slo-1 of nematodes and its interaction with emodepside. *PLoS Negl Trop Dis* 8(12):e3401
- Lee YS, Park YS, Chang DJ, Hwang JM, Min CK, Kaang BK, Cho NJ (1999) Cloning and expression of a G protein-linked acetylcholine receptor from *Caenorhabditis elegans*. *J Neurochem* 72:58–65
- Miledi R, Parker I, Sumikawa K (1983) Recording of single  $\gamma$ -aminobutyrate- and acetylcholine-activated receptor channels translated by exogenous mRNA in *Xenopus* oocytes. *Proc R Soc Lond* 218:481–484
- Siddiqui SZ, Brown DDR, Rao VTS, Forrester SG (2010) An UNC-49 GABA receptor subunit from the parasitic nematode *Haemonchus contortus* is associated with enhanced GABA sensitivity in nematode heteromeric channels. *J Neurochem* 113:1113–1122
- Smart TG, Krishek BJ (1995) *Xenopus* oocyte microinjection and ion-channel expression. In: Boulton AA, Baker GB, Walz W (eds) *Patch-clamp applications and protocols*. Humana Press, Totowa, pp 259–305
- Snutch TP (1988) The use of *Xenopus* oocytes to probe synaptic communication. *Trends Neurosci* 11:250–256
- Stühmer W, Parekh AB (1995) Electrophysiological recordings from *Xenopus* oocytes. In: *Single-channel recording*, Springer, New York, pp 341–356
- Sumikawa K, Houghton M, Emtage JS, Richards BM, Barnard EA (1981) Active multi-subunit ACh receptor assembled by translation of heterologous mRNA in *Xenopus* oocytes. *Nature* 292:862–864
- Weber WM (1999) Ion currents of *Xenopus laevis* oocytes: state of the art. *Biochim Biophys Acta (BBA)-Biomembr* 1421:213–233

## Appendix 2: Chapter II

### A2.1: Manuscript I



# Molecular and pharmacological characterization of an acetylcholine-gated chloride channel (ACC-2) from the parasitic nematode *Haemonchus contortus*

Sarah A. Habibi, Micah Callanan, Sean G. Forrester\*

Applied Bioscience Graduate Program, Faculty of Science, University of Ontario Institute of Technology, 2000 Simcoe Street North, Oshawa, ON, L1H 7K4, Canada

## ARTICLE INFO

### Keywords:

Cholinergic receptor  
Nicotinic acetylcholine receptors (nAChR)  
Acetylcholine-gated chloride channel  
Mutagenesis  
*Haemonchus contortus*  
Anthelmintic

## ABSTRACT

Nematode cys-loop ligand-gated ion channels (LGICs) have been shown to be attractive targets for the development of novel anti-parasitic drugs. The ACC-1 family of receptors are a unique group of acetylcholine-gated chloride channels present only in invertebrates, and sequence analysis suggests that they contain a novel binding site for acetylcholine. We have isolated a novel member of this family, Hco-ACC-2, from the parasitic nematode *Haemonchus contortus* and using site-directed mutagenesis, electrophysiology and molecular modelling examined how two aromatic amino acids in the binding site contributed to agonist recognition. It was found that instead of a tryptophan residue in binding loop B, which essential for ligand binding in mammalian nAChRs, there is a phenylalanine (F200) in Hco-ACC-2. Amino acid changes at F200 to either a tyrosine or tryptophan were fairly well tolerated, where a F200Y mutation resulted in a channel hypersensitive to ACh and nicotine as well as other cholinergic agonists such as carbachol and methacholine. In addition, both pyrantel and levamisole were partial agonists at the wild-type receptor and like the other agonists showed an increase in sensitivity at F200Y. On the other hand, in Hco-ACC-2 there is a tryptophan residue at position 248 in loop C that appears to be essential for receptor function, as mutations to either phenylalanine or tyrosine resulted in a marked decrease in agonist sensitivity. Moreover, mutations that swapped the residues F200 and W248 (ie. F200W/W248F) produced non-functional receptors. Overall, Hco-ACC-2 appears to have a novel cholinergic binding site that could have implications for the design of specific anthelmintics that target this family of receptors in parasitic nematodes.

## 1. Introduction

The Cys-loop (cysteine-loop) superfamily of ligand-gated ion channels (LGICs) are a major class of receptor-coupled ion channels. These channels have been widely studied in invertebrate organisms for decades because they play key roles in the nervous system, making them prime targets for insecticides and nematocides (Del Castillo et al., 1963). The channel contains five protein subunits, encoded by the same or different subunit genes, all situated around a central aqueous pore. Each subunit contains an extracellular N-terminal ligand binding domain, where two cysteine residues, situated 13 amino acid residues apart, form a disulfide bond, as well as four transmembrane domains (TM1-TM4), and an extracellular C-terminus. These subunits can assemble as homo-oligomers, containing one subunit type, or hetero-oligomers, containing multiple subunit types (Sine and Engel, 2006).

Upon ligand binding, these channels elicit fast inhibitory or excitatory neurotransmission. In mammals, excitatory channels include nicotinic acetylcholine receptors (nAChRs) and 5-hydroxytryptamine (5-HT<sub>3</sub>) serotonin receptors, and inhibitory channels include gamma-

aminobutyric acid (GABA) and glycine receptors (Ortells and Lunt, 1995). Invertebrates, specifically parasitic and free-living nematodes, contain a variety of LGIC subunit types which are not found in vertebrates (Jones and Sattelle, 2008). These channels have been shown to be gated by neurotransmitters including GABA (Bamber et al., 1999; Siddiqui et al., 2010), glutamate (Cully et al., 1994), tyramine (Pirri et al., 2009), acetylcholine (ACh) (Putrenko et al., 2005), and serotonin (Ranganathan et al., 2000).

The ligand-binding site of cys-loop receptors is located at the interface of two adjacent subunits, which are loops A-C on the principal subunit and loops D-G on the complementary subunit (Hibbs and Gouaux, 2011). Each receptor has a different ligand-binding domain that contain various residues, which allow for the selection of different molecular agonists. There are key aromatic residues in the binding site of LGICs that have shown to be involved in ligand binding (Beene et al., 2004). Many neurotransmitters contain a cationic center that acts to stabilize the interaction between a cation and the negative electrostatic potential on the face of the aromatic ring. This is known as cation- $\pi$  interactions (Beene et al., 2002). These cation- $\pi$  interactions involve

\* Corresponding author.

E-mail address: [sean.forrester@uoit.ca](mailto:sean.forrester@uoit.ca) (S.G. Forrester).

<https://doi.org/10.1016/j.ijpddr.2018.09.004>

Received 22 August 2018; Received in revised form 17 September 2018; Accepted 17 September 2018

Available online 22 September 2018

2211-3207/ © 2018 The Authors. Published by Elsevier Ltd on behalf of Australian Society for Parasitology. This is an open access article under the CC BY-NC-ND license (<http://creativecommons.org/licenses/by-nc-nd/4.0/>).

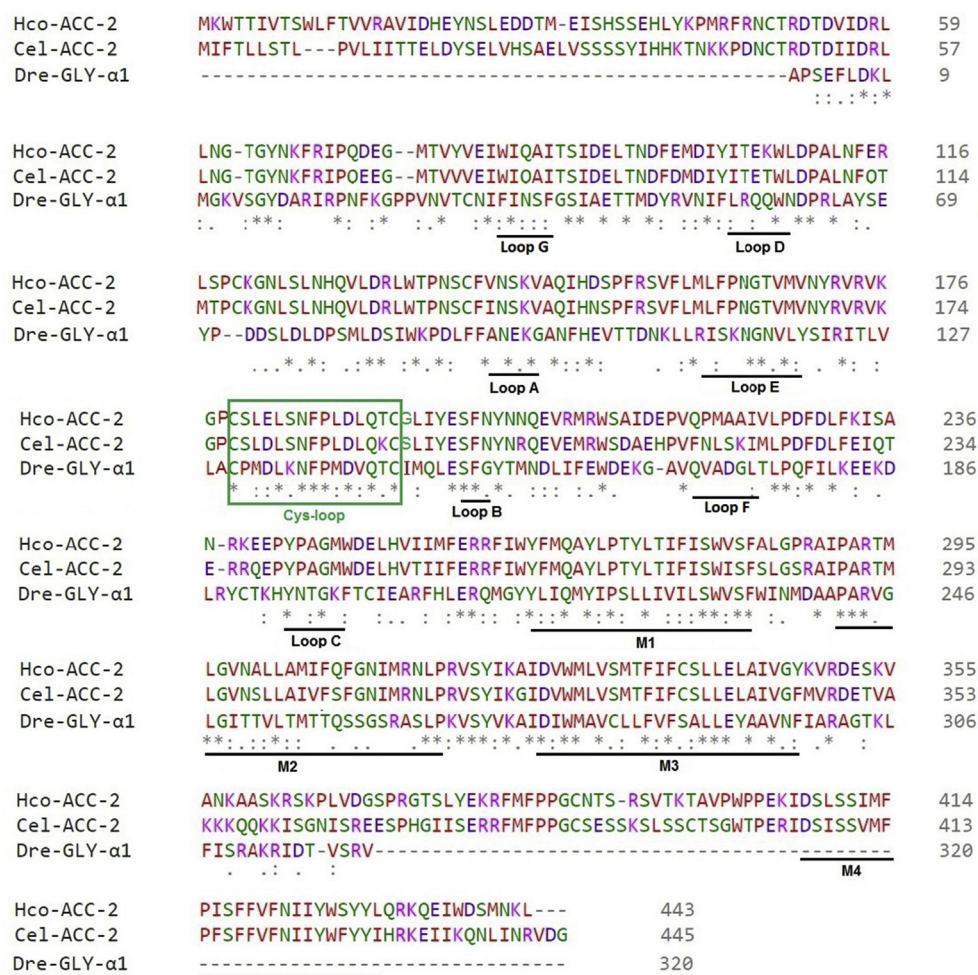


Fig. 1. Protein sequence alignment of the *H. contortus* Hco-ACC-2 receptor with *C. elegans* Cel-ACC-2 and *D. rerio* Dre-GLY-α1 receptors. All seven binding loops (Loop A-G), the characteristic cysteine residues that form the “cys-loop”, and four transmembrane domains (M1-M4) and highlighted with underlines. (\*) indicates identity and (:) indicates similarity.

aromatic amino acids (either phenylalanine, tyrosine, or tryptophan) in the ligand binding region (Dougherty, 1996). While the importance of aromatic residues for the function of the agonist binding pocket is widely shared across the phyla, there is variability across different receptors with respect to the type of aromatic residues that contribute to binding and their location within the binding loops (Lynagh and Pless, 2014). This highlights the promiscuous nature of neurotransmitter binding across a variety of receptors in animals.

Early studies from the mollusk, *Aplysia*, reported the presence of a unique class of acetylcholine receptors in neurons, the acetylcholine-gated chloride channels (ACCs) (Kehoe and McIntosh, 1998). Later, studies identified these receptors in the model nematode *Caenorhabditis elegans* (Putrenko et al., 2005; Wever et al., 2015). In *C. elegans* the ACC-1 family is made up of eight receptor subunit genes, *acc-1*, *-2*, *-3*, and *-4*, and *lgc-46*, *-47*, *-48*, and *-49* (Jones and Sattelle, 2008). The sheep parasite, *Haemonchus contortus*, contains homologues for seven of the ACC-1 gene members, with the absence of *lgc-48* (Laing et al., 2013). As a whole, this family of receptors has potential to be novel antiparasitic drug targets. This is primarily due to the fact that they appear to be expressed in tissues that are sensitive to anthelmintic action, and as sequence analysis suggests, they are not present in mammals and exhibit a unique acetylcholine binding site (Putrenko et al., 2005; Wever et al., 2015). However, the structural components that are important for agonist recognition of this class of cholinergic receptors has not been explored.

Here we have isolated a novel member of the ACC-1 family (Hco-ACC-2) from the parasitic nematode *H. contortus* and investigated the binding site through site-directed mutagenesis and pharmacological analysis. Several introduced point mutations that changed key aromatic residues at the binding site revealed some interesting pharmacological properties. Molecular modelling was used to visualize the structure of the binding pocket and the interaction of key residues with a variety of agonists.

## 2. Methods

### 2.1. Isolation of *hco-acc-2*

*H. contortus* was received from Dr. Prichard (Institute of Parasitology, McGill University). Total RNA was extracted from adult male *H. contortus* using Trizol (Invitrogen, Carlsbad, USA). Complementary DNA (cDNA) was synthesized using the Quantitect Reverse Transcriptase kit from Qiagen (Dusseldorf, Germany), using a unique 3' oligo-dT anchor primer sequence (5'CCTCTGAAGGTTCCAGGATCCACATCTAGATTTTTTTTTTTTTTTTTTTT3'); [where V is either A, C, or G and N is either A, C, G, or T] (Weston et al., 1999). Gene specific primers were generated based on a partial sequence provided by Dr. Robin Beech (McGill University) as part of the genome sequencing project for *H. contortus* (Laing et al., 2013). The original sequence appeared to contain the full 3' end of the gene but was missing the 5'

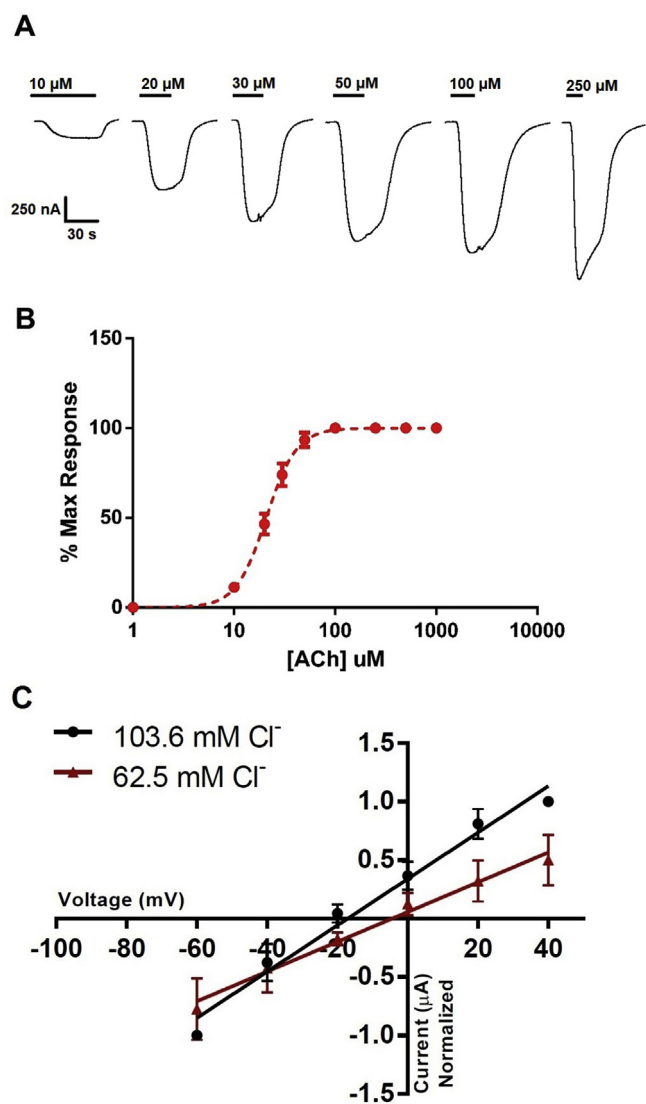


**Fig. 2.** Hco-ACC-2 is an acetylcholine-gated chloride channel. (A) Electrophysiological response of Hco-ACC-2 to increasing concentrations of ACh. (B) Dose-response curve for acetylcholine on the Hco-ACC-2 channel. Standard errors are shown.  $n = 7$  oocytes (C) Current-voltage analysis of the Hco-ACC-2 channel using 103.6 mM Cl<sup>-</sup> and 62.5 mM Cl<sup>-</sup> in ND96 buffer solution. Acetylcholine response were generated using a maximum wild-type ligand saturation concentration of 250 μM. Standard errors are shown.

region that would include the signal peptide cleavage site. The 5' end of the gene was isolated using the 5' rapid amplification of cDNA ends (RACE) protocol (Frohman et al., 1988). Two internal primers were used for the amplification of the 5' end along with a primer specific for the splice-leader 1 sequence (SL1-5'-GGTTTAATTACCCAAGTTT GAG-3') (Van Doren and Hirsh, 1988). The resulting amplicon of predicted size was isolated via a QIAquick Gel Extraction Kit (Qiagen, Dusseldorf, Germany) and sub-cloned into the pGEMT easy™ sequencing vector and was sequenced at Genome Quebec. Amplification of the complete *hco-acc-2* gene was carried out using primers specific to the 5' and 3' end of the gene with the XbaI and BamHI restriction sites and was subsequently cloned into the pGEMHE *Xenopus* expression vector (Zhang et al., 2008). All sequence alignments were produced using ClustalW.

## 2.2. Site-directed mutagenesis

The coding sequence of Hco-ACC-2 was sub-cloned into the

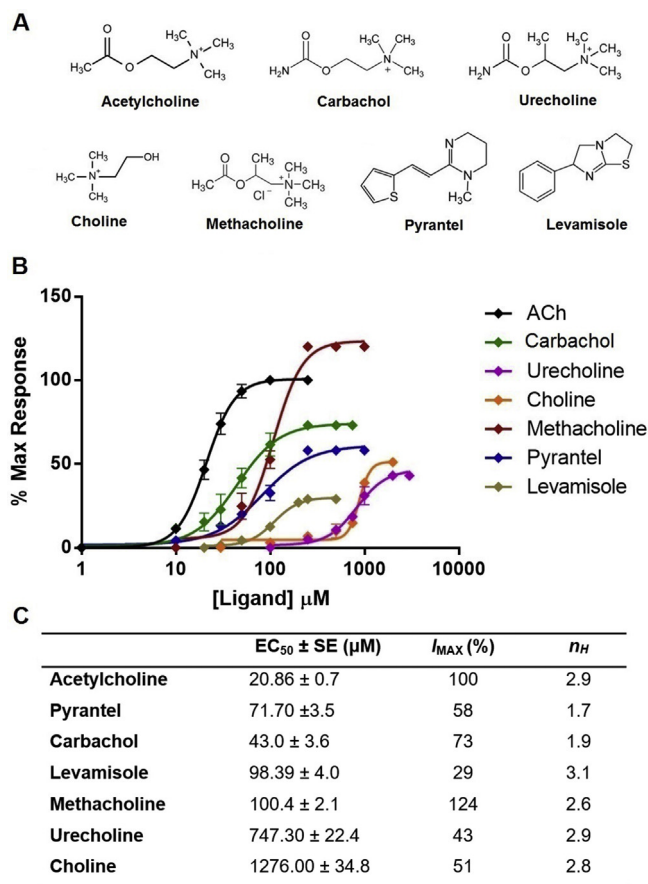


**Fig. 3.** Pharmacology of Hco-ACC-2 (A) Chemical structures for the various molecular agonists used for the characterization of the Hco-ACC-2 binding site. (B) Dose-response curves for each of the listed compounds against the wild-type Hco-ACC-2 channel. Each curve is represented as a percent of the maximum acetylcholine response (250 μM). Partial agonists are those that have a maximum response lower than 100%. (C) Summary of the EC<sub>50</sub> values ± standard error for each compound listed from most sensitive to least. I<sub>max</sub> represents the maximal current response for each agonist.

pGEMHE transcription vector (3022 bp). The introduction of mutations in the Hco-ACC-2 coding sequence was performed using the QuikChange® II Site-Directed Mutagenesis Kit (Agilent Technologies). The primers carrying the specific mutation were generated using QuikChange Primer Design software from Agilent Technologies (QuikChange Primer Design). Five ACC-2 mutants were generated: F200Y, F200W, W248Y, W248F, and F200W/W248F. Point-mutations were confirmed using sequence analysis (Genome Quebec).

## 2.3. Expression in *Xenopus laevis* oocytes

All animal procedures followed the University of Ontario Institute of Technology Animal Care Committee and the Canadian Council on Animal Care guidelines. Expression of channels in oocytes was conducted as outlined in Abdelmassih et al. (2018). Female *Xenopus laevis* frogs were supplied by Nasco (Fort Atkinson, WI, USA). All frogs were housed in a climate controlled room (18 °C) with constant light cycling. Frogs were fed and tanks were cleaned regularly. Frogs were anesthetized with 0.15% 3-aminobenzoic acid ethyl ester methanesulphonate salt (MS-222) buffered with NaHCO<sub>3</sub> to pH 7 (Sigma-Aldrich, Oakville, ON, CA). Surgical removal of a section of the ovary of the frog was performed, and the lobe was defolliculated with a calcium-free oocyte Ringer's solution (82 mM NaCl, 2 mM KCl, 1 mM MgCl<sub>2</sub>, 5 mM HEPES pH 7.5 (Sigma-Aldrich)) (OR-2) containing 2 mg·mL<sup>-1</sup> collagenase-II (Sigma-Aldrich). The oocytes in the defolliculation solution were

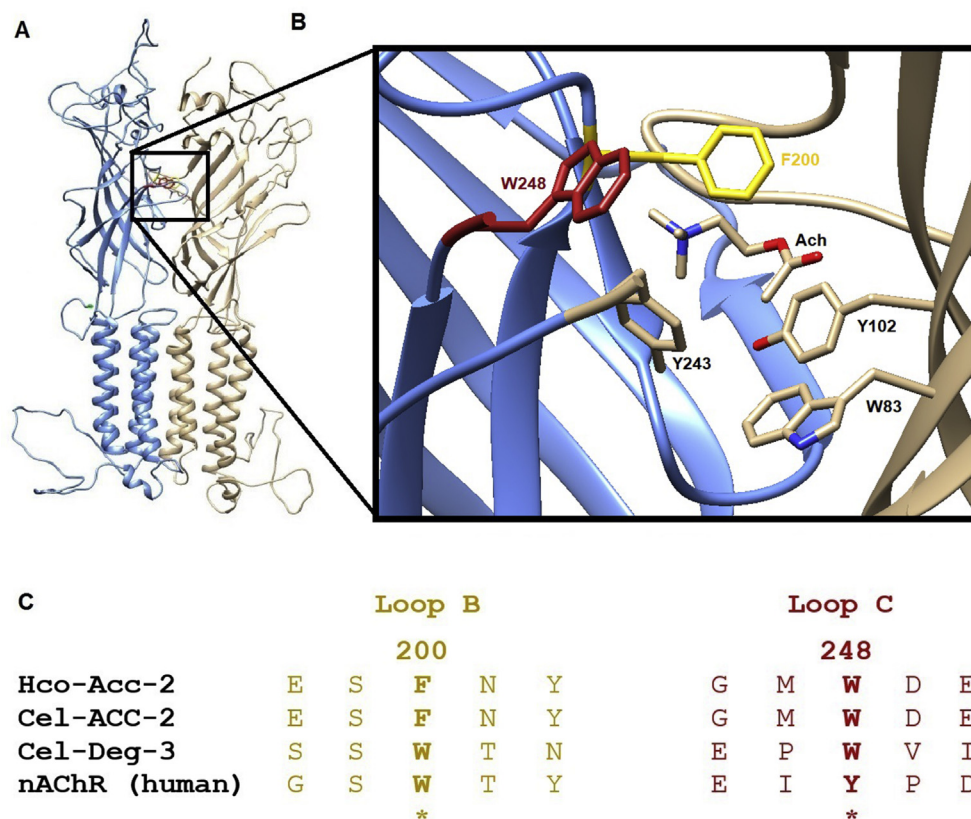


**Fig. 4.** (A) Homology model of Hco-ACC-2 homodimer. The principal and complementary subunits are represented by blue and beige respectively. (B) View of the Hco-ACC-2 binding pocket with acetylcholine docked. Key aromatic residues explored in this study, phenylalanine 200 (yellow) and tryptophan 248 (red) are highlighted. Other aromatic residues that may contribute to the binding site are also indicated. A portion of Loop C is removed for clarity. (C) Protein alignment of the residues found in loop B and C of the Hco-ACC-2 with Cel-ACC-2, Cel-DEG-3 (GenBank accession # CAA98507.1), and the mammalian nAChR. \* indicates the residue position for mutational analysis. (For interpretation of the references to colour in this figure legend, the reader is referred to the Web version of this article.)

incubated at room temperature for 2 h. Collagenase was washed from the oocytes with ND96 solution (1.8 mM CaCl<sub>2</sub>, 96 mM NaCl, 2 mM KCl, 1 mM MgCl<sub>2</sub>, 5 mM HEPES pH 7.5) and allowed one hour to recover at 18 °C in ND96 supplemented with 275 µg·mL<sup>-1</sup> pyruvic acid (Sigma-Aldrich) and 100 µg·mL<sup>-1</sup> of the antibiotic gentamycin (Sigma-Aldrich) (Supplemented ND96). Stage V and VI oocytes were selected for cytoplasmic injection of cRNA.

The pGEMHE vector containing the *hco-acc-2* coding sequence was linearized using the restriction enzyme PstI (New England Biolabs, USA), and used as template for an *in vitro* transcription reaction (T7 mMessage mMachine kit, Ambion, Austin, TX, USA) yielding *hco-acc-2* copy RNA. *X. laevis* oocytes were injected with 50 nl of *hco-acc-2* (0.5 ng·nL<sup>-1</sup>) using the Drummond (Broomall, PA, USA) Nanoject microinjector. The expression of *hco-acc-2* required the co-injection with the copy RNA encoding three accessory proteins, *unc-50*, *unc-74*, and *ric-3.1* (Boulin et al., 2011) which were gifts from Dr. Cédric Neveu (INRA). The injected oocytes were incubated at 18 °C in supplemented ND96 solution. Electrophysiological recordings of the oocytes were conducted between 48 and 72 h after cRNA injection.

#### 2.4. Electrophysiological recordings

Two-electrode voltage clamp electrophysiology was conducted using the Axoclamp 900A voltage clamp (Molecular Devices, Sunnyvale, CA, USA). Glass electrodes were produced using a P-97 Micropipette Puller (Sutter Instrument Co., Novato, CA, USA). The electrodes were backfilled with 3 M KCl and contained Ag|AgCl wires. The following molecules were first dissolved in ND96; Acetylcholine (ACh), Choline Chloride (Choline), Carbamoylcholine Chloride (Carbachol), Acetyl-β-methylcholine Chloride (Methacholine), Carbamyl-β-methylcholine chloride (Urecholine) [Sigma Aldrich], Levamisole Hydrochloride (Levamisole), and Pyrantel Citrate Salt (Pyrantel) [Santa Cruz Biotechnology]. These solutions were perfused over oocytes using the RC-1Z recording chamber (Warner Instruments

Inc., Hamdan, CT, USA). Data was analyzed using Clampex Software v10.2 (Molecular Devices) and all graphs were generated using Graphpad Prism Software v5.0 (San Diego, CA, USA). EC<sub>50</sub> values were determined by dose response curves that had been fitted to the following equation:

$$I_{max} = 1 / \left[ 1 + \left( \frac{EC_{50}}{[D]} \right)^h \right]$$

Where  $I_{max}$  is the maximal response, EC<sub>50</sub> is the concentration of compound required to elicit 50% of the maximal response, [D] is compound concentration, and h is the Hill coefficient. Both EC<sub>50</sub> and h are free parameters, and the curves were normalized to the estimated  $I_{max}$  using 250 µM ACh. Graphpad prism used the equation to fit a sigmoidal curve of variable slopes to the data. Means were determined from at least 5 oocytes from at least two batches of frogs. Significant differences between EC<sub>50</sub> values comparing WT to mutants was performed using Student's T-test with the Bonferroni correction. P-values ≤ 0.01 were considered significant.

Current-voltage relationships were recorded by changing the holding potential from -60 mV to 40 mV in 20 mV increments. At each step the oocyte was exposed to a 250 µM concentration of ACh. For reduced Cl<sup>-</sup> trials, NaCl was partially replaced by Na-gluconate (Sigma) in the ND96 buffer solution, for a final Cl<sup>-</sup> concentration of 62.5 mM. Current-voltage graphs were generated using Graphpad Prism Software v5.0 (San Diego, CA, USA).

#### 2.5. Homology modelling

The template used was the *Danio rerio* alpha-1 glycine receptor (3JAD) which showed the highest homology to Hco-ACC-2. The protein coding sequence of Hco-ACC-2 was aligned to template using SWISS-MODEL which was used in MODELLER v9.15 (Šali and Blundell, 1993) for the generation of the Hco-ACC-2 homodimer. The associated DOPE



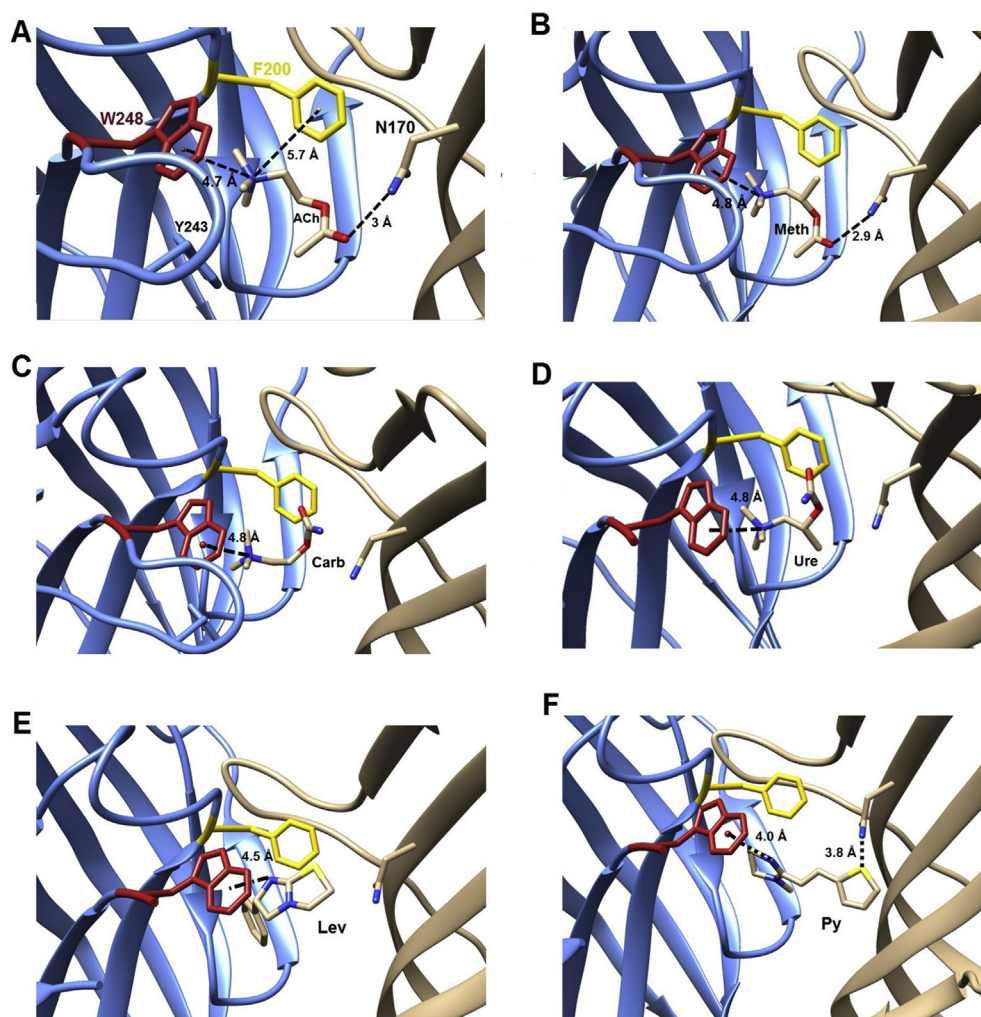


**Fig. 5.** Homology models of Hco-ACC-2 with docked agonists. (A) Acetylcholine (ACh) docked in the binding pocket of the Hco-ACC-2 receptor. Distance between the quaternary amine in ACh with W248 (4.7 Å) and F200 (5.7 Å) are represented by a dotted line and measured in angstroms (Å). Distance between N170 in loop E to the carbonyl oxygen in ACh (3 Å) is also shown. (B) Methacholine (Meth) docked in the Hco-ACC-2 binding pocket. W248 is 4.8 Å away from the quaternary amine of methacholine. N170 is 2.9 Å away from the carbonyl oxygen in methacholine. (C) Carbachol (Carb) docked in the Hco-ACC-2 binding pocket. W248 is 4.8 Å away from the quaternary amine in carbachol. (D) Urecholine (Ure) docked in the Hco-ACC-2 binding pocket. W248 is 4.8 Å away from the quaternary amine in urecholine. (E) Levamisole (Lev) docked in the Hco-ACC-2 binding pocket. (F) Pyrantel (Py) docked in the Hco-ACC-2 binding pocket.

and molpdf scores determined the most energetically favorable model. The final model chosen was visually inspected to ensure the binding loops were in the proper positions. Preparation of the homodimer for agonist docking was carried out using AutoDock Tools. Ligands including ACh and all of the molecules mentioned were obtained from the Zinc database in their energy-reduced extended form. AutoDock Vina was used to simulate docking of each ligand to the homodimers (Trott and Olson, 2010). Pymol was used to visualize the protein homodimer with its associated ligands, and Chimera v1.6.1 (Pettersen et al., 2004) was used to determine the distance between amino acid residues and ligand.

### 3. Results

#### 3.1. Isolation of *hco-acc-2*

The full-length coding sequence of the *hco-acc-2* gene consisted of 1332 nucleotides (GenBank Accession # [KC918364.1](#)). When viewed in the appropriate reading frame, the sequence encodes for a protein containing 443 amino acids (AHM25234.1). The protein sequence contains a signal peptide cleavage site (Signal P; <http://www.cbs.dtu.dk/services/SignalP/>), all seven extracellular binding loops, four transmembrane domains, and the hallmark Cys-loop motif (Fig. 1). The Hco-ACC-2 protein sequences shares 88% similarity to the Cel-ACC-2 protein (Fig. 1). The PAR motif present at the beginning of the transmembrane 2 domain indicates anion selectivity through the channel (Jensen et al., 2002).

#### 3.2. Expression of *hco-acc-2* in *Xenopus oocytes*

Injection of *hco-acc-2* cRNA alone did not result in ACh-sensitive channels. However, the injection of *X. laevis* oocytes with cRNA encoding *hco-acc-2*, and the accessory proteins, *hco-unc-74*, *hco-unc-50*, and *hco-ric-3.1*, resulted in a homomeric ACC-2 channel that was highly sensitive to ACh. ACh currents were in  $\mu$ A range, dose-dependent and desensitizing and were consistent in multiple oocytes from several frogs (Fig. 2A and B). In addition, current-voltage analysis of the Hco-ACC-2 channel was conducted to confirm anion selectivity through the channel. A full  $\text{Cl}^-$  concentration of ND96 (103.6 mM  $\text{Cl}^-$ ) indicated a reverse potential of  $-17.44 \pm 5$  mV ( $n = 4$ ). This is consistent with the calculated Nernst potential for  $\text{Cl}^-$  of  $-18.5$  mV, when assuming an internal  $\text{Cl}^-$  concentration of 50 mM (Kusano et al., 1982). When NaCl was partially replaced with Na-gluconate (final  $\text{Cl}^-$  concentration of 62.5 mM) the reverse potential shifted to  $-3.4 \pm 2$  mV ( $n = 4$ ), which is also consistent with the assumed Nernst potential of  $-5.7$  mV (Fig. 2B).

#### 3.3. Pharmacological analysis

Several cholinergic agonists and anthelmintics were examined. The  $\text{EC}_{50}$  value for ACh was  $21 \pm 0.7$   $\mu\text{M}$  ( $n = 7$ ). The ACh analogue carbachol had an  $\text{EC}_{50}$  of  $43 \pm 3.6$   $\mu\text{M}$  ( $n = 6$ ). Other ACh derivatives, including methacholine, urecholine, and choline also activated the channel with  $\text{EC}_{50}$  values of  $100 \pm 2$   $\mu\text{M}$  ( $n = 6$ ),  $747 \pm 22$   $\mu\text{M}$  ( $n = 10$ ), and  $1276 \pm 35$   $\mu\text{M}$  ( $n = 7$ ), respectively. Currently used

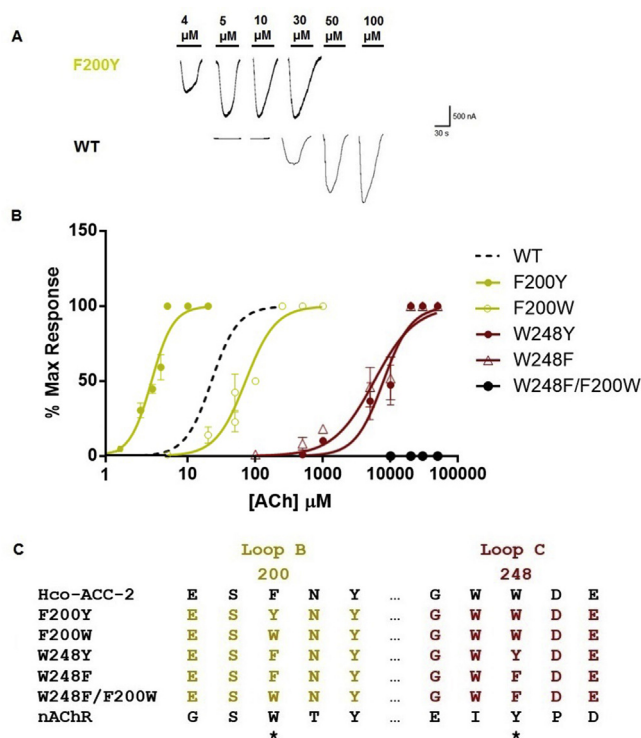


**Fig. 6.** Impact of mutations at key aromatic residues (A) Electrophysiological traces of the F200Y mutant compared to Hco-ACC-2 wild-type. (B) Dose-response curves for the WT and each of the mutated channels with acetylcholine. Loop B and C mutants are represented by yellow and red respectively. (C) Protein alignment of Loop B and C in the Hco-ACC-2 receptor for each of the generated mutants. \* indicates the location of mutational analysis. (For interpretation of the references to colour in this figure legend, the reader is referred to the Web version of this article.)

anthelmintics such as pyrantel and levamisole were partial agonists for the receptor with  $EC_{50}$  values of  $72 \pm 4 \mu$ M ( $n = 6$ ) and  $98 \pm 4 \mu$ M ( $n = 6$ ) respectively. All pharmacological data is represented in Fig. 3. The compounds that showed to be full agonists were ACh and methacholine. All other compounds tested appeared to be partial agonists of the channel (Fig. 3).

### 3.4. Homology modelling

In order to visualize the interaction of agonists with residues in the binding pocket, a homology model was generated for the Hco-ACC-2 dimer using the *D. rerio* glycine receptor 3JAD as template which exhibited the highest homology with Hco-ACC-2. The model chosen, with the lowest DOPE score, is outlined in Fig. 4A. Cys-loop receptors are

**Table 1**

Summary of  $EC_{50}$  values  $\pm$  standard error for each channel with all of the compounds listed. N.R<sup>a</sup> indicates the channel did not respond to concentrations of indicated compound at concentrations  $\geq 1$  mM which is a concentration that elicited a maximal response on the WT channel. N.R<sup>b</sup> indicated that the channel did not respond to concentration up to 20 mM.  $n \geq 5$  oocytes. NR = no response; ND = not determined.

	WT	F200Y	F200W	W248Y	W248F	F200W/W248F
Acetylcholine	$21 \pm 1$	$2.9 \pm 0.1^{**}$	$61 \pm 4^{**}$	$7854 \pm 275^*$	$5600 \pm 1258^*$	N.R <sup>b</sup>
Carbachol	$43 \pm 4$	$9.7 \pm 0.5^{**}$	$67 \pm 4$	N.R <sup>a</sup>	N.R <sup>a</sup>	N.R <sup>b</sup>
Choline	$1276 \pm 35$	$650 \pm 13^{**}$	$4771 \pm 543^*$	N.R <sup>a</sup>	N.R <sup>a</sup>	N.R <sup>b</sup>
Methacholine	$100 \pm 2$	$20 \pm 1^{**}$	$644 \pm 84^{**}$	N.R <sup>a</sup>	N.R <sup>a</sup>	N.R <sup>b</sup>
Urecholine	$747 \pm 22$	$81 \pm 3^{**}$	$2151 \pm 215^{**}$	N.R <sup>a</sup>	N.R <sup>a</sup>	N.R <sup>b</sup>
Levamisole	$98 \pm 4$	$39 \pm 3^{**}$	N.D	N.R <sup>a</sup>	N.R <sup>a</sup>	N.R <sup>b</sup>
Pyrantel	$72 \pm 4$	$44 \pm 2^{**}$	$160 \pm 20$	N.R <sup>a</sup>	N.R <sup>a</sup>	N.R <sup>b</sup>

\*indicates significant difference compared to WT ( $P < 0.01$ ).

\*\*indicates significant difference compared to WT ( $P < 0.001$ ).

NOTE: For each molecule (row), statistical analysis compared  $EC_{50}$  values between WT and each mutant.

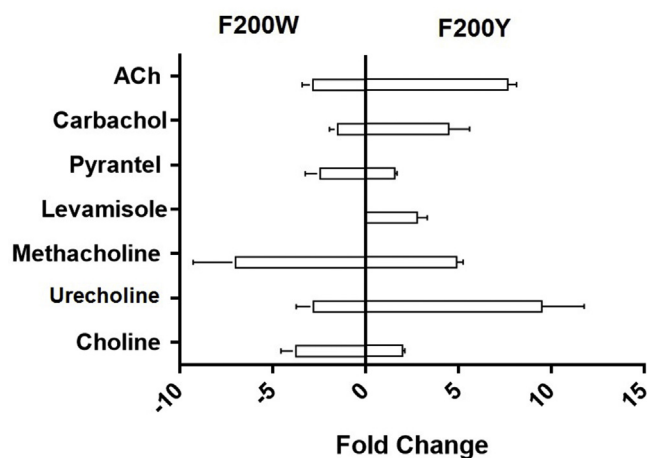


**Fig. 7.** Mutations at F200 have varying effects on agonist sensitivity. Fold changes in  $EC_{50}$  for the loop B mutants (F200Y and F200W) against all of the compounds listed. A positive fold change represents the channel becoming more sensitive to that compound, whereas a negative fold change represents the channel becoming less sensitive.

known to contain an aromatic box in the binding site. The binding site on the primary and complementary subunits appear to be composed of several aromatic residues. Based on sequence alignment of the Hco-ACC-2 protein with the mammalian nAChR, two aromatic residues in binding loops B and C appear to be swapped. The residues that appeared to interact with all agonists were phenylalanine 200 (F200) in loop B, and tryptophan 248 (W248) in loop C. The quaternary amine group in ACh was situated between  $4.7 \text{ \AA}$  and  $5.7 \text{ \AA}$  away from W248 and F200 respectively (Figs. 4B and 5A). The quaternary amine of other molecules such as carbachol, methacholine and urecholine also docked at a similar distance from the two aromatic residues (Fig. 5B, C and D). Partial agonists such as carbachol and urecholine docked in a bent formation (Fig. 5C and D). The anthelmintics levamisole and pyrantel also docked with their quaternary amine close to W248 (Fig. 5E and F). In addition, an asparagine residue (N170) in loop E is also present within the binding pocket, and its hydroxyl group is located  $3 \text{ \AA}$  from the carbonyl oxygen in ACh. The equivalent position in the nAChR is L121 ( $\beta 2$  subunit) (Morales-Perez et al., 2016) which highlights another potential difference in the agonist binding site between ACCs and nAChRs. Methacholine which is also a full agonist docked in a similar orientation as ACh with its carbonyl oxygen within  $3 \text{ \AA}$  from the  $NH_2$  group of N170 (Fig. 5B). Since all agonists appear to dock with their quaternary amine between F200 and W248, these two residues were chosen for further analysis.

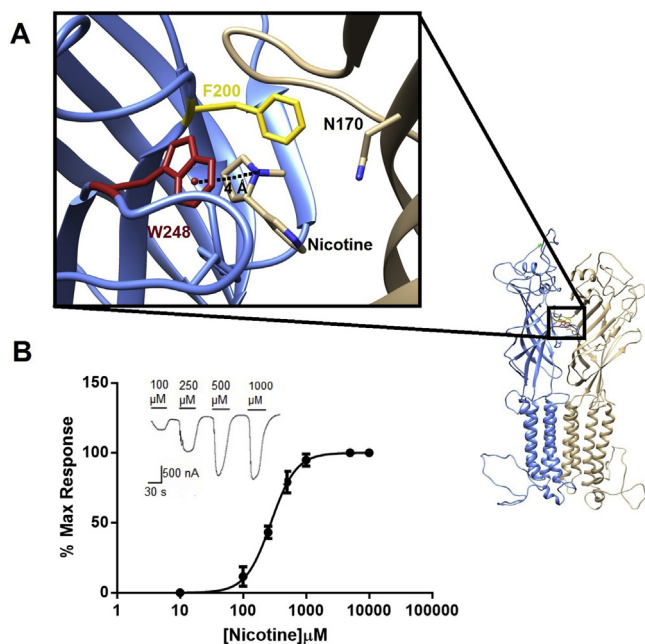


**Fig. 8.** (A) Nicotine docked in the Hco-ACC-2 WT binding pocket. The quaternary amine of nicotine is located 4 Å away from W248. (B) Dose-response curve for the F200Y mutant with nicotine. INSET: Electrophysiological traces of nicotine activation of Hco-ACC-2.  $n = 5$  oocytes.

### 3.5. Mutational analysis

Five Hco-ACC-2 mutants were generated, including F200Y, F200W, W248Y, W248F, and F200W/W248F swap. When the phenylalanine (Phe) at position 200 was replaced with a tyrosine (Tyr) residue, the resulting channel became significantly more sensitive to ACh compared to wild-type (Fig. 6A). The  $EC_{50}$  of the F200Y channel was  $3 \pm 0.1 \mu\text{M}$  ( $n = 5$ ) (Fig. 6B). The mutation of the Phe in loop B to a tryptophan (Trp) resulted in a channel that was slightly less sensitive to ACh, with an  $EC_{50}$  value of  $72 \pm 4 \mu\text{M}$  ( $n = 5$ ) (Fig. 6B). Replacement of Trp at position 248 had a much larger negative impact on the channel, with  $EC_{50}$  values for ACh of  $7854 \pm 275 \mu\text{M}$  ( $n = 5$ ) and  $5600 \pm 1258 \mu\text{M}$  ( $n = 6$ ) for W248Y and W248F, respectively (Fig. 6B). These two mutants did not respond to any of the other compounds at the concentrations tested. The double swap mutation (F200W/W248F) resulted in a channel that was no longer responsive to ACh nor the other compounds (Table 1).

Both the F200Y and F200W single mutants were further characterized using the other agonists listed in Fig. 3A. The F200Y mutation was up to 9-fold more sensitive to all compounds listed, whereas the F200W mutation was up to 7-fold less sensitive (Fig. 7). It appears that both ACh and urecholine were most affected by the F200Y mutation whereas methacholine was most affected by F200W. On the other hand, the sensitivity of the anthelmintic pyrantel was only minimally affected by the two mutations. The resulting  $EC_{50}$  values for each compound is outlined in Table 1. The two Trp mutants, W248Y and W248F, did not respond to any of the other agonists (Table 1). Similarly the double mutant F200W/W248F did not respond to any of the agonists tested (Table 1).

### 3.6. Nicotine activates Hco-ACC-2 F200Y

The Hco-ACC-2 WT channel responded to nicotine at concentrations above 500  $\mu\text{M}$ . It should be noted that some un-injected oocytes showed a small increase in current when exposed to 500  $\mu\text{M}$  nicotine (Data not shown). Therefore, while we believe that the WT channel does respond to high concentrations of nicotine we did not determine an  $EC_{50}$ .

However, since the F200Y mutant responded to lower concentrations of nicotine we conducted dose response experiments which revealed an  $EC_{50}$  of  $277 \pm 8 \mu\text{M}$  ( $n = 5$ ) (Fig. 8B). Nicotine was docked in the binding pocket and its quaternary amine was situated 4 Å away from the center of the W248 benzene ring (Fig. 8A). The N2 quaternary amine in nicotine was 5.5 Å from the F200.

## 4. Discussion

We have identified a member of the ACC-1 family in the parasitic nematode *H. contortus* and investigated its binding site using site-directed mutagenesis, homology modelling and pharmacological analysis. This family of receptors appear to be unique to invertebrates and not present in mammals, making them attractive targets for novel nematocides. This has been validated by research demonstrating that this family of receptors are expressed in tissues that are sensitive to anthelmintic action (Wever et al., 2015). The research described here has examined in detail the structure of the ACC binding site which is important for future research focused on the discovery of novel therapeutics.

The pharmacology of the Hco-ACC-2 receptor can provide some valuable insight into the nature of the binding site. In our analysis, the receptor is least sensitive to choline. The low sensitivity of the receptor to choline is likely due to the molecules smaller size and lack of a carbonyl group which limits its interaction with residues. These features could explain why, compared to the other agonists, there was very little change in sensitivity of choline in the hypersensitive mutant F200Y. Moreover, the comparison between the sensitivities of ACh, carbachol, methacholine and urecholine along with the molecular docking results highlights some interesting trends. For example, all molecules docked with their quaternary amine close to W248. However, both ACh and methacholine, which exhibited maximum efficacy, appear to dock in a similar extended orientation, which places them within 3 Å of N170. On the other hand, carbachol and urecholine, which are both partial agonists, dock in a similar bent orientation, which is more pronounced in urecholine, and places them further away from N170.

One of the key features of ACh binding to mammalian nAChR is the presence of a tryptophan residue that participates in  $\pi$ -cationic interactions with the quaternary amine on ACh. In mammalian nAChRs this tryptophan residue is present in loop B (Beene et al., 2002). However, in ACC receptors there is no tryptophan residue in loop B. Instead, sequence analysis and homology modelling reveal a tryptophan residue present in loop C (W248). W248 is facing into the binding pocket and appears to be within 5 Å of the quaternary amine of the agonists that were docked in this study. While we did not confirm that W248 is participating in a  $\pi$ -cationic interaction with agonists, it is clear that it is essential for the function of Hco-ACC-2. Evidence for the importance of W248 in the function of ACC receptors is highlighted by mutational analysis, which showed that changing W248 to either W248Y or W248F resulted in a severely impacted receptor that did not respond to any agonists other than ACh. This could be partially explained by the removal of the indole nitrogen which is found in tryptophan. The presence of an indole nitrogen causes a large negative electrostatic cloud around this residue, allowing for increased potential of  $\pi$ -cationic interactions (Mecozzi et al., 1996). Since this indole is not present in tyrosine or phenylalanine, it could explain why these mutations were detrimental to receptor function. In addition, the positioning of this tryptophan in loop C could be important in ACC receptor function, as swapping the residues from loop C to B (F200W/W248F) produced a non-functional channel. This phenomenon is reminiscent of the novel nematode 5-HT receptor MOD-1 which also has a tryptophan residue in loop C instead of loop B, as seen in 5-HT<sub>3</sub> receptors (Ranganathan et al., 2000). The loop C tryptophan in the MOD-1 receptor was shown to participate in the essential  $\pi$ -cationic interaction with serotonin which is key for receptor binding (Mu et al., 2003). Interestingly, this loop C

tryptophan is not only present in ACC and MOD-1 receptors but other amine-gated chloride channels such as LGC-55 (tyramine) (Rao et al., 2010) and LGC-53 (dopamine) (Beech et al., 2013) as well as the nematode DEG-3 receptor (Fig. 3). From, an evolutionary perspective it appears that the presence of a tryptophan in loop C is an essential requirement for a diverse array of nematode cys-loop receptors, and their ability to bind to wide range of ligands.

Unlike mammalian nAChRs which exhibit a tryptophan in loop B, the Hco-ACC-2 receptor exhibits a phenylalanine (F200). Mutations at this position provided some additional insight into the structure of the ACC binding site. First, the introduction of a F200W change caused a reduced sensitivity to all agonists, albeit to varying degrees. Carbachol was the least affected by the change while methacholine was most affected. Methacholine is a full agonist for the ACC receptor and differs from ACh with the addition of a methyl group in the backbone, but both appear to bind in a similar orientation in the wildtype receptor. The addition of a bulky tryptophan residue may therefore cause the larger methacholine to shift orientation and reducing its ability to bind and activate the channel. Interestingly, the opposite was found with the F200Y mutation, which increased the sensitivity of all agonists (including nicotine) to varying degrees. Here, urecholine exhibited the highest increase in sensitivity. It is possible the hydroxyl group on tyrosine allows additional hydrogen-bond interactions with surrounding residues, thus changing the structure of the binding site and enhancing agonist (especially urecholine) binding. F200 may also have other roles such as participating in  $\pi$ -cationic interactions with agonists. However, future experiments would have to confirm.

The ACC receptor family appear to be attractive targets for the development of novel anthelmintics. With this in mind we also tested the activity of the anthelmintics levamisole and pyrantel which activate the nematode nAChR (Martin and Robertson, 2007). We found both molecules were partial agonists for the Hco-ACC-2 receptor. However, we were surprised to observe that the mutations we introduced into the receptor minimally effected in their activity. This may highlight the distinct manner at which these anthelmintics bind to the ACC receptors. Molecular models for docked pyrantel and levamisole place both molecules within 5 Å of W248. However, the overall positioning of levamisole and pyrantel within the ACC-2 binding site are clearly different (Fig. 5). How this relates to the differences in efficacy we observed between the two molecules requires further examination.

This study has described the isolation of a member of the ACC family from *H. contortus* and examined two residues in the binding site that are important for agonist recognition. Further research on the essential requirements for agonist recognition of ACC receptor can provide insight into the evolution of cholinergic neurotransmission and may possibly lead to the discovery of novel cholinergic anthelmintics.

## Declarations of interest

None.

## Acknowledgements

This research was funded by grants from Natural Sciences and Engineering Research Council of Canada (Grant #210290) and the Canadian Foundation for Innovation to SGF. The authors declare no conflicts of interest.

## References

Abdelmassih, S.A., Cochrane, E., Forrester, S.G., 2018. Evaluating the longevity of surgically extracted *Xenopus laevis* oocytes for the study of nematode ligand-gated ion channels. *Invertebr. Neurosci.* 18, 1.

Bamber, B.A., Beg, A.A., Twyman, R.E., Jorgensen, E.M., 1999. The *Caenorhabditis elegans* unc-49 locus encodes multiple subunits of a heteromultimeric GABA receptor. *J. Neurosci.* 19, 5348–5359.

Beech, R.N., Callanan, M.K., Rao, V.T.S., Dawe, G.B., Forrester, S.G., 2013.

Characterization of cys-loop receptor genes involved in inhibitory amine neurotransmission in parasitic and free living nematodes. *Parasitol. Int.* 62, 599–605.

Beene, D.L., Brandt, G.S., Zhong, W., Zacharias, N.M., Lester, H.A., Dougherty, D.A., 2002. Cation- $\pi$  interactions in ligand recognition by serotonergic (5-HT<sub>3A</sub>) and nicotinic acetylcholine receptors: the anomalous binding properties of nicotine. *Biochemistry* 41, 10262–10269.

Beene, D.L., Price, K.L., Lester, H.A., Dougherty, D.A., Lummis, S.C.R., 2004. Tyrosine residues that control binding and gating in the 5-hydroxytryptamine<sub>3</sub> receptor revealed by unnatural amino acid mutagenesis. *J. Neurosci.* 24, 9097–9104.

Boulin, T., Fauvin, A., Charvet, C.L., Cortet, J., Cabaret, J., Bessereau, J., Neveu, C., 2011. Functional reconstitution of *Haemonchus contortus* acetylcholine receptors in *Xenopus* oocytes provides mechanistic insights into levamisole resistance. *Br. J. Pharmacol.* 164, 1421–1432.

Del Castillo, J., Morales, T.A., Sanchez, V., 1963. Action of piperazine on the neuromuscular system of *Ascaris lumbricoides*. *Nature* 200, 706.

Cully, D.F., Vassilatis, D.K., Liu, K.K., Pares, P.S., Van der Ploeg, L.H., Schaeffer, J.M., et al., 1994. Cloning of an avermectin-sensitive glutamate-gated chloride channel from *Caenorhabditis elegans*. *Nature* 371, 707.

Van Doren, K., Hirsh, D., 1988. Trans-spliced leader RNA exists as small nuclear ribonucleoprotein particles in *Caenorhabditis elegans*. *Nature* 335, 556.

Dougherty, D.A., 1996. Cation- $\pi$  interactions in chemistry and biology: a new view of benzene, Phe, Tyr, and Trp. *Science* 80 (271), 163.

Frohman, M.A., Dush, M.K., Martin, G.R., 1988. Rapid production of full-length cDNAs from rare transcripts: amplification using a single gene-specific oligonucleotide primer. *Proc. Natl. Acad. Sci. Unit. States Am.* 85, 8998–9002.

Hibbs, R.E., Gouaux, E., 2011. Principles of activation and permeation in an anion-selective Cys-loop receptor. *Nature* 474 (7349), 54–60.

Jensen, M.L., Timmermann, D.B., Johansen, T.H., Schousboe, A., Varming, T., Ahning, P.K., 2002. The  $\beta$  subunit determines the ion selectivity of the GABA<sub>A</sub> receptor. *J. Biol. Chem.* 277, 41438–41447.

Jones, A.K., Sattelle, D.B., 2008. The cys-loop ligand-gated ion channel gene superfamily of the nematode, *Caenorhabditis elegans*. *Invertebr. Neurosci.* 8, 41–47.

Keheoe, J., McIntosh, J.M., 1998. Two distinct nicotinic receptors, one pharmacologically similar to the vertebrate  $\alpha 7$ -containing receptor, mediate Cl<sup>-</sup> currents in *Aplysia* neurons. *J. Neurosci.* 18, 8198–8213.

Kusano, K., Miledi, R., Stinnakre, J., 1982. Cholinergic and catecholaminergic receptors in the *Xenopus* oocyte membrane. *J. Physiol.* 328, 143–170.

Laing, R., Kikuchi, T., Martinelli, A., Tsai, I.J., Beech, R.N., Redman, E., et al., 2013. The genome and transcriptome of *Haemonchus contortus*, a key model parasite for drug and vaccine discovery. *Genome Biol.* 14, R88.

Lynagh, T., Pless, S.A., 2014. Principles of agonist recognition in Cys-loop receptors. *Front. Physiol.* 24 (5), 160.

Martin, R.J., Robertson, A.P., 2007. Mode of action of levamisole and pyrantel, anthelmintic resistance, E153 and Q57. *Parasitology* 134, 1093–1104.

Mecozzi, S., West Jr., A.P., Dougherty, D.A., 1996. Cation- $\pi$  interactions in aromatics of biological and medicinal interest: electrostatic potential surfaces as a useful qualitative guide. *Proc. Natl. Acad. Sci. U. S. A.* 93 (20), 10566–10571.

Morales-Perez, C.L., Noviello, C.M., Hibbs, R.E., 2016. X-ray structure of the human  $\alpha 4\beta 2$  nicotinic receptor. *Nature* 538, 411.

Mu, T.-W., Lester, H.A., Dougherty, D.A., 2003. Different binding orientations for the same agonist at homologous receptors: a lock and key or a simple wedge? *J. Am. Chem. Soc.* 125, 6850–6851.

Ortells, M.O., Lunt, G.G., 1995. Evolutionary history of the ligand-gated ion-channel superfamily of receptors. *Trends Neurosci.* 18, 121–127.

Pettersen, E.F., Goddard, T.D., Huang, C.C., Couch, G.S., Greenblatt, D.M., Meng, E.C., et al., 2004. UCSF Chimera—a visualization system for exploratory research and analysis. *J. Comput. Chem.* 25, 1605–1612.

Pirri, J.K., McPherson, A.D., Donnelly, J.L., Francis, M.M., Alkema, M.J., 2009. A tyramine-gated chloride channel coordinates distinct motor programs of a *Caenorhabditis elegans* escape response. *Neuron* 62, 526–538.

Putrenko, I., Zakikhani, M., Dent, J.A., 2005. *J. Biol. Chem.* 280, 6392–6398.

Ranganathan, R., Cannon, S.C., Horvitz, H.R., 2000. MOD-1 is a serotonin-gated chloride channel that modulates locomotory behaviour in *C. elegans*. *Nature* 408, 470–475.

Rao, V.T.S., Accardi, M.V., Siddiqui, S.Z., Beech, R.N., Prichard, R.K., Forrester, S.G., 2010. Characterization of a novel tyramine-gated chloride channel from *Haemonchus contortus*. *Mol. Biochem. Parasitol.* 173, 64–68.

Šali, A., Blundell, T.L., 1993. Comparative protein modelling by satisfaction of spatial restraints. *J. Mol. Biol.* 234, 779–815.

Siddiqui, S.Z., Brown, D.D.R., Rao, V.T.S., Forrester, S.G., 2010. An UNC-49 GABA receptor subunit from the parasitic nematode *Haemonchus contortus* is associated with enhanced GABA sensitivity in nematode heteromeric channels. *J. Neurochem.* 113, 1113–1122.

Sine, S.M., Engel, A.G., 2006. Recent advances in Cys-loop receptor structure and function. *Nature* 440, 448–455.

Trott, O., Olson, A.J., 2010. AutoDock Vina: improving the speed and accuracy of docking with a new scoring function, efficient optimization, and multithreading. *J. Comput. Chem.* 31, 455–461.

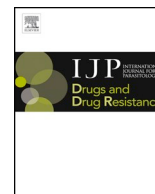
Weston, D., Patel, B., Van Voorhis, W.C., 1999. Virulence in *Trypanosoma cruzi* infection correlates with the expression of a distinct family of sialidase superfamily genes. *Mol. Biochem. Parasitol.* 98, 105–116.

Wever, C.M., Farrington, D., Dent, J.A., 2015. The validation of nematode-specific acetylcholine-gated chloride channels as potential anthelmintic drug targets. *PLoS One* 10, e0138804.

Zhang, J., Xue, F., Chang, Y., 2008. Structural determinants for antagonist pharmacology that distinguish the  $\rho 1$  GABAC receptor from GABA<sub>A</sub> receptors. *Mol. Pharmacol.* 74, 941–951.

## Appendix 3: Chapter III

### A3.1: Manuscript II



## Investigating the function and possible biological role of an acetylcholine-gated chloride channel subunit (ACC-1) from the parasitic nematode *Haemonchus contortus*



Micah K. Callanan<sup>a,1</sup>, Sarah A. Habibi<sup>a,1</sup>, Wen Jing Law<sup>b</sup>, Kristen Nazareth<sup>a</sup>, Richard L. Komuniecki<sup>b</sup>, Sean G. Forrester<sup>a,\*</sup>

<sup>a</sup> Faculty of Science, University of Ontario Institute of Technology, 2000, Simcoe Street North, Oshawa, ON, L1H 7K4, Canada

<sup>b</sup> Department of Biological Sciences, University of Toledo, Toledo, OH, 43606, USA

### ARTICLE INFO

#### Keywords:

Cholinergic receptor

Cys-loop

Ligand-gated chloride channel

Pharynx

*Haemonchus contortus*

### ABSTRACT

The cys-loop superfamily of ligand-gated ion channels are well recognized as important drug targets for many invertebrate specific compounds. With the rise in resistance seen worldwide to existing anthelmintics, novel drug targets must be identified so new treatments can be developed. The acetylcholine-gated chloride channel (ACC) family is a unique family of cholinergic receptors that have been shown, using *Caenorhabditis elegans* as a model, to have potential as anti-parasitic drug targets. However, there is little known about the function of these receptors in parasitic nematodes. Here, we have identified an *acc* gene (*hco-acc-1*) from the sheep parasitic nematode *Haemonchus contortus*. While similar in sequence to the previously characterized *C. elegans* ACC-1 receptor, Hco-ACC-1 does not form a functional homomeric channel in *Xenopus* oocytes. Instead, co-expression of Hco-ACC-1 with a previously characterized subunit Hco-ACC-2 produced a functional heteromeric channel which was 3x more sensitive to acetylcholine compared to the Hco-ACC-2 homomeric channel. We have also found that Hco-ACC-1 can be functionally expressed in *C. elegans*. Overexpression of both *cel-acc-1* and *hco-acc-1* in both *C. elegans* N2 and *acc-1* null mutants decreased the time for worms to initiate reversal avoidance to octanol. Moreover, antibodies were generated against the Hco-ACC-1 protein for use in immunolocalization studies. Hco-ACC-1 consistently localized to the anterior half of the pharynx, specifically in pharyngeal muscle tissue in *H. contortus*. On the other hand, expression of Hco-ACC-1 in *C. elegans* was restricted to neuronal tissue. Overall, this research has provided new insight into the potential role of ACC receptors in parasitic nematodes.

### 1. Introduction

*Haemonchus contortus* is a pathogenic gastrointestinal parasitic nematode that causes severe livestock damage worldwide, particularly in the sheep industry. The disease, known as haemonchosis, leads to severe symptoms in host ruminants including anemia and death (Besier et al., 2016). Traditionally, *H. contortus* is controlled with broad spectrum anthelmintic chemotherapeutics that target different proteins within the parasite. There are multiple classes of these drugs that target cys-loop ligand-gated ion channels, including macrocyclic lactones which specifically target glutamate-gated chloride channels (GluCls) (Forrester et al., 2003; McCavera et al., 2009; Glendinning et al., 2011) and nicotinic acetylcholine receptor (nAChR) agonists such as pyrantel and levamisole (Boulin et al., 2011; Duguet et al., 2016; Blanchard

et al., 2018). Macrocyclic lactones have also been shown to interact with nematode cys-loop GABA receptors (Accardi et al., 2012; Hernando and Bouzat, 2014). There is global concern about the increase in drug resistant populations of *H. contortus* in the field, including documented resistance to more recently developed drugs such as monepantel and derquantel (Raza et al., 2016). This information drives the need for the discovery of novel anthelmintic targets that could be used for the rational design or screening of new and effective anthelmintics.

The cys-loop ligand-gated chloride channel (LGCC) family of receptors is a very attractive group of proteins for drug-target discovery. Information from the *H. contortus* genome suggests that this family of receptors has approximately 35 genes that encode various subunits (Laing et al., 2013). However, approximately half of these potential

\* Corresponding author.

E-mail address: [sean.forrester@uoit.ca](mailto:sean.forrester@uoit.ca) (S.G. Forrester).

<sup>1</sup> Joint first authors.

channels have no confirmed ligand. In addition, many of these channels are either not present in mammals or are sufficiently divergent, suggesting the potential to develop highly specific drugs that will not target host receptors (Laing et al., 2013). However, of the 35 possible LGCC targets in the *H. contortus* genome it is likely that only a subset could be developed as targets for broad-spectrum anthelmintics. This is because the genomes of other parasitic nematodes, particularly human pathogens, appear to contain a significantly lower number of *lgcc* genes with some groups of channels being absent (Williamson et al., 2007; Beech et al., 2013). In addition, several LGCCs are likely to have functions that have no real consequence to the parasite if targeted. Therefore, the most attractive LGCCs from an anthelmintic discovery point of view are those present in a broad range of parasitic nematodes, have a function in the parasitic stage that if bound by an anthelmintic would lead to death or expulsion of the parasite and are not similar to host receptors (Wever et al., 2015). The latter point can be achieved by either targeting unique nematode-specific families of receptors or similar receptors that exhibit unique binding sites for potential drugs.

Previous research has suggested that the acetylcholine-gated chloride channels (ACCs) in *Caenorhabditis elegans* (Putrenko et al., 2005) exhibit the characteristics of promising drug targets. The genes that encode the various subunits of this family are present across the nematode phylum and appear to have fairly broad function in the nematode nervous system (Wever et al., 2015). One of the channels, Cel-ACC-1 exhibits a pharmacology distinct from mammalian cys-loop acetylcholine channels and appears in *C. elegans* to be localized to ventral cord and extrapharyngeal neurons (Wever et al., 2015). Due to their broad role in the *C. elegans* nervous system, the ACC family of receptors appear to be promising targets for effective anthelmintic action against parasitic nematodes (Wever et al., 2015). However, directly extrapolating results from *C. elegans* to parasitic nematodes should be done with caution since the expression patterns of individual LGCCs have been shown in some cases to be different (Portillo et al., 2003).

Here we have isolated a member of the ACC family (Hco-ACC-1) from the parasitic nematode *H. contortus*. Electrophysiological examination revealed that while Hco-ACC-1 does not form a functional homomeric channel in *Xenopus* oocytes, co-expression with a previously characterized subunit (Hco-ACC-2) can form a channel highly sensitive to acetylcholine and carbachol. The ACC-1/2 heteromeric channel was 3x more sensitive to acetylcholine compared to the ACC-2 homomeric channel. When expressed in *C. elegans*, *hco-acc-1*, localizes to pharyngeal neurons and enhances reversal avoidance to octanol demonstrating that *hco-acc-1* can function *in vivo*. In *H. contortus*, ACC-1 may play an essential role in the pharynx as immunolocalization revealed expression in a specific region of the pharyngeal muscle. Overall, this research has provided some novel insight into the possible role of ACC receptors in parasitic nematodes.

## 2. Materials and methods

### 2.1. RNA/cDNA

Total RNA was isolated using Trizol (Invitrogen, Carlsbad, USA) from adult *H. contortus* strain PF23. cDNA was synthesized using the Quantitect Reverse Transcription kit from Qiagen (Dusseldorf, Germany) using a unique 3' anchor sequence primer (5'CCTCTGAAG-GTTCACGGATCCACATCTAGATTTTTTTTTTTTTTTTTTTVN3'); [where V is either A, C, or G and N is either A, C, G, or T] (Weston et al., 1999). The partial *H. contortus* sequence of *acc-1* was initially identified by the Sanger Institute (Cambridge, UK) and used for the creation of gene specific primers. These primers were used in the 5' and 3' rapid amplification of cDNA ends (RACE) protocol (Frohman et al., 1988).

### 2.2. Isolation of *hco-acc-1* and sequence analysis

The 5' end of the *hco-acc-1* gene was amplified using two internal

*hco-acc-1* specific antisense primers [NESTED PRIMER 5' GTTGTCCA AAGCACCTGTGG 3'] and a primer specific for splice leader – 1 sequence (SL1-5'GGTTTAATTACCCAAGTTTGAG3') (Van Doren and Hirsh, 1988) in a PCR using the PTC-100 Programmable Thermal Controller (MJ Research, Inc, Waltham, MA, USA). For the 3' end, two *hco-acc-1* gene specific primers [NESTED PRIMER – 5'GTGACTTACTG GAGCTACTAC 3'] and two primers specific for the 3' oligo-dT anchor sequence were used in a nested PCR reaction. Each amplicon of a predicted size was isolated via gel extraction and subcloned into the pGEMT easy™ vector and sequenced. Amplification of the complete *hco-acc-1* gene was conducted using primers designed targeting 5' and 3' untranslated region. This amplicon was subcloned and sequenced to achieve a consensus sequence. Sequence alignments were produced using ClustalW.

For phylogenetic analysis of the nematode ACC subunit family, the most highly conserved regions of the ligand-binding domain and membrane-spanning regions 1–3 (144 amino acids) were aligned using ClustalW and inputted into PhyML 3.0 to create a phylogenetic tree with 100 bootstrap repetitions. The final formatted tree was produced using FigTree v1.4.3.

### 2.3. Expression in *Xenopus* oocytes

All animal procedures followed the University of Ontario Institute of Technology Animal Care Committee and the Canadian Council on Animal Care guidelines and according to methods outlined in Abdelmassih et al., (2018). *Xenopus laevis* frogs (all female) were supplied by Nasco (Fort Atkinson, WI, USA). The frogs were housed in a room, which was climate controlled, light cycled, and stored in tanks which were regularly cleaned. Frogs were anesthetized with 0.15% 3-aminobenzoic acid ethyl ester methanesulphonate salt (MS-222) buffered with NaHCO<sub>3</sub> to pH 7 (Sigma-Aldrich, Oakville, ON, CA). Surgical removal of a section of the ovary of the frog was performed, and the lobe was defolliculated with a calcium-free oocyte Ringer's solution (82 mM NaCl, 2 mM KCl, 1 mM MgCl<sub>2</sub>, 5 mM HEPES pH 7.5 (Sigma-Aldrich)) (OR-2) containing 2 mg/mL collagenase-II (Sigma-Aldrich). The oocytes in the defolliculation solution were incubated at room temperature for 2 h. Collagenase was washed from the oocytes with ND96 solution (1.8 mM CaCl<sub>2</sub>, 96 mM NaCl, 2 mM KCl, 1 mM MgCl<sub>2</sub>, 5 mM HEPES pH 7.5) and allowed 1 h to recover at 18 °C in ND96 supplemented with 275 µg mL<sup>-1</sup> pyruvic acid (Sigma-Aldrich) and 100 µg mL<sup>-1</sup> of the antibiotic gentamycin (Sigma-Aldrich). Stage V and VI oocytes were selected for cytoplasmic injection of cRNA.

The coding sequence of *hco-acc-1* and *hco-acc-2* (Habibi et al., 2018) was subcloned into the *X. laevis* expression vector pGEMHE (Zhang et al., 2008). The vector was linearized using the restriction enzyme *Pst*I (New England Biolabs, USA), and used as template for an *in vitro* transcription reaction (T7 mMessage mMachine kit, Ambion, Austin, TX, USA) yielding *hco-acc-1* and *hco-acc-2* copy RNA. *X. laevis* oocytes were injected with 50 nl of *hco-acc-1* (0.5 ng/nL), *hco-acc-2* (0.5 ng/nL) or *hco-acc-1/2* (0.25 ng/nl each) using the Drummond (Broomall, PA, USA) Nanoject microinjector. Oocytes were also co-injected with the copy RNA encoding three accessory proteins, *hco-unc-50*, *hco-unc-74*, and *hco-ric-3.1* (Boulin et al., 2011) which were gifts from Dr. Cédric Neveu (INRA). The injected oocytes were incubated at 18 °C in ND96 (96 mM NaCl, 2 mM KCl, 1 mM MgCl<sub>2</sub>, 1.8 mM CaCl<sub>2</sub>, 5 mM HEPES pH 7.5) supplemented with 0.275 µg/mL pyruvate and 50 µg/mL gentamycin. Electrophysiological recordings of the oocytes were conducted between 48 and 72 h after cRNA injection.

### 2.4. Electrophysiological recordings

The Axoclamp 900A voltage clamp (Molecular Devices, Sunnyvale, CA, USA) was used to conduct two electrode voltage clamp electrophysiology. Glass electrodes were produced using a P-97 Micropipette Puller (Sutter Instrument Co., Novato, CA, USA). The electrodes were

backfilled with 3M KCl and contained Ag|AgCl wires, and electrodes with resistances of 1–8 MΩ were selected for recordings. All oocytes were clamped at –60 mV for the entirety of the experiments. Acetylcholine and carbamylcholine (Sigma- Aldrich) were first dissolved in ND96. The resultant solutions were perfused over oocytes using the RC-1Z recording chamber (Warner Instruments Inc., Hamdan, CT, USA). Data was subsequently analyzed using Clampex Software v10.2 (Molecular Devices) and all graphs were generated using Graphpad Prism Software v5.0 (San Diego, CA, USA). Acetylcholine and carbamylcholine (carbachol) EC<sub>50</sub> values were determined by dose response curves which had been fitted to the equation:

$$I_{max} = \frac{1}{1 + \left(\frac{EC_{50}}{D}\right)^h}$$

Where  $I_{max}$  is the maximal response, EC<sub>50</sub> is the concentration of compound required to elicit 50% of the maximal response, [D] is compound concentration, and  $h$  is the Hill coefficient. Both EC<sub>50</sub> and  $h$  are free parameters, and the curves were normalized to the estimated  $I_{max}$ . Graphpad prism used the equation to fit a sigmoidal curve of variable slopes to the data. Dose-response curves comparing Hco-ACC-2 and Hco-ACC-1/2 were conducted in the same week and with the same batch of eggs. Means were determined from at least 4 oocytes from at least two batches of oocytes.

## 2.5. In silico modelling

The protein sequences of Hco-ACC-1 and 2 was aligned to the recently crystalized alpha-1 glycine receptor (3jad) from *Danio rerio* for use in MODELLER v9.15 (Sali and Blundell, 1993) for the generation of the hypothetical Hco-ACC-1/2 heteromeric dimer. The associated DOPE score determined the most energetically favorable model. Preparation of the heteromer for agonist docking was carried out using AutoDock Tools (Morris et al., 2009). ACh and carbachol were obtained from the Zinc database in their energy-reduced form (Irwin et al., 2012). AutoDock Vina (Trott and Olson, 2010) was used to simulate docking of each ligand to the Hco-ACC-1/2 heteromer. Pymol was used to visualize the protein heterodimer with its associated ligand docking, and Chimera v1.6.1 (Pettersen et al., 2004) was used to determine the distance between amino acid residues and ligands.

## 2.6. Immunolocalization in *H. contortus*

Two peptides specific for a portion of the N-terminal region of the Hco-ACC-1 protein (ACC-1.1-YNKHYIPSHPTQVRVDM and ACC-1.2-YQPVQRSRPERNLLSAIRKW) were synthesized commercially and used to immunize two rabbits (21st Century Biochemicals, Marlboro, MA, USA). Peptides were conjugated to the carrier protein ovalbumin and its sequence was initially BLASTed against the *H. contortus* genome database and the NCBI general database to ensure specificity. Whole sera was collected from the animals and subjected to affinity purification using separate columns for each peptide to isolate and purify each antibody separately. Whole antisera was tested for specificity and titer against the immunogenic peptide by ELISA. For immunolocalization two strains of *H. contortus* were used, PF23 and MOF23. Both strains were derived from the same parental strain. However, the PF23 strain was generated by passage through sheep over 23 generations without anthelmintic treatment whereas MOF23 was generated by passage through sheep over 23 generations with increasing dosage of moxidectin at each generation. Further details of the strains can be found in Urdaneta-Marquez et al., (2014). Adult female *H. contortus* worms (strains PF23 and MOF23) were fixed, permeabilized and subsequently digested as previously described (Rao et al., 2009). Worms were subsequently washed 3 times with PBS, and incubated at 4 °C for 72 h with a 1/150 dilution of primary antibody diluted in 0.1% w/v BSA, 0.5% Triton X-100, and 0.05% sodium azide (Sigma) under slight shaking.

The removal of unbound antibodies was conducted by 4 washes of the worms with PBS and a final wash with PBS with 0.1% (v/v) Triton X-100 (PBST). Worms were then incubated at 4 °C with a 1/2000 dilution of Alexa Fluor 448<sup>®</sup> goat anti-rabbit IgG (H + L) secondary antibody for 24 h. Alexa Fluor 488<sup>®</sup> was used due its photostability and sensitivity to detect potentially low abundance proteins such as cys-loop LGCCs. Unbound secondary antibody was removed by 4 washes of the worms with PBS, and a final PBST wash. Worms were mounted on slides using Fluoromount™ Aqueous Mounting Medium (Sigma) and examined. Slides were examined using a Zeiss LSM710 confocal microscope (Carl Zeiss Inc., Canada) equipped with the Zeiss Zen 2010 software package. The lasers used for image acquisition were an Argon 488 nm, with the filter sets adjusted to minimize bleed-through due to spectral overlap.

Several controls were conducted including the omission of primary antibody, a pre-immune control (where 1/50 dilutions of pre-immune serum from experimental rabbits was applied instead of the purified primary antibody), and a peptide absorbed control, where an excess of peptide (50µg/ml) was added to the primary antibody dilution and incubated for 24 h at 4 °C before immunolocalization.

## 2.7. Expression of *acc-1* in *C. elegans*

All transgenic constructs were made by overlap fusion PCR (Hobert, 2002). *H. contortus* and *C. elegans acc-1* cDNAs were fused to *C. elegans acc-1* (5.3 kb) promoter. All transgenes contain sequence encoding a GFP marker (with an *unc-54* 3'-UTR) at the 3'-end of receptor cDNA. PCR products from multiple reactions were pooled and co-injected with coelomocyte-RFP as a screening marker into the appropriate backgrounds (Mello and Fire, 1995). Multiple transgenic lines from each construct were examined. Localization of GFP expression was performed using confocal microscopy.

Well-fed hermaphrodite fourth-stage *C. elegans* larvae carrying a coelomocyte RFP screening marker were picked 24 h prior to assay and incubated overnight at 20 °C. Fresh nematode growth medium (NGM) plates were prepared on the day of assay. Aversive responses were examined off food as described in Chao et al. (2004) and are presented as the time taken to initiate backward locomotion after the presentation of 30% 1-octanol on a hair in front of a forward moving animal.

## 3. Results

### 3.1. Hco-ACC-1 isolation and polypeptide analysis

The final consensus nucleotide product obtained through the RACE procedure was sequenced and shown to consist of 1380 nucleotides and assigned the GenBank accession number AHM25233.1. When translated in the appropriate reading frame, the sequence encodes for a protein containing 459 amino acids with the hallmark Cys-loop motif (Fig. 1a). Additionally, 4 hydrophobic transmembrane domains were identified along with a signal peptide cleavage site (Signal P; <http://www.cbs.dtu.dk/services/SignalP/>). The PAR motif (residues 266–268) was noted in the M2 transmembrane portion of the peptide, indicative of chloride ion selectivity (Jensen et al., 2005). The Hco-ACC-1 peptide shares an 89% similarity with the *C. elegans* ACC-1 subunit. A few key amino acid differences were noted in the major binding loops. Firstly, in ligand binding loop B, a tyrosine (Y178) was identified in the Hco-ACC-1 protein where a phenylalanine (F179) is seen in the analogous position in Cel-ACC-1. Secondly, there are two differences seen in binding loop F. In Hco-ACC-1 two positions P199 and Q201 align to R200 and E201 in Cel-ACC-1 (Fig. 1a). The functional consequences of these differences are not known. In addition, the amino acid sequence of Hco-ACC-1 is identical (except for amino acid 448) to an unnamed protein (CDJ86191.1) deposited to GenBank as part of the *H. contortus* genome sequencing project (Laing et al., 2013).

Using the crystal structure of the *Danio rerio* glycine receptor (PDB 3JAD), a homology model of the ACC receptor (dimer) was generated.



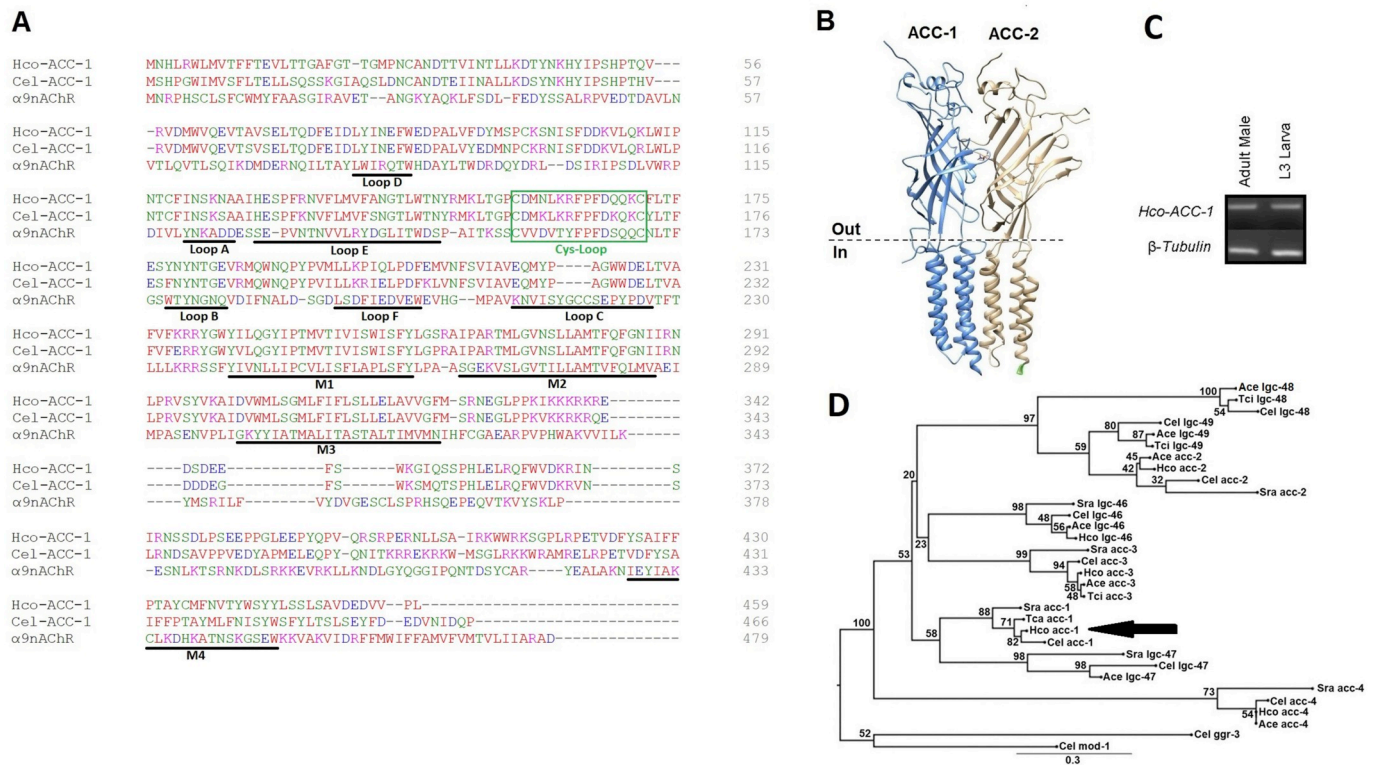


**Fig. 1.** Isolation of *hco-acc-1* and protein sequence analysis. **A.** Protein sequence alignment of *H. contortus* and *C. elegans* ACC-1 with the nAChR. Stars indicate regions of amino acid identity. Dashes represent no alignment between sequences while colons indicate similar amino acids. The 6 ligand binding loops (Loops A-F), 4 transmembrane regions (M1-M4) and the cys-loop are indicated. **B.** Homology model of a hypothetical receptor showing a dimer of Hco-ACC-1 and Hco-ACC-2 that was used for ligand-docking. **C.** End point PCR analysis of the *hco-acc-1* cDNA in the adult male and L3 larval stages of *H. contortus*. PCR reactions were simultaneously performed on the housekeeping gene  $\beta$ -tubulin. Replicate experiments showed a similar trend. No PCR products were detected in negative controls (including negative RT control). **D.** Phylogenetic analysis of the ACC family from various nematodes. Cel - *Caenorhabditis elegans* Hco - *Haemonchus contortus*; Tci - *Teladorsagia circumcincta*; Ace - *Ancylostoma ceylanicum*; Sra - *Strongyloides ratti*; Tca - *Toxocara canis*. Hco-ACC-1 is indicated by arrow.

This crystal structure was selected as template as it shares the highest homology with ACC-1 and 2 of the crystal structures currently in the protein database. A hypothetical heteromer was generated where Hco-ACC-1 was designated the primary subunit and Hco-ACC-2 the complementary subunit. Fig. 1B displays the best model (ie. with lowest DOPE and molpdf scores out of 50 possibilities). Acetylcholine was docked in a  $30 \times 30 \times 30 \text{ \AA}$  box centered between the primary and complementary subunits (between loops A, B and C of the primary and adjacent to loops D, E and F of the complementary subunit).

End-point PCR indicates that *hco-acc-1* is expressed in both the adult male and L3 stage (Fig. 1C) and phylogenetic analysis indicated that Hco-ACC-1 groups with other nematode ACC-1 subunits (Fig. 1D).

### 3.2. Functional characterization of *hco-ACC-1*

Oocytes injected with *hco-acc-1* cRNA alone did not respond to up to 1 mM ACh or carbachol. However, the same batches of oocytes injected with *hco-acc-2* cRNA responded readily to both ACh and carbachol (Fig. 2a and b) with  $EC_{50}$  values similar to those reported in Habibi et al. (2018) of  $19 \pm 1 \mu\text{M}$  ( $n = 5$ ) and  $46 \pm 2 \mu\text{M}$  ( $n = 5$ ), respectively (Fig. 2b). However, co-expression of *hco-acc-1* and 2 produced a channel significantly more sensitive to both ACh and carbachol with  $EC_{50}$  values of  $5.9 \pm 1 \mu\text{M}$  ( $p < 0.001$ ) ( $n = 6$ ) and  $32.5 \pm 3 \mu\text{M}$  ( $p = 0.04$ ) ( $n = 4$ ), respectively. Both the ACC-2 and ACC1/2 channels produced currents that were in the microamp range and desensitized. These responses were observed repeatedly in oocytes from different frogs, but was not seen in eggs injected with water. Current-voltage analysis of the Hco-ACC-1/2 heteromeric channel using full  $\text{Cl}^-$  ND96 (final concentration 103.6 mM  $\text{Cl}^-$ ) indicated a reversal potential of  $-17.7 \pm 5 \text{ mV}$  ( $n = 4$ ) (Fig. 2c) consistent with the calculated Nernst

potential for  $\text{Cl}^-$  of  $-18.5 \text{ mV}$ , assuming 50 mM internal  $\text{Cl}^-$  (Kusano et al., 1982). When NaCl was partially replaced with Na-gluconate in the ND96, the reversal potential shifted to  $-2.1 \pm 1 \text{ mV}$  ( $n = 3$ ), consistent with the predicted Nernst potential of  $-5.7 \text{ mV}$ .

### 3.3. Ligand docking analysis

Docking results clustered all 10 acetylcholine binding poses to the predicted binding location. The dock with the highest affinity ( $-5.4 \text{ kcal}$ ) is shown in Fig. 2d. The acetylcholine quaternary amine group was located directly between W225 (loop C) and Y178 (loop B). This quaternary amine was  $4.3 \text{ \AA}$  away from the center of the W225 aromatic ring suggesting the formation of single pi-cation bond with W225. Similarly, carbachol docked at a similar pose and its quaternary amine was  $4.6 \text{ \AA}$  away from W225 (Fig. 2e).

### 3.4. Immunolocalization

The application of anti-Hco-ACC-1 antibodies was performed on adult female *H. contortus* worms to determine the tissue expression of the ACC-1 protein. Worms from both the PF23 and MOF23 strains were successfully stained, with repeated staining over multiple batches of collected worms. The signal was identified consistently in pharyngeal muscle cells, in the anterior half of the pharynx in both strains (Fig. 3A–D). There were no obvious differences in the signal between *H. contortus* strains. The observed signal was robust and reconstructed stacks of slicing through the Z axis shows the triradiate organization of nematode pharyngeal muscle (supplemental movies 1 and 2). Peptide absorbed controls, pre-immune serum controls and no primary antibody controls displayed no signal beyond background (Fig. 3F and G).

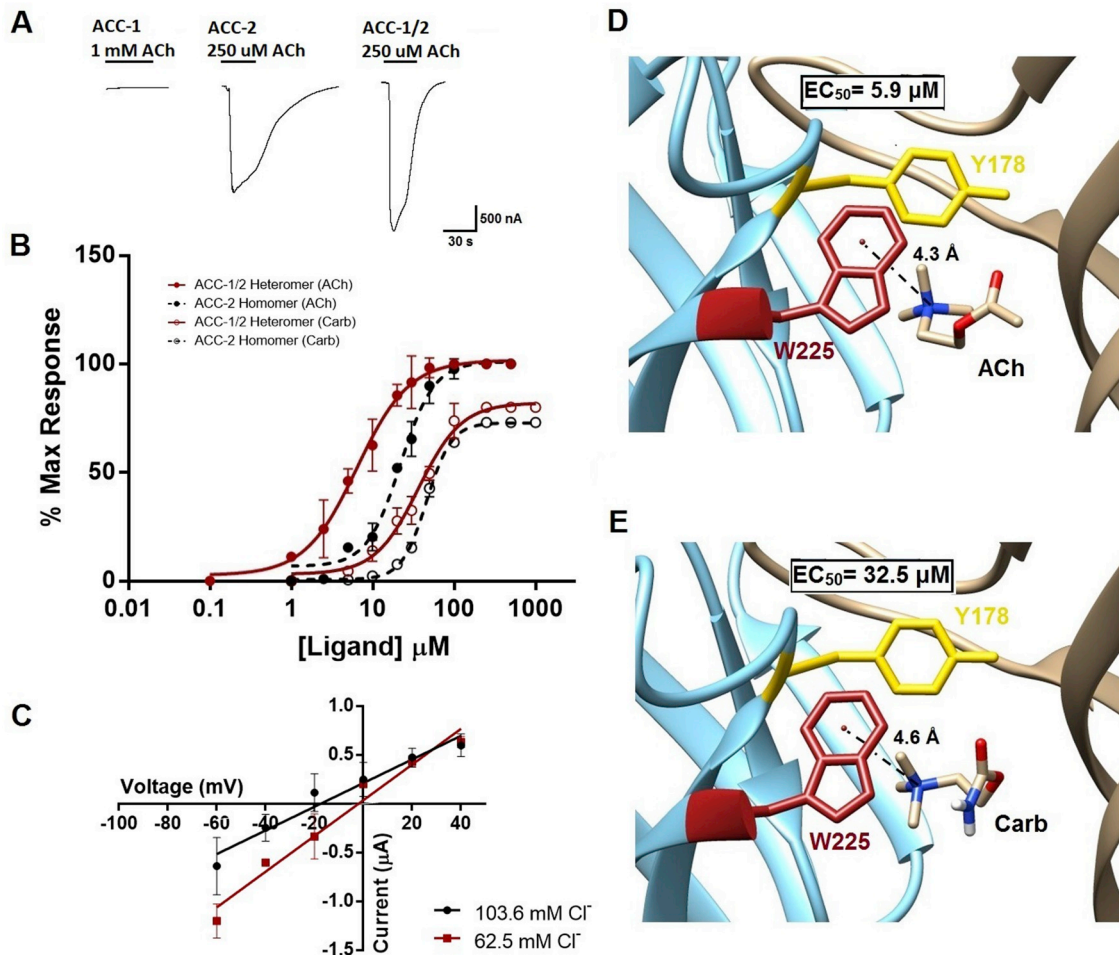


**Fig. 2.** Hco-ACC-1 and Hco-ACC-2 form a functional heteromeric receptor. **A.** Representative electrophysiological traces of the acetylcholine responses to oocytes expressing Hco-ACC-1 alone, Hco-ACC-2 alone and Hco-ACC-1 + 2. **B.** Dose response curves comparing the sensitivities of the Hco-ACC-2 channel and the Hco-ACC-1/2 channel to acetylcholine and carbachol. Each data point is a mean  $\pm$  SEM with  $n \geq 4$ . **C.** Current/Voltage relationship of the Hco-ACC-1/2 channel comparing full  $\text{Cl}^-$  ND96 (103.6 mM) partial  $\text{Cl}^-$  ND96 (62.5 mM). **D.** Ligand docking of acetylcholine to the Hco-ACC1/2 receptor shown the distance of the ligand to W225. **E.** Ligand docking of carbachol to the Hco-ACC-1/2 receptor shown the distance of the ligand to W225.

In addition, no autofluorescence was detected.

Supplementary video related to this article can be found at <https://doi.org/10.1016/j.ijpddr.2018.10.010>.

### 3.5. Expression of *hco-acc-1* in *C. elegans*

To determine whether *hco-acc-1* could function *in vivo* we expressed the gene in *C. elegans*. Aversive responses to 1-octanol have been studied extensively in *C. elegans* and are modulated by a complex locomotory circuit involving an array of sensory and interneurons (Komuniecki et al., 2012, 2014). Both *C. elegans* wild-type and *acc-1* null animals initiate aversive responses to 1-octanol in about 10 s, but the overexpression of either the *C. elegans* or *H. contortus acc-1* genes in wild type-animals, driven by 5.2 kb of the predicted *C. elegans acc-1* promoter, significantly decreased the time taken to initiate an aversive response (Fig. 4). Overexpression of the *H. contortus acc-1* in an *acc-1* null background yielded a similar result, confirming the putative orthology of the two proteins. Fluorescence from an *H. contortus acc-1::gfp* transgene, driven by the same *C. elegans acc-1* promoter was exclusively neuronal and limited to a small number of neurons in both the anterior (Fig. 5) and the posterior (supplemental Figure 1) ends of the worm, similar to published reports for the *C. elegans acc-1* (Pereira et al., 2015).

## 4. Discussion

Here we report the isolation and characterization of an acetylcholine-gated chloride channel from a parasitic nematode. Recently, Wever et al. (2015) provided evidence that the ACC family of receptors were potentially good anthelmintic targets in *C. elegans*. Here *avr-15* (encoding a GluCl subunit) under the control of *acc* promoters exhibited high level of sensitivity to ivermectin demonstrating that the ACC family of receptors function in what was referred to as “essential” tissues. In this case one of the essential tissues was extrapharyngeal neurons (Wever et al., 2015). Interestingly, while we did not observe the localization of Hco-ACC-1 in any neurons in *H. contortus* we consistently found this receptor in pharyngeal muscle tissue. It appears therefore that although ACC-1 localizes to different tissues in *H. contortus* compared to *C. elegans* they both appear to function in tissues that would be considered essential from the point of view of anthelmintic action.

The difference in the localization of ACC receptors between *C. elegans* and *H. contortus* resembles the situation observed with the ivermectin target, the GluCl. In *C. elegans*, GluCl subunits have been localized to pharyngeal muscle and various neurons (Dent et al., 1997, 2000; Laughton et al., 1997), but in *H. contortus*, the GluCl receptors localized thus far were found to be exclusively neuronal (Portillo et al., 2003). However, both nematodes are still very sensitive to ivermectin with respect to both locomotion and pharyngeal pumping (Dent et al., 1997; Wolstenholme, 2012). Here, we have found that Hco-ACC-1

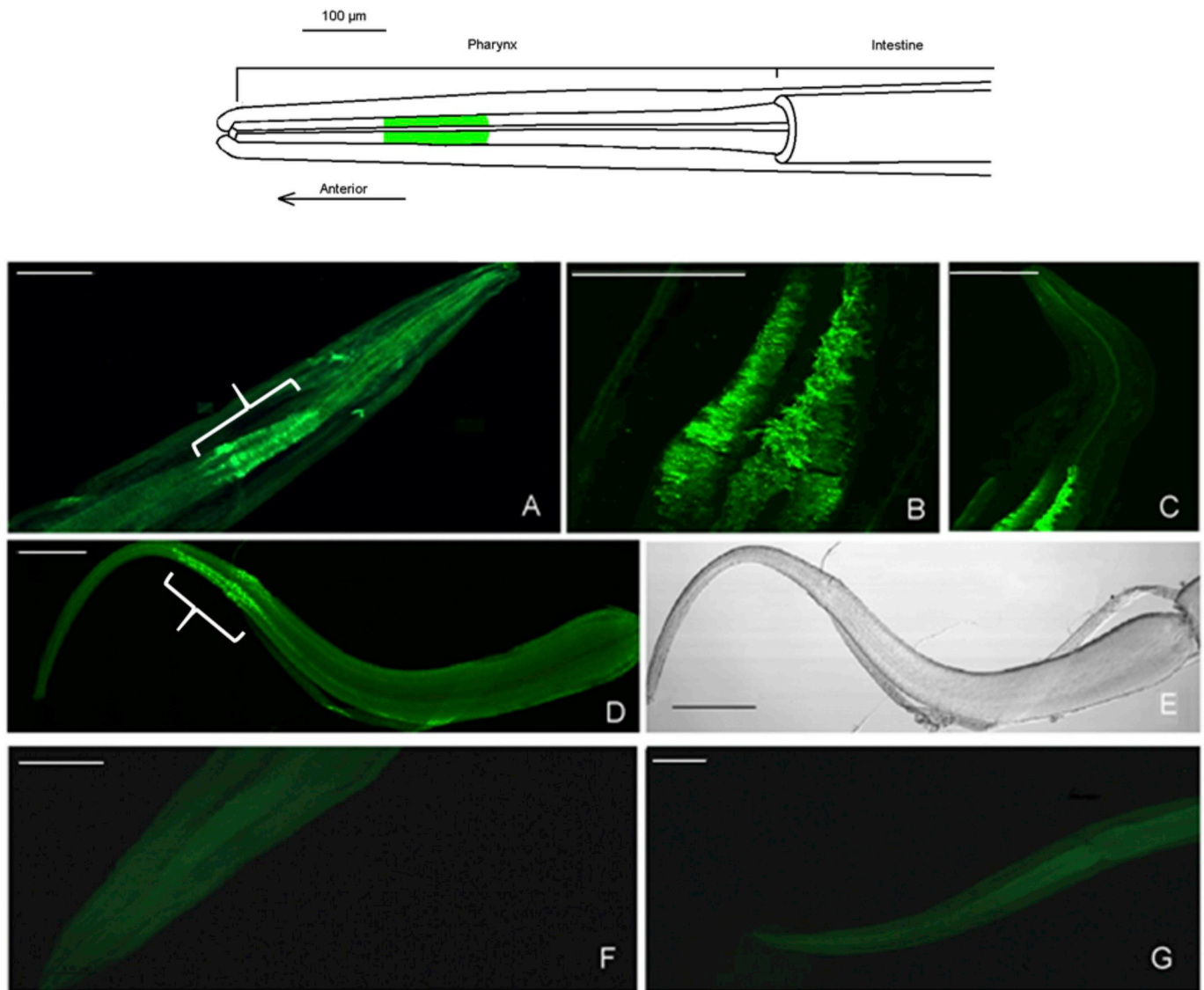


**Fig. 3.** Immunolocalization of Hco-ACC-1 in adult female *H. contortus* worms. A cartoon schematic of the anterior end of the female *H. contortus* adult nematode is shown at the top. Green denotes detected signal in the anterior half of the pharynx seen during immunolocalization experiments. A. 25x magnification of the anterior end of *H. contortus* PF23 strain. B. 40X magnification stack of 25 of 5 µm confocal slices of *H. contortus* PF23 focused on the anterior half of the pharyngeal muscle tissue. C. 25x magnification of a female adult *H. contortus* MOF23 parasite focusing on the anterior end of the worm. D. 25x magnification of isolated pharynx from a female *H. contortus* MOF23 adult worm. E. 25x magnification light micrograph of D. F. Pre-immune serum negative control of *H. contortus* PF23, 25x magnification focusing on anterior end of the worm. G. Peptide-absorbed control of *H. contortus* MOF23 at 10x magnification focusing on the anterior end of the worm. Lines denote 100 µm. (For interpretation of the references to colour in this figure legend, the reader is referred to the Web version of this article.)

localizes to pharyngeal muscle tissue in *H. contortus* but localizes to pharyngeal neurons in *C. elegans*. It is tempting to speculate that like the GluCl<sub>s</sub>, the ACCs family of receptors show different expression patterns but have some overlapping function between *H. contortus* and *C. elegans*. We are in the process of characterizing all additional ACC subunits from *H. contortus* to provide better insight into how conserved the function is between free-living and parasitic nematodes.

An additional difference in ACC-1 between *H. contortus* and *C. elegans* is the results from the oocyte expression experiments. Here we found that unlike Cel-ACC-1 that was reported to form a functional homomeric channel (Putrenko et al., 2005), Hco-ACC-1 does not. However, we have observed that in general the *hco-acc* genes do not express in oocytes as readily as other cyst-loop receptors we have examined in our laboratory. However, co-expression of Hco-ACC-1 and 2 yielded a channel 3x more sensitive to ACh ( $EC_{50}$  5.9 µM) compared to the Hco-ACC-2 homomeric channel. Differences in sensitivities between nematode homomeric and heteromeric channels have also been

observed in the UNC-49 GABA receptor (Bamber et al., 1999; Siddiqui et al., 2010) and the GluCl (Cully et al., 1994). Interestingly, we have found that changing loop B phenylalanine to a tyrosine in Hco-ACC-2 produced a hypersensitive channel with an  $EC_{50}$  of 2.9 µM (Habibi et al., 2018). In Hco-ACC-1 there is a naturally occurring tyrosine (Y178) at the analogous position which may partially explain why the ACC-1/2 heteromeric channel was more sensitive to ACh compared to the ACC-2 homomeric channel. The significance of this naturally occurring tyrosine in Hco-ACC-1 to the *in vivo* function of the receptor is unknown. Moreover, we are still uncertain whether Hco-ACC-1 requires co-expression with additional subunits *in vivo* and while we have found that ACC-1 can co-express with ACC-2 in oocytes we have been unsuccessful, thus far, in determining the tissue location of ACC-2. Thus, we do not know at this time whether Hco-ACC-1 and 2 assemble to form a functional channel *in vivo*. The oocyte experiments merely suggest that the assembly of ACC-1 and ACC-2 is possible.

Examination of the Hco-ACC-1 binding site using *in silico* modelling

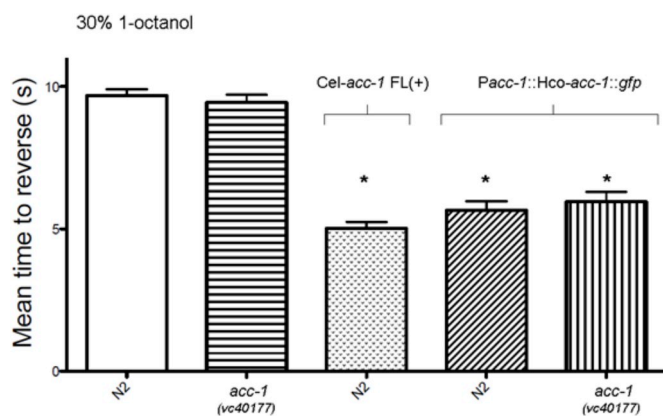


**Fig. 4.** Mean time to reverse of *C. elegans* in the presence of 30% octanol. N2, wild type; ACC-1 vc40177, Cel-ACC-1 knockout strain. PACC-1::ACC-1 FL(+) – overexpression of Cel-ACC-1 in N2 WT. PACC-1::Hco-ACC-1::GFP expression of Hco-ACC-1 in the wild type N2 *C. elegans* strain and the ACC-1 vc40177 (Cel-ACC-1 knockout) strains. Stars denote significant difference ( $P < 0.0005$ ) compared to N2.

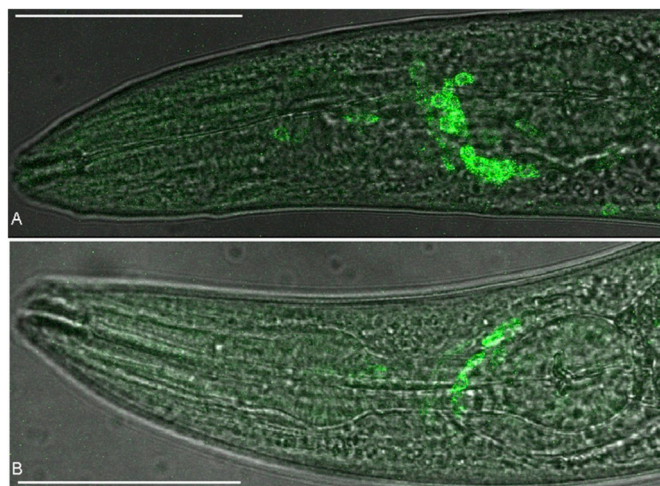


**Fig. 5.** Confocal image of N2 *Caenorhabditis elegans* worms expressing *hco-acc-1* under control of the *cel-acc-1* wild type promoter. Images A and B both show the expression of the construct in neurons near the posterior (terminal bulb) of the pharynx. Line represents 100  $\mu\text{m}$ .

has also highlighted some unique features of this receptor family. Aside from the fact that ACCs are not present in mammals, they also appear to have a unique agonist binding site. The most striking difference between Hco-ACC-1 and both alpha and non-alpha nAChRs is absence of the signature cys-cys motif in binding loop C (see Fig. 1a). Second, the tryptophan residue that has been shown in nAChRs to contribute to a pi-cationic interaction with the quaternary amine of acetylcholine (and carbachol) is still present in ACC-1, but is located in loop C (W225) rather than in the traditional loop B seen in nicotinic receptors and the AChBP (Beene et al., 2002; Celie et al., 2004). Recently, we have shown that this loop C tryptophan is crucial for receptor function in the Hco-ACC-2 receptor (Habibi et al., 2018). Interestingly, a similar shifting of this key tryptophan residue from loop B to C is also seen when we compare serotonin 5-HT<sub>3</sub> and nematode MOD-1 receptors (Mu et al., 2003). A loop C tryptophan is also present in tyramine and dopaminergic chloride channels (Beech et al., 2013), suggesting that it may be important for the ability of nematode cys-loop receptors to respond to a diverse array of molecules. However, it is important to note that the binding site for ACh on the Hco-ACC-1/2 channel could also be on the interface of two ACC-1 or ACC-2 subunits (Habibi et al., 2018) or an ACC-2/1 heterodimer. Further research will be important to determine

the subunit stoichiometry and variation in binding-sites of the ACC family of receptors.

While traditionally characterized as a muscarinic receptor agonist used primarily for the treatment of glaucoma, we have shown that carbachol (carbamylcholine) is an effective agonist at the nematode ACC-1/2 receptor with an EC<sub>50</sub> about 2-fold higher than acetylcholine. Carbachol is also an agonist for muscle nicotinic receptors but with an EC<sub>50</sub> over 10-fold higher compared to acetylcholine (Akk and Auerbach, 1999). Perhaps the structural differences between nAChRs and ACC receptors as outlined above can explain the relatively high sensitivity of carbachol observed in our study. Nevertheless, it is clear that further study of the molecular pharmacology of ACC receptors can provide an excellent opportunity for the study of current AChR agonists and the possible discovery of novel agonists.

In conclusion, this study provides the first investigation of role of ACC receptors in parasitic nematodes. While research using *C. elegans* to evaluate anthelmintic targets is an excellent tool to provide relevant information, research on similar targets in parasitic nematode can provide key information on whether a rational drug design approach might be worthwhile. While there is still much more to be learned about the role of ACC receptors in parasitic nematodes it is clear that comparing the function of the LGCC family in free-living and parasitic nematodes can potentially lead to the discovery of future anthelmintic targets and a better understanding of the evolution of parasitism.

#### Declarations of interest

None.

#### Acknowledgements

Research was funded by the Natural Science and Engineering Council of Canada (NSERC) (Grant #210290) SGF. The funding body played no role in the design or execution of the study. The authors declare no conflict of interest. We thank Paula Ribeiro, McGill University, for the antibodies used in this study and the many years of mentorship and contribution to the field of helminth neurochemistry.

#### Appendix A. Supplementary data

Supplementary data to this article can be found online at <https://doi.org/10.1016/j.ijpddr.2018.10.010>.

#### References

- Abdelmassih, S.A., Cochrane, E., Forrester, S.G., 2018. Evaluating the longevity of surgically extracted *Xenopus laevis* oocytes for the study of nematode ligand-gated ion channels. *Invertebr. Neurosci.* 18, 1.
- Accardi, M.V., Beech, R.N., Forrester, S.G., 2012. Nematode cys-loop GABA receptors: biological function, pharmacology and sites of action for anthelmintics. *Invertebr. Neurosci.* 12 (1), 3–12.
- Akk, G., Auerbach, A., 1999. Activation of muscle nicotinic acetylcholine receptor channels by nicotinic and muscarinic agonists. *Br. J. Pharmacol.* 128 (7), 1467–1476.
- Bamber, B.A., Beg, A.A., Twyman, R.E., Jorgensen, E.M., 1999. The *Caenorhabditis elegans* unc-49 locus encodes multiple subunits of a heteromultimeric GABA receptor. *J. Neurosci.* 19 (13), 5348–5359.
- Beech, R., Callanan, M., Rao, V., Dawe, G., Forrester, S., 2013. Characterization of cys-loop receptor genes involved in inhibitory amine neurotransmission in parasitic and free living nematodes. *Para. Int.* 62, 599–605.
- Beene, D.L., Brandt, G.S., Zhong, W., Zacharias, N.M., Lester, H.A., Dougherty, D.A., 2002. Cation- $\pi$  interactions in ligand recognition by serotonergic (5-HT<sub>3A</sub>) and nicotinic acetylcholine receptors: the anomalous binding properties of nicotine. *Biochemistry* 41, 10262–10269.
- Besier, R.B., Kahn, L.P., Sargison, N.D., Van Wyk, J.A., 2016. The pathophysiology, epidemiology and epidemiology of *Haemonchus contortus* infection in small ruminants. *Adv. Parasitol.* 93, 95–143.
- Blanchard, A., Guégnard, F., Charvet, C.L., Crisford, A., Courtot, E., Sauvé, C., Harmache, A., Duguet, T., O'Connor, V., Castagnone-Sereno, P., Reaves, B., Wolstenholme, A.J., Beech, R.N., Holden-Dye, L., Neveu, C., 2018. Deciphering the molecular determinants of cholinergic anthelmintic sensitivity in nematodes: when novel functional validation approaches highlight major differences between the model *Caenorhabditis elegans* and parasitic species. *PLoS Pathog.* 14 (5), e1006996.

- Boulin, T., Fauvin, A., Charvet, C.L., Cortet, J., Cabaret, J., Bessereau, J., Neveu, C., 2011. Functional reconstitution of *Haemonchus contortus* acetylcholine receptors in *Xenopus* oocytes provides mechanistic insights into levamisole resistance. *Br. J. Pharmacol.* 164, 1421–1432.
- Celie, P.H.N., van Rossum-Fikkert, S.E., van Dijk, W.J., Brejc, K., Smit, A.B., Sixma, T.K., 2004. Nicotine and carbamylcholine binding to nicotinic acetylcholine receptors as studied in AChBP crystal structures. *Neuron* 41, 907–914.
- Chao, M., Komatsu, H., Fukuto, H., Dionne, H., Hart, A., 2004. Feeding status and serotonin rapidly and reversibly modulate a *Caenorhabditis elegans* chemosensory circuit. *Proc. Natl. Acad. Sci. Unit. States Am.* 101, 15512–15517.
- Cully, D.F., Vassilatis, D.K., Liu, K.K., Paress, P.S., Van der Ploeg, L.H., Schaeffer, J.M., Arena, J.P., 1994. Cloning of an avermectin-sensitive glutamate-gated chloride channel from *Caenorhabditis elegans*. *Nature* 371 (6499), 707–711.
- Dent, J.A., Smith, M.M., Vassilatis, D.K., Avery, L., 2000. The genetics of ivermectin resistance in *Caenorhabditis elegans*. *Proc. Natl. Acad. Sci. U. S. A.* 14;97 (6), 2674–2679.
- Dent, J.A., Davits, M.W., Avery, L., 1997. *avr-15* encodes a chloride channel subunit that mediates inhibitory glutamatergic neurotransmission and ivermectin sensitivity in *Caenorhabditis elegans*. *EMBO J.* 16 (19), 5867–5879.
- Duguet, T.B., Charvet, C.L., Forrester, S.G., Wever, C.M., Dent, J.A., Neveu, C., Beech, R.N., 2016. Recent duplication and functional divergence in parasitic nematode levamisole-sensitive acetylcholine receptors. *PLoS Neglected Trop. Dis.* 10 (7), e0004826.
- Forrester, S.G., Prichard, R.K., Dent, J.A., Beech, R.N., 2003. *Haemonchus contortus*: HcGluCl $\alpha$  expressed in *Xenopus* oocytes forms a glutamate-gated ion channel that is activated by ibotenate and the antiparasitic drug ivermectin. *Mol. Biochem. Parasitol.* 129, 115–121.
- Frohman, M.A., Dush, M.K., Martin, G.R., 1988. Rapid production of full-length cDNAs from rare transcripts: amplification using a single gene-specific oligonucleotide primer. *Proc. Natl. Acad. Sci. U.S.A.* 85, 8998–9002.
- Glendinning, S.K., Buckingham, S.D., Sattelle, D.B., Wonnacott, S., Wolstenholme, A.J., 2011. Glutamate-gated chloride channels of *Haemonchus contortus* restore drug sensitivity to ivermectin resistant *Caenorhabditis elegans*. *PLoS One* 6 (7), e22390.
- Habibi, S.A., Callanan, M., Forrester, S.G., 2018. Molecular and pharmacological characterization of an acetylcholine-gated chloride channel (ACC-2) from the parasitic nematode *Haemonchus contortus*. *Int. J. Parasitol. Drugs Drug Resist.* <https://doi.org/10.1016/j.ijpddr.2018.09.004>. (in press).
- Hernando, G., Bouzat, C., 2014. *Caenorhabditis elegans* neuromuscular junction: GABA receptors and ivermectin action. *PLoS One* 9 (4), e95072.
- Hobert, O., 2002. PCR fusion-based approach to create reporter gene constructs for expression analysis in transgenic *C. elegans*. *Biotechniques* 32, 728–730.
- Irwin, J.J., Sterling, T., Mysinger, M.M., Bolstad, E.S., Coleman, R.G., 2012. ZINC: a free tool to discover chemistry for biology. *J. Chem. Inf. Model.* 23;52 (7), 1757–1768.
- Jensen, M.L., Pedersen, L.N., Timmermann, D.B., Schousboe, A., Ahring, P.K., 2005. Mutational studies using a cation-conducting GABAA receptor reveal the selectivity determinants of the Cys-loop family of ligand-gated ion channels. *J. Neurochem.* 92 (4), 962–972.
- Kusano, K., Miledi, R., Stinnakre, J., 1982. Cholinergic and catecholaminergic receptors in the *Xenopus* oocyte membrane. *J. Physiol. (Lond.)* 328, 143–170.
- Komuniecki, R., Hapiak, V., Harris, G., Bamber, B., 2014. Context-dependent modulation reconfigures interactive sensory-mediated microcircuits in *Caenorhabditis elegans*. *Curr. Opin. Neurobiol.* 29, 17–24.
- Komuniecki, R., Harris, G., Hapiak, V., Wragg, R., Bamber, B., 2012. Monoamines activate neuropeptide signaling cascades to modulate nociception in *C. elegans*: a useful model for the modulation of chronic pain? *Invertebr. Neurosci.* 12 (1), 53–61.
- Laing, R., Kikuchi, T., Martinelli, A., Tsai, I.J., Beech, R.N., Redman, E., Holroyd, N., Bartley, D.J., Beasley, H., Britton, C., Curran, D., Devaney, E., Gilbert, A., Hunt, M., Jackson, F., Johnston, S.L., Kryukov, I., Li, K., Morrison, A.A., Reid, A.J., Sargison, N., Saunders, G.I., Wasmuth, J.D., Wolstenholme, A., Berriman, M., Gilleard, J.S., Cotton, J.A., 2013. The genome and transcriptome of *Haemonchus contortus*, a key model parasite for drug and vaccine discovery. *Genome Biol.* 28;14 (8) R88.
- Laughton, D.L., Lunt, G.G., Wolstenholme, A.J., 1997. Reporter gene constructs suggest that the *Caenorhabditis elegans* avermectin receptor beta-subunit is expressed solely in the pharynx. *J. Exp. Biol.* 200, 1509–1514.
- McCavera, S., Rogers, A.T., Yates, D.M., Woods, D.J., Wolstenholme, A.J., 2009. An ivermectin-sensitive glutamate-gated chloride channel from the parasitic nematode, *Haemonchus contortus*. *Mol. Pharmacol.* 75, 1347–1355.
- Mello, C., Fire, A., 1995. DNA transformation. *Methods Cell Biol.* 48, 451–482.
- Morris, G.M., Huey, R., Lindstrom, W., Sanner, M.F., Belew, R.K., Goodsell, D.S., Olson, A.J., 2009. AutoDock4 and AutoDockTools4: automated docking with selective receptor flexibility. *J. Comput. Chem.* 30 (16), 2785–2791.
- Mu, T.W., Lester, H.A., Dougherty, D.A., 2003. Different binding orientations for the same agonist at homologous receptors: a lock and key or a simple wedge? *J. Am. Chem. Soc.* 11;125 (23), 6850–6851.
- Pereira, L., Kratsios, P., Serrano-Saiz, E., Sheftel, H., Hobert, O., et al., 2015. A cellular and regulatory map of the cholinergic nervous system of *C. elegans*. *Elife*, e12432.
- Petersen, E.F., Goddard, T.D., Huang, C.C., Couch, G.S., Greenblatt, D.M., Meng, E.C., Ferrin, T.E., 2004. UCSF Chimera—a visualization system for exploratory research and analysis. *J. Comput. Chem.* 25 (13), 1605–1612.
- Portillo, V., Jagannathan, S., Wolstenholme, A.J., 2003. Distribution of glutamate-gated chloride channel subunits in the parasitic nematode *Haemonchus contortus*. *J. Comp. Neurol.* 462 (2), 213–222.
- Putrenko, I., Zakikhani, M., Dent, J.A., 2005. A family of acetylcholine-gated chloride channel subunits in *Caenorhabditis elegans*. *J. Biol. Chem.* 280 (8), 6392–6398.
- Rao, V., Siddiqui, S., Prichard, R., Forrester, S., 2009. A dopamine-gated ion channel (HcGGR3\*) from *Haemonchus contortus* is expressed in the cervical papillae and is associated with macrocyclic lactone resistance. *Mol. Biochem. Parasitol.* 166 (1), 54–61.
- Raza, A., Lamb, J., Chambers, M., Hunt, P., Kotze, A., 2016. Larval development assay reveal the presence of sub-populations showing high- and low-level resistance in a monepantel (Zolvix®)-resistant isolate of *Haemonchus contortus*. *Vet. Parasitol.* 220, 77–82.
- Šali, A., Blundell, T.L., 1993. Comparative protein modelling by satisfaction of spatial restraints. *J. Mol. Biol.* 234, 779–815.
- Siddiqui, S.Z., Brown, D.D., Rao, V.T., Forrester, S.G., 2010. An UNC-49 GABA receptor subunit from the parasitic nematode *Haemonchus contortus* is associated with enhanced GABA sensitivity in nematode heteromeric channels. *J. Neurochem.* 113 (5), 1113–1122.
- Trott, O., Olson, A.J., 2010. AutoDock Vina: improving the speed and accuracy of docking with a new scoring function, efficient optimization, and multithreading. *J. Comput. Chem.* 30;31 (2), 455–461.
- Urdaneta-Marquez, L., Bae, S.H., Janukavicius, P., Beech, R., Dent, J., Prichard, R., 2014. A dyf-7 haplotype causes sensory neuron defects and is associated with macrocyclic lactone resistance worldwide in the nematode parasite *Haemonchus contortus*. *Int. J. Parasitol.* 44 (14), 1063–1071.
- Van Doren, K., Hirsh, D., 1988. Trans-spliced leader RNA exists as small nuclear ribonucleoprotein particles in *Caenorhabditis elegans*. *Nature* 6;335 (6190), 556–559.
- Weston, D., Patel, B., Van Voorhis, W.C., 1999. Virulence in *Trypanosoma cruzi* infection correlates with the expression of a distinct family of sialidase superfamily genes. *Mol. Biochem. Parasitol.* 98, 105–116.
- Wever, C., Farrington, D., Dent, J., 2015. The validation of nematode-specific acetylcholine-gated chloride channels as potential anthelmintic drug targets. *PLoS One* 2210 (9).
- Williamson, S.M., Walsh, T.K., Wolstenholme, A.J., 2007. The cys-loop ligand-gated ion channel gene family of *Brugia malayi* and *Trichinella spiralis*: a comparison with *Caenorhabditis elegans*. *Invertebr. Neurosci.* 7 (4), 219–226.
- Wolstenholme, A.J., 2012. Glutamate-gated chloride channels. *J. Biol. Chem.* 287 (48), 40232–40238.
- Zhang, J., Xue, F., Chang, Y., 2008. Structural determinants for antagonist pharmacology that distinguish the rho1 GABAC receptor from GABAA receptors. *Mol. Pharmacol.* 74 (4), 941–951.

## A3.2: Supplementary Information

### A3.2.1: Figures:

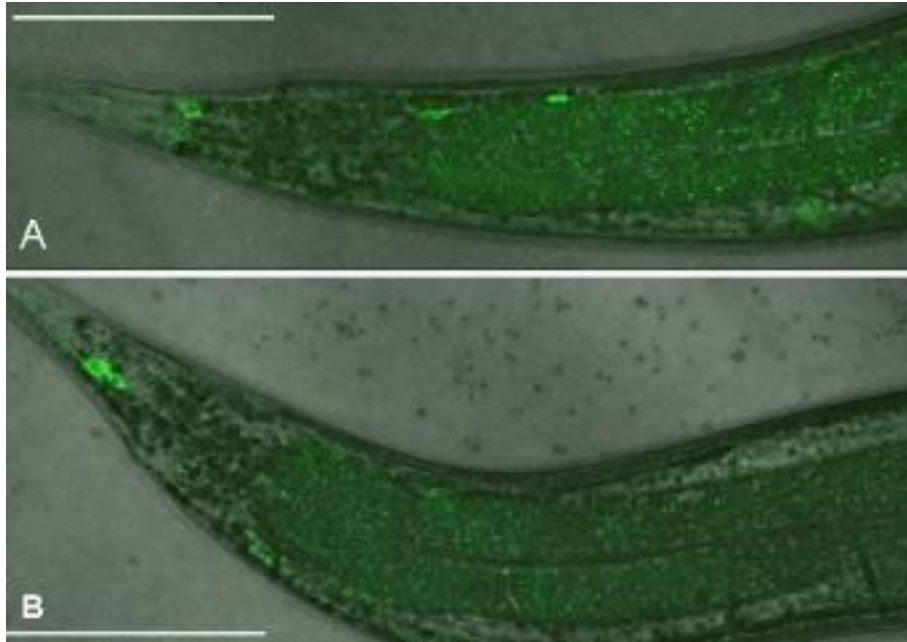


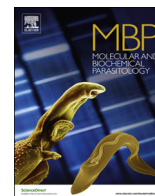
**Figure 1:** Confocal images of the tail region of N2 *C. elegans* worms expressing *hco-acc-1* under control of the *cel-acc-1* wild type promoter.

Video 1: <https://doi.org/10.1016/j.ijpddr.2018.10.010>.

Video 2: <https://doi.org/10.1016/j.ijpddr.2018.10.010>.

## Appendix 4: Chapter IV

### A4.1: Manuscript III



# Isolation and characterization of a novel member of the ACC ligand-gated chloride channel family, Hco-LGC-46, from the parasitic nematode *Haemonchus contortus*

Sarah A. Habibi<sup>a</sup>, Stephen M. Blazie<sup>b</sup>, Yishi Jin<sup>b</sup>, Sean G. Forrester<sup>a,\*</sup>

<sup>a</sup> Applied Bioscience Graduate Program, Faculty of Science, Ontario Tech University, 2000 Simcoe Street North, Oshawa, ON, L1H 7K4, Canada

<sup>b</sup> Neurobiology Section, Division of Biological Sciences, University of California, San Diego, La Jolla, CA, 92093, United States



## ARTICLE INFO

### Keywords:

*Haemonchus contortus*  
Aldicarb sensitivity  
Parasitic nematode  
Cys-loop receptor  
Ion channels

## ABSTRACT

The ACC-1 family of cys-loop receptors are ligand-gated chloride channels sensitive to acetylcholine (ACh), and are only present in invertebrates. Studies of this family of inhibitory receptors has provided insight into how they bind and respond to ACh in a manner vastly different from nicotinic acetylcholine receptors and appear to be present in tissues that are relevant to anthelmintic action. Here, we have identified two members of the ACC-1 family from the parasitic nematode *Haemonchus contortus*, Hco-LGC-46 and Hco-ACC-4. Hco-LGC-46 is an ACC subunit that has never been previously expressed and pharmacologically characterized. We found that Hco-LGC-46 when expressed in *Xenopus laevis* oocytes forms a functional homomeric channel that is responsive to the cholinergic agonists ACh and methylcholine. *hco-lgc-46* expressed in a *C. elegans lgc-46* null strain (*ok2900*) suppressed hypersensitivity to aldicarb in a manner similar to *cel-lgc-46*. It was also found that Hco-LGC-46 assembles with Hco-ACC-1 and produces a receptor that is over 5-fold more sensitive to ACh and responds to the cholinergic agonists methylcholine and carbachol. In contrast, the co-expression of Hco-LGC-46 with Hco-ACC-4 resulted in non-functional channels in oocytes. Hco-ACC-4 also appears to form heteromeric channels with a previously characterized subunit, Hco-ACC-2. Co-expression of Hco-ACC-4 with Hco-ACC-2 resulted in a functional heteromeric channel with an EC<sub>50</sub> value similar to that of the Hco-ACC-2 homomeric channel. However, the maximum currents generated in the ACC-4/ACC-2 channel were significantly ( $p < 0.005$ ) lower than those from the ACC-2 homomeric channel. Overall, this is the first report confirming that *lgc-46* encodes an acetylcholine-gated chloride channel which when co-expressed with *acc-4* results in reduced receptor function or trafficking in oocytes.

## 1. Introduction

Ion channels have been extensively studied, due to the role they play in fast synaptic neurotransmission in the nervous system of vertebrate and invertebrate organisms. The cys-loop (cysteine-loop) superfamily of ligand-gated ion channels are a major class of receptor-coupled ion channels that play a significant role in the nervous system of invertebrates, making them prime targets for nematocides [1]. These channels have been shown to be gated by neurotransmitters such as, gamma-aminobutyric acid (GABA) [2,3], glutamate [4], tyramine [5], serotonin [6], and acetylcholine [7].

Cholinergic neurotransmission is mediated by ACh receptors including nicotinic ACh receptors (nAChRs), which are cation-selective channels that result in neuro-excitation in the presence of agonists. However, early studies of the mollusk, *Aplysia*, revealed a population of

receptors that resulted in neuro-inhibition in the presence of ACh [8]. Further investigation in the free-living nematode *Caenorhabditis elegans* led to the identification of the inhibitory acetylcholine-gated chloride channel (ACC-1) family of cys-loop receptors [7,9]. The entire family is encoded by eight receptor subunit genes, named *acc-1*, *-2*, *-3*, and *-4*, and *lgc-46*, *-47*, *-48*, and *-49* [10]. Of these eight genes, 7 have been identified in the sheep parasite *Haemonchus contortus*, with the absence of *lgc-48* [11]. The ACC-1 family is of interest since they are nematode specific receptors that do not contain homologs in mammalian species [7]. In addition, they are shown to be present in anthelmintic relevant tissues, such as pharyngeal neurons in *C. elegans* [9] and pharyngeal muscle in *H. contortus* [12], making them prime candidates for the development of novel pharmaceuticals.

Recent work by our group identified and pharmacologically characterized two members of the ACC-1 family, ACC-1 and ACC-2, from *H.*

\* Corresponding author.

E-mail address: [sean.forrester@uoit.ca](mailto:sean.forrester@uoit.ca) (S.G. Forrester).

<https://doi.org/10.1016/j.molbiopara.2020.111276>

Received 30 October 2019; Received in revised form 24 March 2020; Accepted 25 March 2020

Available online 06 April 2020

0166-6851/ © 2020 Elsevier B.V. All rights reserved.



*contortus*. We found that Hco-ACC-2 forms a functional homomeric channel when expressed in *Xenopus laevis* oocytes [13]. Although Hco-ACC-1 does not form a function homomeric receptor on its own, it does associate with Hco-ACC-2 to form a heteromeric receptor which exhibits increased sensitivity to acetylcholine compared to the ACC-2 homomeric channel [12]. Immunolocalization of Hco-ACC-1 revealed specific expression in the anterior part of the pharynx of adult *H. contortus*, revealing a potential role in parasite feeding [12].

Aside from ACC-1 through -4, very little is known about the other members of the ACC-1 family. However, it has been shown that in *C. elegans* LGC-46 and ACC-4 are strongly expressed in cholinergic motor neurons [14,15]. Specifically they are localized to presynaptic terminals on these neurons and are involved in synaptic vesicle release [15]. This suggests the possibility that LGC-46, ACC-4, and other members of the ACC-1 family have the ability to form heteromeric channels. However, to date only ACC-1 through -4 have been expressed and functionally characterized in *Xenopus* oocytes [7,12,13] so it is unknown whether other members, such as LGC-46, can form ACh-gated chloride channels.

Here, we report the first pharmacological characterization of the LGC-46 receptor from the parasitic nematode *H. contortus*. We found that LGC-46 forms a functional homomeric receptor which is sensitive to acetylcholine and other cholinergic ligands. In addition, the co-expression of LGC-46 with ACC-1 results in an acetylcholine receptor that is 5x more sensitive to ACh compared to the LGC-46 homomeric channel. In contrast, the co-expression of ACC-4 with LGC-46 inhibited receptor function in *Xenopus* oocytes. Our data suggests that LGC-46 interacts with both ACC-2 and ACC-4 in oocytes, but only the LGC-46/ACC-2 channel is functional.

## 2. Methods

### 2.1. Isolation of *hco-lgc-46* and *hco-acc-4*

Whole adult *H. contortus* were received from Dr. Prichard (Institute of Parasitology, McGill University). Total RNA was extracted from adult male *H. contortus* worms using Trizol (Invitrogen, Carlsbad, USA). Complementary DNA (cDNA) was synthesized using the Quantitect Reverse Transcriptase kit from Qiagen (Dusseldorf, Germany), using a unique 3' oligo-dT anchor primer sequence (5'CCTCTGAAGGTTTCAGGATCCACATCTAGATTTTTTTTTTTTTTTTTTTVN3'); [where V is either A, C, or G and N is either A, C, G, or T] [16]. Gene specific primers were generated based on a full sequence provided by Dr. Robin Beech (McGill University) as part of the genome sequencing project for *H. contortus* [11]. Amplification of the complete *hco-lgc-46* and *hco-acc-4* genes was carried out using primers specific to the 5' and 3' end of the gene with XbaI and XmaI restrictions sites. *hco-lgc-46* and *hco-acc-4* were subcloned into the *X. laevis* expression vector pGEMHE [17].

### 2.2. Expression in *Xenopus laevis* oocytes

All animal procedures followed the Ontario Tech University Animal Care Committee and the Canadian Council on Animal Care guidelines. Channels were expressed in *X. laevis* oocytes according to [18]. Female *X. laevis* frogs were supplied by Nasco (Fort Atkinson, WI, USA). Animals were fed and tanks were cleaned regularly. Frogs were housed in a climate-controlled room (18 °C) with continuous light cycling. Frogs were anesthetized with 0.15 % 3-aminobenzoic acid ethyl ester methanesulphonate salt (MS-222) buffered with NaHCO<sub>3</sub> to pH 7 (Sigma-Aldrich, Oakville, ON, CA). Surgical removal of a section of the ovary of the frog was performed, and the lobe was defolliculated with a calcium-free oocyte Ringer's solution (82 mM NaCl, 2 mM KCl, 1 mM MgCl<sub>2</sub>, 5 mM HEPES pH 7.5 (Sigma-Aldrich) (OR-2) containing 2 mg/mL collagenase-II (Sigma-Aldrich). The oocytes in the defolliculation solution were incubated at room temperature for 2 h. Collagenase was washed from the oocytes with ND96 solution (1.8 mM CaCl<sub>2</sub>, 96 mM NaCl, 2

mM KCl, 1 mM MgCl<sub>2</sub>, 5 mM HEPES pH 7.5) and allowed one hour to recover at 18 °C in ND96 supplemented with 275 µg/mL pyruvic acid (Sigma-Aldrich) and 100 µg/mL of the antibiotic gentamycin (Sigma-Aldrich) (Supplemented ND96). Stage V and VI oocytes were selected for cytoplasmic injection of cRNA.

The pGEMHE vector containing the *hco-lgc-46*, *hco-acc-1*, *hco-acc-2*, and *hco-acc-4* coding sequences were linearized using SphI or NheI (New England Biolabs, USA), and used as templates for an *in vitro* transcription reaction (T7 mMessage mMachine kit, Ambion, Austin, TX, USA) yielding copy RNA corresponding to each gene. *X. laevis* oocytes were injected with 50 nl of each subunit gene (0.5 ng/µL) alone or in combination (0.25 ng/µL each) using the Drummond (Broomall, PA, USA) Nanoject microinjector. Oocytes were also co-injected with the *H. contortus* genes *unc-50*, *unc-74*, and *ric-3.1*, which encode accessory proteins [19]. The injected oocytes were incubated at 18 °C in supplemented ND96 solution. Electrophysiological recordings of the oocytes were conducted between 48 and 72 h after cRNA injection.

### 2.3. Electrophysiological recordings

Two-electrode voltage clamp electrophysiology was conducted using the Axoclamp 900A voltage clamp (Molecular Devices, Sunnyvale, CA, USA). Glass electrodes were produced using a P-97 Micropipette Puller (Sutter Instrument Co., Novato, CA, USA). The electrodes were backfilled with 3 M KCl and contained Ag|AgCl wires. The following molecules were first dissolved in ND96; Acetylcholine (ACh), Carbamoylcholine Chloride (Carbachol), Acetyl-β-methylcholine Chloride (Methacholine), Levamisole Hydrochloride (Levamisole), and Pyrantel Citrate Salt (Pyrantel) [Santa Cruz Biotechnology]. These solutions were perfused over oocytes using the RC-1Z recording chamber (Warner Instruments Inc., Hamdan, CT, USA). Data was analyzed using Clampex Software v10.2 (Molecular Devices) and all graphs were generated using Graphpad Prism Software v5.0 (San Diego, CA, USA). EC<sub>50</sub> values were determined by dose response curves that had been fitted to the following equation:

$$I_{max} = 1 / \left[ 1 + \left( \frac{EC_{50}}{[D]} \right)^h \right]$$

Where  $I_{max}$  is the maximal response, EC<sub>50</sub> is the concentration of compound required to elicit 50 % of the maximal response, [D] is compound concentration, and  $h$  is the Hill coefficient. Both EC<sub>50</sub> and  $h$  are free parameters, and the curves were normalized to the estimated  $I_{max}$ . Graphpad prism used the equation to fit a sigmoidal curve of variable slopes to the data. Means were determined from at least 7 oocytes from at least three batches of frogs.

Current-voltage relationships were recorded by changing the holding potential from -60 mV to 40 mV in 20 mV increments. At each step the oocyte was exposed to either a 1 or 10 mM concentration of ACh. For reduced Cl<sup>-</sup> trials, NaCl was partially replaced by Na-glucuronate (Sigma) in the ND96 buffer solution, for a final Cl<sup>-</sup> concentration of 62.5 mM. Current-voltage graphs were generated using Graphpad Prism Software v5.0 (San Diego, CA, USA).

### 2.4. In silico modelling

The protein coding sequences of Hco-LGC-46 and Hco-ACC-1 were aligned with the *Danio rerio* alpha-1 glycine receptor (3JAD). MODELLER v9.21 software [20] was used for the generation of the Hco-LGC-46 homodimer and Hco-ACC-1/Hco-LGC-46 heterodimer. Both homodimer and heterodimers were prepared for agonist docking using AutoDock Tools. Ligands were obtained from PubChem in their energy-reduced form. AutoDock Vina was used to simulate docking of each ligand to the homo- or hetero-dimers. Pymol was used to visualize the protein models with their associated ligands, and Chimera v1.6.1 [21] was used for the generation of figures.

## 2.5. Expression of *hco-lgc-46* in *C. elegans*

The *C. elegans* strain (*ok2900*) is a knockout strain for *lgc-46* and the mutant worms are hypersensitive to aldicarb [15], an inhibitor of acetylcholine esterase, compared to WT. To generate *Punc-17β::hco-lgc-46*, we amplified *hco-lgc-46* cDNA from pGEM *hco-lgc-46* using the primers YJ12412 and YJ12414 (Supplementary data T1). We used Gibson Assembly (NEB, Ipswich, MA) to clone the resulting amplicon downstream of the *Punc-17β* promoter sequence within expression vector pCZGY1091 [15], which was amplified using primers YJ12416 and YJ12417. *Punc-17β* is the sequence 498 bp upstream of the annotated (WS220) *C. elegans unc-17* start codon and is active only in *C. elegans* cholinergic motor neurons [22]. Two independent transgenic lines expressing *Punc-17β-hco-lgc-46* from transmitting extrachromosomal arrays were generated by injecting *Punc-17β-hco-lgc-46* (15 ng/μl), *Pmyo-2::mCherry* (pCFJ90) co-injection marker (2.5 ng/μl), and 100bp DNA ladder (82.5 ng/μl) into the *lgc-46(ok2900)* background using standard *C. elegans* microinjection procedure [23]. The *lgc-46(ok2900)* + empty vector transgenic line included as a control in our aldicarb assay was generated by injecting the empty pCZGY1091 plasmid (15 ng/μl), which contains *Punc-17β* and not the *hco-lgc-46* cDNA, along with *Pmyo-2::mCherry* (pCFJ90, 2.5 ng/μl), and 100bp DNA ladder (82.5 ng/μl) into the *lgc-46(ok2900)* background. Construction of the extrachromosomal array line expressing *Punc-17β-cel-lgc-46* was reported previously [15]. In transgenic animals with *Pmyo-2* co-injection marker, no toxicity was observed. Aldicarb response was assessed using one-day old young adults on NGM plates seeded with OP50, containing 500 μM aldicarb. Paralysis was defined as absence of movement in response to touch three times with a platinum wire pick and was assessed over a 5 h period. Two independent trials involving  $n = 15$  worms per line were performed on different days. For each trial, the proportion of non-paralyzed worms at each time point was averaged and these results are reported in Fig. 6.

## 3. Results

### 3.1. Isolation of *hco-lgc-46* and *hco-acc-4*

The full-length cDNA of the *hco-lgc-46* gene consisted of 1569 nucleotides (GenBank Accession # MN402460). The sequence encodes a protein containing 522 amino acids. The full-length coding sequence of the *hco-acc-4* gene consisted of 1239 nucleotides (GenBank Accession #AHM25235.1) and encodes a protein containing 412 amino acids (KC918365.1). Both protein sequences contain all seven extracellular binding loops, four transmembrane domains, and the Cys-loop motif (Fig. 1). The Hco-LGC-46 protein sequence shares 74 % similarity to the Cel-LGC-46 protein (Fig. 1). The Hco-ACC-4 protein sequence shares 86 % similarity with Cel-ACC-4. The PAR motif present at the beginning of the transmembrane 2 domain is indicative of anion selectivity [24].

### 3.2. Expression of *hco-lgc-46* and *hco-acc-1* in *Xenopus oocytes*

Upon injection of *X. laevis* oocytes with cRNA encoding Hco-LGC-46, along with the accessory proteins Hco-UNC-74, Hco-UNC-50, and Hco-RIC-3.1, a homomeric LGC-46 channel is formed (Fig. 2A). The EC<sub>50</sub> value for the Hco-LGC-46 homomeric channel in response to ACh was 893 ± 200 μM (Fig. 2C). The Hco-LGC-46 channel also responded to ACh derivative, methacholine, with an EC<sub>50</sub> value of 7348 ± 900 μM (Fig. 2A and C). However, the Hco-LGC-46 channel did not respond to 20 μM carbachol. The Hco-ACC-1/Hco-LGC-46 channel was more sensitive to ACh compared to the Hco-LGC-46 homomeric channel (Fig. 2A and B). The EC<sub>50</sub> value for the Hco-ACC-1/Hco-LGC-46 heteromeric channel in response to ACh was 166 ± 4 μM (Fig. 2C). The heteromeric channel also responded to derivatives, carbachol and methacholine, with EC<sub>50</sub> values of 1680 ± 70 μM and 3990 ± 600 μM, respectively (Fig. 2C). Carbachol was a partial agonist of the heteromeric channel,

whereas for both the Hco-LGC-46 and Hco-LGC-46/ACC-1 channel, methacholine was a weak partial agonist. Neither the Hco-LGC-46 homomeric channel nor the Hco-ACC-1/Hco-LGC-46 heteromeric channel respond to the cholinergic anthelmintics 20 μM levamisole or 20 μM pyrantel.

Current-voltage analysis of the Hco-LGC-46 channel was conducted to confirm anion selectivity (Fig. 3A). A full Cl<sup>-</sup> concentration of ND96 (103.6 mM Cl<sup>-</sup>) indicated a reverse potential of -17.44 ± 5 mV ( $n = 5$ ). This is consistent with the calculated Nernst potential for Cl<sup>-</sup> of -24.5 mV, when assuming an internal Cl<sup>-</sup> concentration of 50 mM [25]. When NaCl was partially replaced with Na-gluconate (final Cl<sup>-</sup> concentration of 62.5 mM) the reverse potential shifted to -3.4 ± 2 mV ( $n = 5$ ), which is also consistent with the assumed Nernst potential of -5.7 mV (Fig. 3A). Current-voltage analysis of the Hco-ACC-1/LGC-46 channel indicated reverse potentials of -27.7 mV and -1.1 mV when recorded in full and partial chloride concentrations respectively (Fig. 3B).

### 3.3. Homology modelling

To aid in understanding how the agonists sit in the binding pocket, homology models were generated. The Hco-LGC-46 homodimer and a Hco-ACC-1/Hco-LGC-46 heterodimer were produced using the *D. rerio* glycine receptor 3JAD as template. This template was chosen as it contained the highest homology with the ACC-1 family of receptors. The model for the Hco-LGC-46 homodimer is outlined in Fig. 4A. The binding site appears to be composed of several aromatic residues. Docking of channel activators, ACh and methacholine, is outlined in Fig. 4B and C. The quaternary amine on ACh is located 5.6 Å from W259. The asparagine (N182) in loop E is located 3.3 Å away from the carbonyl oxygen in ACh, allowing for potential hydrogen bond interactions to occur. Both ACh and Meth dock in an extended orientation in the LGC-46 binding pocket. However, the quaternary amine of methacholine is shifted away from W259. The model for the Hco-ACC-1/Hco-LGC-46 heteromeric channel is outlined in Fig. 5A. Similar to the homomeric model, the binding site of the heteromeric channel is composed of many aromatic residues. Docking of agonists, ACh, Carbachol, and Methacholine, is shown in Fig. 5B–D. The quaternary amine on ACh and carbachol is located 5.2 Å from W225, whereas this amine in methacholine is located 5.6 Å away from W225. The Y178 residue in loop B is 2.7 Å from N179 allowing for an increase in potential hydrogen bonding in the binding pocket. When looking at how each molecule docks in the binding pocket, we can see a similar extended orientation for each.

### 3.4. Expression of *hco-lgc-46* in *C. elegans*

To assess whether *hco-lgc-46* can function *in vivo* we took advantage of a *lgc-46* null strain *ok2900* which is hypersensitive to aldicarb, an acetylcholine esterase inhibitor that causes paralysis over time [15]. Compared to WT, *lgc-46(ok2900)* animals were much more sensitive to 500 μM aldicarb assessed over 5 h (Fig. 6). Expressing *cel-lgc-46* or *hco-lgc-46* specifically in the cholinergic motor neurons (*Punc-17β*) was sufficient to partially suppress aldicarb hypersensitivity. While we did not observe complete suppression, the level is similar to that reported in Takayanagi-Kiya et al. [15] (Fig. 6).

### 3.5. Expression of *Hco-ACC-4* in oocytes

Similar to the *C. elegans* version of *acc-4* [7], injection of *hco-acc-4* cRNA alone in oocytes did not result in a functional ACh-sensitive channel. In addition, the co-injection of cRNA encoding *hco-lgc-46* with *hco-acc-4* did not result in the expression of a sensitive heteromeric channel (Fig. 7). The co-injection of *hco-acc-4* with *hco-acc-2* resulted in a channel that was sensitive to ACh. The resulting ACC-4/ACC-2 receptor had an EC<sub>50</sub> value of 25 ± 0.3 μM which is similar to the ACC-2



**Fig. 1.** Protein sequence alignment of the *H. contortus* Hco-LGC-46 and Hco-ACC-4 receptors with *C. elegans* Cel-LGC-46 and Cel-ACC-4 and *D. rerio* Dre-GLY- $\alpha$ 1 receptors. All five binding loops (Loop A-E), the characteristic cysteine residues that form the “cys-loop”, and four transmembrane domains (M1-M4) and highlighted with underlines. (\*) indicates identity and (:) indicates similarity.

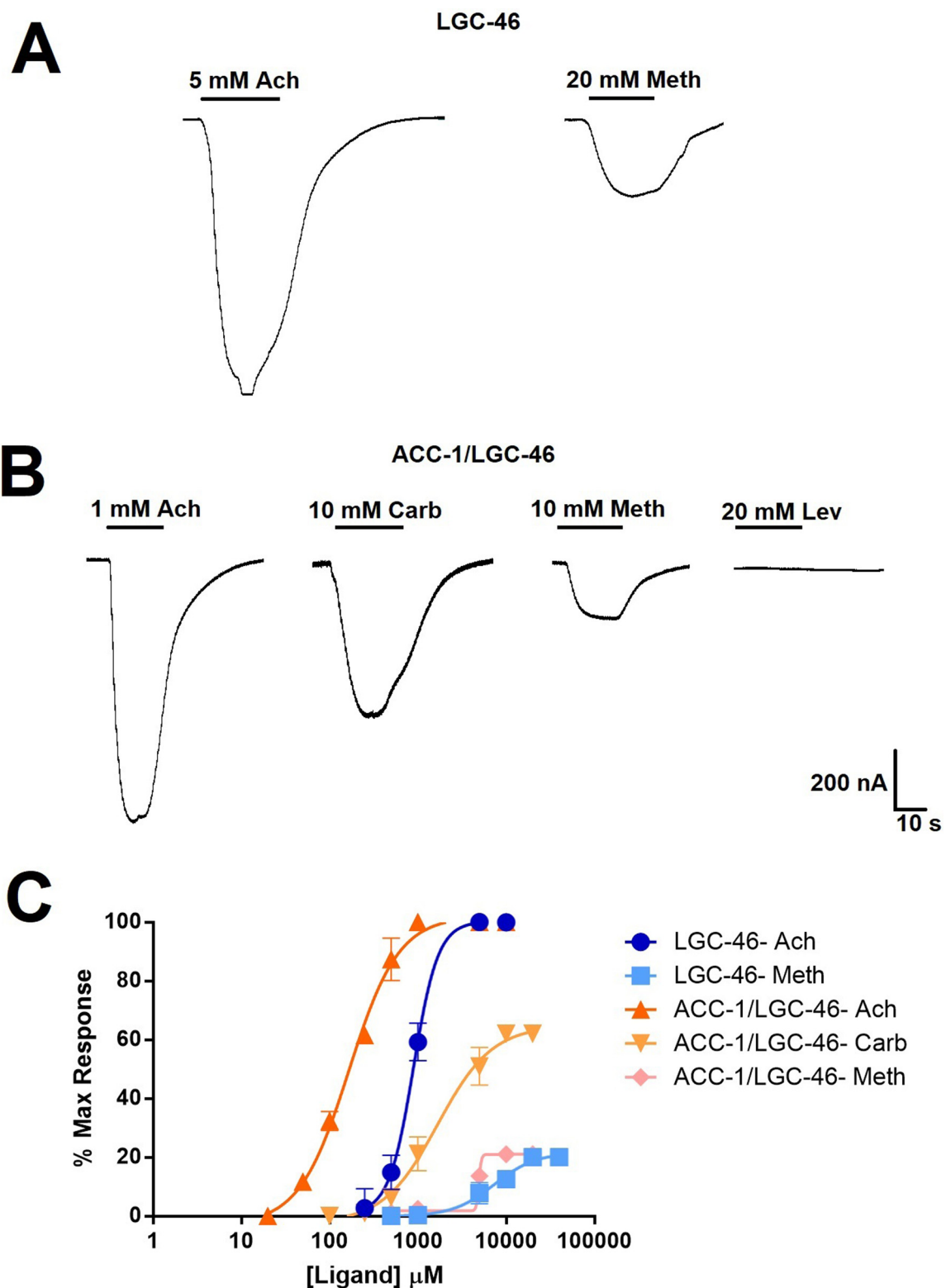


**Fig. 2.** (A) Maximal electrophysiological response of the Hco-LGC-46 receptor in response to acetylcholine and methacholine. (B) Maximal electrophysiological response of the Hco-ACC-1/Hco-LGC-46 heteromeric receptor in the presence of acetylcholine, carbachol, methacholine, and levamisole. (C) Dose-response curves of the Hco-LGC-46 and Hco-ACC-1/Hco-LGC-46 receptors in the presence of ligands shown. Standard errors are shown.  $n \geq 7$  oocytes. Each curve is represented as a percent of the maximum acetylcholine response. Partial agonists are those that have a maximum response lower than 100 %.

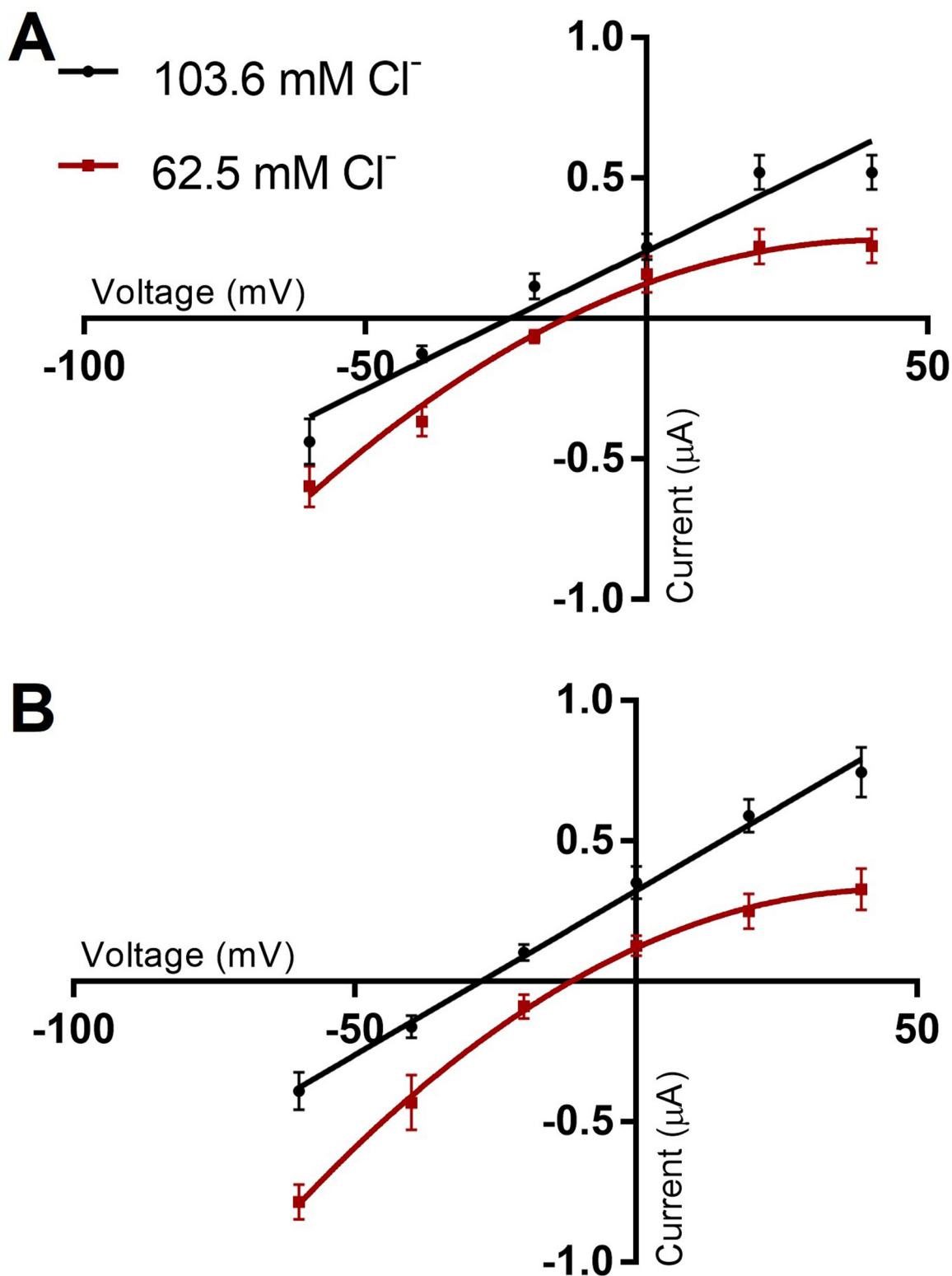


**Fig. 3.** (A) Current-voltage analysis of the Hco-LGC-46 channel using 103.6 mM Cl<sup>-</sup> and 62.5 mM Cl<sup>-</sup> buffer solutions. Acetylcholine response was generated using a maximum concentration. The indicated reverse potentials were -17.44 mV and -3.4 mV when recorded in full and partial chloride concentrations respectively. Standard errors are shown. (B) Current-voltage analysis of the Hco-LGC-46/ACC-1 channel using 103.6 mM Cl<sup>-</sup> and 62.5 mM Cl<sup>-</sup> buffer solutions. Acetylcholine response was generated using a maximum concentration. The indicated reverse potentials were -27.7 mV and -1.1 mV when recorded in full and partial chloride concentrations respectively.

homomeric channel  $21 \pm 0.7 \mu\text{M}$  [13]. However, the maximum current produced by the channel in the presence of ACC-4/ACC-2 channel was significantly lower ( $p < 0.005$ ) when compared to ACC-2 alone (Fig. 7). This is consistent with results obtained for the *C. elegans* ACC-4/ACC-2

subunits expressed in oocytes [7].

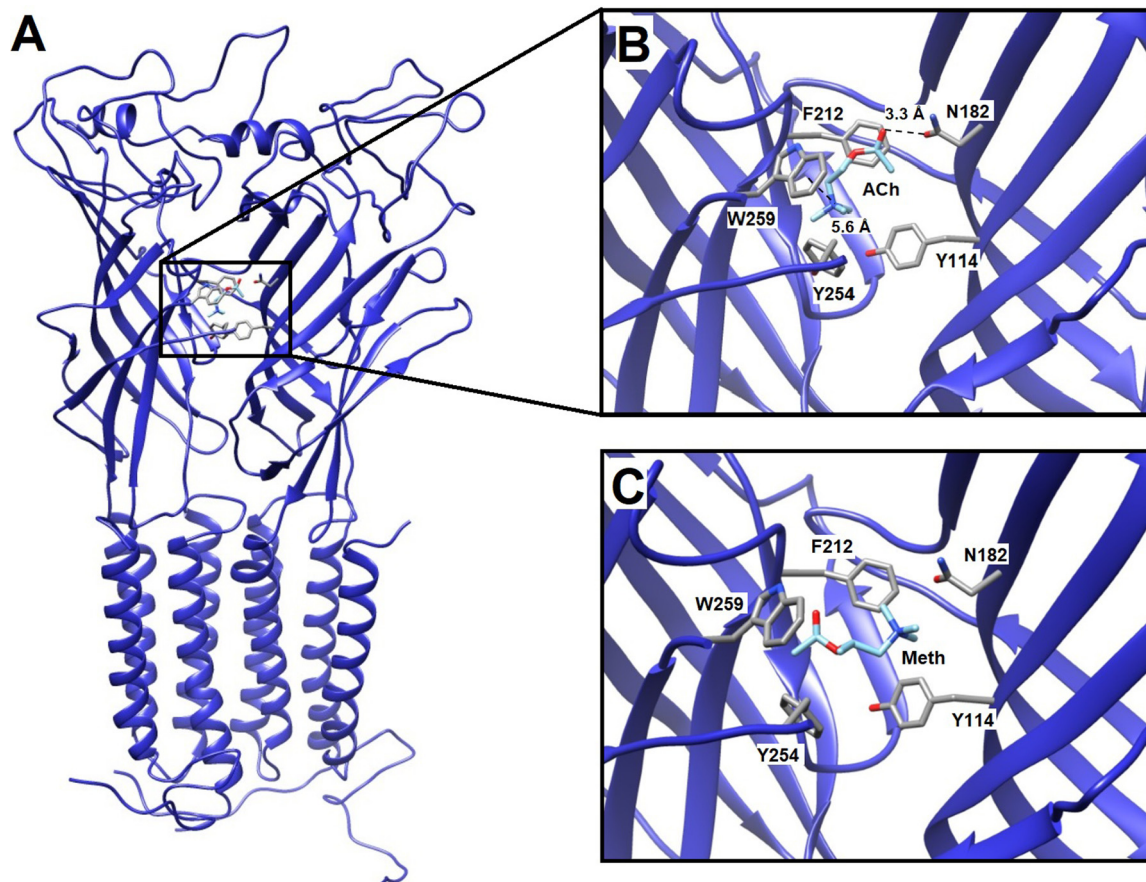


Fig. 4. (A) Homology model of Hco-LGC-46 homodimer. The principal and complementary subunits are represented by the colour blue. (B) View of the Hco-LGC-46 binding pocket with acetylcholine docked. Key aromatic residues in binding pocket are highlighted and distances to tryptophan (W259) and asparagine (N182) are shown. (C) View of the Hco-LGC-46 binding pocket with methacholine docked. \*A portion of Loop C is removed from the images for clarity.

#### 4. Discussion

We have identified and cloned the *Hco-lgc-46* gene from the parasitic nematode *H. contortus*, which encodes a member of the ACC-1 family of cys-loop ligand-gated chloride channels in nematodes. This unique family of inhibitory receptors is only present in nematode species, and thus provides an opportunity for exploration as new potential anthelmintic targets. In addition, phylogenetic analysis has revealed members of the ACC-1 family are present in a vast number of parasitic nematode species [12]. Previously it has been shown that members of this family from *H. contortus* combine to form homomeric and heteromeric channels that are highly sensitive to acetylcholine [12,13]. Here, we report that Hco-LGC-46 expressed in *Xenopus* oocyte can form a homomeric channel and a heteromeric channel with Hco-ACC-1 [12], that responds to cholinergic agonists, albeit at much higher concentrations than previously reported for other members of this family. Hco-LGC-46 when expressed in *C. elegans* cholinergic motor neurons partially suppresses aldicarb hypersensitivity in a similar manner to Cel-LGC-46, confirming that Hco-LGC-46 can function *in vivo*. Whether Hco-LGC-46 functions in a similar manner in *H. contortus* is unknown at this time. We have found previously that ACC-1 is expressed in different tissues in *C. elegans* vs *H. contortus* [12], so it is possible that there are differences in LGC-46 function between nematodes.

The pharmacology of Hco-LGC-46 and Hco-LGC-46/Hco-ACC-1 receptors, provide insight into the nature of the binding site. The Hco-LGC-46 receptor is minimally sensitive to the partial agonist methacholine (Meth). When referring to the model, Meth can be seen docked in an extended orientation surrounded by aromatic residues in the binding pocket. In mammalian nAChRs a tryptophan residue in loop B

has been shown to be a key player in ACh binding where it forms a cationic pi interaction with the quaternary amine of ACh [26]. In nematode ACCs however, this key tryptophan residue is found in loop C [13]. In the Hco-LGC-46 receptor we see Meth docking with its quaternary amine directed away from this tryptophan residue, W259, possibly explaining its lower sensitivity on the receptor. On the other hand, the Hco-LGC-46 receptors appears to be more sensitive to ACh. In the LGC-46 homodimer model ACh docks with its quaternary amine 5.6 Å from the tryptophan residue (W259) in loop C which would allow essential cation pi interactions to occur.

When Hco-LGC-46 was co-expressed with Hco-ACC-1 we generate a receptor that is over 5-fold more sensitive to ACh. Interestingly, when other members of the ACC-1 family are co-expressed with Hco-ACC-1, increased receptor sensitivity is also observed [12]. A pharmacological summary of the ACC-1 family of receptors in response to the cholinergic ligands and anthelmintics can be found in Table 1. Upon analysis of sequence alignments, it is noted that Hco-ACC-1 contains a tyrosine residue (Y178) in binding loop B, whereas the Hco-LGC-46 receptor contains a phenylalanine (F212) in the equivalent position. The presence of a tyrosine residue in loop B has been shown to contribute to hypersensitivity of these receptors when expressed in *Xenopus* oocytes [13]. The addition of the hydroxyl group in the ACC-1/LGC-46 channel places the tyrosine residue (Y178) within 2.7 Å of the amine group found on nearby asparagine (N179), allowing for hydrogen bond interactions to occur and provides a possible reason for increased channel activation. If Hco-ACC-1 is responsible for this increased receptor sensitivity it may indicate that it is playing the role of the principle subunit in pentamer formation (ie contributing this loop B tyrosine). Similarly, the Hco-ACC-1/Hco-LGC-46 receptor was 2-fold more sensitive to

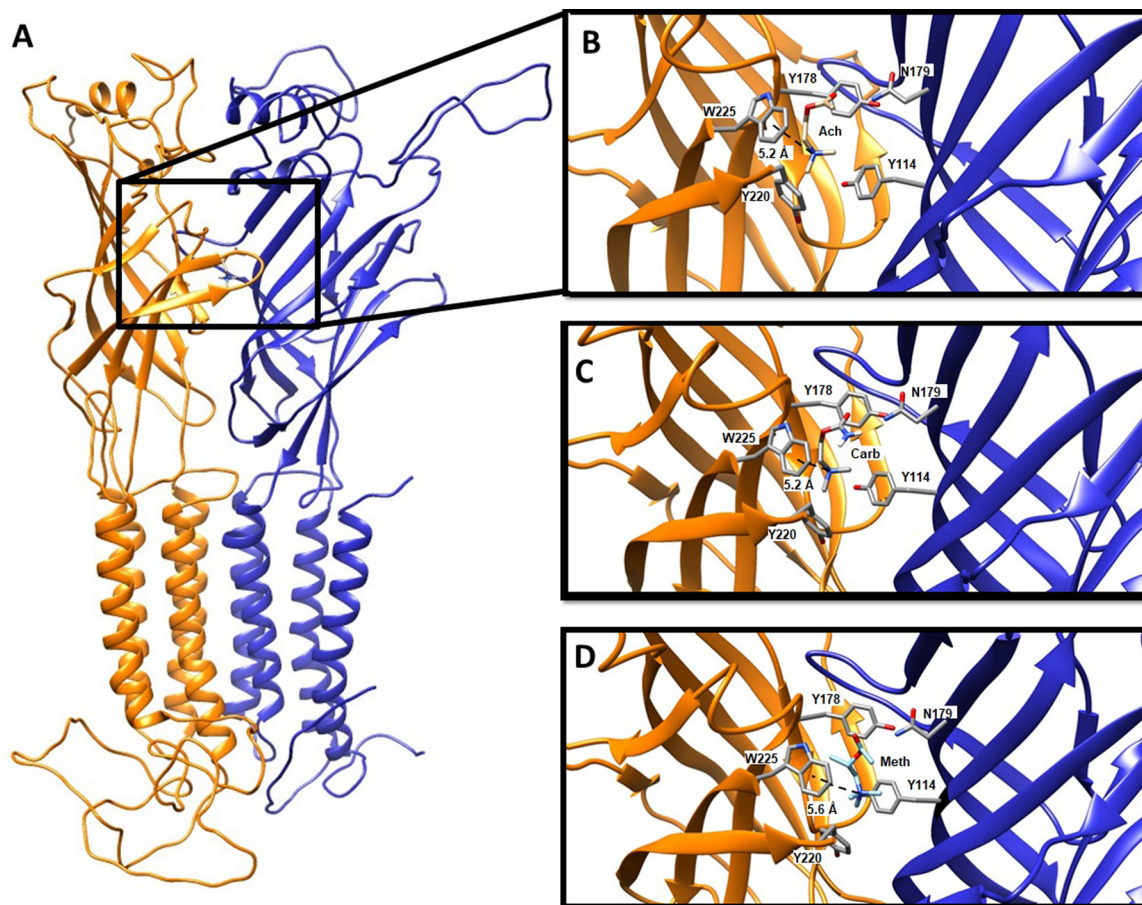


**Fig. 5.** (A) Homology model of Hco-ACC-1/ Hco-LGC-46 heterodimer. Hco-ACC-1 and LGC-46 are the principal and complimentary subunits, and are represented by the colours orange and blue, respectively. (B) View of the Hco-ACC-1/Hco-LGC-46 binding pocket with acetylcholine docked. (C) View of the Hco-ACC-1/Hco-LGC-46 binding pocket with carbachol docked. (D) Methacholine docked in binding pocket. Key aromatic residues in binding pocket are highlighted and distance to tryptophan (W225) is shown. \*A portion of Loop C is removed from the images for clarity.

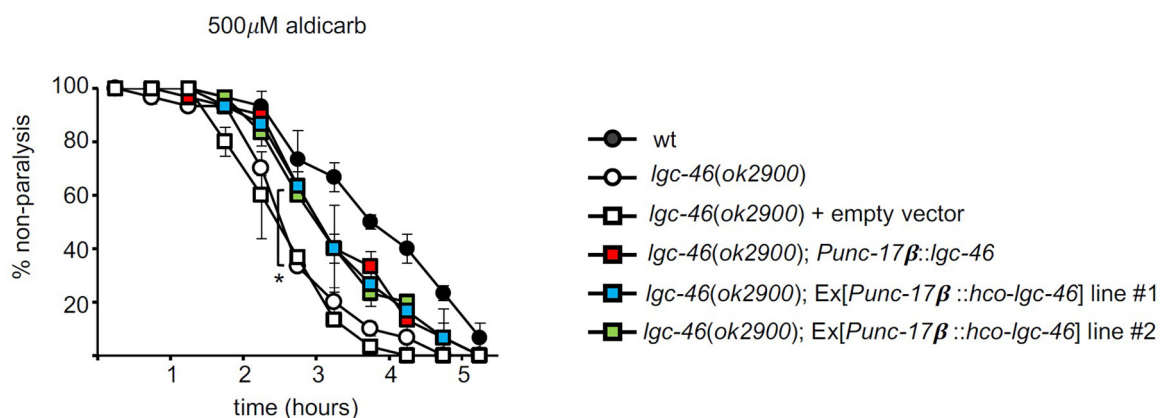


**Fig. 6.** Expression of Hco-LGC-46 partially rescues aldicarb hypersensitivity of *C. elegans* *lgc-46(ok2900)*. Results show the comparison between one extra-chromosomal array line expressing *C. elegans* LGC-46 and two independent lines expressing Hco-LGC-46 and under a cholinergic motor neuron specific promoter (*Punc-17β*). When restored to this subset of the nervous system, both *C. elegans* and Hco-LGC-46 partially rescue aldicarb hypersensitivity in the *lgc-46* genetic null (*ok2900*) background. The empty vector control line carries a plasmid containing *Punc-17β* without the *hco-lgc-46* cDNA insert in the *lgc-46(ok2900)* transgenic background. All transgenic lines express co-injection marker *Pmyo-2::mCherry*. Results are from two independent experiments of  $n = 15$  worms per group, performed on different days. Each data point is the mean % non-paralysis  $\pm$  SEM. \*:  $p < 0.05$  by two-way ANOVA and Bonferroni post-hoc test.

Meth, compared to Hco-LGC-46 homomer, and was responsive to ACh derivative carbachol. Both methacholine and carbachol were partial agonists of the ACC-1/LGC-46 receptor. Finally, neither the Hco-LGC-46 nor the Hco-ACC-1/Hco-LGC-46 receptors responded to nAChR anthelmintics pyrantel or levamisole, which have shown to have some

activity at the Hco-ACC-2 channel. This could indicate differences in the agonist binding site even within members of the ACC-1 family of receptors.

When Hco-LGC-46 was co-expressed with Hco-ACC-4 we observed no receptor functionality. It is unknown at this time whether the

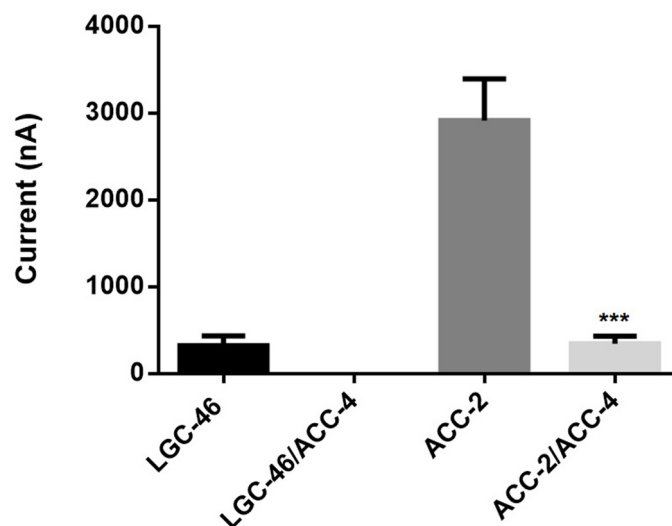


Fig. 7. Average maximal currents shown for the Hco-LGC-46 and Hco-ACC-2 receptors in comparison to the heteromeric channels with Hco-ACC-4 present. Standard errors are shown,  $n = 5$ ). \*\*\* indicates significant difference between ACC-2 and ACC-2/ACC-4 currents ( $P < 0.005$ ).

Table 1

Pharmacological summary of ACC-1 family of receptors from *H. contortus* in response to various cholinergic ligands and nAChR anthelmintics. Pharmacological responses are represented by  $EC_{50} \pm SE$ . N.R refers to no observed response of receptor to 20 mM concentration of ligand.

	ACC-2 <sup>a</sup>	ACC-1/ACC-2 <sup>b</sup>	LGC-46	ACC-1/LGC-46	LGC-46/ACC-4
Acetylcholine	$20.86 \pm 0.7 \mu M$	$5.9 \pm 1 \mu M$	$893 \pm 200 \mu M$	$166 \pm 4 \mu M$	N.R
Carbachol	$43.0 \pm 3.6 \mu M$	$32.5 \pm 3 \mu M$	N.R	$1680 \pm 70 \mu M$	N.R
Methacholine	$100.4 \pm 2.1 \mu M$	–	$7348 \pm 900 \mu M$	$3990 \pm 600 \mu M$	N.R
Levamisole	$98.39 \pm 4.0 \mu M$	–	N.R	N.R	N.R
Pyrantel	$71.7 \pm 3.5 \mu M$	–	N.R	N.R	N.R

<sup>a</sup> Data from Habibi et al. [13].

<sup>b</sup> Data from Callanan et al. [12]).

presence of ACC-4 is preventing the expression of LGC-46 in oocytes, or if it is forming a unique heteromeric receptor which is no longer sensitive to cholinergic ligands. Interestingly, nematodes that possess LGC-46 also possess ACC-4, and those lacking one also lack the other [9]. When analyzing the sequence alignments of these two subunits we see that in loop C of the ACC-4 receptor, the key tryptophan residue that has been shown to form essential cation pi interactions in other nematode cys-loop receptors [27] is missing, and instead there is a phenylalanine. Prior research from our group has shown that the substitution of this tryptophan residue for a phenylalanine severely impacts the function of the resulting receptor that is over 200 times less sensitive to ACh compared to wild-type [13]. If LGC-46 and ACC-4 were forming a heteromeric channel where the binding site is at the interface of the two subunits, this could possibly explain the reason for the inhibited function. In *C. elegans* ACC-4 and LGC-46 have been shown to function together in pre-synaptic cholinergic neurons by regulating synaptic vesicle release. Specifically, *lgc-46* gain-of function mutants showed suppressed activity in the *acc-4* knock-outs, indicating the role of ACC-4 in LGC-46 function [15]. However, while our results provide evidence for an interaction between ACC-4 and LGC-46 in oocytes the interaction appears to negatively affect channel function. Since there are no detectable currents in the ACC-4/LGC-46 receptor, we are unable to conclude whether the result is due to expression of receptor, or changes made to the binding site.

In *C. elegans*, ACC-4 has been shown to negatively impact the function of other ACC-1 family members such as ACC-2, where no currents were detected from the channel [7]. During our investigation we saw a similar observation with ACC-2 and ACC-4, where the presence of ACC-4 significantly ( $p < 0.005$ ) reduced the current flowing through the channel in the presence of ACh with little change in the

$EC_{50}$ . This suggests that ACC-4 is negatively impacting expression and not necessarily the agonist binding site in the ACC-4/ACC-2 channel.

#### CRediT authorship contribution statement

**Sarah A. Habibi:** Conceptualization, Data curation, Formal analysis, Writing - original draft, Writing - review & editing. **Stephen M. Blazie:** Data curation, Formal analysis, Writing - original draft, Writing - review & editing. **Yishi Jin:** Funding acquisition. **Sean G. Forrester:** Conceptualization, Writing - original draft, Writing - review & editing, Funding acquisition.

#### Acknowledgements

This study was funded by a grant from the Natural Science and Engineering Research Council of Canada to SGF and an NIH NS grant (NS R37 035546) to YJ

#### Appendix A. Supplementary data

Supplementary material related to this article can be found, in the online version, at doi:<https://doi.org/10.1016/j.molbiopara.2020.111276>.

#### References

- [1] J. Del Castillo, T.A. Morales, V. Sanchez, Action of piperazine on the neuromuscular system of *Ascaris lumbricoides*, *Nature* 200 (4907) (1963) 706.
- [2] B.A. Bamber, A.A. Beg, R.E. Twyman, E.M. Jorgensen, The *Caenorhabditis elegans* unc-49 locus encodes multiple subunits of a heteromultimeric GABA receptor, *J. Neurosci.* 19 (13) (1999) 5348–5359.
- [3] S.Z. Siddiqui, D.D.R. Brown, V.T.S. Rao, S.G. Forrester, An UNC-49 GABA receptor



- subunit from the parasitic nematode *Haemonchus contortus* is associated with enhanced GABA sensitivity in nematode heteromeric channels, *J. Neurochem.* 113 (5) (2010) 1113–1122.
- [4] D.F. Cully, D.K. Vassilatis, K.K. Liu, P.S. Paress, L.H. Van der Ploeg, J.M. Schaeffer, J.P. Arena, Cloning of an avermectin-sensitive glutamate-gated chloride channel from *Caenorhabditis elegans*, *Nature* 371 (6499) (1994) 707.
- [5] J.K. Pirri, A.D. McPherson, J.L. Donnelly, M.M. Francis, M.J. Alkema, A tyramine-gated chloride channel coordinates distinct motor programs of a *Caenorhabditis elegans* escape response, *Neuron* 62 (4) (2009) 526–538.
- [6] R. Ranganathan, S.C. Cannon, H.R. Horvitz, MOD-1 is a serotonin-gated chloride channel that modulates locomotory behaviour in *C. elegans*, *Nature* 408 (6811) (2000) 470–475.
- [7] I. Putrenko, M. Zakikhani, J.A. Dent, A family of acetylcholine-gated chloride channel subunits in *Caenorhabditis elegans*, *J. Biol. Chem.* 280 (8) (2005) 6392–6398.
- [8] J. Kehoe, J.M. McIntosh, *Aplysia* Two distinct nicotinic receptors, one pharmacologically similar to the vertebrate  $\alpha 7$ -containing receptor, mediate Cl currents in neurons, *J. Neurosci.* 18 (20) (1998) 8198–8213.
- [9] C.M. Wever, D. Farrington, J.A. Dent, The validation of nematode-specific acetylcholine-gated chloride channels as potential anthelmintic drug targets, *PLoS One* 10 (9) (2015) e0138804.
- [10] A.K. Jones, D.B. Sattelle, The cys-loop ligand-gated ion channel gene superfamily of the nematode, *Caenorhabditis elegans*, *Invert. Neurosci.* 8 (1) (2008) 41–47.
- [11] R. Laing, T. Kikuchi, A. Martinelli, L.J. Tsai, R.N. Beech, E. Redman, N. Holroyd, D.J. Bartley, H. Beasley, C. Britton, The genome and transcriptome of *Haemonchus contortus*, a key model parasite for drug and vaccine discovery, *Genome Biol.* 14 (8) (2013) R88.
- [12] M.K. Callanan, S.A. Habibi, W.J. Law, K. Nazareth, R.L. Komuniecki, S.G. Forrester, Investigating the function and possible biological role of an acetylcholine-gated chloride channel subunit (ACC-1) from the parasitic nematode *Haemonchus contortus*, *Int. J. Parasitol. Drugs Drug Resist.* 8 (3) (2018) 526–533.
- [13] S.A. Habibi, M. Callanan, S.G. Forrester, Molecular and pharmacological characterization of an acetylcholine-gated chloride channel (ACC-2) from the parasitic nematode *Haemonchus contortus*, *Int. J. Parasitol. Drugs Drug Resist.* 8 (3) (2018) 518–525.
- [14] L. Pereira, P. Kratsios, E. Serrano-Saiz, H. Sheftel, A.E. Mayo, D.H. Hall, J.G. White, B. LeBoeuf, L.R. García, U. Alon, A cellular and regulatory map of the cholinergic nervous system of *C. elegans*, *Elife* 4 (2015) e12432.
- [15] S. Takayanagi-Kiya, K. Zhou, Y. Jin, Release-dependent feedback inhibition by a presynaptically localized ligand-gated anion channel, *Elife* 5 (2016) e21734.
- [16] D. Weston, B. Patel, W.C. Van Voorhis, Virulence in *Trypanosoma cruzi* infection correlates with the expression of a distinct family of sialidase superfamily genes, *Mol. Biochem. Parasitol.* 98 (1) (1999) 105–116.
- [17] J. Zhang, F. Xue, Y. Chang, Structural determinants for antagonist pharmacology that distinguish the  $\rho 1$  GABAC receptor from GABAA receptors, *Mol. Pharmacol.* 74 (4) (2008) 941–951.
- [18] S.A. Abdelmassih, E. Cochrane, S.G. Forrester, Evaluating the longevity of surgically extracted *Xenopus laevis* oocytes for the study of nematode ligand-gated ion channels, *Invert. Neurosci.* 18 (1) (2018) 1.
- [19] T. Boulin, A. Fauvin, C.L. Charvet, J. Cortet, J. Cabaret, J. Bessereau, C. Neveu, Functional reconstitution of *Haemonchus contortus* acetylcholine receptors in *Xenopus* oocytes provides mechanistic insights into levamisole resistance, *Br. J. Pharmacol.* 164 (5) (2011) 1421–1432.
- [20] A. Šali, T.L. Blundell, Comparative protein modelling by satisfaction of spatial restraints, *J. Mol. Biol.* 234 (3) (1993) 779–815.
- [21] E.F. Pettersen, T.D. Goddard, C.C. Huang, G.S. Couch, D.M. Greenblatt, E.C. Meng, T.E. Ferrin, UCSF Chimera—a visualization system for exploratory research and analysis, *J. Comput. Chem.* 25 (13) (2004) 1605–1612.
- [22] N.K. Charlie, M.A. Schade, A.M. Thomure, K.G. Miller, Presynaptic UNC-31 (CAPS) is required to activate the Gas pathway of the *Caenorhabditis elegans* synaptic signaling network, *Genetics* 172 (2) (2006) 943–961.
- [23] C.C. Mello, J.M. Kramer, D. Stinchcomb, V. Ambros, Efficient gene transfer in *C. elegans*: extrachromosomal maintenance and integration of transforming sequences, *EMBO J.* 10 (12) (1991) 3959–3970.
- [24] M.L. Jensen, D.B. Timmermann, T.H. Johansen, A. Schousboe, T. Varming, P.K. Ahring, The  $\beta$  subunit determines the ion selectivity of the GABAA receptor, *J. Biol. Chem.* 277 (44) (2002) 41438–41447.
- [25] K. Kusano, R. Miledi, J. Stinnakre, Cholinergic and catecholaminergic receptors in the *Xenopus* oocyte membrane, *J. Physiol.* 328 (1) (1982) 143–170.
- [26] D.L. Beene, G.S. Brandt, W. Zhong, N.M. Zacharias, H.A. Lester, D.A. Dougherty, Cation- $\pi$  interactions in ligand recognition by serotonergic (5-HT<sub>3A</sub>) and nicotinic acetylcholine receptors: the anomalous binding properties of nicotine, *Biochemistry* 41 (32) (2002) 10262–10269.
- [27] T.-W. Mu, H.A. Lester, D.A. Dougherty, Different binding orientations for the same agonist at homologous receptors: a lock and key or a simple wedge? *J. Am. Chem. Soc.* 125 (23) (2003) 6850–6851.

## A4.2: Supplementary Information

### A2.4.1: Tables

Table 1: Cloning primers used to generate *Punc-17β::hco-lgc-46*:

<b>primer</b>	<b>Sequence (5' to 3')- uppercase are sequences annealing to <i>hco-lgc-46</i></b>
YJ12412	tcttggtcaaATGTATTACATCACTTTCCTACTATTGCTGCT
YJ12414	attcgatatcCTAGCCATCTGAGCGTAGGTAGTG
YJ12416	AGATGGCTAGgatatcgaattcctgcagccccg
YJ12417	TGTAATACATtgaacaagagatgcggaataagaaagact

Table 2: Homology scores of top 5

<b>Template</b>	<b>ID</b>	<b>Identity (% homology)</b>
<b>alpha-1 glycine receptor by single particle electron cryo-microscopy, strychnine-bound state</b>	3JAD	34.47
alpha-1 glycine receptor by single particle electron cryo-microscopy, glycine-bound state	3JAE	34.47
Human Glycine Receptor alpha-3 Bound to AM-3607, Glycine, and Ivermectin	5VDI	34.11
<i>C. elegans</i> glutamate-gated chloride channel (GluCl) in complex with Fab and ivermectin	3RHW	31.97
<i>C. elegans</i> glutamate-gated chloride channel (GluCl) in complex with Fab in a non-conducting conformation	4TNV	31.47

Appendix 5 – Copyright Permission from Co-Authors

## Copyright Permission Letter

July 7, 2020

**Publication Titles:** 1) Molecular and pharmacological characterization of an acetylcholine-gated chloride channel (ACC-2) from the parasitic nematode *Haemonchus contortus*. 2) Investigating the function and possible biological role of an acetylcholine-gated chloride channel subunit (ACC-1) from the parasitic nematode *Haemonchus contortus*. 3) Isolation and characterization of a novel member of the ACC ligand-gated chloride channel family, Hco-LCG-46, from the parasitic nematode *Haemonchus contortus*. 4) Evaluating the longevity of surgically extracted *Xenopus laevis* oocytes for the study of nematode ligand-gated ion channels.

I am preparing my Doctor of Philosophy thesis for submission to the School of Graduate and Postdoctoral Studies at the University of Ontario Institute of Technology (Ontario Tech) in Oshawa, Ontario, Canada. I am seeking your permission to include a manuscript version of the following paper(s) as a chapter in the thesis:

Habibi, S.A., Callanan, M. and Forrester, S.G. (2018) Molecular and pharmacological characterization of an acetylcholine-gated chloride channel (ACC-2) from the parasitic nematode *Haemonchus contortus*. *International Journal for Parasitology: Drugs and Drug Resistance*. 8(3): 518-525

Callanan, M., Habibi, S.A.\*, Law, W.J., Nazareth, K., Komuniecki, R., and Forrester, S.G. (2018) Investigating the function and possible biological role of an acetylcholine-gated chloride channel subunit (ACC-1) from the parasitic nematode *Haemonchus contortus*. *International Journal for Parasitology: Drugs and Drug Resistance*. 8(3): 526-533 \*Joint first author

Habibi, S.A., Blazie, S., Jin, Y. and Forrester, S.G. (2019) Isolation and characterization of a novel member of the ACC ligand-gated chloride channel family, Hco-LCG-46, from the parasitic nematode *Haemonchus contortus*. *Molecular & Biochemical Parasitology*. 237(111276)

Abdelmassih, S.A., Cochrane, E. and Forrester, S.G. (2018) Evaluating the longevity of surgically extracted *Xenopus laevis* oocytes for the study of nematode ligand-gated ion channels. *Invertebrate Neuroscience*. 18(1): 1-6

Canadian graduate theses are reproduced by the Library and Archives of Canada (formerly National Library of Canada) through a non-exclusive, world-wide license to reproduce, loan, distribute, or sell theses. I am also seeking your permission for the material described above to be reproduced and distributed by the LAC (NLC). Further details about the LAC (NLC) thesis program are available on the LAC (NLC) website ([www.nlc-bnc.ca](http://www.nlc-bnc.ca)).

Full publication details and a copy of this permission letter will be included in the thesis.

Yours sincerely,  
Sarah Habibi

Permission is granted for:

a) The inclusion of the material described above in your thesis.

b) For the material described above to be included in the copy of your thesis that is sent to the Library and Archives of Canada (formerly National Library of Canada) for reproduction and distribution.

Name: Sean Forrester

Title: Associate Professor

---

Signature: 

Date (dd/mmm/yyyy): 07/07/2020

---

### Copyright Permission Letter

July 7, 2020

**Publication Title:** Evaluating the longevity of surgically extracted *Xenopus laevis* oocytes for the study of nematode ligand-gated ion channels.

I am preparing my Doctor of Philosophy thesis for submission to the School of Graduate and Postdoctoral Studies at the University of Ontario Institute of Technology (Ontario Tech) in Oshawa, Ontario, Canada. I am seeking your permission to include a manuscript version of the following paper(s) as a chapter in the thesis:

Abdelmassih, S.A., Cochrane, E. and Forrester, S.G. (2018) Evaluating the longevity of surgically extracted *Xenopus laevis* oocytes for the study of nematode ligand-gated ion channels. *Invertebrate Neuroscience*. 18(1): 1-6

Canadian graduate theses are reproduced by the Library and Archives of Canada (formerly National Library of Canada) through a non-exclusive, world-wide license to reproduce, loan, distribute, or sell theses. I am also seeking your permission for the material described above to be reproduced and distributed by the LAC (NLC). Further details about the LAC (NLC) thesis program are available on the LAC (NLC) website ([www.nlc-bnc.ca](http://www.nlc-bnc.ca)).

Full publication details and a copy of this permission letter will be included in the thesis.

Yours sincerely,  
Sarah Habibi

Permission is granted for:

- a) The inclusion of the material described above in your thesis.
- b) For the material described above to be included in the copy of your thesis that is sent to the Library and Archives of Canada (formerly National Library of Canada) for reproduction and distribution.

Name: Everett Cochrane

Title:

---

Signature:



Date (dd/mmm/yyyy) 07/07/2020

---

## Copyright Permission Letter

July 7, 2020

**Publication Title:** Investigating the function and possible biological role of an acetylcholine-gated chloride channel subunit (ACC-1) from the parasitic nematode *Haemonchus contortus*.

I am preparing my Doctor of Philosophy thesis for submission to the School of Graduate and Postdoctoral Studies at the University of Ontario Institute of Technology (Ontario Tech) in Oshawa, Ontario, Canada. I am seeking your permission to include a manuscript version of the following paper(s) as a chapter in the thesis:

Callanan, M., Habibi, S.A. \*, Law, W.J., Nazareth, K., Komuniecki, R., and Forrester, S.G. (2018) Investigating the function and possible biological role of an acetylcholine-gated chloride channel subunit (ACC-1) from the parasitic nematode *Haemonchus contortus*. *International Journal for Parasitology: Drugs and Drug Resistance*. 8(3): 526-533 \*Joint first author

Canadian graduate theses are reproduced by the Library and Archives of Canada (formerly National Library of Canada) through a non-exclusive, world-wide license to reproduce, loan, distribute, or sell theses. I am also seeking your permission for the material described above to be reproduced and distributed by the LAC (NLC). Further details about the LAC (NLC) thesis program are available on the LAC (NLC) website ([www.nlc-bnc.ca](http://www.nlc-bnc.ca)).

Full publication details and a copy of this permission letter will be included in the thesis.

Yours sincerely,  
Sarah Habibi


Permission is granted for:

- a) The inclusion of the material described above in your thesis.
- b) For the material described above to be included in the copy of your thesis that is sent to the Library and Archives of Canada (formerly National Library of Canada) for reproduction and distribution.

Name: Kristen Nazareth

Title: Miss

---

Signature: 

Date (dd/mmm/yyyy) 07/07/2020

---

## Copyright Permission Letter

July 7,  
2020

**Publication Title:** 1) Molecular and pharmacological characterization of an acetylcholine-gated chloride channel (ACC-2) from the parasitic nematode *Haemonchus contortus*. 2) Investigating the function and possible biological role of an acetylcholine-gated chloride channel subunit (ACC-1) from the parasitic nematode *Haemonchus contortus*.

I am preparing my Doctor of Philosophy thesis for submission to the School of Graduate and Postdoctoral Studies at the University of Ontario Institute of Technology (Ontario Tech) in Oshawa, Ontario, Canada. I am seeking your permission to include a manuscript version of the following paper(s) as a chapter in the thesis:

Habibi, S.A., Callanan, M. and Forrester, S.G. (2018) Molecular and pharmacological characterization of an acetylcholine-gated chloride channel (ACC-2) from the parasitic nematode *Haemonchus contortus*. *International Journal for Parasitology: Drugs and Drug Resistance*. 8(3): 518-525

Callanan, M., Habibi, S.A.\*, Komuniecki, R., Law, W.J., and Forrester, S.G. (2018) Investigating the function and possible biological role of an acetylcholine-gated chloride channel subunit (ACC-1) from the parasitic nematode *Haemonchus contortus*. *International Journal for Parasitology: Drugs and Drug Resistance*. 8(3): 526-533 \*Joint first author

Canadian graduate theses are reproduced by the Library and Archives of Canada (formerly National Library of Canada) through a non-exclusive, world-wide license to reproduce, loan, distribute, or sell theses. I am also seeking your permission for the material described above to be reproduced and distributed by the LAC (NLC). Further details about the LAC (NLC) thesis program are available on the LAC (NLC) website ([www.nlc-bnc.ca](http://www.nlc-bnc.ca)).

Full publication details and a copy of this permission letter will be included in the thesis.

Yours  
sincerely,  
Sarah Habibi

Permission is granted for: a) The inclusion of the material described above in your thesis. b) For the material described above to be included in the copy of your thesis that is sent to the Library and Archives of Canada (formerly National Library of Canada) for reproduction and



distribution.

Name: Micah Callanan

Title: Mr.

A handwritten signature in black ink, appearing to read 'Micah Callanan', written in a cursive style.

Signature:

Date (dd/mm/yyyy) 07/07/2020

Copyright Permission Letter

July 7, 2020

**Publication Title:** Isolation and characterization of a novel member of the ACC ligand-gated chloride channel family, Hco-LCG-46, from the parasitic nematode *Haemonchus contortus*.

I am preparing my Doctor of Philosophy thesis for submission to the School of Graduate and Postdoctoral Studies at the University of Ontario Institute of Technology (Ontario Tech) in Oshawa, Ontario, Canada. I am seeking your permission to include a manuscript version of the following paper(s) as a chapter in the thesis:

Habibi, S.A., Blazie, S., Jin, Y. and Forrester, S.G. (2019) Isolation and characterization of a novel member of the ACC ligand-gated chloride channel family, Hco-LCG-46, from the parasitic nematode *Haemonchus contortus*. *Molecular & Biochemical Parasitology*. 237(111276)

Canadian graduate theses are reproduced by the Library and Archives of Canada (formerly National Library of Canada) through a non-exclusive, world-wide license to reproduce, loan, distribute, or sell theses. I am also seeking your permission for the material described above to be reproduced and distributed by the LAC (NLC). Further details about the LAC (NLC) thesis program are available on the LAC (NLC) website ([www.nlc-bnc.ca](http://www.nlc-bnc.ca)).


Full publication details and a copy of this permission letter will be included in the thesis.

Yours sincerely,  
Sarah Habibi

Permission is granted for:

- a) The inclusion of the material described above in your thesis.
- b) For the material described above to be included in the copy of your thesis that is sent to the Library and Archives of Canada (formerly National Library of Canada) for reproduction and distribution.

Name: Stephen Blazie Title: Postdoctoral Fellow

Signature:  Date (dd/mmm/yyyy) 10/7/2020

### Copyright Permission Letter

July 7, 2020

**Publication Title:** Investigating the function and possible biological role of an acetylcholine-gated chloride channel subunit (ACC-1) from the parasitic nematode *Haemonchus contortus*.

I am preparing my Doctor of Philosophy thesis for submission to the School of Graduate and Postdoctoral Studies at the University of Ontario Institute of Technology (Ontario Tech) in Oshawa, Ontario, Canada. I am seeking your permission to include a manuscript version of the following paper(s) as a chapter in the thesis:

Callanan, M., Habibi, S.A. \*, Law, W.J., Nazareth, K., Komuniecki, R., and Forrester, S.G. (2018) Investigating the function and possible biological role of an acetylcholine-gated chloride channel subunit (ACC-1) from the parasitic nematode *Haemonchus contortus*. *International Journal for Parasitology: Drugs and Drug Resistance*. 8(3): 526-533 \*Joint first author

Canadian graduate theses are reproduced by the Library and Archives of Canada (formerly National Library of Canada) through a non-exclusive, world-wide license to reproduce, loan, distribute, or sell theses. I am also seeking your permission for the material described above to be reproduced and distributed by the LAC (NLC). Further details about the LAC (NLC) thesis program are available on the LAC (NLC) website ([www.nlc-bnc.ca](http://www.nlc-bnc.ca)).

Full publication details and a copy of this permission letter will be included in the thesis.

Yours sincerely,  
Sarah Habibi

Permission is granted for:

- a) The inclusion of the material described above in your thesis.
- b) For the material described above to be included in the copy of your thesis that is sent to the Library and Archives of Canada (formerly National Library of Canada) for reproduction and distribution.

Name: Wen Jing Law

Title: Dr.

---

Signature: *Wen Jing Law*

Date (dd/mmm/yyyy): 03/09/2020

---

## Copyright Permission Letter

July 7, 2020

**Publication Title:** Isolation and characterization of a novel member of the ACC ligand-gated chloride channel family, Hco-LCG-46, from the parasitic nematode *Haemonchus contortus*.

I am preparing my Doctor of Philosophy thesis for submission to the School of Graduate and Postdoctoral Studies at the University of Ontario Institute of Technology (Ontario Tech) in Oshawa, Ontario, Canada. I am seeking your permission to include a manuscript version of the following paper(s) as a chapter in the thesis:

Habibi, S.A., Blazie, S., Jin, Y. and Forrester, S.G. (2019) Isolation and characterization of a novel member of the ACC ligand-gated chloride channel family, Hco-LCG-46, from the parasitic nematode *Haemonchus contortus*. *Molecular & Biochemical Parasitology*. 237(111276)

Canadian graduate theses are reproduced by the Library and Archives of Canada (formerly National Library of Canada) through a non-exclusive, world-wide license to reproduce, loan, distribute, or sell theses. I am also seeking your permission for the material described above to be reproduced and distributed by the LAC (NLC). Further details about the LAC (NLC) thesis program are available on the LAC (NLC) website ([www.nlc-bnc.ca](http://www.nlc-bnc.ca)).

Full publication details and a copy of this permission letter will be included in the thesis.

Yours sincerely,  
Sarah Habibi

Permission is granted for:

- a) The inclusion of the material described above in your thesis.
- b) For the material described above to be included in the copy of your thesis that is sent to the Library and Archives of Canada (formerly National Library of Canada) for reproduction and distribution.

Name: Yishi Jin

Title: Professor

---

Signature:

Date (dd/mmm/yyyy) July 7, 2020

---

### Copyright Permission Letter

July 7, 2020

**Publication Title:** Investigating the function and possible biological role of an acetylcholine-gated chloride channel subunit (ACC-1) from the parasitic nematode *Haemonchus contortus*.

I am preparing my Doctor of Philosophy thesis for submission to the School of Graduate and Postdoctoral Studies at the University of Ontario Institute of Technology (Ontario Tech) in Oshawa, Ontario, Canada. I am seeking your permission to include a manuscript version of the following paper(s) as a chapter in the thesis:

Callanan, M., Habibi, S.A.\*, Law, W.J., Nazareth, K., Komuniecki, R., and Forrester, S.G. (2018) Investigating the function and possible biological role of an acetylcholine-gated chloride channel subunit (ACC-1) from the parasitic nematode *Haemonchus contortus*. *International Journal for Parasitology: Drugs and Drug Resistance*. 8(3): 526-533 \*Joint first author

Canadian graduate theses are reproduced by the Library and Archives of Canada (formerly National Library of Canada) through a non-exclusive, world-wide license to reproduce, loan, distribute, or sell theses. I am also seeking your permission for the material described above to be reproduced and distributed by the LAC (NLC). Further details about the LAC (NLC) thesis program are available on the LAC (NLC) website ([www.nlc-bnc.ca](http://www.nlc-bnc.ca)).

Full publication details and a copy of this permission letter will be included in the thesis.

Yours sincerely,  
Sarah Habibi

Permission is granted for:

- a) The inclusion of the material described above in your thesis.
- b) For the material described above to be included in the copy of your thesis that is sent to the Library and Archives of Canada (formerly National Library of Canada) for reproduction and distribution.

Name: RICHARD KOMUNIECKI

Title: DISTINGUISHED UNIVERSITY PROFESSOR  
UNIVERSITY OF TOLEDO  
(Emeritus)

Signature: Richard Komuniecki

Date (dd/mmm/yyyy): 09 JULY 2020